



Universidad de Oviedo

Departamento de Química Física y Analítica

**DISPOSITIVOS ELECTROANALÍTICOS
MINIATURIZADOS: ESTRATEGIAS
PARA LA MEJORA DE LA SEPARACIÓN
Y LA DETECCIÓN**

TESIS DOCTORAL

Isabel Álvarez Martos

2013

TABLE OF CONTENTS

| | |
|---|------------|
| RESUMEN | i |
| SCIENTIFIC PUBLICATIONS | iii |
| I. Peer-reviewed Journal Papers | iii |
| <i>Related with this Thesis</i> | iii |
| <i>Other contributions not related with this Thesis</i> | iv |
| II. Book Chapters | iv |
| III. Conference Papers (Proceedings) | iv |
| IV. Conference Contributions | iv |
| <i>Oral communications</i> | iv |
| <i>Poster communications</i> | v |
| LIST OF TABLES AND FIGURES | VII |
| INTRODUCTION | IX |
| 1. From Capillary Electrophoresis to Microfluidics | 1 |
| 1.1. Brief History of Capillary Electrophoresis (CE) | 1 |
| 1.2. Principles of Capillary Electrophoresis | 3 |
| 1.2.1. Electrokinetic phenomena (EKP) | 4 |
| 1.2.2. Separation parameters to be considered | 7 |
| 1.3. Current Trends in Analytical Chemistry: Miniaturization | 9 |
| 1.3.1. Benefits and drawbacks of miniaturization | 10 |
| REFERENCES | 12 |
| 2. Electrochemistry as Detection Method | 15 |
| 2.1. Principles of the Electrochemical Detection (ED) | 16 |
| 2.1.1. Mass transfer processes | 16 |
| 2.1.2. Electrochemical cell | 17 |
| 2.1.2.1. Working electrode materials | 18 |
| 2.1.3. Electrochemical techniques | 19 |
| 2.1.3.1. Voltammetry | 19 |
| 2.1.3.2. Amperometry | 22 |
| 2.1.4. Microelectrodes | 23 |
| 2.2. Electrochemical Detection in Miniaturized Analytical Devices | 25 |
| 2.3. Nanotechnological Approaches towards Improved Sensitivity | 26 |
| 2.3.1. Carbon-based nanomaterials | 27 |
| 2.3.1.1. Carbon nanotubes (CNTs) | 27 |

| | |
|---|-----------|
| 2.3.1.1.1. Functionalized carbon nanotubes | 28 |
| 2.3.1.1.2. Carbon nanotubes for electrochemical sensing | 30 |
| 2.3.1.1.3. Growth of carbon nanotubes | 31 |
| REFERENCES | 33 |
| 3. Materials for Miniaturized Analytical Devices | 37 |
| 3.1. Inorganic Materials | 38 |
| 3.2. Polymers | 39 |
| 3.2.1. Elastomers | 39 |
| 3.2.2. Thermoplastics | 40 |
| 3.2.3. Thermosets | 41 |
| 3.3. Paper | 41 |
| REFERENCES | 44 |
| 4. Towards Improved Separation Efficiency: The Role of the Surface | 47 |
| 4.1. Dynamic Coatings | 48 |
| 4.2. Permanent Coatings | 51 |
| REFERENCES | 53 |
| 5. Target Analytes | 57 |
| 5. 1. Catecholamines | 57 |
| 5.1.1. Clinical interest | 57 |
| 5.1.2. Methods of analysis | 58 |
| 5.2. Heavy Metals | 60 |
| 5.2.2. Methods of analysis | 61 |
| REFERENCES | 62 |
| OBJECTIVES | 65 |
| RESULTS & DISCUSSION | 69 |
| CHAPTER 1: SEPARATION EFFICIENCY IMPROVEMENT | 71 |
| 1.1. Background | 73 |
| 1.2. Research & Development | 77 |
| Book Chapter | 79 |
| <i>Improving the Separation in Microchip Electrophoresis by Surface Modification</i> | |
| John Wiley & Sons, Inc. (2013) Chapter 6 | |
| Article 1 | 139 |
| <i>Poly (acrylic acid) Microchannel Modification for the Enhanced Resolution of Catecholamines Microchip Electrophoresis with Electrochemical Detection</i> | |
| Anal. Chim. Acta 724 (2012) 136-143. | |
| Article 2 | 161 |

| | |
|--|------------|
| <i>Ionic Liquids as Modifiers for Glass and SU-8 Electrochemical Microfluidic Chips Sens. Actuators B: Chem. 188 (2013) 837-846</i> | |
| Article 3 | 187 |
| <i>Poly(glycidyl methacrylate) Derivatives as Modifiers in Microfluidic Devices for the Improvement of Catecholamines Separation (considering for publication)</i> | |
| CHAPTER 2: SENSITIVITY IMPROVEMENT | 217 |
| 2.1. Background | 219 |
| 2.2. Research & Development | 225 |
| Article 4 | 227 |
| <i>Manufacture of Carbon Microelectrodes by Laser Lithography for Electrochemical Detection</i> | |
| <i>J. Micro/Nanolith. MEMS MOEMS 10 (2011) 043013-1.</i> | |
| Article 5 | 241 |
| <i>Electrochemical Properties of Spaghetti and Forest like Carbon Nanotubes Grown on Glass Substrates (considering for publication)</i> | |
| CHAPTER 3: NOVEL MATERIALS | 265 |
| 3.1. Background | 267 |
| 3.2. Research & Development | 271 |
| Article 6 | 273 |
| <i>Paper/Transparency-based Analytical Devices for the Sensitive Detection of Lead and Cadmium (unpublished results)</i> | 273 |
| | 273 |
| CONCLUSIONS | 291 |

RESUMEN

Actualmente, la miniaturización es una de las principales tendencias en todos los campos científicos y particularmente en la Química Analítica. En este contexto, las técnicas de separación y especialmente la electroforesis, han sido pioneras en el desarrollo de dispositivos analíticos miniaturizados (Microchips de Electroforesis, MEs). Estos se incluyen dentro de los dispositivos denominados “lab-on-a-chip” (LOC), capaces de integrar todas las etapas de análisis en un dispositivo portátil. En lo que se refiere a su aplicación clínica, también pueden considerarse dispositivos “point-of-care” (POC), desarrollados con el objetivo de realizar análisis descentralizados en el punto de diagnóstico o tratamiento.

Con el fin de obtener dispositivos con altas prestaciones analíticas, el trabajo realizado en la presente memoria puede ser estructurado en tres partes: la modificación de los microcanales (para mejorar la selectividad), la obtención de un sistema de detección electroquímico miniaturizado y competitivo (para mejorar la sensibilidad), y la introducción de nuevos materiales (con el fin de obtener “zero-cost” análisis).

Los microchips de electroforesis son dispositivos analíticos miniaturizados que pretenden ser una potente técnica de separación. La separación de los analitos va a depender de dos factores: (i) los fenómenos electrocinéticos involucrados en la separación que dependen de la acumulación de cargas en la pared del microcanal y (ii) de la interacción de los analitos con el material inmovilizado. Por ello es de gran importancia la modificación superficial de microcanales, especialmente cuando se trata de analitos con una relación masa/carga parecida. Las estrategias propuestas en esta memoria para la consecución de este objetivo pueden ser clasificadas en dos grandes grupos modificaciones estáticas y dinámicas, dependiendo de si son irreversibles o si se producen por adición del modificador a la disolución reguladora (fase pseudoestacionaria). A lo largo de los estudios aquí realizados se han evaluado polímeros comerciales (poliácido acrílico), polímeros de síntesis propia (derivados del polimetil metacrilato) y modificadores orgánicos de reciente introducción (líquidos iónicos). Todos ellos han demostrado ser necesarios para conseguir la separación de especies estructuralmente muy parecidos, como son las catecolaminas (moléculas además de gran interés desde el punto de vista clínico dada su relación con enfermedades como el Alzheimer).

Dados los pequeños volúmenes de muestra empleados, estos dispositivos miniaturizados requieren un sistema de detección muy sensible. En los estudios recogidos en

esta Tesis los nanotubos de carbono crecidos directamente sobre la superficie han demostrado ser un material electródico apropiados para la detección de las catecolaminas. Dado que la medida que se realiza es una medida electroquímica interfacial, el estado de la superficie es muy importante. Por ello, se evaluaron la influencia de distintos parámetros como catalizadores e intercapas, pretratamientos, densidad e influencia de la orientación en la señal electroquímica. Por otro lado, la detección electroquímica ofrece muchas posibilidades, entre ellas el empleo de electrodos miniaturizados y de más de un electrodo a la vez para obtener la señal analítica (array). Esta estrategia además se caracteriza por la obtención de mejores sensibilidades. Así, se describen los primeros pasos y pruebas hacia la consecución de este objetivo, mediante el diseño de máscaras por métodos fotolitográficos.

La parte final de esta Tesis está basada en la integración de la detección electroquímica en dispositivos analíticos miniaturizados realizados en materiales de bajo coste, los denominados “paper-based analytical devices”. En la realización de esta Tesis se han evaluado tanto papel de filtro como transparencias, demostrando su potencial en la detección de metales pesados, como el plomo o el cadmio.

SCIENTIFIC PUBLICATIONS

I. Peer-reviewed Journal Papers

Related with this Thesis

- 1) S. J. Antuña Presa, A. Fernández Gavela, I. Álvarez Martos, M.T. Fernández Abedul, A. Costa García, M.G. Granda, M. Rodríguez Lastra, J. Rodríguez García. "Manufacture of Carbon Microelectrodes by Laser Lithography for Electrochemical Detection". J. Micro/Nanolith. MEMS MOEMS 10 (2011) 043013-1 (DOI: 10.1117/1.3661993).
- 2) I. Álvarez-Martos, M.T. Fernández-Abedul, A. Anillo, J.L. García-Fierro, F.J. García-Alonso, A.Costa-García. "Poly(acrylic acid) Microchannel Modification for the Enhanced Resolution of Catecholamines Microchip Electrophoresis with Electrochemical Detection". Anal. Chim. Acta 724 (2012) 136-143 (DOI: 10.1016/j.aca.2012.02.053).
- 3) I. Álvarez-Martos, F.J. García Alonso, Adela Anillo, P. Arias-Abrodo, M.D. Gutiérrez-Álvarez, A. Costa-García, M.T. Fernández-Abedul. "Ionic Liquids as Modifiers for Glass and SU-8 Electrochemical Microfluidic Chips". Sens. Actuators B: Chem. 188 (2013) 837-846 (DOI: <http://dx.doi.org/10.1016/j.snb.2013.07.068>).
- 4) I. Álvarez-Martos, A. Fernández-Gavela, J. Rodríguez-García, N. Campos-Alfaraz, A.B. García-Delgado, D. Gómez-Plaza, A. Costa-García, M.T. Fernández-Abedul. "Electrochemical Properties of Spaghetti and Forest like Carbon Nanotubes Grown on Glass Substrates" (Sens. Actuators B: Chem. under review).
- 5) I. Álvarez-Martos, R. Alonso-Bartolomé, V. Mulas Hernández, F.J. García Alonso, A. Anillo, A. Costa-García, M.T. Fernández-Abedul. "Poly(glycidyl methacrylate) Derivatives as Modifiers in Microfluidic Devices for the Improvement of Catecholamines Separation". (Macromolecules, under review).

Table 1. Impact Factor of the articles contained in this Thesis (year 2012).

| Journal | Impact Factor | Area | Ranking | Publication Status |
|---|---------------|-----------------------|---------|---|
| Journal of Micro-Nanolithography MEMS and MOEMS | 1.148 | Optics | 42/80 | Published |
| Analytica Chimica Acta | 4.387 | Chemistry, Analytical | 7/75 | Published |
| Sensors and Actuators B: Chemical | 3.535 | Chemistry, Analytical | 11/75 | One Published and other under consideration for publication |
| Macromolecules | 5.521 | Polymer Science | 3/83 | Considering for Publication |

Source: ISI Web of Knowledge

Other contributions not related with this Thesis

- 1) A. Fernández Gavela, S.J. Antuña Presa, M. García Granda, I. Álvarez Martos, M.T. Fernández Abedul, A. Costa García, M. Rodríguez Lastra, J. Rodríguez García. *“Refractive Index and Thickness Evaluation of Monomode and Multimode Step-index Planar Optical Waveguides Using Longitudinal Section Magnetic (LSM) and Longitudinal Section Electric (LSE) Formulation”*. PIER B 46 (2013) 213-231.

II. Book Chapters

- 1) M.T. Fernández-Abedul, I. Álvarez-Martos, F.J. García-Alonso, A. Costa-García, *“Improving the Separation in Microchip Electrophoresis by Surface Modification”*. Capillary Electrophoresis and Microchip Capillary Electrophoresis: Principles, Applications, and Limitations, First Edition, Edited by Carlos D. Garcia, Karin Y. Chumbimuni-Torres, and Emanuel Carrilho. John Wiley & Sons, Inc, NY, (2013) Chapter 6 (ISBN: 780470572177).

III. Conference Papers (Proceedings)

- 1) A. Fernández Gavela, S.J. Antuña Presa, M. García Granda, I. Álvarez Martos, M.T. Fernández Abedul, A. Costa García, M. Rodríguez Lastra, J. Rodríguez García. *“New Theoretical Proposal for Planar Optical Waveguides Characterization from Effective Indexes Measurements”*. (ISBN: 978-84-695-4327-6). XVII Simposium Nacional de la Unión Científica Internacional de Radio (URSI). 12-14 September (2012), Elche, Spain.
- 2) I. Álvarez-Martos, R. Alonso-Bartolomé, A. Fernández-Gavela, J. Rodríguez-García, N. Campos-Alfaraz, A.B. García-Delgado, D. Gómez-Plaza, A. Costa-García, M.T. Fernández-Abedul. *“Forest and Disordered Carbon Nanotubes: Sensitivity Improvement of Electrochemical Detection in Miniaturized Devices”* (ISBN: 978-3-9813484-2-2). 14th International Meeting on Chemical Sensors (IMCS). 20-23 May (2012), Nuremberg, Germany.

IV. Conference Contributions

Oral communications

- 1) I. Álvarez-Martos, M.T. Fernández-Abedul, A. Anillo-Abril, F.J. García-Alonso, A. Costa-García, *“Carboxylic Multi-walled Nanotubes as Immobilized Stationary Coating in Glass Capillary Electrophoresis Microchips for Catecholamines Detection”* (Poster + flash communication). III Workshop on Analytical Nanoscience and Nanotechnology. 16-18 September (2009), Oviedo, Spain.
- 2) I. Álvarez-Martos, M.T. Fernández-Abedul, F.J. García Alonso, A. Costa-García, *“Poly(acrylic acid) Modified Glass-MCEs for Catecholamines Electrochemical Detection”* (Poster + flash communication). II International Workshop of Analytical Miniaturization. 7-8 June (2010), Oviedo, Spain.

- 3) I. Álvarez-Martos, A. Fernández-Gavela, J. Rodríguez-García, N. Campos-Alfaraz, A.B. García-Delgado, D. Gómez-Plaza, A. Costa-García, M.T. Fernández-Abedul. *“Direct Growth of Carbon Nanotubes for Miniaturized Analytical Devices”* (Oral invited conference). VI Workshop en Nanociencia y Nanotecnología Analíticas. 8-9 July (2013), Alcalá de Henares, Spain.

Poster communications

- 1) I. Álvarez-Martos, M.T. Fernández-Abedul, F.J. García Alonso, A. Costa-García, *“Improving Cathecolamines Resolution by Poly-acrylic Acid Modification of Microchannel Walls in Glass Capillary Electrophoresis Microchips”*. 3th Lab-on-a-chip European Congress. 19-20 May (2009) Stockholm, Sweden.
- 2) I. Álvarez-Martos, R. Alonso-Bartolomé, M.T. Fernández-Abedul, F.J. García Alonso, A. Costa-García, *“Static Coatings for Cathecolamines Detection in Glass Capillary Electrophoresis Microchips”*. 13th International Conference on Electroanalysis (ESEAC). 20-24 June (2010), Gijón, Spain.
- 3) S.J. Antuña Presa, A. Fernández Gavela, M. Rodríguez Lastra, I. Álvarez Martos, M.T. Fernández Abedul, A. Costa García, J. Rodríguez García. *“Fabrication of Master Micromolds for Microchannels Replication to be Applied in Biosensors”*. XI Eurotrode. 1-4 April (2012), Barcelona, Spain.
- 4) I. Álvarez-Martos, R. Alonso-Bartolomé, A. Fernández-Gavela, J. Rodríguez-García, N. Campos-Alfaraz, A.B. García-Delgado, D. Gómez-Plaza, A. Costa-García, M.T. Fernández-Abedul. *“Forest and Disordered Carbon Nanotubes: Sensitivity Improvement of Electrochemical Detection in Miniaturized Devices”*. 14th International Meeting on Chemical Sensors. 20-23 May (2012), Nuremberg, Germany.
- 5) I. Álvarez-Martos, A. Fernández-Gavela, J. Rodríguez-García, N. Campos-Alfaraz, A.B. García-Delgado, D. Gómez-Plaza, A. Costa-García, M.T. Fernández-Abedul. *“Direct Growth of Forest and Disordered Carbon Nanotubes on Glass for Use in Miniaturized Analytical Devices”*. III International Workshop of Analytical Miniaturization. 11-12 June (2012), Barcelona, Spain.

LIST OF TABLES AND FIGURES

Table 1. Impact Factor of the articles contained in this Thesis (year 2012).

Table 2. Modes of capillary electrophoresis: Capillary Zone Electrophoresis (CZE), Capillary Gel Electrophoresis (CGE), Micellar Electrokinetic Chromatography (MEKC), Capillary Electrochromatography (CEC), Capillary Isoelectric Focusing (CIEF), Capillary Isotachopheresis (CITP) (information adapted from ref. [20]).

Table 3. Common types of microelectrodes and their diffusion fields.

Table 4. Classification of materials employed in miniaturized analytical devices fabrication and their properties.

Table 5. μ PADs common fabrication techniques.

Table 6. Receptors activated by dopamine (DA), norepinephrine (NE) and epinephrine (E).

Figure 1. Capillary Electrophoresis (CE) timeline.

Figure 2. Schematic representation of a Capillary Electrophoresis system.

Figure 3. Migration velocity (v_{tot}) of molecules with different nature (cation, neutral and anion) as a contribution of electrophoretic (v_{ep}) and electroosmotic (v_{EOF}) velocities. Schematic representation of the electrical double layer on a negatively charged surface.

Figure 4. Microchip electrophoresis schematic drawing for single channel design, and two injector configurations (single-T and twin-T), where: A is the buffer inlet, B the detection reservoir, C the sample reservoir and D the sample waste.

Figure 5. Classification of velocity profiles.

Figure 6. Classification of the electrochemical techniques based on current or potential measurements [potential (E), current (i), and time (t)].

Figure 7. Miniaturization of the electrochemical cell.

Figure 8. Potential-time and current-potential waveforms for cyclic voltammetry, where: E_i (initial potential), E_f (switching potential), E_{pc} (cathodic peak potential), E_{pa} (anodic peak potential), i_{pc} (cathodic peak current), and i_{pa} (anodic peak current).

Figure 9. Potential-time and current-potential waveforms for square wave voltammetry, where: ESW (pulse amplitude), ΔE_{SW} (step potential), τ (stair case period), t_1 and t_2 (current measures), E_p (peak potential), and i_p (peak current).

Figure 10. Potential-time and current-time waveforms for chronoamperometry.

Figure 11. Classification of the microchip electrophoresis electrochemical detection in function of the working electrode (WE) location.

Figure 12. Classification of the different carbon structures according to the number of dimensions on the nanometric scale.

Figure 13. Diagrams of A) SWCNTs and MWCNTs with typical dimensions (length, width and separation distance), and B) the three main ways in which graphene sheet is rolled.

Figure 14. Growth modes of carbon nanotubes by chemical vapor deposition.

Figure 15. Fabrication techniques for polymer-based microfluidic devices.

Figure 16. Classification of the surface modification methods for microfluidic devices.

Figure 17. Aggregated structures from single-chained surfactants (micelle) or from double-chained surfactants (bilayer and vesicle).

Figure 18. Structures of the most commonly used ionic liquids in capillary electrophoresis.

Figure 19. Approaches for the surface modification with polymers.

Figure 20. Structures of the catecholamines.

Figure 21. Cyclization reactions for dopamine conversion into quinone [23].

Figure 22. Objectives of the Thesis divided into microfluidic device functions.

INTRODUCTION

INTRODUCTION

1. From Capillary Electrophoresis to Microfluidics

During the last years there has been a growing trend towards the miniaturization of analytical devices and their components [1,2] but, why is this tendency so important? Why the use of microfluidic devices?

By definition, microfluidics is considered as the science of manipulating small amounts of liquids in μ -size channels. They offer attractive advantages over classic techniques which make them able to meet the more every day demanded zero-cost and fast-response analysis, small sample volumes, and in-field or point-of-care analysis [3]. Therefore, microfluidic devices are an extremely versatile tool of analysis capable of covering a wide range of bio-applications (high-throughput drug screening, single cell analysis, drug delivery and therapeutics ...) [4], detect warfare agents and explosive compounds [5], food [6] or environmental analysis [7], among others. The three entirely different research fields responsible of encouraging microfluidics since 90s are biodefense, molecular biology and microelectronics [8].

However, before becoming widespread, every technology has challenges to overcome. In the field of microfluidics these are not only related to their commercialization, where a lot of work must be done in order to achieve the complete integration of all the components into a single device, but also with the search of new surface properties and materials as well as sensitive detection systems, which meet the needs of society.

1.1. Brief History of Capillary Electrophoresis (CE)

Electrophoresis as an analytical technique was first introduced by the Swedish chemist Arne Tiselius in 1930 [9]. Although his apparatus was complex (U-shaped tube with electrodes at each end), Tiselius was able to separate the five most abundant proteins in human serum and quantify their levels. This early form of electrophoresis was replaced in the 1950s by the called *Zone Electrophoresis* (ZE) which relies on the separation of molecules in a solid support (e.g. filter paper, agarose and polyacrylamide gels or cellulose acetate) [10]. Although zone electrophoresis provides efficient separations (allowing its application in the analysis of biological macromolecules), the long analysis times (separation speed is limited by Joule heating and only low voltages can be applied), the poor reproducibility, difficulties in detection and its complicated automation are among its main drawbacks. Therefore, it is generally not possible to develop quantitative assays.

Electrophoresis in narrow tubes arises to overcome the above mentioned problems. The first in describing an electrophoretic separation of molecules in a glass tube (internal diameter of 3 mm approximately) and the detection of the separated compounds by ultraviolet absorption (UV) was Hjertén in 1967 [11]. The small volume of the tube improves the dissipation of heat, which allows the application of higher voltages, leading to high-speed analysis. However, electrophoresis in a tube did not become popular until 1981, when Jorgenson and Luckas [12] demonstrated the high-resolution power of *Capillary Zone Electrophoresis* (CZE). They show the potential of *Capillary Electrophoresis* (CE) as an analytical technique, using fused silica capillaries with internal diameter of 75 μm and on-column fluorescence detection. This technique enables the separation of charged analytes which are separated based on their mass-to-charge ratios however, neutral compounds cannot be separated.

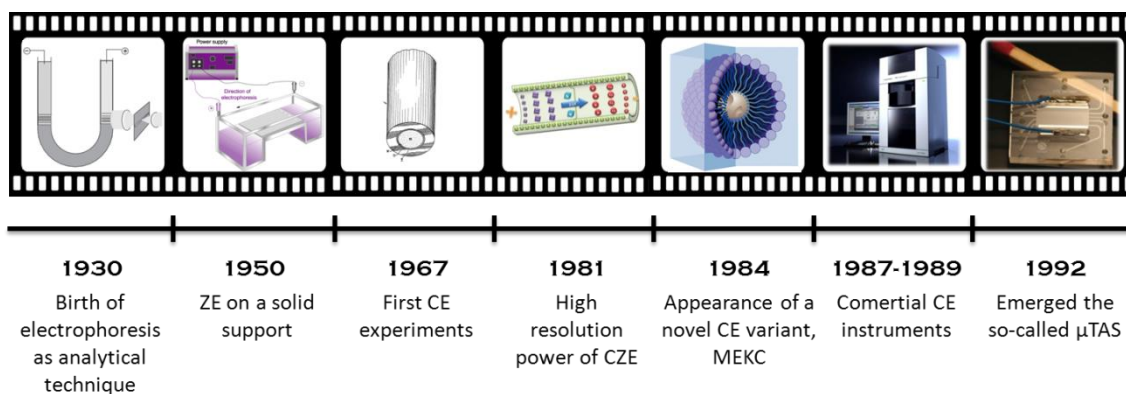


Figure 1. *Capillary Electrophoresis (CE) timeline.*

A novel variant of capillary electrophoresis, which enabled the separation of neutral compounds, was introduced in 1984 by Terabe [13]. In this version, called *Micellar Electrokinetic Chromatography* (MEKC), a charged surfactant (*e.g.* sodium dodecyl sulphate) is added to the mobile phase at concentrations above its critical micelle concentration. This causes the separation of non-polar compounds due to differing degrees of partition (distribution between the mobile phase and micelles) into the charged micelle.

The first commercial CE automated instruments were introduced in 1987-1989 by Microphoretic Systems (Sunnyvale, CA, USA), Applied Biosystems (Foster City, CA, USA) and Beckman Coulter (Fullerton, CA, USA). Since then, there have been many advances with a tremendous impact on the progress of science. The most ambitious and important example is the Human Genome Project (HGP) with the goal of determining the complete nucleotide sequence of the human genome in a short period of time [14,15]. It should be said that, the success of this project was possible thanks to the introduction of DNA sequencers based on

capillary electrophoresis [16] which allow the sequence of 14.8 billion DNA base pairs in just nine months.

Recent efforts have been focused on miniaturized instrumentation in order not only to enhance the performance of the analytical devices but also to reduce analysis times, reagents consumption and equipment costs. In 1992, *Manz et al.* [17] employed the silicon technology to integrate capillary electrophoresis into a microchip format, emerging the so-called *Miniaturized Total Analysis Systems* (μ TAS) and an exciting new field (*microfluidic devices*) which continues growing today.

1.2. Principles of Capillary Electrophoresis

Capillary electrophoresis can be described as a high-efficient separation technique carried out in capillaries based solely on the differences in the electrophoretic mobilities of charged species (analytes) either in aqueous or non-aqueous background electrolyte solutions. These can also contain additives, whose interactions with analytes are able to alter their electrophoretic mobility [18].

This technique offers some remarkable advantages when it is compared to other separation techniques such as high efficient separations, short analysis times (usually within 10 min), small sample volumes (less than pg or nL), low consumption of reagents and inexpensive columns but, one of the most important comes from its ability to separate both charged and non-charged molecules and the employment of aqueous solutions instead of organic solvents (making it more environmental-friendly) [19]. Moreover, one key feature is the relative simplicity of the instrumentation which could be easily miniaturized and automated.

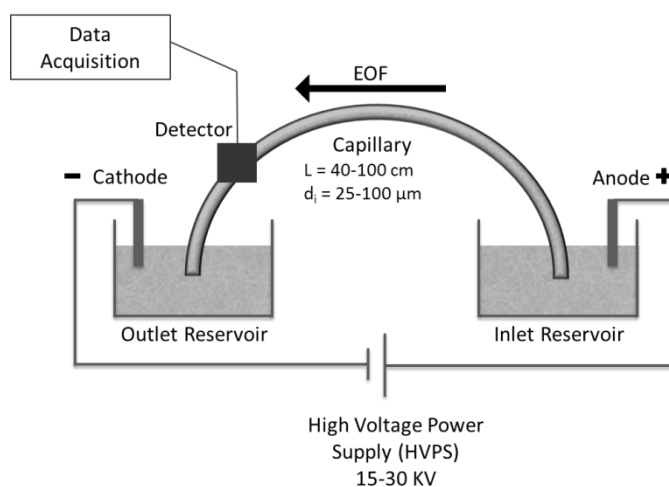


Figure 2. Schematic representation of a Capillary Electrophoresis system.

A schematic diagram of a CE system is illustrated in **Figure 2**. The basic instrumentation setup consists of an anode and a cathode which are placed in the inlet and outlet buffer reservoirs respectively, and connected to a High Voltage Power Supply (HVPS). The typical applied voltages across the capillary (internal diameter about 25-100 μm) are comprised between 15-30 KV. As a result, an electric field is created in the capillary (usually made of fused-silica) which allows charged molecules to migrate. Finally, a detector is placed downstream towards the end of the capillary and it is usually connected with a data acquisition system.

Table 2. Modes of capillary electrophoresis: Capillary Zone Electrophoresis (CZE), Capillary Gel Electrophoresis (CGE), Micellar Electrokinetic Chromatography (MEKC), Capillary Electrochromatography (CEC), Capillary Isoelectric Focusing (CIEF), Capillary Isotachopheresis (CITP) (information adapted from ref. [20]).

| | MODE | BASIS | | APPLICATIONS | |
|----------------------|----------------------|-------------------|--|--|--|
| CONTINUOUS SYSTEM | KINETIC PROCESS | CZE | Free solution mobilities | | Drugs, environmental analysis, organic and inorganic species, peptides and proteins |
| | | CGE | Size and charge | | Oligonucleotide purity analysis, anti-sense gene therapy, DNA sequencing, PCR product analysis, DNA forensics and proteins |
| | | MEKC | Hydrophobic/ionic interactions with micelles | | Amino acids, nucleotides, vitamins, pharmaceuticals, aromatic hydrocarbons, explosives ... |
| STEADY-STATE PROCESS | CIEF | Isoelectric point | | Separation of isoforms, immunoglobulins and hemoglobins and other biological solutions | |
| | DISCONTINUOUS SYSTEM | CITP | Moving boundaries | | Preconcentration step prior CZE, MEKC or CGE |

Another remarkable feature of CE is its versatility, which is partially derived from its numerous modes of operation. There is a huge variety of separation modes, which can be accessed only by modifying the buffer solution composition or separation conditions. Thus, the choice of an adequate mode is going to be mainly defined by the analytical problem under consideration. A description of the basic capillary electrophoresis separation methods is comprised in **Table 2**.

1.2.1. Electrokinetic phenomena (EKP)

Electrokinetic phenomena (those involving tangential fluid motion adjacent to a charged surface [21]) belong to the oldest branch of surface and colloid science, which arose from the concept of the electrical double layer (EDL). The most remarkable application of this effect is its use in separation techniques [22,23].

Focusing on capillary electrophoresis, the electrophoretic separation emerges from the difference in velocity of charged particles which migrate under the influence of an *electric field* (V). Thus, as **Figure 3** displays (left side), the overall migration velocity (v_{tot}) is the sum of two migration processes, which take place simultaneously and have different velocities: the *electrophoretic velocity* (v_{ep}) and the *electroosmotic velocity* (v_{eo}). In addition, both velocities are determined by its *mobility* (μ) and the *electric field strength* of the medium (E), which is directly proportional to the applied voltage and inversely proportional to the *capillary length*, L).

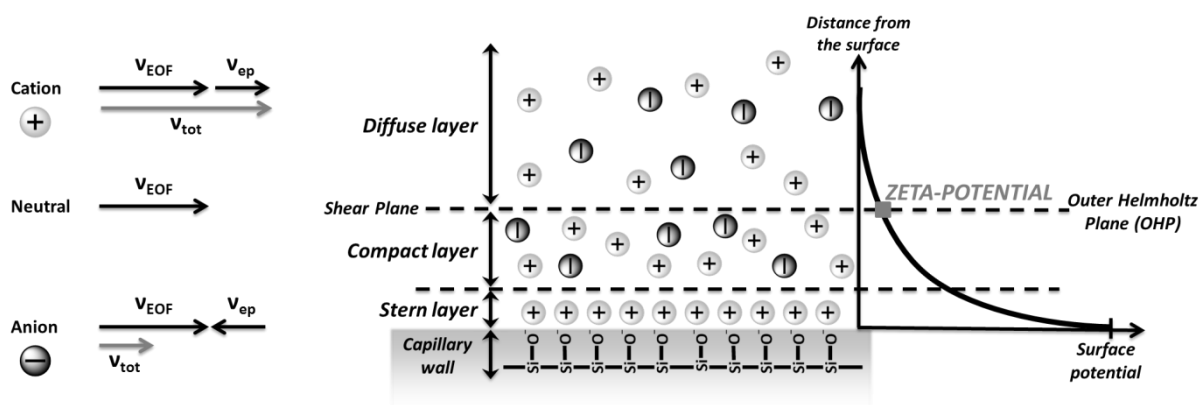


Figure 3. Migration velocity (v_{tot}) of molecules with different nature (cation, neutral and anion) as a contribution of electrophoretic (v_{ep}) and electroosmotic (v_{EOF}) velocities. Schematic representation of the electrical double layer on a negatively charged surface.

The following equations show that the electrophoretic and electroosmotic mobilities are influenced by different parameters. While μ_{ep} depends on the physical features of the particle [mainly *charge* (q) and *radius* (r)] μ_{EOF} does it on the surface charge on capillary walls [mainly

solution *dielectric constant* (ϵ) and *zeta potential* (ζ). The dependence of both mobilities with the medium *viscosity* (η) should be noted.

$$v = v_{ep} + v_{EOF} = (\mu_{ep} + \mu_{EOF})E = (\mu_{ep} + \mu_{EOF}) VL^{-1} \quad (1)$$

$$\mu_{ep} = \frac{q}{6\pi r\eta} \quad (2)$$

$$\mu_{EOF} = \frac{\epsilon\zeta}{\eta} \quad (3)$$

Special mention deserves the so-called **Electroosmotic Flow** (EOF), an electrophoretic phenomena that generates the bulk solution flow toward the cathode within the capillary. This flow results from the effect of the applied electric field on the solution double layer at the capillary wall, which is schematically illustrated in **Figure 3** (right side). The EOF is strongly controlled by the ionization of the acidic silanol groups (SiOH) which are on the inner part of the capillary. At pH>3 these groups are dissociated resulting in a negative charged surface. In order to maintain the electro-neutrality, cations build up near the surface leading to the so-called *Stern layer* (where the ions are strongly bounded). Outside this layer, ions of opposite polarities form an electrically neutral *diffusion layer* (where ions are less firmly attached). When the voltage is applied, a part of the electrical double layer is set into motion, causing a net solution flow through the capillary. This effect could be considered as an “electric pump” [24]. On the other hand, solvent molecules located close to the wall within the *surface of shear* will not move under the influence of an electric field. It should be noted that the EOF is mainly determined by the so-called zeta potential, which drops logarithmically with the electrical double layer distance [25].

The double layer is usually thin compared with channel dimensions, and this allows flow at the walls of the capillary, resulting in a flat profile, minimizing dispersion and enabling higher peak efficiencies than those of separation techniques with pressure-driven flow profiles [26].

The zeta potential, and as a result the electroosmotic flow, is going to be under the influence of the capillary wall surface conditions, which is mainly influenced by [27]:

- *pH of the buffer solution.* This parameter affects the protonation/deprotonation equilibria of the silanol groups present on the surface of the capillary wall, influencing the charge density. Thus, the zeta potential increases with increasing pH because at high pH values silanol groups are more deprotonated.

- *Ionic strength of the buffer solution.* This parameter influences the degree in which the surface charge is shielded. An increase in ionic strength results in a thicker double layer, and has the effect of decreasing the zeta potential. Furthermore, high ionic strength buffer solution is also going to generate high currents and an important Joule heating.
- *Temperature.* Generally, the zeta potential increases 1.75 % per °C.
- *Counterion valence and size.* These parameters are typically less important but, it has to be considered that they influence the zeta potential by affecting the surface adhesion equilibrium, by changing the exact location of the OHP, and by affecting the thickness of the diffuse double layer. In most cases a reduction in zeta potential is observed with high valence and size ions.

1.2.2. Separation parameters to be considered

Separation in electrophoresis is based on differences in the species mobility, which is dependent on the width and the difference in migration time. The quantitative measure of separation performance in CE is the **Resolution** (R_s). This parameter is defined as the separation of two peaks in terms of their average peak width at base ($t_{m2} > t_{m1}$) [28].

$$R_s = \frac{t_{m2} - t_{m1}}{\frac{W_{p1} + W_{p2}}{2}} = \frac{2 t_{m2} - t_{m1}}{W_{p1} + W_{p2}} \quad (4)$$

Where t_m is the *migration time* of the analyte, defined as the time required for the analyte to move through the *effective length* of the capillary (L_{eff}), that is, from the sample introduction point to the detection point, and W_p is the *peak width* measured at its base. When $R_s = 1.5$, the separation of two peaks is essentially complete, and they are considered baseline resolved.

The measure of the process efficiency is given by the **number of theoretical plates** (N).

$$N = \frac{(\mu_{ep} - \mu_{EOF})L_{eff}V}{2D} \quad (5)$$

Where D is the *diffusion coefficient* of the analyte.

In case of electrophoretic measurements this value can be determined by this equation:

$$N = 5.54 \frac{t_m}{W_{1/2}}^2 \quad (6)$$

Where $W_{1/2}$ is the peak width at half-height.

Thus, the best separation efficiencies are going to be achieved with higher applied voltages, in capillaries long enough to dissipate the heat generated. A high value of N is also going to result in narrow peaks as a consequence of the short time the analyte spends in the capillary. Even though, in capillary electrophoresis there are a large number of parameters that also affect the separation efficiency (diffusion, Joule heat, electrophoretic dispersion, wall adsorption, capillary dimensions ...) [29,30] and, therefore it is essential to know how a change in one of them will affect the others. The ones involved in band-broadening are particularly important:

- *Diffusion*. The factors that affect the extent of the band-broadening are mainly the molecule's size and time. The first is given by the Stokes-Einstein equation (7), and is less important in larger (slower diffusion) than in smaller substances, as well as in solutions with higher viscosities or lower temperatures. The second is the time that the molecule is in the capillary, which decreases with increasing applied voltage.

$$D = \frac{k T}{6\pi\eta r} \quad (7)$$

Where, k is the Boltzmann constant, T the temperature, η the viscosity and r the radius of the molecule.

Particular mention deserves the so-called *Joule heating*, which is often the most important band-broadening cause in electrophoresis. Heat depends on the applied voltage and the time within the system. When there is a rise in temperature the solution viscosity usually decreases, leading to increased diffusion coefficient and band-broadening. Furthermore, if the heat is not distributed uniformly, the temperature will not be the same throughout the capillary, obtaining regions with different densities and rates of diffusion.

- *Electromigration dispersion*. This effect is observed when the concentration of sample ions is comparable to that of the background solution. Under such conditions, the local electrical conductivity is altered in the vicinity of the

sample, which alters the effective migration speed of the sample ions and the concentration distribution, generating a non-linear transport problem [31].

- *Geometry of the capillary.* Sometimes it is necessary to extend the capillary length to improve resolution (*e.g.* closely migrating species) or to increase the internal diameter of the capillary (*e.g.* increasing the path length) but, the separation quality can be significantly compromised due to sample dispersion.
- *Adsorption.* The analyte-wall interaction can modify the zeta potential in a non-uniform way. This induces axial pressure gradients, so that the flow is no longer uniform throughout the capillary, resulting in shear-induced dispersion of the sample. This effect is particularly important for species such as proteins, DNA or peptides which adsorb strongly on capillary walls [32].

1.3. Current Trends in Analytical Chemistry: Miniaturization

Simplification (ease of implementation or use), automation (electromechanical self-operation) and miniaturization (small scale) are recognized as the main trends in modern Analytical Chemistry [33-35]. It appears from this description that microfluidic microfabricated devices, which ideally perform all the analytical steps (sample preparation, analyte separation and detection) in one system, satisfactorily fulfill the final objective of the Analytical field. Therefore, in the last years, an important growth in the use of these devices has been witnessed.

These devices could be defined as those made by using microtechnology with at least one dimension between 100 nm to 500 μm , which allow fluids movement through channels, chambers or conduits [36]. Special mention deserves the so-called *Microchip Electrophoresis* (ME), which arise as a result of capillary electrophoresis miniaturization. This fact makes that both techniques have also several common features. However, there are some important differences that have practical consequences, and which have to be considered:

- *Type of injection.* While conventional CE systems are equipped with pressure systems for hydrodynamic injections, in ME this is performed electrokinetically, avoiding the need of pumps.
- *Separation channel.* It is considerably reduced in length, allowing the application of higher electric fields with lower voltages.

- *Buffer and sample reservoirs.* They are smaller than in CE, so the volumes employed in ME are roughly an order of magnitude smaller than in CE.

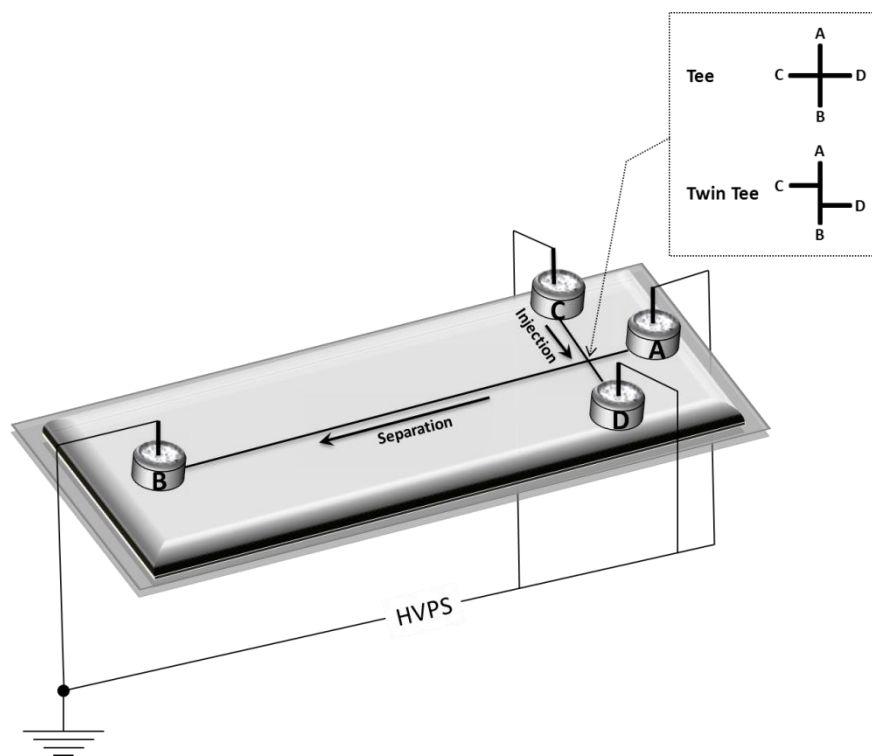


Figure 4. Microchip electrophoresis schematic drawing for single channel design, and two injector configurations (single-T and twin-T), where: A is the buffer inlet, B the detection reservoir, C the sample reservoir and D the sample waste.

The classic design of a microfluidic chip consists of a long separation channel that intersects a shorter injection channel and includes reservoirs at the end of each [37]. This is known as “single-channel” or “single-T”. As **Figure 4** exhibits, the sample injection is generally performed by applying a voltage of several hundred volts between sample (C) and sample waste (D) reservoirs, which typically represents an injection volume of 50-100 μL . The separation is carried out by applying a voltage of 1-4 KV between buffer (A) and detection (B) reservoirs. Finally analytes are detected when they reach the detection window downstream.

1.3.1. Benefits and drawbacks of miniaturization

From the practical point of view, miniaturization has inherent advantages giving the possibility of making portable analysis devices and even laboratories for in-field use. These features allow automated analysis and, in general, lower costs and energy consumption as well as higher speed, providing the opportunity of creating new markets and applications.

On the other hand, “micro” in this context implies small dimensions leading to tiny sample volumes (nanoliter to femtoliters), which can reduce the required amount of solvents and reagents. This also leads to shorter time required to perform the complete analysis (high throughput), for instance, it can drop from minutes to seconds, which can be critical for medical applications [2].

It is noteworthy that the physical and chemical properties such as capillary forces, surface roughness or chemical interactions are different in small-scale devices. On the one hand, miniaturized devices have a higher surface area to volume ratio than traditional CE systems, which allows a greater dissipation of the heating. Such heating is frequently referred to as *Joule heating*, which usually leads to the detrimental effect of nonlinear flow, causing band broadening [38] as it was mentioned in *section 1.2.2*. This feature can lead to increased performance, higher sensitivity and increased resolution of separation, allowing the separation of compounds traditionally difficult to separate by capillary electrophoresis [39]. Although high surface area to volume ratio can be extremely advantageous, it can also be detrimental, leading to adsorbed molecules onto the surface of the microchannel and decreasing the transport efficiency [40].

Another important characteristic at the microscale is that viscosity and surface tension become more and more dominant while gravity and inertia lose their relative importance. These dominant forces provide well-defined flow characteristics, such as regularly shaped fluid and laminar flow [41,42]. Thus, when an electric field is applied, the fluid flow can be easily controlled [43], which is of paramount importance when an accurately control is necessary as for example, in biological or clinical applications [44]. On the other hand, the electroosmotic flow offers another important advantage over pressure-driven flows: it provides uniform velocity profiles (velocity is constant all along the microchannel except very close to the wall), which allows low sample dispersion (**Figure 5**).

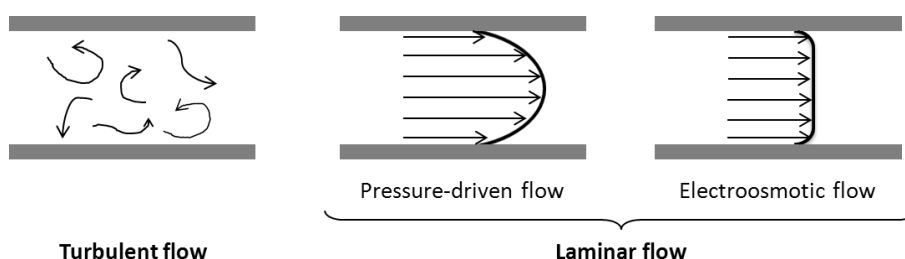


Figure 5. Classification of velocity profiles.

REFERENCES

- [1] M. Miró, E.H. Hansen. *Anal. Chim. Acta* 750 (2012) 3-15.
- [2] A. Rios, M. Zougagh, M. Avila. *Anal. Chim. Acta* 740 (2012) 1-11.
- [3] G.M. Whitesides. *Lab Chip*. 13 (2013) 11–13.
- [4] L.Y. Yeo, H.-C. Chia, P.P.Y. Chan, J.R. Friend. *Small* 7 (2010) 12-48.
- [5] J. Wang. *Anal. Chim. Acta* 507 (2004) 3-10.
- [6] A. Martín, D. Vilela, A. Escarpa. *Electrophoresis* 33 (2012) 2212-2227.
- [7] L. Marle, G.M. Greenway. *Trac-Trend. Anal. Chem.* 24 (2005) 795-802.
- [8] G.M. Whitesides. *Nature* 442 (2006) 368-373.
- [9] A. Tiselius. *Trans. Faraday Soc*, 33 (1937) 524-531.
- [10] R. Westermeier. Chapter 1 in *Electrophoresis in Practice: A Guide to Methods and Applications of DNA and Protein Separations*. Willey-VCH Verlag GmbH & Co. KGaA, Weinheim (2005) 9-43.
- [11] S. Hjertén. *Chromatogr. Rev.* 9 (1967) 122-219.
- [12] J.W. Jorgenson, K.D. Lukacs. *Anal. Chem.* 53 (1981) 1298-1302.
- [13] S. Terabe, K. Otsuka, K. Ichikawa, A. Tsuchiya, T. Ando. *Anal. Chem.* 56 (1984) 111-113.
- [14] J.C. Venter, M.D. Adams, E.W. Myers, P.W. Li. *et al. Science* 291 (2001) 1304-1351.
- [15] E.S. Lander, L.M. Linton, B. Birren, C. Nusbaum *et al. Nature* 409 (2001) 860-921.
- [16] N.J. Dovichi, J. Zang. *Angew. Chem. Int. Ed.* 39 (2000) 3924-4468.
- [17] A. Manz, N. Graber, H.M. Widmer. *Sensor. Actuat. B-Chem* 1 (1990) 244-248.
- [18] M.-L. Riekkola, J.Å. Jönsson, R.M. Smith. *Pure Appl. Chem.* 76 (2004) 443-451.
- [19] M.C. Breadmore. *J. Chromatogr. A* 1221 (2012) 42-55.
- [20] D. Heiger. High Performance Capillary electrophoresis, Agilent Technologies (<http://www.colby.edu/chemistry/CH332/laboratory/Agilent%20CE%20Primer.pdf>)
- [21] A.V. Delgado, F. González-Caballero, R.J. Hunter, L.K. Koopal, J. Lyklema. *Pure Appl. Chem.* 77 (2005) 1753-1805.
- [22] P.G. Righetti. *J. Chromatogr. A* 1079 (2005) 24-40.
- [23] S. Wall. *Curr. Opin. Colloid In.* 15 (2010) 119-124.
- [24] K.D. Altria. Chapter 1 in *Capillary Electrophoresis Guidebook: Principles, Operation and Applications*. Springer (1996) 3-13.
- [25] C. Schwer, E. Kenndler. *Anal. Chem.* 63 (1991) 1801-1807.
- [26] A. Manz, C.S. Effenhauser, N. Burggraf, D.J. Harrison, K. Seiler, K. Fluri. *J. Micromech. Microeng.* 4 (1994) 257-265.
- [27] B.J. Kirby, E.F. Hasselbrink Jr. *Electrophoresis* 25 (2004) 187-202.
- [28] IUPAC. *Compendium of Chemical Terminology*, 2nd ed. (the "Gold Book"). Compiled by A. D. McNaught and A. Wilkinson. Blackwell Scientific Publications, Oxford (1997).

- [29] M.L. Marina, A. Rios, M. Valcárcel. Chapter 1 in *Analysis and Detection by Capillary Electrophoresis*. Elsevier (2005) 1-28.
- [30] J.P. Landers. Chapter 1 in *Handbook of Capillary and Microchip Electrophoresis and Associated Microtechniques*. CRC Press, Taylor & Francis Group (2008) 4-74.
- [31] S. Ghosal, Z. Chen. *J. Fluid. Mech.* 697 (2012) 436-454.
- [32] S. Ghosal. *J. Fluid. Mech.* 491 (2003) 285-300.
- [33] J. Wang. *Trac-Trend. Anal. Chem.* 21 (2002) 226-232.
- [34] M. Ryvolová, J. Preisler, D. Brabazon, M. Macka. *Trac-Trend. Anal. Chem.* 9 (2010) 339-353.
- [35] Y. Peng, D.E. Austin. *Trac-Trend. Anal. Chem.* 30 (2011) 1560-1567.
- [36] P. Wilding, T. Joos, L.J. Kricka, L. Shi. *Pure Appl. Chem.* 78 (2006) 677-684.
- [37] http://www.micruxfluidic.com/products-microfluidic_chip.html#su8ed
- [38] N.J. Petersen, R.P.H. Nikolajsen, K.B. Mogensen, J.P. Kutter. *Electrophoresis* 25 (2004) 253-269.
- [39] D.J. Beebe, G.A. Mensing, G.M. Walker. *Annu. Rev. Biomed. Eng.* 4 (2002) 261-286.
- [40] S. Pennathur, C.D. Meinhart, H.T. Soh. *Lab. Chip.* 8 (2008) 20-22.
- [41] S. Takayama, E. Ostuni, P. LeDuc, K. Naruse, D.E. Ingber, G.M. Whitesides. *Nature* 411 (2001) 1016-1016.
- [42] T.M. Squires, S.R. Quake. *Rev. Mod. Phys.* 77 (2005) 977-1026.
- [43] C. Zhang, K. Khoshmanesh, A. Mitchell, K. Kalantar-zadeh. *Anal. Bioanal. Chem.* 396 (2010) 401-420.
- [44] Q. Zhang, R.H. Austin. *BioNanoSci.* 2 (2012) 277-286.

2. Electrochemistry as Detection Method

Miniaturized separation devices, particularly microfluidic chips, have demonstrated a huge potential as analytical tool, leading to the next generation in chemical separation/detection technologies [1]. Given their enormous potential, there is a need for developing compatible detection systems, which provide a reproducible and accurate quantitative analysis. Indeed, detection has been one of the main challenges for ME, since they need very sensitive detection techniques as a consequence of the small sample volumes.

Detection systems employed on these devices can be categorized into conventional (optical, electrochemical and mass spectrometry) and unconventional (infrared, Raman spectroscopy, nuclear magnetic resonance, surface plasmon resonance, thermal lens detection ...) [2] methods. Among conventional detection schemes it could be found:

- Optical methods, which comprise the detection by monitoring the light properties of the analyte. They are classified in two main groups: those that require an external source of radiation, such as lasers (LIF) or light-emitting diodes (LEDs) [3], and those that do not require an external source of radiation (chemiluminescence, CL) [4].
- Electrochemical sensing is based on the electrical properties measurement of species that undergo redox reactions, being the amperometric and contactless conductivity detections the most widespread [5].
- Mass spectrometry detection is able to monitor the trajectory of ions in electric and/or magnetic fields, which elucidate the mass and charge of the ions [6,7].

Much of the works on microfluidic chips are based on optical and electrochemical methods due to their selectivity and sensitivity. However, whereas the first requires a large and expensive supporting optical system, and is limited to analytes that are fluorescent or are liable to derivatization with a fluorophore, electrochemical methods can be easily miniaturized without loss of performance. Moreover, they are compatible with lithographic techniques, their response is not dependent on optical path length or sample turbidity. On the other side, there are many more compounds exhibiting electroactivity than native fluorescence [8].

In this section, a brief overview of electrochemistry, and particularly of the electrochemical techniques employed in the development of this Thesis, is given in order to introduce a few fundamental concepts.

2.1. Principles of the Electrochemical Detection (ED)

Electrochemistry is the branch of the chemistry which deals with the interrelation between electrical current and chemical effects. The available techniques are extremely varied, and as illustrated **Figure 6**, they can be mainly classified based on measurements of current or potential.

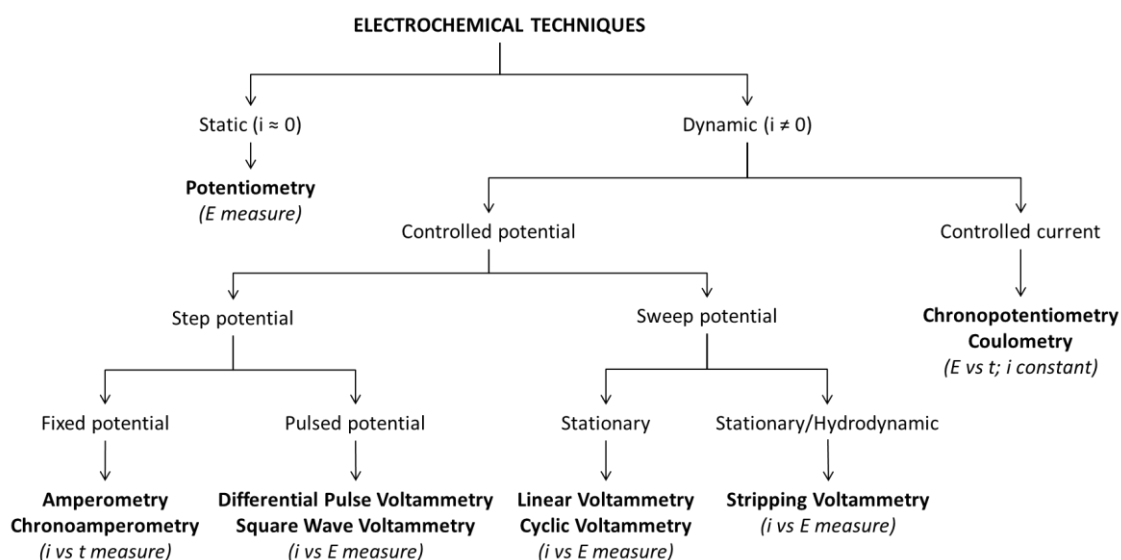


Figure 6. Classification of the electrochemical techniques based on current or potential measurements [potential (E), current (i), and time (t)].

2.1.1. Mass transfer processes

In general, the electrochemical signal has two contributions: the faradaic current (resulting from redox reactions) and the capacitive current (property of the interface between the electrode and the solution).

The magnitude of the *capacitive current* is going to be a function of the working electrode area and the scan rate. For instance, in cyclic voltammetry the capacitive current increases proportionally to the scan rate. Nevertheless, in many cases it is smaller than the faradaic one, so it can be ignored. On the other hand, there are two main factors that contribute to the *faradaic current*: the rate at which the molecules are transported to and from the electrode (mass transport), and the rate at which electrons pass between the electrode and the solution.

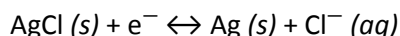
The rate of mass transport is one of the major factors influencing the faradaic current, which can be accomplished by three main modes: *diffusion* (movement of a species under the

influence of a concentration gradient), *migration* (movement of a charged molecule in an electric field), and *convection* (species movement because of stirring or density gradients) [9]. Most electrochemical theory is based on the assumption that the system is diffusion-controlled. In some cases, however, the analyte is highly attracted to the electrode and will be adsorbed.

2.1.2. Electrochemical cell

In spite of having the possibility of using different techniques, it is considered that all share the basic components, *i.e.* three-electrode cell and the electronic circuit for controlling and measuring the current or the potential (potentiostat). The three-electrode cell consists of a working electrode, WE (sensible to the analyte's concentration), reference electrode, RE (provides a constant potential against the WE), and counter electrode CE (with larger area than the working electrode).

The *working electrode* could be made in various materials ranging from metals (gold, platinum, silver ...) to different forms of carbon (paste, ink, graphite ...), and geometries. The *counter electrode* is usually a thin platinum wire, and the *reference electrode* is commonly a silver/silver chloride (Ag/AgCl) system, which is based on the following redox couple:



The typical Ag/AgCl reference electrode consists of a silver wire, which is anodized (coated with a thin film of AgCl), immersed in a saturated solution of potassium chloride (KCl), and a porous plug acting as a salt bridge. This reference electrode should provide a constant potential, and it is crucial that its potential remains constant over time in order to assign any change in current to the WE.

The trend towards analytical devices miniaturization has made that traditional bulky electrochemical cells have started to be replaced by other miniaturized, which can be considered as disposable (**Figure 7**). Thus, microfabrication techniques, including thick-film and thin-film processes, have made a considerable impact on the production of these three-electrode microsystems.

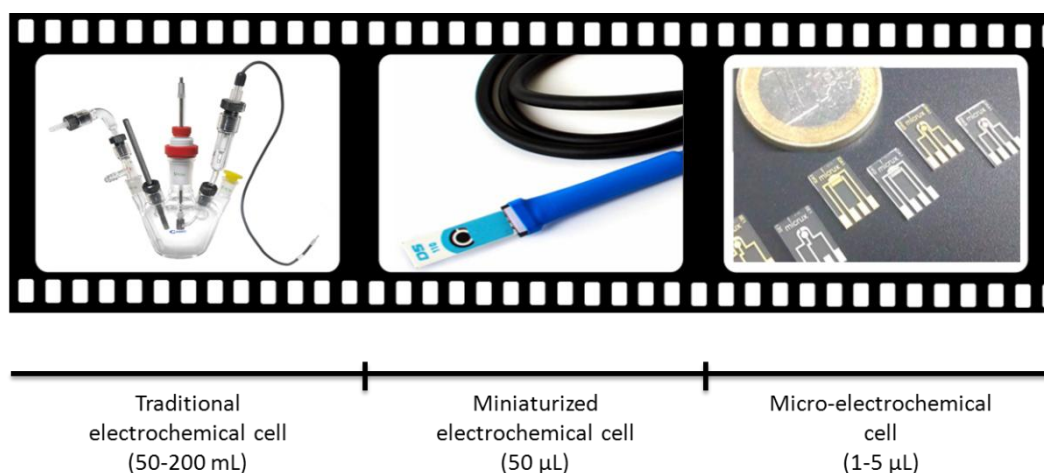


Figure 7. Miniaturization of the electrochemical cell.

The thick-film approach, represented by screen-printed electrodes, is generally simpler and cheaper than the thin-film, but it is limited to electrode structures larger than 100 μm . Fabrication of those electrodes relies on printing patterns, which contain the cell design, on plastic or ceramic substrates. The electrochemical behavior of these electrodes is going to be dependent on the ink composition, the printing technique, and curing conditions (*e.g.* temperature, pressure). On the other hand, thin-film approach, such as sputtering or evaporation, is based on metal film deposition onto the substrate. In this case a pattern is also needed, but it has a resolution in the order of few tens of micrometers [10]. In many cases the RE is a metal (*e.g.* Au, Ag, Pt ...) or carbon, and it is often termed as *pseudo-reference electrode* since it lacks the usual salt reservoir (*e.g.* KCl) and salt bridge, providing a constant but unknown potential, which is dependent on the buffer solution nature [11].

2.1.2.1. Working electrode materials

The *working electrode* represents the most important part of the electrochemical cell. Thus, the choice of an adequate material is critical to the experimental success, and its selection depends primarily on: favorable redox behavior of the analyte at the electrode material (fast, no electrode fouling ...), the potential window should be as wide as possible, measures should be reproducible. In addition it should be cheap, easily machined, and with low toxicity [12].

The materials employed as working electrodes could be classified into noble metals (gold [13], platinum [14], bismuth [15], silver [16] ...) and carbon [17]. In general, *noble metals* show higher conductivity resulting in low background currents, and usually have better sensitivity than carbon. Among these, platinum is likely the favorite, demonstrating good electrochemical behavior and ease fabrication but, its biggest disadvantage is the high cost.

Gold electrodes behave similarly to platinum, but have limited usefulness in the positive potential range due to the oxidation of its surface. Moreover, all metals are amenable of undergo corrosion or passivation (salt film on the surface).

On the other hand, *carbon materials* normally have a wider potential window, but the electrochemical processes usually are slower than in metals. There are many types of carbon used as working electrodes through the bibliography, including glassy-carbon [18], carbon inks (different inks printed on plastic or ceramic substrates) [19], carbon paste (consisting of graphite powder mixed with an inert matrix such as Nujol, paraffin, epoxy resin ...) [20], pencil lead [21], diamond-based materials [22], etc.

2.1.3. Electrochemical techniques

The choice of the technique to use depends on the analytical purpose, for instance amperometry is ideally suited for the analyte detection in flow systems, and stripping voltammetry when a much more sensitive detection technique is required. In the following section it is included a more thorough explanation of the techniques employed in the development of this Thesis is included.

Among all the existing electrochemical techniques, voltammetry and amperometry are those employed in this work.

2.1.3.1. Voltammetry

1) Cyclic Voltammetry (CV)

This is a widely used electroanalytical technique for studying the analyte redox process or characterized the electrode behavior. It is based on varying the applied potential at a working electrode in both forward and reverse directions while monitoring the current. The important parameters in a cyclic voltammogram are the anodic and cathodic peak potentials (E_{pa} and E_{pc}) and the anodic and cathodic peak currents (i_{pa} and i_{pc}).

The working electrode is subjected to a triangular potential sweep, whereby the potential rises from a starting value (E_i) to a final value (E_f) then returns back to the start potential at a constant scan rate (**Figure 8**), which can vary from a few millivolts per second to a hundred volts per second.

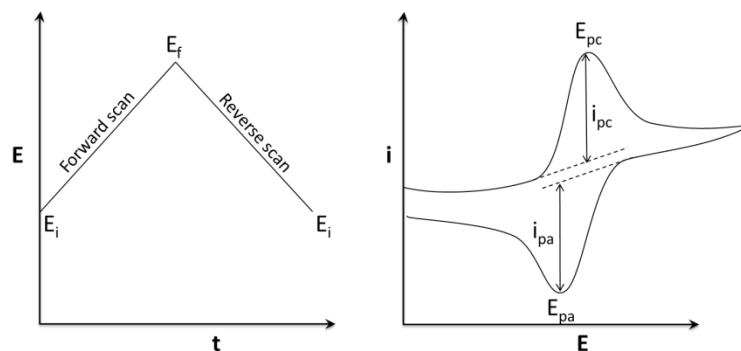


Figure 8. Potential-time and current-potential waveforms for cyclic voltammetry, where: E_i (initial potential), E_f (switching potential), E_{pc} (cathodic peak potential), E_{pa} (anodic peak potential), i_{pc} (cathodic peak current), and i_{pa} (anodic peak current).

If the electron transfer process is fast, the reaction is said to be *electrochemically reversible*. In this case the anodic and cathodic peak currents are equal (the ratio i_{pa}/i_{pc} is 1), and the separation between peak potentials is given by:

$$\Delta E = E_{pa} - E_{pc} = \frac{59 \text{ mV}}{n} \quad (8)$$

The peak current for a reversible system is given by the *Randles-Sevcik* equation.

$$i_p = 2.69 \cdot 10^{-5} n^{3/2} A D^{1/2} \nu^{1/2} C \quad (9)$$

Where:

n is the number of electrons involved in the redox reaction.

A is the area of the working electrode (cm^2).

D is the diffusion coefficient of the electroactive species ($\text{cm}^2 \text{s}^{-1}$).

ν is the scan rate (V s^{-1}).

C is the concentration of the electroactive species at the electrode (mol cm^{-3}).

From this equation it can be concluded that for a reversible process under diffusion conditions, the peak current is directly proportional to the square root of the scan rate.

2) Square wave voltammetry (SWV)

With the aim of increasing speed and sensitivity, other forms of voltammetry have been checked over the years. They are called pulsed techniques, and one of the most employed is the square-wave voltammetry. One of the main characteristics of this technique is its capability to reject the capacitive currents, leading to increased signal-to-noise ratios at the same time that it provides high sensitivity and speed analysis.

As illustrated in **Figure 9**, this wave form differs from that used at cyclic voltammetry measurements. In this case the starting potential is a average of the extreme potentials of the square-wave pulse. Thus, the waveform can be considered as a train of pulses towards higher and lower potentials. The square wave is characterized by the pulse amplitude (E_{SW}), which corresponds to one-half of the peak-to-peak amplitude of the square-wave signal. The duration of each pulse ($t_p = \tau/2$) is one-half the staircase period, the frequency ($f = 1/\tau$) is reciprocal to the staircase period, and the potential increment (ΔE_{SW}) is the height of the staircase waveform [23]. The current is sampled twice during each square-wave cycle, once at the forward pulse (t_1) and once at the end of the reverse pulse (t_2) providing an enhanced net current, especially for reversible processes. Thus, the peak shape is symmetric and the current is proportional to the analyte concentration. Capacitive current decays exponentially with time, increasing thus the sensitivity of measurements.

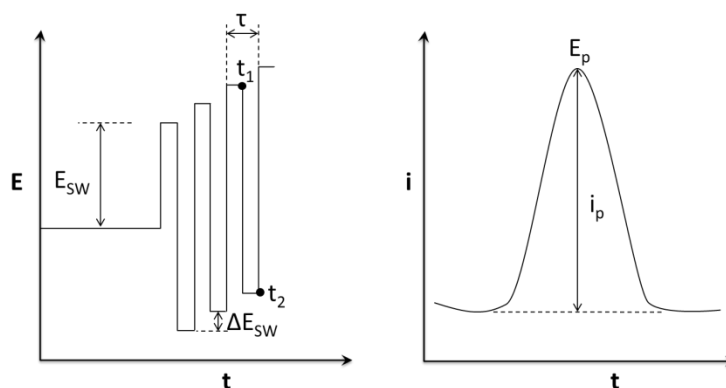


Figure 9. Potential-time and current-potential waveforms for square wave voltammetry, where: E_{SW} (pulse amplitude), ΔE_{SW} (step potential), τ (stair case period), t_1 and t_2 (current measures), E_p (peak potential), and i_p (peak current).

3) Stripping voltammetry

This technique belongs to the so-called preconcentration techniques. They are characterized by the lower limits of detection of any commonly used electroanalytical techniques, which make them ideal for trace analysis. Stripping analysis is basically a two-step technique: the first one (*deposition step*) in which the analyte is preconcentrated onto or into the working electrode, and the second one (*stripping*) in which the previously preconcentrated analyte is dissolved by applying a potential scan. In the stripping step any of the existing potential waveforms can be used (*i.e.* differential pulse, square wave, linear sweep, or staircase), but due to their excellent features (discrimination of the background currents, faster analysis and higher sensitivities) square wave is the most common [24]. Stripping analysis

can be classified into different versions depending on the deposition step: anodic stripping voltammetry (ASV), cathodic stripping voltammetry (CSV), and adsorptive stripping voltammetry (AdSV).

2.1.3.2. Amperometry

Amperometry is one of a family of electrochemical methods in which a constant potential is applied to the working electrode, using the same three electrode cell configuration as in cyclic voltammetry, and the current is constantly measured as a function of time.

The chronoamperometry deserves particular mention. In this technique the potential applied leads to a maximum value of the current, which decreases then exponentially as the analyte at the electrode is depleted.

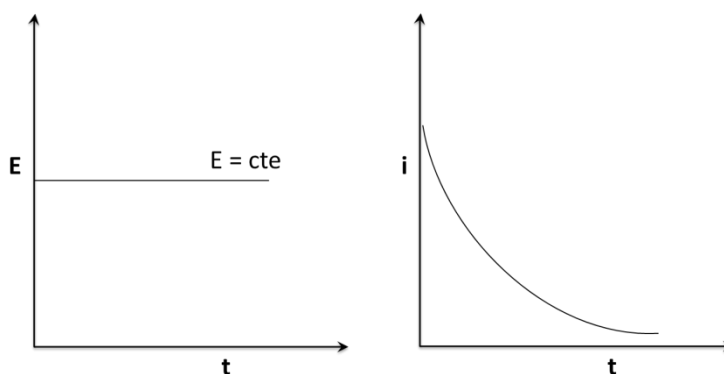


Figure 10. Potential-time and current-time waveforms for chronoamperometry.

For a planar electrode in unstirred solution, if the mass transport is only diffusion-controlled, then the current-time dependence is given by the *Cottrell equation* [25].

$$i = \frac{nFAD C^*}{\zeta} \quad (10)$$

If the mass transfer is governed by diffusion, then $\zeta = \sqrt{\pi D t}$, and the peak current is:

$$i = \frac{nFAD^{1/2} C^*}{\pi^{1/2} t^{1/2}} \quad (11)$$

Where:

n is the number of electrons in the redox reaction.

F is the Faraday constant ($C \text{ mol}^{-1}$).

A is the area of the electrode (cm^2).

D is the diffusion coefficient of the species ($\text{cm}^2 \text{s}^{-1}$).

C^* is the concentration of the analyte (mol cm^{-3}).

t is the time (s).

ζ is the thickness of the diffusion layer (cm).

From the equation, it could be seen that the current is inversely proportional to the square root of time.

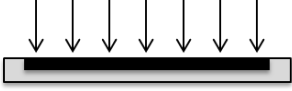
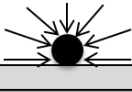

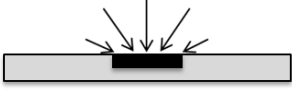

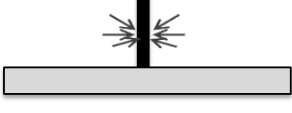
2.1.4. Microelectrodes

As it was said before, miniaturization is a growing trend in the field of Analytical Chemistry not only in separation devices but also in the detection systems. Microelectrodes, or ultramicroelectrodes (UME), are commonly defined as electrodes which have at least one dimension (thickness, width or radius) between 0.1 and 50 μm [26]. The most common geometric shapes include discs, spheres, hemispheres, rings or bands and, in general, they can be classified in two groups: single microelectrodes or various microelectrodes (array) [27].

As a consequence of their small size, a number of advantages are gained:

- *The rate of mass transport is enhanced.* The diffusion current contribution from the edges (radial diffusion) of the microelectrode becomes more important than in macroelectrodes (linear diffusion) (**Table 3**). As a consequence of the electrode size reduction, the rate of mass transport increases (faradaic current), while the capacitive current decreases (as a result of the reduced double-layer). Therefore, microelectrodes exhibit improved signal-to-noise ratios and sensitivities higher than macroelectrodes
- *Possibility of working in high resistance solutions* due to their almost negligible Ohmic drop (iR). This allows electrochemical measurements to be made in solvents with high resistance like benzene, toluene, and acetonitrile, among others.
- *Lower response times.*
- In case of microelectrode arrays, *increased current intensity.*
- They are *cheaper*, *small volumes* needed, and measurements are *simple* to carry out.

Table 3. Common types of microelectrodes and their diffusion fields.

| Common Geometries | | |
|-------------------|--------------------|--|
| Type of electrode | Critical dimension | Diffusion field |
| Macro-electrode | — |  |
| Sphere | Radius |  |
| Hemisphere | Radius |  |
| Micro-electrode | Disc | Radius |
| Band | Width |  |
| Ring | Width |  |
| Fiber | Radius |  |

These properties have captured much interest in the field of electrochemistry during the last decade to overcome the problems of conventional macroelectrodes (*e.g.* increase the potential window, obtain high spatial and temporal resolution in biological samples ...) [28].

Because of their small size, the electrochemical behavior of microelectrodes can appear markedly different from that observed at conventional electrodes. For example, in case of cyclic voltammetry measurements the current-potential waveform has a sigmoidal shape. A constant current (limiting current) is yielded, which is independent of the scan rate.

The ongoing interest in nanotechnology and the need of doing electrochemistry in increasingly small spaces (neurotransmitters release, single cell analysis ...) have given rise to even smaller electrodes, such as nanoelectrodes. They are generally defined as electrodes with at least one dimension less than 100 nm, in which benefits detailed above are magnified. For example, the dramatic decrease in capacitive currents together with the dominance of radial diffusion, allow measurements to be done on nanosecond time scales [29,30].

2.2. Electrochemical Detection in Miniaturized Analytical Devices

One of the major challenges in miniaturized analytical devices is the proper placement of the detection system. Thus, the detector design should ensure well-defined mass transport, minimal band broadening, electrical isolation from the separation voltage (failure on this leads to increased noise as well as probable damage to the potentiostat) as well as high sensitivity, tunable selectivity (*via* the applied potential), simple handling, and long-term stability [31].

To fulfill these requirements various detector configurations have been proposed, depending on the electrode position regarding the flow direction (flow-by, flow-onto, and flow-through) [12] or the microchannel (end-channel, off-channel, and in-channel) [32]. The former can be applied to all miniaturized analytical devices while the latter is more typical of microfluidic chips.

- *End-channel.* Is the most often used amperometric detection configuration. The electrode is placed 5-20 μm from the end of the separation channel. This configuration allows the separation voltage to dissipate prior to reach the working electrode [33]. Even though this strategy is simple and easy, one of its main drawbacks is the peak dispersion and band broadening due to the gap between the channel output and the electrode [34]. It is subdivided in two approaches: on-chip and off-chip [35].
- *In-channel.* In this configuration the WE is located inside the separation channel, because the potentiostat is electrically isolated. The benefit of this approach is the substantial improvement in plate height and peak symmetry as compared with the end-channel detection [36].
- *Off-channel.* A decoupler is placed in the separation channel ahead of the working electrode, and serves as a path to ground. The decoupler is usually made of palladium (Pd) or platinum (Pt), because of their capability of absorbing hydrogen gas bubbles, which are formed on its surface owing to the electrochemical reaction [37]. It has been demonstrated that this configuration reduces band broadening when compared with that implying the end-channel detection.

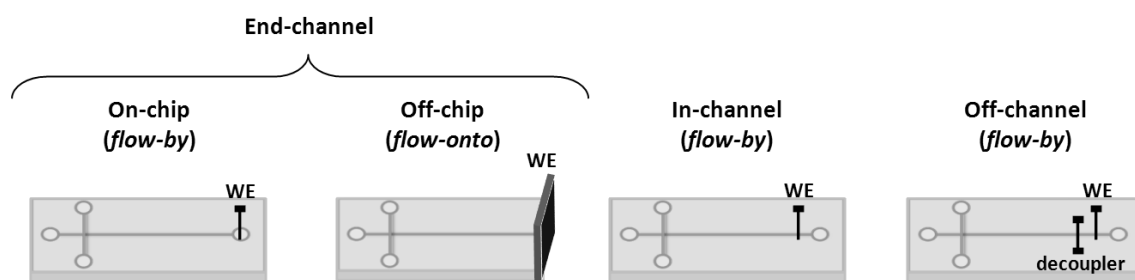


Figure 11. Classification of the microchip electrophoresis electrochemical detection in function of the working electrode (WE) location.

The success of this kind of devices is going to be also related to the material of the working electrode, whose choice is mainly determined by the redox behavior of the target analyte and the background current over the applied potential [8]. A lot of work has been done in the last decade with the aim of achieving more stable and sensitive detection systems [38-40]. For example, in case of organic molecules (catecholamines, phenols, aromatic amines, ...), carbon materials have proved to be the most adequate choice due to their large potential window, resistance to fouling, low background noise and favorable electron transfer [41].

2.3. Nanotechnological Approaches towards Improved Sensitivity

The discovery of novel materials, processes, and phenomena at the nanoscale opens up new opportunities for the development of innovative nanostructured materials, which can be endowed with unique nanostructures and properties. This nanomaterial science revolution has provided particles with virtually unlimited size and shape, including spherical, amorphous, aggregates, rods, tubes, cubes, triangles or cones. Their chemical composition can be just as different as their shape, consisting of polymers or copolymers, inorganic structures or metals and semiconductors [42]. Furthermore, new symmetrical organic structures have burst in the nanometer scale, the so-called carbon-based nanomaterials (fullerenes, carbon nanotubes and graphene, fibers ...) [43].

Very often, both shape and composition are going to determine the suitability of the nanoparticle for a particular purpose. The materials world, has an interest towards the preparation of materials with improved properties (mechanical, magnetic, optical, electrical, and a host of other depending on the application). This allows finding applications as varied as sunscreens and cosmetics, paints, tissue engineering, sensors, construction, energy, electronics, textile ... [44,45].

Carbon-based nanomaterials, and especially carbon nanotubes (CNTs), are an excellent choice to fulfill the need of better sensitivities in miniaturized electroanalytical devices due to their good electrical conductivity, low capacitance which arises from their one-dimensional nature, and the thickness of the electrochemical double layer, being comparable to nanotube diameter [46].

2.3.1. Carbon-based nanomaterials

Carbon-based nanomaterials can be defined as those in which the “nanocomponent” is pure carbon. If we defined a nanomaterial as that having at least one dimension smaller than 100 nm, then carbon-based nanomaterials can be classified in groups, depending on the number of dimensions in the nanometric scale (**Figure 12**) [47,48].

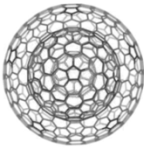
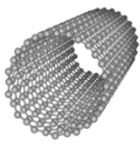
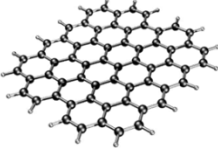
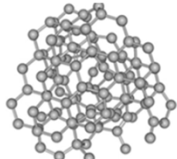
| | 0D | 1D | 2D | 0D |
|---------------------------------------|---|---|--|---|
| Dimensions at nanometric scale | All | One | Two | None |
| Structures | Nanodiamond Carbon onions Fullerenes | Nanotubes Nanofibers | Graphene | Amorphous carbon |
| |  |  |  |  |

Figure 12. Classification of the different carbon structures according to the number of dimensions on the nanometric scale.

Among all the available structures, special mention deserves carbon nanotubes (CNTs). On the basis of their unique open tubular structure, which favors fast ion and electron transfer [49], they have been broadly employed as electrodes with the aim of increasing their electrical properties [50].

2.3.1.1. Carbon nanotubes (CNTs)

A new era in carbon nanomaterials began in 1952 when Radushkevich and Lukyanovich first observed by transmission electron microscopy (TEM) carbon products in tubular form (carbon filaments) [51]. Then, in 1991 arise carbon nanotubes, which were first reported by Iijima *et al.* [52]. They can be described as sheets of graphene rolled up to make a tube. From the geometric point of view, there is a restriction regarding the tube diameter. Calculations have shown that tubular configuration is energetically less favorable beyond a diameter value of 2.5 nm [53], which causes that the commonly available CNTs have diameters ranging in 0.4-

2.5 nm. On the other hand, there is no such restriction related to nanotube length, which only depends on the specific conditions of the method employed at the synthesis. Taking into account the number of sheets, they can be classified in two main groups (**Figure 13**): single-wall carbon nanotubes, SWCNTs (a single sheet wrapped into a cylindrical tube) and multi-wall carbon nanotubes, MWCNTs (which comprise an array of concentric cylinders with diameters of 1.4-100 nm) [54].

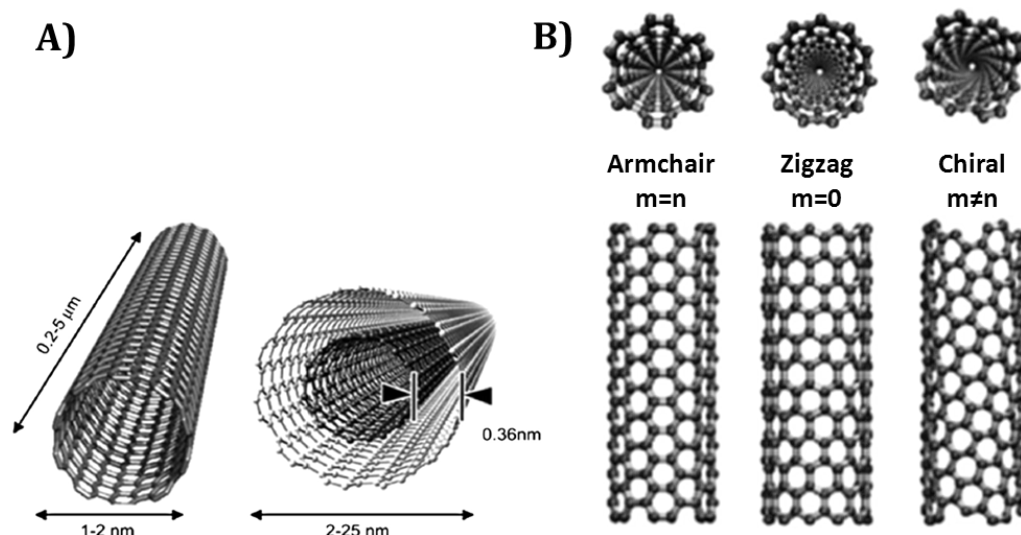


Figure 13. Diagrams of A) SWCNTs and MWCNTs with typical dimensions (length, width and separation distance), and B) the three main ways in which graphene sheet is rolled.

Another remarkable feature of these materials comes from the way in which the graphene sheet is rolled around the tube, which makes that the C=C bonds are no longer planar; this means that the hybridization of carbon atoms are no longer pure sp^2 (as in graphene), and with decreasing tube diameter, an increasing percentage of sp^3 character occurs. This is supposed to make the CNTs surface a bit more reactive than graphene, thereby inducing a unique versatile electronic behavior.

The electrical properties of nanotubes depend sensitively on the (m, n) indices, which represent the beginning and the end of a lattice vector in the graphene plane, and therefore on the diameter and chirality. Thus, for the structures represented in **Figure 13**, armchair tubes should be always of metallic nature, while zigzag and chiral should be semiconducting [55].

2.3.1.1.1. Functionalized carbon nanotubes

A great variety of carbon nanotubes derivatives can be obtained by their functionalization, which is based on the interaction between the active molecule and the nanotube carbon atoms. However, this is not a trivial task, since the carbon atoms on CNTs

walls are chemically stable (because of the aromatic nature of the bond), resulting on inert structures. Therefore, significant efforts have been directed towards developing methods to modify CNTs surface properties. Based on the reactivity of carbon nanotubes, the functionalization reactions can be divided in [47,56]:

- *Chemical functionalization.* Formation of covalent bonds between the functional group and the carbon atoms of the CNTs. This linkage can take place directly in the sidewalls of grown carbon nanotubes (sidewall functionalization), or by means of carboxylic groups and defects generated by the previously oxidized CNTs (defect functionalization). In the former, it is necessary to carry out a previous reaction using high reactive molecules (*e.g.* fluorine) and then replaced fluorine groups by carboxylic, amino and/or hydroxyl functions. In the latter, CNTs are first oxidized to generate oxygen-containing groups (hydroxyl, carbonyl and/or carboxylic) and then the reaction to form the covalent bond is performed (amidation, esterification, thiolation or silanization).
- *Physical functionalization.* This strategy is based on non-covalent interactions, mainly by van der Waals and Π - Π stacking forces between nanotube and molecule. Another procedure included in this group is the so-called endohedral method, in which pure elements (gold and silver), small molecules (metal oxides) or small proteins are inserted in the inner cavity of CNTs. This insertion often takes place at defect sites located at sidewalls or ends.

There are plenty of reasons which make carbon nanotubes functionalization an extremely important task (*e.g.* to achieve their solubility in common organic solvents and/or water [57], to improve the selectivity for target analytes in solid-phase extraction [58] or their behavior as drug delivery systems [59], to employ them in sensors [60] ...).

As a result of this interest, *electrochemical functionalization*, which involves the creation of active species from a precursor in the vicinity of a working electrode, has become an elegant tool for CNTs functionalization in a selective and controlled way. In this case the active species are formed because of charge transfer between the electrode (where the CNTs are located) and the precursor. This strategy is usually performed by applying a constant potential or current over an extended period of time, or even by successive complete voltammetric scans [61,62].

In the concrete case of CNTs *electrochemical oxidation*, consisting on the treatment of raw CNTs with strong oxidizing agents (H_2SO_4 , HNO_3 , HCl , NaOH ...) [63] under any of the above described conditions, nanotubes show carboxylic groups in the regions where the oxidative damage took place. The presence of oxygenated groups on carbon nanotubes is important for improving not only their solubility but also their electron transfer properties [64].

Otherwise, the synthesized CNTs usually contain carbonaceous impurities (e.g. amorphous carbon and carbon nanoparticles) and catalyst particles (e.g. transition metal catalysts and catalyst support), which often hinder the fully demonstration of the electronic properties of CNTs. Therefore, it is highly recommended that as-produced CNTs are purified before use, being the electrochemical oxidation a particularly efficient way to transform waste into valuable products [65].

2.3.1.1.2. Carbon nanotubes for electrochemical sensing

Because of the high electrochemically accessible CNTs surface area, combined with their high electronic properties, these materials are extremely attractive as electrodes. One of the main problems related with the employment of CNTs as working electrode material is their insolubility in conventional solvents, becoming essential their modification prior to use. To this end, different approaches have been proposed through the bibliography mainly based on CNTs dispersion [66] by sonication (applying ultrasound energy to agitate particles in a solution), calendaring processes (three roll mills which employ the shear force to mix, disperse or homogenize the material), ball milling (grinding method used to obtain extremely fine powder), stir (mixing method in which the dispersion results depend on the size and shape of a propeller), extrusion (twin screw rotate at high speed creating a high shear flow), etc. [56]. However, these methods have a serious drawback, since during the process, especially in case of sonication, a large number of defects are inevitably created on CNTs sidewalls, and in some cases, CNTs are even fragmented into smaller pieces. These damaging effects result in a disruption of the π electron system, which is detrimental to electrical transport properties, considering that the defect sites are the responsible of the electron transference. Sometimes the addition of surfactants and polymer as dispersing agents (substance added to a suspension to prevent particles settling or clumping) is quite helpful for achieving CNTs dispersion [67,68], although this alters CNTs intrinsic properties.

The challenge is thus, the incorporation of carbon nanotubes to the electrode surface without losing their electrical properties. Within this context, many efforts have been put forward to develop methods that are less harmful to the nanotube structure. This strategy is

based on *in situ* growth of CNTs on the electrode surface [69], mainly with two configurations: non-oriented (disordered or spaghetti) and oriented (forest or vertically aligned) [70]. With such route, CNTs with specific configurations can be employed as electrode material, avoiding tedious treatment procedures [71], in addition to be an ideal method for integrating electrochemical detection in miniaturized electroanalytical devices [72].

Particular attention deserves carbon nanotubes in oriented configuration, since the rate of electron transfer between the electrode surface and the redox couple has been shown to be dependent on the orientation of the nanotube, being almost 40 times faster through vertically aligned tubes than through randomly dispersed [73]. As reported Compton *et al.* the origin of these electrocatalytic properties is at the end of the tube and along the tube where defect sites exist, in which the electron transfer process is abnormally faster than that on the side walls of the nanotube [74].

2.3.1.1.3. Growth of carbon nanotubes

The most commonly used techniques in the last 20 years are arc discharge, laser ablation and chemical vapor deposition (CVD) [65,69], being the last one the most feasible and widespread synthesis method today. While the basic growth procedure is considered to be very closely related in most fabrication techniques, the exact mechanism are still the source of much debate [75]. As a rule, it consists on the catalytic decomposition of a volatile carbon source (C_nH_m) into carbon and hydrogen atoms, then hydrogen goes away, and carbon diffuses into metal particles until they become saturated. Finally, the as-diffused carbon precipitates and crystallizes (graphitization), which forming a cylinder under the right conditions (CNT) [76].

Depending on catalyst-substrate interaction the graphitization process will be different. Thus, the cylinder can be created either by "*base growth*" (catalyst strong attachment) or "*tip growth*" (catalyst weak attachment). In first case, the nanotube grows upwards from the metal particle that remain fixed on the substrate, whereas in second case, particles detach and move at the head of the growing nanotube, which stops when the metal is fully covered with excess carbon, ceasing its catalytic activity (**Figure 14**). It has been also observed that for the same source of carbon, catalyst and substrate both processes are viable thus, the growth mechanism is going to be mainly influenced by experimental conditions [77].

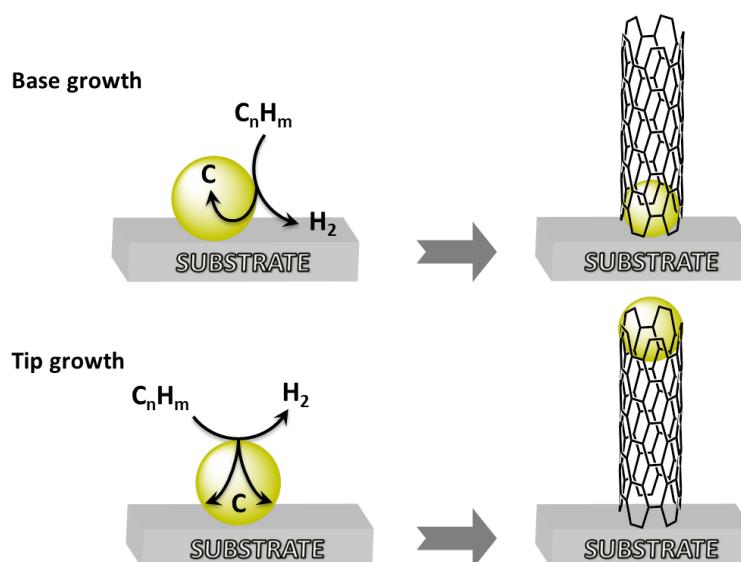


Figure 14. Growth modes of carbon nanotubes by chemical vapor deposition.

Some of the parameters involved in carbon nanotubes growth by CVD are: the temperature, gas composition/flow rate, and catalyst nature/size. The catalyst is a key factor that should be considered as it is going to decide not only the diameter of the tube but also the orientation. They are frequently nanometer-size particles obtained from the reduction of transition metals (Fe, Co, Ni, Ag, Au, Cu, Pd ...) or their alloys (Fe-Ni, Ni-Co, Cu-Cr, Ni-Mo, Pd-Cr-Pt ...) [78]. The most widespread are Fe, Co and Ni because: (i) the high carbon diffusion rate in these metals, and (ii) their high melting point and low vapor pressure, which offers a wide temperature window.

There are two main methods for preparing the catalyst: impregnating the substrate with a solution of a salt of the desired transition metal catalyst or evaporating it (sputtering) [79]. In both cases, the catalyst is then reduced to form the metal nanoparticles on which the CNTs are going to be grown. In addition, they can be classified in: homogeneous (carbon source and catalyst volatile) or heterogeneous (catalyst supported on the substrate), as well as pre-made (nanoparticles deposited on the substrate) or *in-situ* made (from organometallic compounds) [80].

REFERENCES

- [1] A. González Crevillén, M. Hervás, M.A. López, M.C. González, A. Escarpa. *Talanta* 74 (2007) 342-357.
- [2] P.J. Viskari, J.P. Landers. *Electrophoresis* 27 (2006) 1797-1810.
- [3] B.J. de Kort, G.J. de Jong, G.W. Somsen. *Anal. Chim. Acta* 766 (2013) 13-33.
- [4] F. Opekar, K. Stulík. *Electrophoresis* 32 (2011) 795-810.
- [5] J.J.P. Mark, R. Scholz, F.-M. Matysik. *J. Chromatogr. A* 1267 (2012) 45-64.
- [6] R.D. Oleschuck, D.J. Harrison. *Trac-Trend Anal. Chem.* 19 (2000) 379-388.
- [7] F. Kitagawa, K. Otsuka. *J. Pharmaceut. Biomed.* 55 (2011) 668-678.
- [8] A. Rios, A. Escarpa, B. Simonet. Chapter 6 in *Miniaturization of Analytical Systems: Principles, Designs, and Applications*. John Wiley & Sons, New York (2009) 213-261.
- [9] M. Ciobanu, J.P. Wilburn, M.L. Krim, D.E. Cliffel. Chapter 1 in *Handbook of Electrochemistry*. Elsevier, The Netherlands (2007) 1-28.
- [10] X. Xu, S. Zhang, H. Chen, J. Kong. *Talanta* 80 (2009) 8-18.
- [11] H. Kahlert. Chapter 11 in *Handbook of Reference Electrodes*. Springer-Verlag Berlin Heidelberg (2013) 289-305.
- [12] J. Wang. *Analytical Electrochemistry*. John Wiley & Sons, New York (2006) 67-112.
- [13] S. Laschi, I. Palchetti, M. Mascini. *Sens. Actuators B* 114 (2006) 460-465.
- [14] J.P. Metters, F. Tan, R.O. Kadara, C.E. Banks. *Anal. Methods* 4 (2012) 1272-1277.
- [15] L. Wang. *Electroanalysis* 17 (2005) 1341-1346.
- [16] J.-M. Zen, C.-C. Yang, A.S. Kumar. *Anal. Chim. Acta* 464 (2002) 229-235.
- [17] C.M.A. Brett, A.M.O. Brett. Chapter 7 in *Electrochemistry: Principles, Methods, and Applications*. Oxford University Press (1993) 129-149.
- [18] M.M.P.S. Neves, H.P.A. Nouws, C. Delerue-Matos. *J. Food Drug Anal.* 18 (2010) 353-357.
- [19] O. Domínguez Renedo, M.A. Alonso-Lomillo, M.J. Arcos Martínez. *Talanta* 73 (2007) 202-219.
- [20] D. Bellido-Milla, L.M. Cubillana-Aguilera, M.E. Kaoutit, M.P. Hernández-Artiga, J.L. Hidalgo-Hidalgo de Cisneros, I. Naranjo-Rodríguez, J.M. Palacios-Santander. *Anal. Bioanal. Chem.* 405 (2013) 3525-3539.
- [21] J. Wang, A.-N. Kawde, E. Sahlin. *Analyst* 125 (2000) 5-7.
- [22] J. Roeser, N.F.A. Alting, H.P. Permentier, A.P. Brunis, R. Bischoff. *Anal. Chem.* 85 (2013) 6626-6632.
- [23] V. Mirceski, S. Komorsky-Lovric, M. Lovric. Chapter 1 in *Square-Wave Voltammetry: Theory and Application*. Springer-Verlag Berlin Heidelberg (2007) 1-12.
- [24] S.P. Kounaves. Chapter 37 in *Handbook of Instrumental Techniques for Analytical Chemistry*. Prentice-Hall, New Jersey (1997) 709-725.

- [25] A.J. Bard, L.R. Faulkner. Chapter 5 in *Electrochemical Methods: Fundamentals and Applications*. John Wiley & Sons, New York (2001) 156-225.
- [26] C.M.A. Brett, A.M.O. Brett. Chapter 5 in *Electrochemistry: Principles, Methods, and Applications*. Oxford University Press, New York (1993) 82-102.
- [27] K. Stulik, C. Amatore, K. Holub, V. Marecek, W. Kutner. *Pure Appl. Chem.* 72 (2000) 1483-1492.
- [28] X.-J. Huang, A.M. O'Mahony, R.G. Compton. *Small* 7 (2009) 776-788.
- [29] D.W.M. Arrigan. *Analyst* 129 (2004) 1157-1165.
- [30] S.M. Oja, M. Wood, B. Zhang. *Anal. Chem.* 85 (2013) 473-486.
- [31] J. Wang. *Talanta* 56 (2002) 223-231.
- [32] D.J. Fischer, M.K. Hulvey, A.R. Regel, S.M. Lunte. *Electrophoresis* 30 (2009) 3324-3333.
- [33] X. Huang, R.N. Zare, S. Sloss, A.G. Ewing. *Anal. Chem.* 63 (1991) 189-192.
- [34] R.S. Martin, K.L. Ratzlaff, B.H. Huynh, S.M. Lunte. *Anal. Chem.* 74 (2002) 1136-1143.
- [35] W.R. Vandaveer IV, S.A. Padas-Farmer, D.J. Fischer, C.N. Frankenfeld, S.M. Lunte. *Electrophoresis* 25 (2004) 3528-3549.
- [36] D.B. Gunasekara, M.K. Hulvey, S.M. Lunte. *Electrophoresis* 32 (2011) 832-837.
- [37] M.H. Ghanim, M.Z. Abdullah. *Talanta* 85 (2011) 28-34.
- [38] M. Pumera. *Electrophoresis* 28 (2007) 2113-2124.
- [39] M. Pumera. *Electrophoresis* 27 (2006) 244-256.
- [40] C.A. Croushore, J.V. Sweedler. *Lab Chip* 13 (2013) 1666-1676.
- [41] W.R. Vandaveer, S.A. Padas-Farmer, D.J. Fischer, C.N. Frankenfeld, S.M. Lunte. *Electrophoresis* 25 (2004) 3528-3549.
- [42] C.M. Welch, R.G. Compton. *Anal. Bioanal. Chem.* 384 (2006) 601-619.
- [43] G.T. Hermanson. Chapter 14 in *Bioconjugate Techniques*. Elsevier (1996) 582-626.
- [44] M.G. Lines. *J. Alloy. Compd.* 449 (2008) 242-245.
- [45] K. Arivalagan, S. Ravichandran, K. Rangasamy, E. Karthikeyan. *Int. J. Chem. Tech. Res.* 3 (2011) 534-538.
- [46] S. Rosenblatt, Y. Yaish, J. Park, J. Gore, V. Sazonova, P.L. McEuen. *Nano Lett.* 2 (2002) 869-872.
- [47] J.L. Delgado, M.A. Herranz, N. Martín. *J. Mater. Chem.* 18 (2008) 1417-1426.
- [48] H. Jiang, P.S. Lee, C. Li. *Energy Environ. Sci.* 6 (2013) 41-53.
- [49] G. Lota, K. Fic, E. Frackowiak. *Energy Environ. Sci.* 4 (2011) 1592-1605.
- [50] P. Yañez-Sedeño, J. Riu, J.M. Pingarron, F.X. Rius. *Trac-Trend Anal. Chem.* 29 (2010) 939-953.
- [51] L.V. Radushkevich, V.M. Lukyanovich. *Soviet. J. Phys. Chem.* 26 (1952) 88-95.
- [52] S. Iijima. *Nature* 354 (1991) 56-58.
- [53] J. Tersoff, R.S. Ruoff. *Phys. Rev. Lett.* 73 (1994) 676-679.

- [54] N. Tagmatarchis, M. Prato. *Pure Appl. Chem.* 77 (2005) 1675-1684.
- [55] H. Dai. *Surf. Sci.* 500 (2002) 218-241.
- [56] P.-C. Ma, N.A. Siddiqui, G. Marom, J.-K. Kim. *Compos. Part A-Appl. S.* 41 (2010) 1345-1367.
- [57] Y.-P. Sun, K. Fu, Y. Lin, W. Huang. *Acc. Chem. Res.* 35 (2002) 1096-1104.
- [58] C.H. Latorre, J.A. Méndez, J.B. García, S.G. Martín, R.M.P. Crecente. *Anal. Chim Acta* 749 (2012) 16-35.
- [59] G. Pastorin. *Pharm. Res.* 26 (2009) 746-769.
- [60] I. Capek. *Adv. Colloid Interfac.* 150 (2009) 63-89.
- [61] J.L. Bahr, J. Yang, D.V. Kosynkin, M.J. Bronikowski, R.E. Smalley, J.M. Tour. *J. Am. Chem. Soc.* 123 (2001) 6536-6542.
- [62] K. Balasubramanian, M. Burghard. *J. Mater. Chem.* 18 (2008) 3071-3083.
- [63] J. Zhang, H. Zou, Q. Qing, Y. Yang, Q. Li, Z. Liu, X. Guo, Z. Du. *J. Phys. Chem. B* 107 (2003) 3712-3718.
- [64] A. Doepke, C. Han, T. Back, W.D. Cho, D.D. Dionysiou, V. Shanov, H.B. Halsall, W.R. Heineman. *Electroanalysis* 24 (2012) 1501-1508.
- [65] Q. Zhang, J.-Q. Huang, W.-Z. Qian, Y.-Y. Zhang, F. Wei. *Small* 9 (2013) 1237-1265.
- [66] T. Premkumar, R. Mezzenga, K.E. Geckeler. *Small* 8 (2012) 1299-1313.
- [67] E.E. Tkalya, M. Ghislandi, G. de With, C.E. Koning. *Curr. Opin. Colloid In.* 17 (2012) 225-232.
- [68] Y.Y. Huang, E.M. Terentjev. *Polymers* 4 (2012) 275-295.
- [69] J.P. Metters, C.E. Banks. *Vacuum* 86 (2012) 507-519.
- [70] A. Merkoçi, M. Pumera, X. Ilopis, B. Pérez, M. del Valle, S. Alegret. *Trac-Trend Anal. Chem.* 24 (2005) 826-838.
- [71] G. Atthipalli, Y. Tang, A. Star, J.L. Gray. *Thin Solid Films* 520 (2011) 1651-1655.
- [72] R.H. Baughman, A.A. Zakhidov, W.A. de Heer. *Science* 297 (2002) 787-792.
- [73] J.J. Gooding, A. Chou, J. Liu, D. Losic, J.G. Shaper, D.B. Hibbert. *Electrochem. Commun.* 9 (2007) 1677-1683.
- [74] C.E. Banks, R.R. Moore, T.J. Davies, R.G. Compton. *Chem. Commun.* 16 (2004) 1804-1805.
- [75] M. Monthieux, P. Serp, E. Flahaut, M. Razafinimanana, C. Laurent, A. Peigney, W. Basca, J.-M. Broto. Chapter 3 in *Springer Handbook of Nanomaterials*. Springer-Verlag Berlin Heidelberg (2010) 47-101.
- [76] S.B. Sinnott, R. Andrews, D. Qian, A.M. Rao, Z. Mao, E.C. Dickey, F. Derbyshire. *Chem. Phys. Lett.* 315 (1999) 25-30.
- [77] M. Kumar. Chapter 8 in *Carbon Nanotubes-Synthesis, Characterization, Applications*. InTech, China (2011) 147-170. Available from: <http://www.intechopen.com/books/carbon-nanotubes-synthesis-characterization-applications/carbonnanotube-synthesis-and-growth-mechanism>.
- [78] X. Qi, C. Qin, W. Zhong, C. Au, X. Ye, Y. Du. *Materials* 3 (2010) 4142-4174.

[79] A.-C. Dupuis. Prog. Mater. Sci. 50 (2005) 929-961.

[80] A. Kukovecz, G. Kozma, Z. Kónya. Chapter 5 in Springer Handbook of Nanomaterials (2013) 147-169.

3. Materials for Miniaturized Analytical Devices

During the last years microfluidic chips have been gaining attention, leading to the development of a wide and diverse range of applications (genomic and proteomic [1,2], drug analysis [3], environmental [4], food [5] etc.). However, selecting the most suitable material for a specific application is not a trivial task. There are several considerations that need to be carefully assessed in order to know if the chosen material is going to be a viable substrate [6]:

- *Support a stable EOF.* If the electroosmotic flow is not stable, there could be changes in analyte mobility. This leads to irreproducible results, making peak identification by migration time difficult, and affecting separation efficiencies.
- *Optical transmission.* This is only applicable in case of optical detection systems in which the substrate must be optically transparent at monitoring wavelengths.
- *Easily micromachined.* Microfluidic devices require the fabrication of channels with micrometer dimensions. Thus, the chosen material should provide easy access to such structures with high reproducibility.
- *Surface chemistry.* In many applications the material surface need to be altered with the aim of modifying/suppressing the EOF or improving separation efficiencies. Therefore, it is very useful that it has well established, stable and diverse modification chemistries.
- *Compatibility with the running buffer.* Molecules separation sometimes can require the employment of organic solvents and therefore, the material must not swell, crack, or dissolve in the running buffer.
- *Good thermal/electrical properties.* To reduce the Joule heating when high voltages are needed.

As **Table 4** exhibits, the materials employed in microfluidic devices fabrication can be organized into three broad categories: inorganic, polymeric (divided into elastomers, thermoplastics and thermosets), and paper [7]. It is important to consider the advantages and disadvantages of each.

Table 4. Classification of materials employed in miniaturized analytical devices fabrication and their properties.

| | MATERIALS | | | | | |
|----------------------------------|--------------|-------|------------------|----------------|-------------|----------|
| | Inorganic | | Polymers | | | Paper |
| | Silicon | Glass | Elastomers | Thermoplastics | Thermosets | |
| Possible geometries | Limited (2D) | | Many (2D and 3D) | | | Lots |
| Mechanical stability | High | | Very low | Low | High | High |
| Thermal stability | High | | Low | Low | Medium | Medium |
| Acid stability | High | | High | High | High | High |
| Organic solvent stability | High | | Low | Low | Medium-high | High |
| Alkaline stability | Limited | High | High | High | High | High |
| Optical transparency | No | High | High | High | Limited | No |
| EOF mobility | Good | | Good | Low | Good | No |
| Material price | Medium-high | | Low | Low | Medium | Very low |

3.1. Inorganic Materials

In the early days microfluidic devices were based on inorganic materials, such as silicon, glass or quartz, in which microchannel networks were etched adopting those well-established methodologies employed in microelectronics industry, such as photolithography, and dry or wet etching [8].

Among these, *silicon* was used as basic material for fabricating microfluidic devices because it possesses good thermal conductivity and is resistant to high temperatures; therefore, it is suitable for applications requiring a relatively high operating temperature, such as for polymerase chain reaction (PCR) and for bioreactors [9]. Nevertheless, it is not transparent to visible and UV light (needed in case of optical detection), and its breakdown voltage is relatively low (≈ 500 V) thereby, it is seldom used. In comparison, *quartz* wafer has superior optical properties but, it is not widely used due to its high cost and difficult fabrication.

In contrast to silicon and quartz, *glass* substrates are less expensive, optically transparent throughout the visible spectrum, and not electrically conductive. Moreover, they have a well understood surface chemistry (allowing easy modification), good mechanical stability, and show an excellent compatibility with organic solvents. Therefore, glass seems to

be an ideal substrate for ME fabrication. However, glass-based microfluidic devices are usually fabricated by wet etching, which limits the dimensions of achieved microstructures, is expensive and time-consuming. Even though glass has inherent drawbacks, it has been the major inorganic material used in microfluidic chips fabrication [10].

To overcome today challenges (add novel functionalities or processing capability) new materials are incessantly being investigated. Thus, ceramic-based microfluidics, especially low-temperature cofired ceramic (LTCC), have been proposed as an alternative to other inorganic materials, as they bring faster processing times and allow easy creation of 3D architectures [11].

3.2. Polymers

Polymers are long-chain organic molecules with a carbon backbone, whose chemical properties (and names) are defined by functional groups attached. They have gained significant attraction after Whitesides *et al.* demonstrated the potential of poly(dimethyl siloxane) (PDMS) for fabricating microfluidics by employing soft lithography technique [12]. Polymer-based microchips are easy to fabricate (channels can be sealed thermally or by using adhesives), and their use reduces the time, complexity, and cost of prototyping and manufacturing [13]. Notwithstanding, they have some disadvantages compared with glass wafers, since more care must be taken to control their surface chemistry, and they are often incompatible with organic solvents and high temperatures (**Table 4**).

There are various methods of fabrication (**Figure 15**), usually based on three families of techniques: polymer micromachining/laser ablation (using direct writing processes such as drilling, sawing, laser ...), injection molding/hot embossing (involves the high pressure injection of melted thermoplastic pellets into a heated master mold), and polymer casting (also known as soft lithography, and based on the replica of a mold) [14,15].

3.2.1. Elastomers

Among these polymers, PDMS is an excellent material for the fabrication of microfluidic systems because of its desirable characteristics, such as inexpensive, flexible, non-toxic, and optically transparent (down to 230 nm). Moreover, it can be sealed reversibly to itself (and a range of other materials) by van der Waals molecular interactions with the surface, or it can be sealed irreversibly (after exposure to air plasma) by formation of covalent bonds [16]. Even though it is valuable for rapid prototyping, and commonly used in microfluidic applications,

PDMS is a hydrophobic surface, which can show nonspecific adsorption of proteins and other molecules, poor wettability with aqueous solutions, formation of bubbles and, in general, commercially avoided [17]. Thus, hybrid PDMS/glass microchips are commonly employed in the literature to overcome these drawbacks [18].

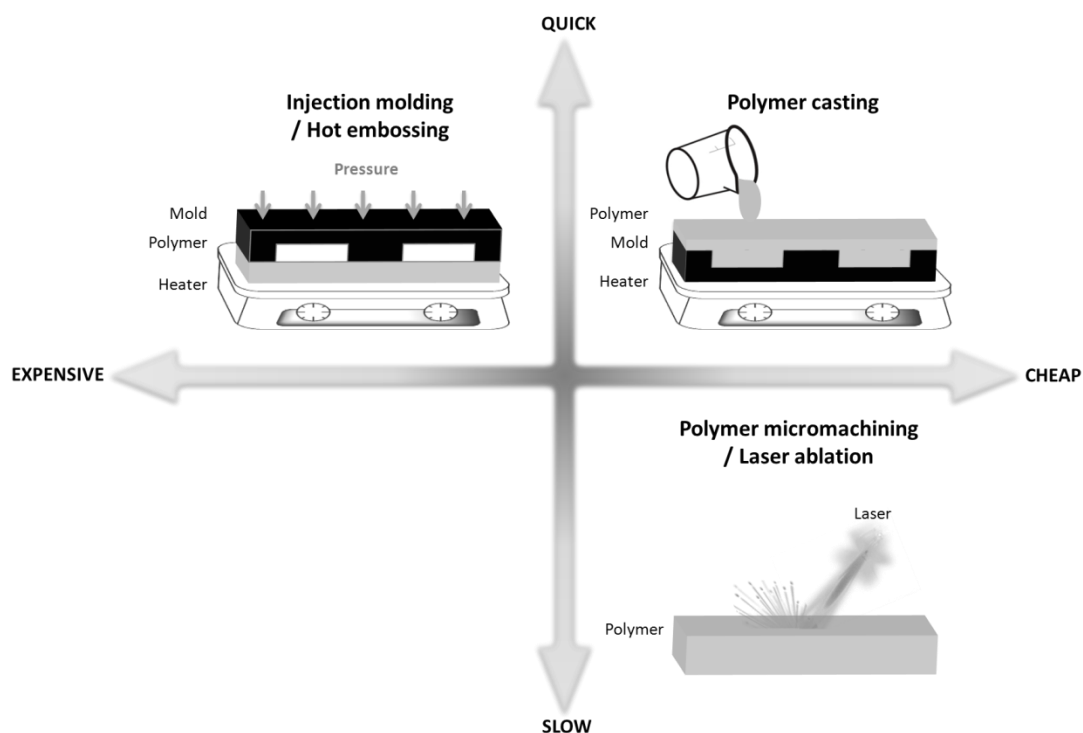


Figure 15. Fabrication techniques for polymer-based microfluidic devices.

3.2.2. Thermoplastics

Thermoplastics are densely cross-linked polymers that are moldable when heated to their glass transition temperature but retain their shape when cooled. These kinds of materials have been investigated as an alternative solution to the fabrication of disposable ME for their durability, optical transparency, and stiffness compared with elastomers [19]. To date, there are a huge variety of these polymers, including poly(methyl methacrylate) (PMMA), polystyrene (PS), polycarbonate (PC), polyethylene (PE), cyclic-olefin copolymer (COC), etc [20].

Early developments in thermoplastic microfluidic systems were largely focused on the use of PC and PMMA due to their wide availability, high optical transmission in the visible wavelengths, and well-characterized molding parameters [21,22]. However, special care has to be taken when dealing with these materials for separation purposes because they may be deteriorated by organic solvents. To overcome this problem, COC [23] or fluoro-polymers (like

fluorinated ethylene-propylene, FEP) [24] have emerged as highly attractive materials, which allow the fabrication of cost-effective and solvent resistant devices.

3.2.3. Thermosets

Thermoset or duroplastics are heavily cross-linked polymers produced when heated molecules chemically interact and form a permanent three-dimensional network. If the curing process has taken place once, the polymer remains stiff even if reheated, as it involves an irreversible chemical reaction. In principle they cannot be bonded through thermal pressure, solvents or laser because their chains cannot diffuse into foreign material to get entangled [25]. Typical examples of these polymers are bakelite, epoxy resins, polyimide (Kapton®) into others.

Epoxy-based photoresists, like SU-8, has shown to be a very suitable material for ME production owing to its capability of achieving layers of few hundred microns by spin-coating and being stable against many acids, bases and solvents [26-28].

Recently, thermoset polyester (TPE), formed by the polymerization of polyester and styrene through UV or heat [29], was explored proven to be a very promising material because it merges ease fabrication and cost effectiveness of PDMS, with higher separation efficiencies and increased stability [30].

3.3. Paper

Filter paper is a well-known material as it has been commonly used for chromatography and filtration purposes [31]. Nevertheless, with the recent interest in the development of point-of-care (POC) devices, which perform the analysis at or near the site where the patient is located, paper has attracted again the attention of researchers in order to develop paper-based analytical devices (μ PADs). These systems combine some of the capabilities of conventional microfluidic devices with the simplicity of diagnostic strip tests. Moreover, they should meet the ASSURED criteria, i.e. Affordable by those at risk of infection, Sensitive (few false-negatives), Specific (few false-positives), User-friendly (simple to perform and requiring minimal training), Rapid (to enable treatment at first visit) and Robust (not require refrigerated storage), Equipment-free, and Deliverable to end-users [32].

When there is the need of developing new microfluidic platforms, the choice of an adequate material is the first issue to consider. Thus, paper is an ideal candidate to provide these near zero-cost devices. As substrate, paper is thin, lightweight, available in a wide range

of thicknesses and easy to store and transport, disposable, inexpensive, biocompatible, easy to modify and pattern by the existing fabrication technologies, and is available with a huge variety of properties [33]. Following this trend, other cheap materials have been recently introduced, such as cotton yarn and thread [34,35], cloth [36,37] or transparency sheets [38].

There are several techniques reported in the literature for the fabrication of these devices [39], and they are summarized in **Table 5**. The fundamental principle underlying them is to pattern hydrophobic channels, by which solutions are moved. In case of paper, thread and cloth the flow is mainly caused by capillarity and evaporation (instead of external and/or complex pumping systems) while, for transparency it is necessary an electrokinetic pumping of solutions [40].

In general, the bulk of μ PADs are based on colorimetric assays, which provide a “yes/no” detection of analytes [41,42]. This strategy offers several advantages (portability, affordability and simplicity), but it is normally not capable of doing quantitative analysis [43]. On the other hand, highly selective and sensitive detection is possible by employing electrochemical techniques [44,45]. Notice that electrochemical measurements performed on paper differ from those in free solution owing to the presence of the cellulose matrix, which blocks part of the electrode surface. In contrast, the sensitivity can be increased due to the capillarity of paper, which can drive the transport of analytes over the electrode surface [46].

There are several examples of successful electroanalytical systems already use [47,48]. Even though, research on paper-based microfluidic devices is still at an early stage and significant efforts will be needed in this field with the aim of providing point-of-care devices for a wide range of applications.

Table 5. Common fabrication techniques

| FABRICATION TECHNIQUES | | | | |
|-------------------------|------------|--------------|------------------------|------|
| | Resolution | Cost | High-throughput method | Ref |
| Cutting | Very low | Very low | No | [49] |
| Drawing | Very low | Very low | No | [50] |
| Plotting | Low | Low | Yes | [51] |
| Wax | High | Low | Yes | [52] |
| Ink-jet | High | Low-moderate | Yes | [53] |
| Toner | High | Low-moderate | Yes | [40] |
| Printing | Moderate | Very low | Yes | [54] |
| Flexographic | High | Moderate | Yes | [55] |
| Transfer | Moderate | Low | Yes | [56] |
| Photolithography | High | Moderate | Yes | [57] |

REFERENCES

- [1] G.H.W. Sanders, A. Manz. *Trac-Trend. Anal. Chem.* 19 (2000) 364-378.
- [2] S. Liu, A. Guttman. *Trac-Trend. Anal. Chem.* 23 (2004) 422-431.
- [3] E. Al-Hetlani. *Electrophoresis* 34 (2013) 1262-1272.
- [4] L. Marle, G.M. Greenway. *Trac-Trend. Anal. Chem.* 24 (2005) 795-802.
- [5] A. Martín, D. Vilela, A. Escarpa. *Electrophoresis* 33 (2012) 2212-2227.
- [6] H. Shadpour, H. Musyimi, J. Chen, S.A. Soper. *J. Chromatogr. A* 1111 (2006) 238-251.
- [7] P.N. Nge, C.I. Rogers, A.T. Woolley. *Chem. Rev.* 113 (2013) 2550-2583.
- [8] P. Abgrall, A.-M. Gué. *J. Micromech. Microeng.* 17 (2007) R15-R19.
- [9] E. Menegatti, D. Berardi, M. Messina, I. Ferrante, O. Giachino, B. Spagnolo, G. Restagno, L. Cognolato, D. Roccatello. *Autoimmun. Rev.* 12 (2013) 814-820.
- [10] F. Shang, E. Guihen, J.D. Glennon. *Electrophoresis* 33 (2012) 105-116.
- [11] A. Vasudev, A. Kaushik, K. Jones, S. Bhansali. *Microfluid. Nanofluid.* 14 (2013) 683-702.
- [12] J.R. Anderson, D.T. Chiu, R.J. Jackman, O. Cherniavskaya, J.C. McDonald, H. Wu, S.H. Whitesides, G.M. Whitesides. *Anal. Chem.* 72 (2000) 3158-3164.
- [13] J.C. McDonald, G.M. Whitesides. *Accounts Chem. Res.* 35 (2002) 491-499.
- [14] A. de Mello. *Lab Chip* 2 (2002) 31N-36N.
- [15] E. Sollier, C. Murray, P. Maoddi, D. Di Carlo. *Lab Chip* 11 (2011) 3752-3765.
- [16] J.C. McDonald, D.C. Duffy, J.R. Anderson, D.T. Chiu, H. Wu, O.J.A. Schueller, G.M. Whitesides. *Electrophoresis* 21 (2000) 27-40.
- [17] C.-C. Lin, J.-H. Wang, H.-W. Wu, G.-B. Lee. *JALA* 15 (2010) 253-274.
- [18] C.W. Beh, W. Zhou, T.-W. Wang. *Lab Chip* 20 (2012) 4120-4127.
- [19] C.-W. Tsao, D.L. De Voe. *Microfluid. Nanofluid.* 6 (2009) 1-16.
- [20] K. Liu, Z.H. Fan. *Analyst* 136 (2011) 1288-1297.
- [21] Y. Chen, L. Zhang, G. Chen. *Electrophoresis* 29 (2008) 1801-1814.
- [22] M.T. Koesdjojo, C.R. Koch, V.T. Remcho. *Anal. Chem.* 81 (2009) 1652-1659.
- [23] Y. Ladner, G. Crétier, K. Faure. *Electrophoresis* 33 (2012) 3087-3094.
- [24] W.H. Grover, M.G. von Muhlen, S.R. Manalis. *Lab Chip* 8 (2008) 913-918.
- [25] H. Becker, C. Gärtner. *Anal. Bioanal. Chem.* 390 (2008) 89-111.
- [26] P. Abgrall, V. Conedera, H. Camon, A.-M. Gue, N.-T. Nguyen. *Electrophoresis* 28 (2007) 4539-4551.
- [27] N. Nordman, T. Sikanen, M.-E. Moilanen, S. Aura, T. Kotihao, S. Franssila, R. Kostianen. *J. Chromatogr. A* 1218 (2011) 739-745.
- [28] R.S. Lima, P. Augusto, G.C. Leao, A.M. Monteiro, M.H. de Oliveira Piazzetta, A.L. Gobbi, L.H. Mazo, E. Carrilho. *Electrophoresis* (2013). DOI: 10.1002/elps.201300167.

- [29] G.S. Fiorini, G.D.M. Jeffries, D.S.W. Lim, C.L. Kuyper, D.T. Chiu. *Lab. Chip* 3 (2003) 158-163.
- [30] J.A. Vickers, B.M. Dressen, M.C. Weston, K. Boonsong, O. Chailapakul, D.M. Cropek, C.S. Henry. *Electrophoresis* 28 (2007) 1123-1129.
- [31] Y.-Q. Huang, J.-Q. You, J. Zhang, W. Sun, L. Ding, Y.-Q. Feng. *J. Chromatogr. A* 1218 (2011) 7371-7376.
- [32] D. Mabey, R.W. Peeling, A. Ustianowsky, M.D. Perkins. *Nat. Rev.* 2 (2004) 231-240.
- [33] A.W. Martinez, S.T. Phillips, E.M. Carrilho, G.M. Whitesides. *Anal. Chem.* 82 (2010) 3-10.
- [34] M. Reches, K.A. Mirica, R. Dasgupta, M.D. Dickey, M.J. Butte, G.M. Whitesides. *ACS Appl. Mater. Inter.* 2 (2010) 1722-1728.
- [35] G. Zhou, X. mao, D. Juncker. *Anal. Chem.* 84 (2012) 7736-7743.
- [36] A. Nilghaz, D.H.B. Wicaksono, D. Gustiono, F.A.A. Majid, E. Supriyanto, M.R.A. Kadir. *Lab Chip* 12 (2012) 209-218.
- [37] F. Vatansever, R. Burtovyy, B. Zdyrko, K. Ramaratnam, T. Andruk, S. Minko, J.R. Owens, K.G. Kornev, I. Luzinov. *ACS Appl. Mater. Inter.* 4 (2012) 4541-4548.
- [38] B.H.-P. Cheong, V. Diep, T. Wah Ng, O.W. Liew. *Anal. Biochem.* 422 (2012) 39-45.
- [39] X. Li, D.R. Ballerini, W. Shen. *Biomicrofluidics* 6 (2012) 011301-13.
- [40] E.F.M. Gabriel, C.L. do Lago, A.L. Gobbi, E. Carrilho, W.K.T. Coltro. *Electrophoresis* 34 (2013) 2169-2176.
- [41] W. Dungchai, O. Chailapakul, C.S. Henry. *Anal. Chim. Acta* 674 (2010) 227-233.
- [42] A. Apilux, W. Siangproh, N. Praphairaksit, O. Chailapakul. *Talanta* 97 (2012) 388-394.
- [43] Y. Liu, Y. Sun, K. Sun, L. Song, X. Jiang. *J. Mater. Chem.* 20 (2010) 7305-7311.
- [44] W. Dungchai, O. Chailapakul, C.S. Henry. *Anal. Chem.* 81 (2009) 5821-5826.
- [45] M. Santhiago, J.B. Wydallis, L.T. Kubota, C.S. Henry. *Anal. Chem.* 85 (2013) 5233-5239.
- [46] E.J. Maxwell, A.D. Mazzeo, G.M. Whitesides. *MRS Bulletin* 38 (2013) 309-314.
- [47] Z.H. Nie, F. Deiss, X.Y. Liu, O. Akbulut, G.M. Whitesides. *Lab Chip* 10 (2010) 3163-3169.
- [48] J.L. Delaney, E.H. Doeven, A.J. Harsant, C.F. Hogan. *Anal. Chim. Acta* 790 (2013) 56-60.
- [49] W. Wang, W.-Y. Wua, W. Wang, J.-J. Zhu. *J. Chromatogr. A* 1217 (2010) 3896-3899.
- [50] A. Russo, B.Y. Ahn, J.J. Adams, E.B. Duoss, J.T. Bernhard, J.A. Lewis. *Adv. Mater.* 23 (2011) 3426-3430.
- [51] D.A. Bruzewicz, M. Reches, G.M. Whitesides. *Anal. Chem.* 80 (2008) 3387-3392.
- [52] E. Carrilho, A.W. Martinez, G.M. Whitesides. *Anal. Chem.* 81 (2009) 7091-7095.
- [53] X. Li, J. Tian, G. Garnier, W. Shen. *Colloid. Surface. B* 76 (2010) 564-570.
- [54] S. Wang, L. Ge, X. Song, J. Yu, S. Ge, J. Huang, F. Zeng. *Biosens. Bioelectron.* 31 (2012) 212-218.
- [55] J. Olkkonen, K. Lehtinen, T. Erho. *Anal. Chem.* 82 (2010) 10246-10250.
- [56] Y. Lu, B. Lin, J. Qin. *Anal. Chem.* 83 (2011) 1830-1835.

[57] A.W. Martinez, S.T. Phillips, M.J. Butte, G.M. Whitesides. *Angew. Chem. Int. Ed.* 46 (2007) 1318–1320.

4. Towards Improved Separation Efficiency: The Role of the Surface

In capillary electrophoresis, it is well known that the performance of electrophoretic separations can be remarkably enhanced by the appropriate surface modification. Thus, capillary coatings have been widespread applied with the aim of controlling the electroosmotic flow [1] and for the suppression of the analyte-wall interaction [2]. Therefore, the manipulation of surface properties is going to be even more important in miniaturized analytical devices, especially in microfluidic chips, for several reasons [3]:

- In microfluidic devices both the precision and a robust injection process are of great importance. These rely on a controlled EOF to ensure a reproducible sample plug.
- The limited length of the microfluidic device separation channel compared with the capillaries employed in conventional CE makes surface coatings essential to increase separation efficiencies and resolution.

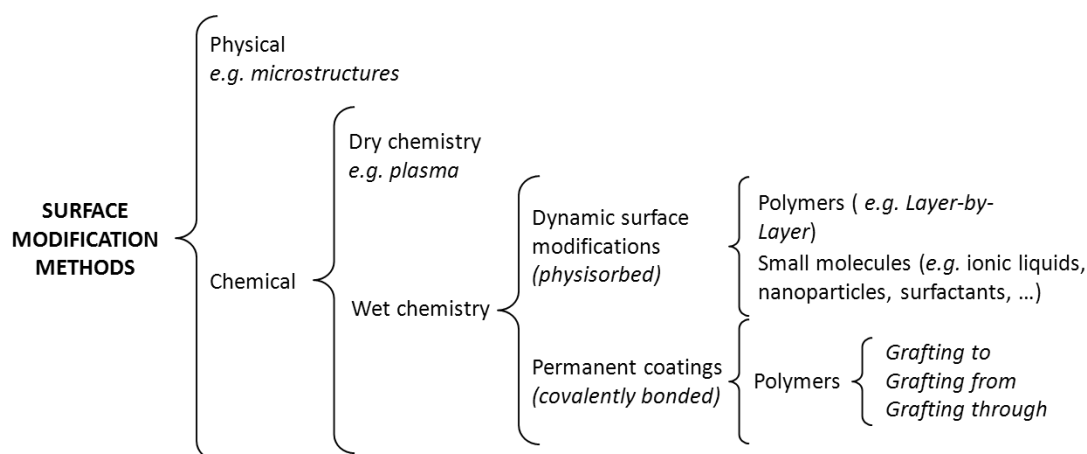


Figure 16. Classification of the surface modification methods for microfluidic devices.

Surface modification methods can be classified, depending on how the process affects the surface, in two broad categories: physical and chemical. In the former case, while the chemical composition of the surface is not altered, physical state of the surface is modified [4,5]. This is often carried out by the use of lasers, temperature, ion beams ... [6]. In the latter case, a change in the chemistry of the surface is introduced, which provides a layer with different properties and surface charge compared to the bulk material.

The methods for *chemical modification* can be classified into: dry (by using reactive plasmas) and wet processes (rely on the principles of organic/inorganic chemistry for the formation of new surface chemical functionalities). Among dry methods, the use of reactive

plasmas (air, oxygen, ammonia, argon ...) has been gaining popularity, most likely due to its compatibility with microfabrication techniques. On the other hand, two main approaches can be found based on the attachment of the coating to the capillary wall surface: dynamic coatings (physisorbed) and permanent coatings (covalently bonded) [3]. In permanent coatings, chemical compounds (often polymers) are covalently bound to surface functional groups (*via* cross-linking, sol-gel chemistry, silanization ...) [7], while in dynamic they are strongly adsorbed on the surface. Dynamic modifications are characterized by being a reversible process, which can be accomplished by rinsing with a solution containing the modifier prior the analysis or by adding the modifier to the background solution or the sample. Chemical modifications by wet chemistry are going to be discussed in more detail, because this has been the approach chosen for the development of this Thesis. A more deeply description of the common modifiers for microfluidic chips can be found in the book chapter included also in this memory.

4.1. Dynamic Coatings

Dynamic wall modifications are attractive methods because they are experimentally ease to carry out, and they allow to overcome the common problem of achieving a homogeneous capillary wall chemical derivatization. However, one of the main drawbacks comes from the lack of robustness of the coating layer, due to the weak interactions between the surface and the modifier.

A large variety of natural and synthetic (charged and neutral) **polymers** have been tested, and various coating strategies have been developed in the pursuit of a better dynamic coating [8,9]. The polymer physisorption can be described as a reversible process based on their self-assembly on the capillary wall. Due to its versatility and simplicity, layer-by-layer (**Figure 19**) has become a particularly attractive technique to improve the surface functional properties, which involves the consecutive adsorption of oppositely charged polyelectrolytes creating multilayers [10]. When a polyelectrolyte multilayer is employed, two are the main parameters affecting the resolution and peak efficiencies of analytes: thickness (the number of layers) and charge (it determines the direction and magnitude of the EOF). In general, it is required the deposition of more than one layer to control the EOF magnitude and direction in microfluidic systems [11]. However, Sui *et al.* demonstrate that this can be achieved employing only a single polyelectrolyte layer [12].

Neutral polymers are more frequently employed as sieving matrix in order to avoid analyte-wall electrostatic interactions [13], while charged polymers are developed for specific problems, such as faster separations, reversed EOF, and enhanced separation of complex analyte mixtures [14]. The efficiency of the dynamic coating is going to be determined by the robustness of binding to the capillary wall surface as well as pH, buffer solution and analyte's nature. For instance, poly(vinyl alcohol)-based polymers bind more strongly to glass surfaces than other polymers like cellulose derivatives. Thus, it is not easily washed off, providing a robust and stable coating.

Small molecule additives are able to reduce protein adsorption, either by providing electrostatic shielding between the cationic protein and anionic capillary wall, or by reducing the effective surface charge due to a molecule-negatively charged surface association. Among the most common small molecule additives are amines [15], and surfactants [16], while nanoparticles (large surface area-to-volume ratio particles, ideal for low mass-transfer process) [17,18] and ionic liquids (water-miscible and high-conductive molten salts at room temperature with synergistic effects with surfactants) [19] arise as novel approaches.

For their capability of interact with deprotonated silanol groups, *amines* are the more widespread small molecule employed for surface modification. The behavior of these species is determined by the number of free amine groups (as they increase inhibit better the protein adsorption). Thus, monoamines are poor preventers of this effect, while polyamines offer almost a total inhibition [20].

Surfactants (amphiphilic molecules with a hydrophobic tail and a hydrophilic head group) are a special class of small molecule additives. When they are in solution, and their concentration is greater than the critical micelle concentration (CMC), free monomers are aggregated to each other in order to minimize the repulsive interaction between hydrocarbon chains and water. These aggregates can be classified in bilayers, micelles or vesicles (**Figure 17**) depending on their structure, which also define their performance as capillary coatings. For example, while single-chained surfactants (*e.g.* cetyltrimethylammonium bromide, CTAB) generally must be maintained in the buffer solution to be effective (typically only used as dynamic coating), double-chained surfactants (*e.g.* didodecyldimethylammonium bromide, DDAB) are able to form semi-permanent coatings (no need to be maintained in the buffer solution) [21].

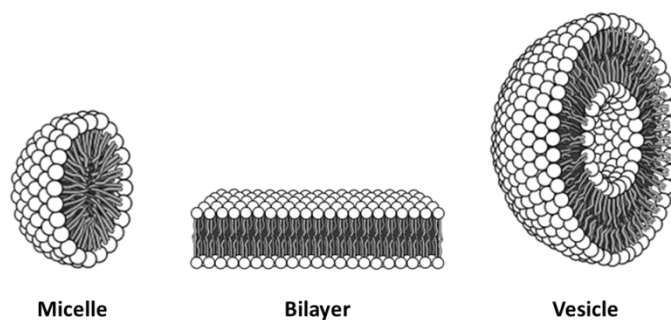


Figure 17. Aggregated structures from single-chained surfactants (micelle) or from double-chained surfactants (bilayer and vesicle).

In general, *ionic liquids (ILs)* are defined as salts, which are made up of a bulky organic cation and an organic/inorganic anion (**Figure 18**), being liquid at room temperature. In this case their properties, such as high conductivity, wide temperature range, negligible vapor pressure, good thermal stability, tunable viscosity and miscibility with water and organic solvents are dependent on the type and size of both anion and cation [22]. When ILs are included in the background solution, they change the analyte migration behavior. In the majority of cases the resolution is connected with the cation, which plays two main roles (i) coating the capillary wall, modifying the EOF, and (ii) interacting with the analyte in the buffer solution.

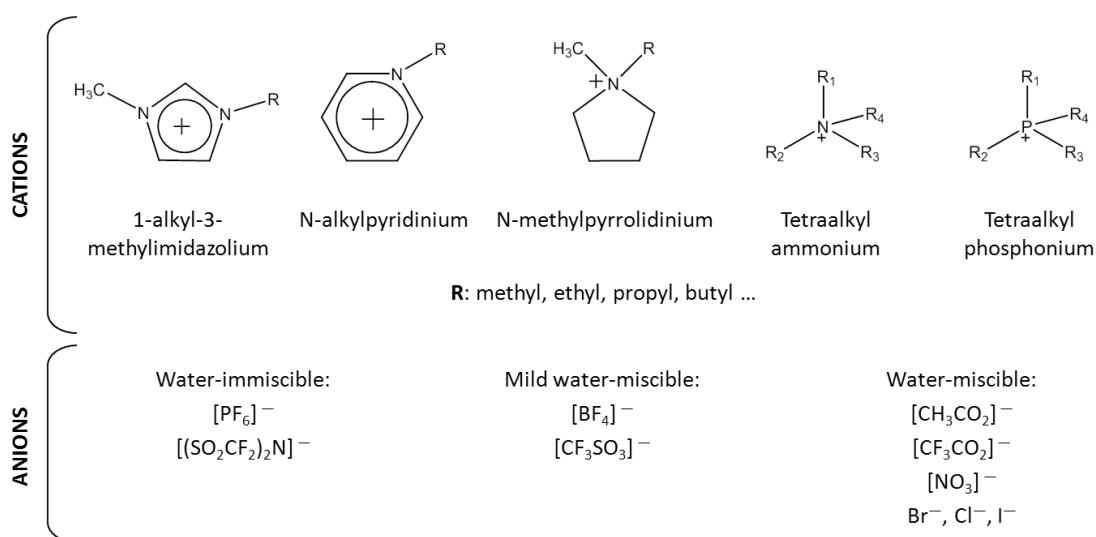


Figure 18. Structures of the most commonly used ionic liquids in capillary electrophoresis.

Nanoparticles (NPs) have been recently introduced in separation science. They have proven to possess a huge versatility with regard to chemical functional groups [amino (NH_2), thiol (SH), carboxyl (COOH) ...], composition (zeolite, latex, metal oxides, gold, silver ...), size and shape. Moreover, NPs can be charged or uncharged and, their area-to-volume ratio is huge compared with the bulk material.

4.2. Permanent Coatings

These coatings have a long-term stability so they are often regarded as the most effective way for surface modification. Even when the coating procedure is usually more time-consuming than in dynamic ones and thus, it is not suitable for disposable devices, they are attractive for reusable devices (e.g. glass microfluidic chips) [3].

When a coating is employed, there are two main reasons considered as responsible of EOF changes: (i) zeta-potential alteration by shielding the Si—OH groups of the capillary wall surface, and (iii) local viscosity increases.

Especially mention deserves the so-called *self-assembled monolayers* (SAMs). They are frequently alkylchlorosilanes ($\text{R-SiO}_3\text{Cl}$) coordinated with the hydroxylated substrate through Si—O—Si bonds, or alkanethiolates (R-SH) chemisorbed (mainly to metal substrates) *via* electrostatic interaction like RS^-Au^+ [23]. In both cases alkyl chains remain closed-packed. Most often, SAMs are made of small organic molecules with lengths around few nanometers, providing thin polymer layers [24]. Their properties are largely determined by their terminal functional group, creating an adhesion layer on which biomolecules or cells can be immobilized [25-27], or preventing unwanted adsorption [28], whose resistance is strongly influenced by the alkyl length [29].

Polymers are the most widespread covalent modifiers. Different approaches have been developed over the years with the aim of obtaining permanent coatings, mainly *via* either Si—O—Si—C or Si—C bonds. The first can be hydrolyzed at $\text{pH} > 8$ resulting in the coating destruction, while the second is more stable to hydrolysis [30] and allows the employment of higher pH values, which is important as the buffer solution pH relies on the stability of this bonding. Thus, the modifiers currently employed in capillary electrophoresis and microfluidic devices can be classified into “grafting to”, “grafting from” or “grafting from” in function of how the coating is grown (**Figure 19**). In all cases, there are two common steps prior the polymer coating process, first the surface activation (e.g. plasma, $\text{H}_2\text{SO}_4/\text{H}_2\text{O}_2$...) and then the derivatization (commonly known as silanization).

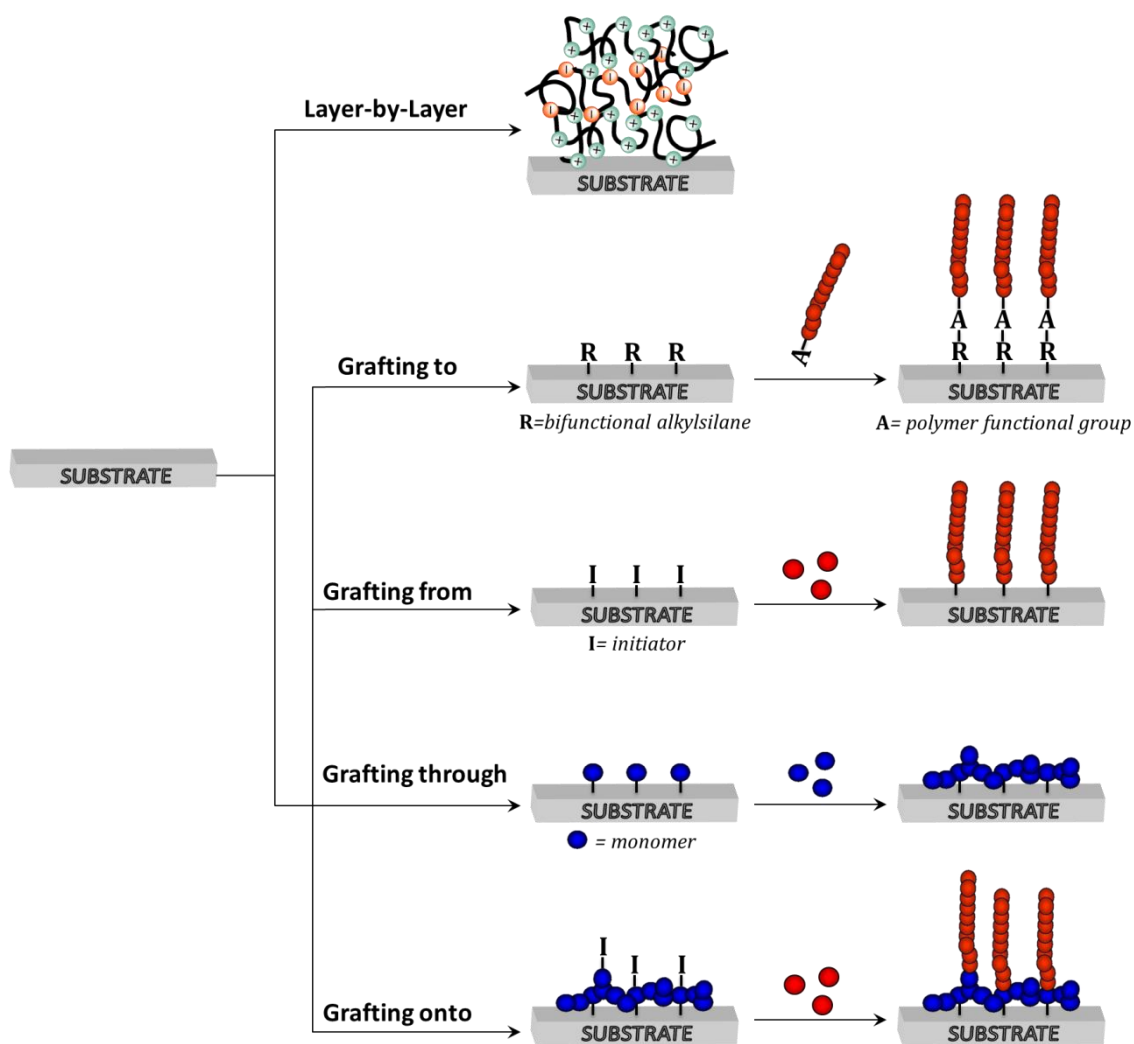


Figure 19. Approaches for the surface modification with polymers.

Surface *derivatization* is usually performed by employing alkylsilanes as bifunctional cross-linkers owing to their quickly reaction with polymers to form the above commented stable siloxane bond (Si—O—Si). These molecules are formed by two different reactive groups: the silyl head ($-\text{SiOR}_3$) and the organic reactive [31]. While the former group undergoes reaction with the surface hydroxyl groups (resulting in a robust anchorage organosilane-substrate), the latter are used to functionalize the surface with different groups. It is noteworthy that small changes in the structure of the alkyl group will decide the organic group reactivity as well as the bond stability [32]. However, this reaction has some remarkable drawbacks, such as it is time-consuming (1-36 h), usually requires high temperatures (above 110°C), and inert atmosphere.

The “*grafting to*” approach is characterized by the reaction between a prepolymerized polymers and the surface reactive sites (alkylsilane previously immobilized). A wide range of polymers have been immobilized in microfluidic devices by this technique. Among the most

widely employed are poly(ethyleneimine) (PEI) for improving sensitivity of enzyme-linked immunosorbent assays [33], and poly(ethylene glycol) (PEG) [34-36] or oxidized dextran [37] for reducing the adsorption of proteins by suppressing the EOF. Even though also other polymers, such as hyperbranched polyglycerols (HPGs) in order to prevent nonspecific protein adsorption and increase the selective capture of positively charged proteins [38], or allylhydridopolycarbosilane (AHPCS) showing an excellent solvent resistance and a highly stable EOF [39]. Through this technique only a small amount of polymer is going to be immobilized on the surface thus, these coatings will present low grafting density and thickness. Therefore, in cases where a high density coating is required, another approach has to be followed.

The need of preparing polymer monoliths in small areas with low polydispersities has led to the emergence of the so-called “*grafting from*” methods [40], wherein the polymer is grown inside the capillary starting from the radical sites on the substrate (initiators). This polymerization process can be initiated by means of UV exposure, electron beam irradiation, depending on the method, which are grouped into free radical polymerization and controlled/living radical polymerization (CRP) [41]. In the latter, great progress has been made in recent years as they provide more homogeneous polymers than the former method. In the particular case of microfluidic devices, atom transfer radical polymerization (ATRP) [42] is the most frequently used CRP method. Thus, poly(ethylene glycol) [43] or poly(N-vinylpyrrolidone) [44], have been grafted on PMMA and PDMS surfaces respectively in order to obtain anti-biofouling miniaturized analytical devices, quaternary ammonium poly(dimethylaminoethyl methacrylate)-based brushes were prepared for improving the hydrophilicity of PDMS substrates and preventing non-specific protein adsorption [45], poly(ethylene glycol)-modified β -cyclodextrins were introduced onto PDMS surfaces with the aim of preparing photocontrolled reversible surfaces for cardiac biomarkers and fatty acid proteins analysis [46].

One of the last grafting approaches for microfluidics is the so-called “*grafting through*”, which is employed to obtain copolymer coatings. For instance, Llopis *et al.* applied this method to a PMMA microfluidic chip with the aim of improving DNA electrophoretic separation [47]. Thus, the protocol was based on the immobilization of methacrylic acid (monomer) on a pre-aminated surface. The resulting terminal groups then serve as scaffold for subsequent acrylamide polymerization.

There is one last method for achieving polymer permanent coatings, known as “*grafting onto*” polymerization [48], which has not been reported yet for microfluidic devices. In this case a polymeric backbone is grafted onto a macro initiator (polymer with a reactive group, previously synthesized on the substrate) [49].

REFERENCES

- [1] D. Belder, H. Husmann, J. Warmke. *Electrophoresis* 22 (2001) 666-672.
- [2] R. Haselberg, L. van der Sneppen, F. Ariese, W. Ubachs, C. Gooijer, G.J. de Jong, G.W. Somsen. *Anal. Chem.* 81 (2009) 10172-10178.
- [3] D. Belder, M. Ludwig. *Electrophoresis* 24 (2003) 3595-3606.
- [4] A.D. Stroock, G.M. Whitesides. *Acc. Chem. Res.* 36 (2003) 597-604.
- [5] Y. Lu, Y.-L. Hu, X.-H. Xia. *Talanta* 79 (2009) 1270-1275.
- [6] S. Prakash, M.B. Karacor, S. Banerjee. *Surf. Sci. Rep.* 64 (2009) 233-254.
- [7] J. Zhou, A.V. Ellis, N.H. Voelcker. *Electrophoresis* 31 (2010) 2-16.
- [8] I. Peric, E. Kenndler. *Electrophoresis* 24 (2003) 2924-2934.
- [9] A. Pallandre, B. de Lambert, R. Attia, A.M. Jonas, J.-L. Viovy. *Electrophoresis* 27 (2006) 584-610.
- [10] M.W. Kamade, K.A. Fletcher, M. Lowry, I.M. Warner. *J. Sep. Sci.* 28 (2005) 710-718.
- [11] K. Boonsong, M.M. Caulum, B.M. Dressen, O. Chailapakul, D.M. Crokek, C.S. Henry. *Electrophoresis* 29 (2008) 3128-3134.
- [12] Z. Sui, J.B. Schlenoff. *Langmuir* 20 (2004) 6026-6031.
- [13] H. Wang, D. Wang, J. Wang, H. Wang, J. Gu, C. Han, Q. Jin, B. Xu, C. He, L. Cao, Y. Wang, J. Zhao. *J. Chromatogr. A* 1216 (2009) 6343-6347.
- [14] J. Horvath, V. Dolnik. *Electrophoresis* 22 (2001) 644-655.
- [15] C.A. Lucy, A.M. MacDonald, M.D. Gulcev. *J. Chromatogr. A* 1184 (2008) 81-105.
- [16] P.G. Righetti, C. Gelfi, B. Verzola, L. Castelletti. *Electrophoresis* 22 (2001) 603-611.
- [17] C. Nilsson, S. Birnbaum, S. Nilsson. *J. Chromatogr. A* 1168 (2007) 212-224.
- [18] E. Guihen. *Trac-Trend Anal. Chem.* 46 (2013) 1-14.
- [19] Y. Xu, E. Wang. *J. Chromatogr. A* 1216 (2009) 4817-4823.
- [20] B. Verzola, C. Gelfi, P.G. Righetti. *J. Chromatogr. A* 868 (2000) 85-99.
- [21] J.E. Melanson, N.E. Baryla, C.A. Lucy. *Anal. Chem.* 72 (2000) 4110-4114.
- [22] S.A. Forsyth, J.M. Pringle, D.R. MacFarlane. *Aust. J. Chem.* 57 (2004) 113-119.
- [23] A. Ulman. *Chem. Rev.* 96 (1996) 1533-1554.
- [24] A. Pallandre, B. de Lambert, R. Attia, A.M. Jonas, J.-L. Viovy. *Electrophoresis* 27 (2006) 584-610.
- [25] J.T. Koepsel, W.L. Murphy. *Langmuir* 25 (2009) 12825-12834.
- [26] N.P. Westcott, M.N. Yousaf. *Electrophoresis* 30 (2009) 3381-3385.
- [27] J.T. Koepsel, W.L. Murphy. *Chem. Bio.Chem.* 13 (2012) 1717 - 1724.
- [28] R.S. Kane, S. Takayama, E. Ostuni, D.E. Ingber, G.M. Whitesides. *Biomaterials* 20 (1999) 2363-2376.
- [29] J. Lu, M.L. Lee. *Electrophoresis* 27 (2006) 3533-3546.

- [30] E.A.S. Doherty, R.J. Meagher, M.N. Albarghouthi, A.E. Barron. *Electrophoresis* 24 (2003) 34-54.
- [31] A. Marechal, R. El-Debs, V. Dugas, C. Demesmay. *J. Sep. Sci.* 36 (2013) 2049-2062.
- [32] B.H. Northrop, R.N. Coffey. *J. Am. Chem. Soc.* 134 (2012) 13804–1381.
- [33] Y. Bai, C.G. Koh, M. Boreman, Y.-J. Juang, I.-C. Tang, L.J. Lee, S.-T. Yang. *Langmuir* 22 (2006) 9458-9467.
- [34] Z. Zhang, X. Feng, Q. Luo, B.-F. Liu. *Electrophoresis* 30 (2009) 3174-3180.
- [35] Z. Zhang, X. Feng, F. Xu, X. Liu, B.-F. Liu. *Electrophoresis* 31 (2010) 3129-3136.
- [36] P.Y. Yeh, Z. Zhang, M. Lin, X. Cao. *Langmuir* 28 (2012) 16227–16236.
- [37] J.-J. Feng, A.-J. Wang, J. Fan, J.-J. Xu, H.-Y. Chen. *Anal. Chim. Acta* 658 (2010) 75-80.
- [38] P.Y. Yeh, N.A.A. Rossi, J.N. Kizhakkedathu, C.A. Mu. *Microfluid. Nanofluid.* 9 (2010) 199–209.
- [39] M. Li, D.P. Kim. *Lab. Chip.* 11 (2011) 1126-1131.
- [40] Q.S. Kang, X.F. Shen, N.N. Hu, M.J. Hu, H. Liao, H.Z. Wang, Z.K. He, W.H. Huang. *Analyst* 138 (2013) 2613-2619.
- [41] H. Wang, X. Dong, M. Yang. *Trac-Trend Anal. Chem.* 31 (2012) 96-108.
- [42] L. Lanotte, S. Guido, C. Misbah, P. Peyla, L. Bureau. *Langmuir* 28 (2012) 13758–13764.
- [43] J. Liu, T. Pan, A.t. Woolley, M.L. Lee. *Anal. Chem.* 76 (2004) 6948-6955.
- [44] Z. Wu, W. Tong, W. Jiang, X. Liu, Y. Wang, H. Chen. *Colloid. Surface. B* 96 (2012) 37-43.
- [45] Q. Tu, J.-C. Wang, R. Liu, J. He, Y. Zhang, S. Shen, J. Xu, J. Liu, M.-S. Yuan, J. Wang. *Colloid. Surface. B* 102 (2013) 361-370.
- [46] Y. Zhang, L. Ren, Q. Tu, X. Wang, R. Liu, L. Li, J.-C. Wang, W. Liu, J. Xu, J. Wang. *Anal. Chem.* 83 (2011) 9651-9659.
- [47] S.L. Llopis, J. Osiri, S.A. Soper. *Electrophoresis* 28 (2007) 984-993.
- [48] H. Gao, K. Matyjaszewski. *J. Am. Chem. Soc.* 129 (2007) 6633-6639.
- [49] S. Morsch, W.C.E. Schofield, J.P.S. Badyal. *Langmuir* 27 (2011) 14151-14159.

5. Target Analytes

5.1. Catecholamines

There are several compelling reasons for studying catecholamines [dopamine (DA), norepinephrine (NE) and epinephrine (E)] over and above their uniqueness, as they act as neurotransmitters or hormones at the central (CNS) and peripheral (PNS) nervous systems. Although these three catecholamines have similar structures (**Figure 20**), their physiological and pathological functions in the CNS and PNV are quite different, being considered as important biomarkers for diagnosis, therapy and prognosis of several neuroendocrine and cardiovascular disorders. It is noteworthy that dopamine is the precursor of norepinephrine and then of epinephrine in the biosynthetic pathways of these neurotransmitters [1].

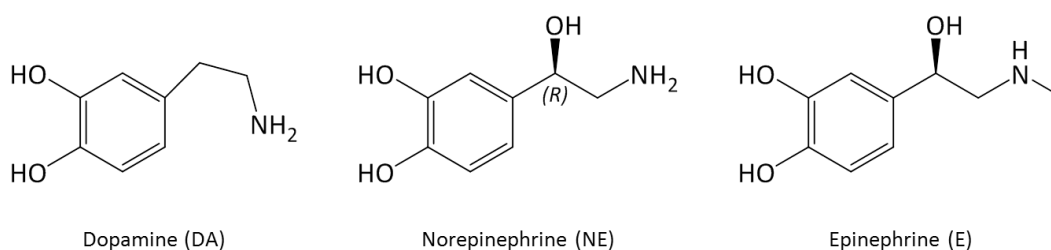


Figure 20. Structures of the catecholamines.

Because of their chemistry, these catecholamines have three properties in common (i) they cannot be used orally, (ii) they have a brief duration of action, and (iii) they cannot cross the blood-brain barrier [2].

5.1.1. Clinical interest

The fact that catecholamines have different effects from the clinical point of view comes from their selective activation of specific receptors. This information is represented in **Table 6** for usual therapeutic doses.

Table 6. Receptors activated by dopamine (DA), norepinephrine (NE) and epinephrine (E).

| Catecholamines | Receptors Activated | | | | |
|----------------|---------------------|------------|-----------|-----------|----------|
| | α_1 | α_2 | β_1 | β_2 | Dopamine |
| DA | ✓ | | ✓ | | ✓ |
| NE | ✓ | ✓ | ✓ | | |
| E | ✓ | ✓ | ✓ | ✓ | |

Dopaminergic neurons are the main source of **dopamine** production in the body. Despite the fact that they correspond to less than 1 % of the total number of brain neurons [3], they play an important role in the regulation of several aspects of basic brain functions, including motor control, motivation, learning and working memory [4]. Therefore, dopamine regulation is going to be responsible not only of both mental and physical health, but also the pharmacology of psychotherapeutic drugs and drugs of abuse.

For instance, among the major neurodegenerative disorders associated with *dopamine loss* are schizophrenia [5,6] and Parkinson [7] diseases but, the lack of dopamine can be also related with other pathologies such as depression, some sleep disorders, and inability to focus on a task. On the other hand, abnormally *high dopamine* levels may cause compulsive behavior, and may indicate a catecholamine-producing tumor, such as neuroblastoma, pheochromocytoma and paraganglioma [8,9].

From the therapeutic point of view, dopamine has been indicated for shock treatment, heart or renal failures, due to its ability of increasing renal blood flow.

Norepinephrine, also known as noradrenaline, is considered the primary neurotransmitter in the peripheral sympathetic nervous system, which is responsible of human cardiovascular control. This catecholamine, along with dopamine, has come to be recognized as indicator of attention and focus disorders, stress and depression [10]. Moreover, *elevated levels* of norepinephrine are also related with heart failure [11]. Thus, it stimulates ventricular contraction and act as vasoconstrictor (in blood vessels of the skin, viscera, and mucous membranes), increasing cardiac output and blood pressure [12].

There are various evidences to support that **epinephrine**, also known as adrenaline, has been implicated in the addictive and positively reinforcing effects of alcohol [13]. On the other hand, it has some therapeutic uses, such as (i) topical bleeding controlled (hemostasis), (ii) delayed adsorption of local anesthetics or (iii) anaphylactic shock treatment when injected. However, it can cause adverse effects such as hypertensive crisis, dysrhythmias, angina pectoris or hyperglycemia [2].

5.1.2. Methods of analysis

It seems clear that the analysis of catecholamines is a very important task, and demands the development of reliable analytical methods in order to achieve the separation and quantification of these molecules.

Due to their closely related structures catecholamines need a powerful separation technique prior detection. They have been routinely determined in clinical laboratories by high performance liquid chromatography (HPLC) [14,15], and significant improvements in the specificity have been achieved by coupling it with fluorescence, electrochemical, chemiluminescence or mass spectrometry detection [16]. However, when chromatographic methods are compared with *capillary electrophoresis*, the general conclusion is that CE offers important advantages for life science. Not only for their high separation efficiency (allowing separations with a large number of theoretical plates), and selectivity under properly conditions (enabling the separation of most diverse type of compounds), but also their shorter times of analysis, and the need of lower sample volumes [17]. What is more, sample volume requirements can place limitations on how HPLC can be used for real sample analysis, being well suited only to situations where sample volumes are not limited [18,19]. On the other side, the application of electrophoretic based-microfluidics to biological analysis is among the major advances in the last decade. Compared with conventional capillary electrophoresis, they provide extra advantages, including fastest analysis, smaller sample volume and reagent consumption or disposability, constituting high efficient platforms for simultaneous analysis not only for catecholamines but also for a large number of biological compounds [20,21].

Nowadays, the majority of traditional methods for detecting catecholamines, which relied mainly on the creation of detectable fluorophores, are obsolete. Although they are still used in some clinical laboratories, fluorescent methods have been replaced by new methods with the aim of improving the analytical sensitivity, accuracy and clinical suitability, being the most employed those based on *electrochemistry detection*. The chemistry of catecholamines is largely dominated by the nucleophilic amino group, which acts as an excellent target for derivatization agents. However, some important derivatives employed in fluorescence detection techniques require a free primary amino group, and therefore they cannot be applied to epinephrine. On the other hand, the ease oxidation of the catechol ring (**Figure 21**) is another property that has also been employed with analytical purposes. Thus, electroanalytical techniques, which are based on the catecholamines oxidation at an anodic surface, are appealing as an improved alternative for the detection of these compounds [22].

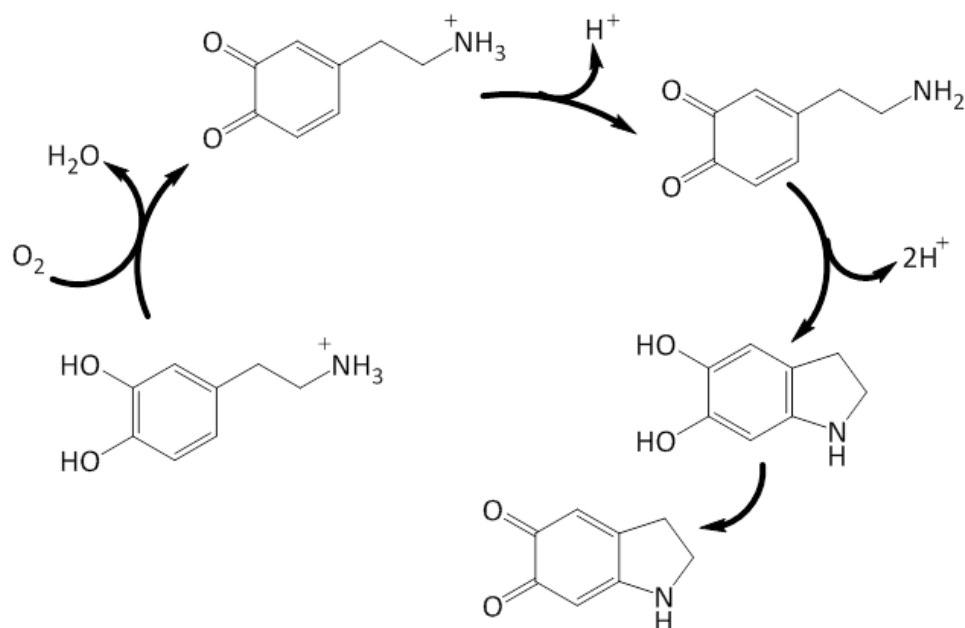


Figure 21. Cyclization reactions for dopamine conversion into quinone [23].

5.2. Heavy Metals

The World Health Organization (WHO) establish heavy metals as potential harmful to people and the environment [24]. These metals are notable for their wide environmental dispersion (soils and rocks, air and water), their tendency to accumulate in some tissues and their overall potential to be toxic even in minor levels. Certain metals (*e.g.* Fe or Cu) in small quantities are essential for a healthy life. Nevertheless, other are xenobiotic (compound foreign to a living organism) [25] and, even trace levels are extremely toxic.

The main threats to human health from heavy metals are associated with lead (Pb), cadmium (Cd), mercury (Hg) and arsenic (As) and could be explained by their tendency to form complexes with nitrogen, sulfur, or oxygen biological matter, generating changes in proteins molecular structure, breaking hydrogen bonds, or inhibiting the enzymatic activity. These are some of the reasons that explain their toxicological and carcinogenic effects, such as those affecting the central nervous system (Hg^{2+} , Pb^{2+} , As^{2+}), the kidney or liver (Cd^{2+} , Hg^{2+} , Pb^{2+}), or skin, bones or teeth (Cd^{2+}) [26].

This explains the ongoing search to develop highly selective and sensitive detection systems for detecting trace metals.

5.2.2. *Methods of analysis*

Current trend towards the development of rapid, low-cost, and friendly-use techniques for *in situ* heavy metals monitoring have made that standardized techniques, like graphite furnace atomic absorption spectrometry and inductively coupled emission spectroscopy, are being replaced due to their time-consumption and costly equipment. With the aim of overcoming these problems, a number of optical (light absorption and light emission fluorescence) and electrochemical (chemically modified and nanostructured electrodes) based-techniques have arisen in the last years [27].

However, the emergent needs for developing zero-cost and in-field analytical tools for heavy metals analysis have made that the last efforts have been focused on the development of paper-based analytical devices. Thus, some colorimetric methods have been proposed for sensing Cu^{2+} , Ag^+ , Cd^{2+} , Hg^{2+} , Pb^{2+} ... [28,29]. Especial mention deserves the electrochemical techniques, which shows numerous advantages for this particular trend, such as faster analysis, good selectivity and sensitivity. These benefits have been magnified by their recently integration in paper-based devices where they show to be well suited for trace-metal content analysis in water samples [30,31].

REFERENCES

- [1] G. Eisenhofer, I.J. Kopin, D.S. Goldstein. *Pharmacol. Rev.* 56 (2004) 331-249.
- [2] <http://www.elsevieradvantage.com/samplechapters/9781437735826.pdf>
- [3] S.J. Chinta, J.K. Andersen. *Int. J. Biochem. Cell Biol.* 37 (2005) 942-946.
- [4] D.S. Goldstein, G. Eisenhofer, K.M. McCarty. *Catecholamines: Bridging Basic Science with Clinical Medicine.* Academic Press (1998).
- [5] K.L. Davis, R.S. Kahn, G. Ko, M. Davidson. *Am. J. Psychiatr.* 148 (1991) 1474-1486.
- [6] O. Guillin, A. Abi-Dargham, M. Laruelle. *Int. Rev. Neurobiol.* 78 (2007) 1-39.
- [7] J. Lotharius, P. Brundin. *Nat. Rev. Neurosci.* 3 (2002) 932-942.
- [8] M.M. Kushnir, F.M. Urry, E.L. Frank, W.L. Roberts, B. Shushan. *Clin. Chem.* 48 (2002) 323-331.
- [9] W.H.A. de Jong, E.G.E. de Vries, B.H.R. Wolffenbuttel, I.P. Kema. *J. Chromatogr. B* 878 (2010) 1506-1512.
- [10] T.D. Jr Geraciotti, D.G. Baker, N.N. Ekhatior, S.A. West, K.K. Hill, A.B. Bruce, D. Schmidt, B. Rounds-Kugler, R. Yehuda, P.E. Jr Keck, J.W. Kasckow. *Am. J. Psychiatry* 158 (2001) 1227-1230.
- [11] R.S. Kramer, D.T. Mason, E. Braunwald. *Circulation* 38 (1968) 629-634.
- [12] J.M. Foody, M.H. Farrel, H.M. Krumholz. *JAMA-J. Am. Med. Assoc.* 287 (2002) 883-889.
- [13] M. Linnoila. *Research on Alcohol and Alcoholism.* 13 (1989) 355-357.
- [14] W.H.A. de Jong, E.G.E. de Vries, I.P. Kema. *Clin. Biochem.* 44 (2011) 95-103.
- [15] J. Bicker, A. Fortuna, G. Alves, A. Falcao. *Anal. Chim. Acta* 768 (2013) 12-34.
- [16] M. Tsunoda. *Anal. Bioanal. Chem.* 386 (2006) 506-514.
- [17] Z. Deyl, F. Tagliaro, I. Miksik. *J. Chromatogr. B* 656 (1994) 3-27.
- [18] T. Lapainis, J.V. Sweedler. *J. Chromatogr. A* 1184 (2008) 144-158.
- [19] M. Perry, Q. Li, R.T. Kennedy. *Anal. Chim. Acta* 653 (2009) 1-22.
- [20] H.-F. Li, Z.W. Cai, J.-M. Lin. *Anal. Chim. Acta* 565 (2006) 183-189.
- [21] C. Cakal, J.P. Ferrance, J.P. Landers, P. Caglar. *Anal. Bioanal. Chem.* 398 (2010) 1909-1917.
- [22] E.C.Y. Chan, P.C.L. Ho. Chapter 7 in *Chromatographic Methods in Clinical Chemistry and Toxicology.* John Wiley & Sons, New York (2007) 101-119.
- [23] Y. Lin, Z. Zhang, L. Zhao, X. Wang, P. Yu, L. Su, L. Mao. *Biosens. Bioelectron.* 25 (2010) 1350-1355.
- [24] Guidelines for drinking water quality, third Ed. The World Health Organization (WHO) (2008) 145-196.
- [25] IUPAC. *Compendium of Chemical Terminology*, 2nd ed. (the "Gold Book"). Compiled by A. D. McNaught and A. Wilkinson. Blackwell Scientific Publications, Oxford (1997).
- [26] I. Järup. *Brit. Med. Bull.* 68 (2003) 167-182.
- [27] G. Aragay, J. Pons, A. Merkoçi. *Chem. Rev.* 111 (2011) 3433-3458.

- [28] N. Ratnarathorn, O. Chailapakul, C.S. Henry, W. Dungchai. *Talanta* 99 (2012) 552-557.
- [29] L. Feng, X. Li, H. Li, W. Yang, L. Chen, Y. Guan. *Anal. Chim. Acta* 780 (2013) 74-80.
- [30] Z. Nie, C.A. Nijhuis, J. Gong, X. Chen, A. Kumachev, A.W. Martinez, M. Narovlyansky, G.M. Whitesides. *Lab Chip* 10 (2010) 477-483.
- [31] J. Shi, F. Tang, H. Xing, H. Zheng, L. Bi, W. Wang. *J. Braz. Chem. Soc.* 23 (2012) 1124-1130.

OBJECTIVES

OBJECTIVES

The studies included in this Thesis deal with several important parameters involved in the **achievement of a robust microfluidic analytical device**, which have been chosen for their capability of integrating all the analysis steps, at the same time in a single device. Thus, the objectives and therefore, the content of the following chapters, are related with the three main important parts of these devices: separation, detection and substrate (**Figure 22**).

- ▢ The **first objective** (Chapter 1) is devoted to improve the separation of three catecholamines with closely related structures (dopamine, norepinephrine and epinephrine) by employing microchannel coatings.
- ▢ The **second objective** (Chapter 2) is aimed at sensitivity enhancement of the electrochemical detection system, due to the low detection limits required for target analytes.
- ▢ The **third objective** (Chapter 3) deals with the fabrication of these microfluidic devices in novel materials, particularly the ones designed on paper, which have been recently introduced.

The specific objectives are more detailed in each chapter.

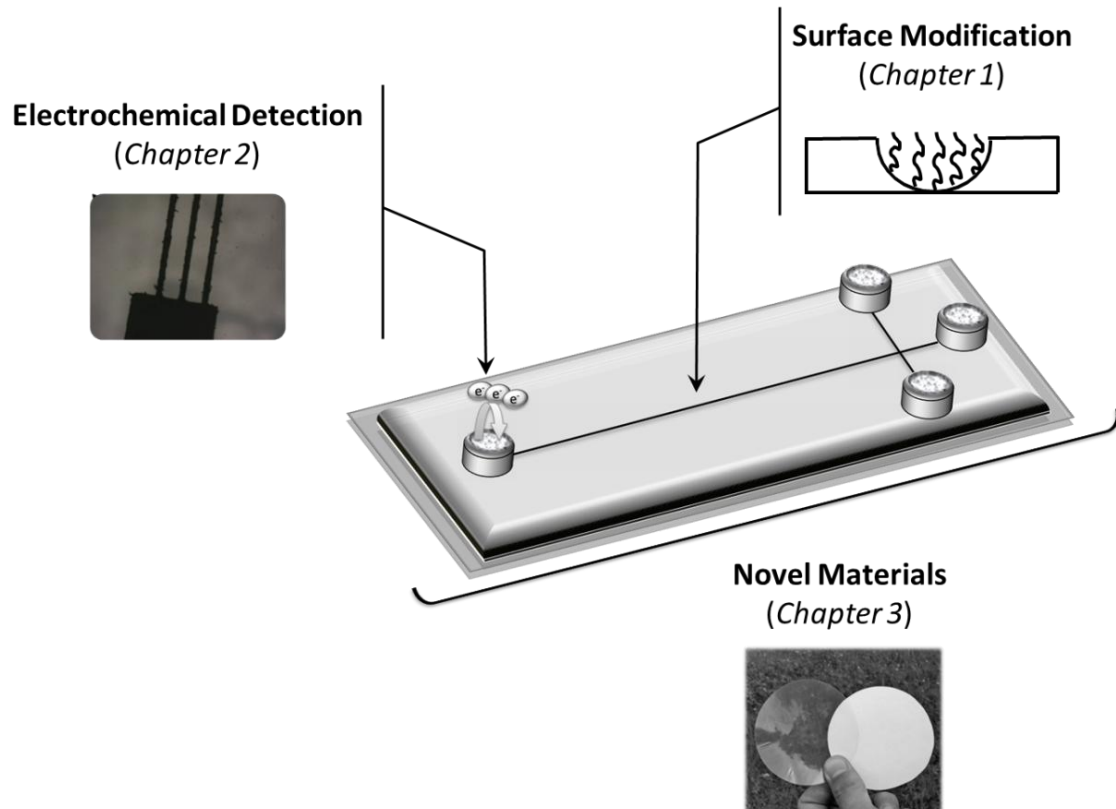


Figure 22. Objectives of the Thesis divided into microfluidic device functions.

RESULTS & DISCUSSION

RESULTS & DISCUSSION

CHAPTER 1: SEPARATION EFFICIENCY IMPROVEMENT

1.1. Background

1.2. Research & Development:

- ▣ **Book Chapter:** Improving the Separation in Microchip Electrophoresis by Surface Modification.
 - ▣ **Article 1:** Poly (acrylic acid) Microchannel Modification for the Enhanced Resolution of Catecholamines Microchip Electrophoresis with Electrochemical Detection.
 - ▣ **Article 2:** Ionic liquids as Modifiers for Glass and SU-8 Electrochemical Microfluidic chips.
 - ▣ **Article 3:** Poly(glycidyl methacrylate) Derivatives as Modifiers in Microfluidic Devices for the Improvement of Catecholamines Separation.
-

1.1. Background

Background

As outlined in the Objectives section, one critical parameter involved in the success of a microfluidic device lies in analytes effective separation. One of the most particularly attractive strategies to achieve this goal is the inner wall surface modification, which allows the introduction of different functional groups, being capable to: reduce or increase the interactions between analytes and microchannel walls, as well as the compatibility with biological samples or, change the electroosmotic flow.

The purpose of this research part of the Thesis was the **development and evaluation of new surface coatings that could contribute to achieve more robust microfluidic devices**. To accomplish this goal three catecholamines (dopamine, norepinephrine and epinephrine) were chosen as model analytes. The separation of these compounds is a demanding task owing to their clinical relevance (neurotransmitters related with many neurological diseases) and their closely related structures (**Figure 20**) leading to nearly identical electrophoretic behavior, which makes almost impossible their separation in microfluidic devices without a suitable surface modification.

Based on this, the specific aims of this section are summarized below.

- ▣ To give an overview that serves as a brief introduction to the conventionally employed chemical modifiers and, the most important techniques used for surface coating (**Book Chapter**).
- ▣ To obtain a coating that remains substantially stable during the useful lifetime of the microfluidic chip. With this aim a covalent approach was proposed in **Article 1**. Thus, poly (acrylic acid) was chosen for the development of this part of the work because of its capability of bearing different charge only by manipulating the conditions inside the device (*e.g.* pH) and its capability to interact with catecholamines. Furthermore, glass possesses a number of attributes that make it an ideal material for microfluidic devices (*i.e.* it is extremely chemically robust, do not swell and, is compatible with a wide variety of chemicals, including organic solvents). This, coupled with its well-known chemistry (silica-based capillaries utilized in capillary electrophoresis have been modified through the time with a wide range of compounds) leads to an easily way of controlling the surface properties.

- ▣ To test new promising chemical modifiers like ionic liquids not only as surface coating but also its influence in the electrochemical detection properties (**Article 2**). For their properties (miscibility with water and high conductivity) ionic liquids are attracting a great deal of research in the last decade but, they have not been extensively studied yet in microfluidic chips. Moreover, this is the first time that ionic liquids were employed in SU-8 photoresist microchips. In this case, a dynamic approach (based on the addition of ionic liquids in the background solution) was chosen for its versatility and less time consuming.

- ▣ To synthesize a group of homemade polymers (cationic, anionic and neutral) which allow choosing the optimal coating depending on the target analytes nature (**Article 3**). Herein, inspired in the extraordinary versatility of the epoxy group chemistry, different poly(glicidil methacrylate) based polymers were designed and tested as SU-8 microfluidic chips surface modifiers.

This Thesis is presented in the format “*Thesis by Publications*”. The Chapter 1 in particular, contains both published and unpublished papers, which have been reformatted to word files with the aim of achieving a consistent presentation within this Thesis (the content remains unchanged).

1.2. Research & Development

Book Chapter

*Improving the Separation in Microchip
Electrophoresis by Surface Modification*

John Wiley & Sons, Inc. (2013) Chapter 6

Capillary Electrophoresis and Microchip Capillary Electrophoresis

Principles, Applications, and Limitations

Chapter 6: Improving the Separation in Microchip Electrophoresis by Surface Modification

M. Teresa Fernández-Abedul^a, Isabel Álvarez-Martos^a, Francisco Javier García Alonso^b, Agustín Costa-García^a

^a*Departamento de Química Física y Analítica, Universidad de Oviedo, Asturias, Spain*

^b*Departamento de Química Orgánica e Inorgánica, Universidad de Oviedo, Asturias, Spain*

ABSTRACT

Microchip electrophoresis devices are a powerful tool of analytical chemistry. Much research is made in order to overcome the limitations imposed by the current challenges such as enhancement of sensitivity and selectivity. Surface chemistry becomes of paramount importance due to the high area-to-volume ratio and therefore, strategies to improve its characteristics are continuously made. In this chapter, the different aspects related to surface modification of microchannels is commented with special emphasis on the chemical modification through surfactants, ionic liquids, nanoparticles, and polymers.

1. Introduction

Analytical Chemistry is a well-established discipline but also a very vivid and young one. The analytical process solving problems by translating the socio-economic or scientific-technological statement into an analytical problem related to some of the four known questions: What and how much? How structured? How bound? and/or How distributed? [1]. The process followed to find the answers is well structured and usually starts with a sampling step and continues with the sample preparation or pretreatment step. Once the sample has been conditioned for measurement, an optimized methodology is followed to obtain the analytical signal that will give the chemical information, commonly an electronic signal. This will help in understanding and solving the analytical problem. In this context, the main goals of Analytical Chemistry are to obtain more (bio)chemical information with better quality, increasingly using less materials, time, cost, and risk for personnel and the environment. This is summarized in three basic and interconnected trends, namely, automation, simplification, and miniaturization [2]. The last one is a basic trend shared with many technical and scientific areas. One of the best examples is the development of analytical devices with extremely small size, including operations such as sample injection, separation (i.e., capillary electrophoresis, CE), and detection [3]. This milestone started a new period that involves an intensive research line in microfluidics (manipulation of fluids in channels with dimensions of tens of micrometers), in order to achieve important technological improvements [4,5] in addition to relevant applications [6,7] that lead to real “lab-on-a-chip” (LOC) devices.

The use of flow systems had produced an important advance in Analytical Chemistry, since many methodologies that were performed in discrete steps could be automated [*i.e.*, flow injection analysis (FIA) methodologies]. Now, miniaturization has opened up many possibilities of transferring methods already matured or developing new ones. The latest developments with regard to technology, standard operations, and applications have been reviewed recently [8]. This field, also referred as micro total analysis systems (μ TAS), is highly interdisciplinary and has served as a focal point to bring together research fields from different disciplines. On the other hand, achieving real μ TAS or LOC devices involves integration of the multiple steps performed in conventional analysis systems. However, not all analytical steps are equally incorporated and the incidence level of miniaturization is not homogeneous. Concerning separation techniques, CE has demonstrated to be a robust technique with relevance in projects of paramount importance [9] and an invaluable help to pathologists and doctors in the evaluation of patients' status [10]. The fusion of the two principles (μ TAS

devices and CE), which is denoted microchip electrophoresis (ME) (at the beginning it was named microchip capillary electrophoresis, MCE), is extremely promising, with many different unexplored paths. Research in this field is active and new developments are being continuously reported [11]. However, limitations are still there and solutions need to be found for continuous improvement of the methodologies. Enhancement of sensitivity and selectivity is among the main goals.

2. Strategies for Improving Separations

The determination of closely related analytes, with very similar structures, is still a challenge. Quantitation of analytes in complex matrices has required the use of different strategies in order to differentiate the analyte from a mixture of interfering substances. Complex pretreatments are sometimes performed in order to execute this separation. In some cases, even when pretreatments are performed, similar molecules are present in the sample. Moreover, it has to be taken into account that two related molecules can both be relevant analytes and they have to be in the same sample for simultaneous determination. This is the field of separation techniques, using different approaches for separating molecules. Requirements are increasing continuously and with time, more similar molecules must be separated.

2.1. Selection of an adequate technique: ME

Strategies for resolving signals coming from related analytes are a field of active research. For example, resolution of peaks by means of voltammetric techniques is commonly performed through electrode modification. Polymeric films with electrocatalytic activity have been combined with carbon electrodes for the voltammetric resolution of dopamine (DA) [12] or epinephrine (EP) [13] in the presence of ascorbic and uric acids. However, to distinguish between chemical species that are involved in diffusion-controlled, one-electron electrolysis processes, it is required that their E° values differ by at least 0.118V [14], and therefore combination with separation techniques is usually required. Even with the use of these techniques, the challenge is still there. Strategies to improve resolution in CE, including the use of nonaqueous capillary electrophoresis (NACE) or the use of isoelectric buffers or ionic liquids (ILs) as additives, have been reported [15].

An important example of these aims (improvement of the separation between similar molecules) is the resolution of very structurally related molecules such as chiral analytes [16,17], in which a special strategy has to be employed [18]. A high-speed ME method for the

enantiomeric separation of (R,S)-naproxen using methyl- β -cyclodextrin was compared with CE methodology [19]. Poly(ethylene glycol)-functionalized polymeric microchips were fabricated and evaluated for the electrophoretic chiral separation of 10 different D,L-amino acid pairs with the addition of β -cyclodextrin as chiral selector in the running buffer [20]. A different strategy for enantioseparation was the *in situ* molecular imprinting of the microchannel wall for separation of model enantiomers Boc-D-Trp and Boc-L-Trp, detected amperometrically [21].

2.2. Microchannel design

Referring to their dimensions, CE (diameter) and microchip electrophoresis (microchannel width and height) work on the same scale, both on the order of micrometers. However, a great difference in dimensions is found in the length: capillaries are usually between 50 and 100 cm, whereas separation microchannels are around 5 cm, 10 times smaller. It has been shown that resolution in free zone electrophoresis is directly proportional to the square root of separation length [22]. Therefore, increasing the separation channel length will lead to an increase in resolution between closely eluting analytes. Nevertheless, the microfabrication procedure is not usually considered for very long microchips because of the equipment employed ultraviolet (UV) insolation or laser equipment, spin coaters, etc.]. Consequently, the increase in length is made through serpentine microchannels with incorporated turns [23]. However, it has to be kept in mind that this design increases analyte dispersion [24] and requires an optimized design [25].

2.3. Selection of an appropriate ME material

A different possibility that ME offers (and actually it is one of its major advantages) is the employment of different materials. Owing to the limited separation channel length, the resolution obtainable in ME is in practice often lower than that in classical CE. Accordingly, the optimization of resolution is of great importance. In conventional CE, fused silica is nearly exclusively used as capillary material. However, quite diverse materials can be employed for microchip fabrication. The similarity between glass (microchip) and fused silica (capillary) made this material one of the first developed in the ME field together with some examples of silicon and quartz. However, the properties of polymers were quickly highlighted and microchips were manufactured in various materials with technologies different from those employed in conventional CE, as is extensively commented upon throughout the literature. As examples, polymeric materials such as polydimethylsiloxane (PDMS) [26,27], poly(methyl methacrylate) (PMMA) [28,29], polycarbonate (PC) [30], and poly(ethylene terephthalate)

(PET) [31,32] are among the most employed for ME devices and also those consisting of cyclic olefin polymers such as Zeonex/Zeonor [33,34] and thermoplastic olefinic polymer of amorphous structure (TOPAS) [35] have been employed. The silicone elastomer PDMS is very popular for the ease of fabrication that allows speed in creating new fluidic designs and complex multilayer channel networks, but incompatibility with most nonpolar solvents [36] and surface instability have created the need for analogous materials that address these issues. One such polymer is thermoset polyester (TPE) [37,38], which can be shaped by a replica molding process similar to PDMS, allowing for rapid prototyping of fluidic designs, but with a surface stability and solvent resistance similar to those of glass. The use of polyester toner has also been reported [39], in addition to the use of EPON SU-8 resin [40,41], typically employed as sacrificial material in photolithographic processes, or elastomeric polyurethane (PU) [42]. Moreover, microchip materials such as low-temperature co-fired ceramics [43] or paper, inexpensive material easy to use and specifically designed for developing countries [44] can be employed.

More recently, a new commercial hybrid ceramic polymer,Ormocomp, was introduced for the fabrication of microfluidic separation chips. This organic–inorganic polymer structure natively resists biofouling; even so, it can be used in intact protein analysis without prior surface modification [45]. A different strategy can be employed for generating materials that allow the fabrication of microfluidic devices: synthesis of block copolymers. As an example, a polydimethylsiloxane–poly(ethylene oxide) (PDMS–PEO) vinyl-terminated block copolymer has been synthesized *via* a simple hydrosilylation reaction between hydride-terminated PDMS and PEO divinyl ether [46]. This prepolymer can be subsequently cross-linked into an elastomer in a second hydrosilylation reaction involving a methylhydrosiloxane–dimethylsiloxane copolymer. The presence of the PEO block in the prepolymer chain results in a much more hydrophilic material following cross-linking. The length of the PDMS–PEO prepolymer chain and the multifunctional hydride cross-linker chains dictate the durability of the elastomeric material. Another possibility, which is commented upon in the section Surface Modification, is the use of materials obtained by copolymerization, that is, an acrylic copolymer such as poly(glycidyl methacrylate)-*co*-(methyl methacrylate) (PGMAMMA) [47] or poly(ethylene glycol) (PEG)-functionalized acrylic copolymer [48,49].

Apart from the consideration of the microchip material, it has to be taken into account that hybrid microchips are commonly employed. Microfabrication of channels is usually made in one of the plates of the microchip and the other plate can be different (*e.g.*, PDMS–glass and

silicon–PDMS). Differences with microchips in which both plates are made of the same material are very possible and have to be considered.

Comparison of the analytical performance of electrophoresis microchannels fabricated in different materials has been reported. In this way, the performance of microchips fabricated with different technologies in quartz, glass, PMMA, and PDMS has been studied [50]. Characteristics of PDMS and glass microchips have been evaluated in the separation of peptides [51]. Similarly, different PDMS and glass microchips and also polyester toner chips micromachined by a direct printing process using an office laser printer have been compared [52], in addition to the surface chemistry and optical properties of SU-8 and glass microchips [53].

The fact that ME devices have been manufactured in all these materials, very different in properties and characteristics, suggests the great potential of this methodology. As will be commented upon later, ME is still under development and researchers are still looking for the material with the best performance. The main goal in this area is the optimization of the separations, which relates to the surface of the microchannel, which in turns depends on the material and also on the treatments of the surface. For example, the surface of native PDMS does not contain ionizable surface groups to produce a significant zeta potential when it is in contact with solution. Electrokinetic pumping, the method by which solution flow is induced within the microchannels, relies on the electroosmotic force generated as a result of an electrical double layer. The lack of surface ionizable groups prevents PDMS from generating significant electroosmotic flow (EOF) [54]. Therefore, separations are affected by the microchannel material responsible for EOF and the state of its surface.

Apart from the improvement of the separation in terms of resolution between adjacent peaks, solving problems such as microchannel hydrophobicity is pursued. Such hydrophobicity makes it more difficult to wet the channels and easily form air bubbles. Moreover, adsorption of molecules on the surface that even penetrate spontaneously into the polymer matrix (e.g., PDMS) can occur and the EOF can be unstable and poorly controlled [54,55]. Therefore, it can be said that, in general, the main motivation for finding an adequate material is the control of the EOF in order to improve the precision of migration times but also to perform a robust injection. Another important goal is the reduction of analyte–wall interactions.

2.4. Optimization of the working conditions

It is known that molecules migrate under the electric field following two different electrokinetic effects: electrophoretic and EOF. Apart from the material, the background electrolyte (BGE) conditions, which affect the apparent mobility of molecules, especially the pH of the running buffer, are dominant factors in the separation of analytes [56]. Moreover, operational conditions such as separation voltage, injection time, and injection format have to be carefully optimized. However, when the differences in molecules are very small and also dependent on the material, the use of appropriate conditions is not sufficient. In these cases, modification of the microchannel surface is a possible strategy for improving the separations.

2.5. Surface modification

The field of microfluidics is moving very fast on the research front, but the number of real-world, routine applications is still limited. One probable reason is that the very richness of the field also increases the already large number of challenges that must be solved before a robust practical system can be achieved. As commented upon in a review on surface treatment and characterization [57], surface interactions and treatments are among these challenges, being in contrast to what happens in CE, in their infancy. Another limitation is the moderate number of surface characterization methods that can be applied inside a capillary or microchannel. Microfluidic systems are often assembled by the bonding of flat substrates. It is therefore often possible to transpose to microfluidics the developments in the chemical physics of surfaces. It has to be taken into account that the devices have a large surface area-to-volume ratio and, therefore, the state of the surface becomes very important. Changes in the surface will undoubtedly have a positive/ negative influence on separations.

The number of microchip materials and surface chemistries prohibit an exhaustive account of methodologies here and, moreover, has been adequately dealt with elsewhere. Revisions on the surface modification in ME have been reported [58-65]. Since modification of chips was driven by different aims, this is sometimes the criterion for making a classification of the modification procedures: modulation of the EOF, solid-phase extraction, suppression of protein adsorption, electrophoretic separations, or design of biochips/ arrays [61]. On the other hand, in other revisions [58,60], classification into dynamic coating with surface-active compounds that presents physical adsorption, and permanent coating with molecules that are covalently bound through functional groups, is made. Subclassification attending to the material, glass/quartz, or plastic devices is possible. Several approaches for surface modification of glass substrates have been transferred from classical capillaries in CE to ME,

but various different approaches were generated for the new materials employed in ME. Concretely, most of the developments are made for polymers [18,58,61,62], which are cheaper and employ simpler fabrication procedures, PDMS being the most popular [58,62,66]. In reported reviews, the special case of wall [60] / permanent [62] coatings for protein separations is considered. In this chapter, the most important modifiers employed in ME as a strategy for improving the resolution are commented upon. As a summary, in **Fig. 1** all the considerations that have to be taken into account when a surface modification is going to be performed and the criteria that can be followed for classifying the modification procedures are schematized.

2.5.1. Surface micro- and nanostructuring

Microchannel surfaces can be modified by different means. One of these is to construct on the microchannels special micro- and nanostructures that differentiate the passage of similar molecules. Electrophoresis over nanopatterned surfaces has some analogies with gel electrophoresis, taking into account that the gel is replaced by nanofabricated structures. Depending on the dimensions, they can act as a sieving matrix. The main advantage of such structures is the uniformity of spacing and size of the obstacles and their robustness for repeated use [67]. Surface morphology or surface roughness of the microchannels undoubtedly has an effect on separation quality; the influence of surface microstructures on the separation efficiency in glass ME has been evaluated for the model system DA–EP, molecules that differ only in a hydroxyl group [68]. However, even though these structures have been applied to the separation of small analytes, the main application is found for large molecules, such as DNA. Thus, nanochannels with crosssections as small as 10 nm x 50 nm allow the elongation of very long biopolymers by space confinement. They can be gently elongated and analyzed [69]. Special networks such as nanoslit arrays were imprinted in PMMA, cyclic olefin copolymer (COC), and PC fluidic devices using a nanoimprinting tool for studying the double-stranded DNA electrokinetic transport mobility [70]. Nanoscaled structures inside microchannels such as nanopillar, nanoball, and nanofibers contribute to obtaining higher performances in DNA separations [71]. In these cases, the flow passes through the different motifs and, since the size of analytes approaches that of the structures, transport is affected and separation can be improved. Actually, a rectangular array of micropillars was used to replace gels [polyacrylamide (PA) or agarose] to perform electrokinetic separation, since the microarray mimicked a highly diluted gel [72]. Instead of using a regular array of posts or holes, size separation of DNA molecules can be achieved by using anodic porous alumina as a separation medium [73]. The bed of the microfluidic channel

was made of a porous alumina membrane having nanoscale pores on its surface. Larger molecules eluted first as the small ones are much more frequently trapped by the nanopores. This is a field that is probably going to increase with the development of nanotechnology, and promising work on the modification with ordered structures of controlled dimensions is expected.

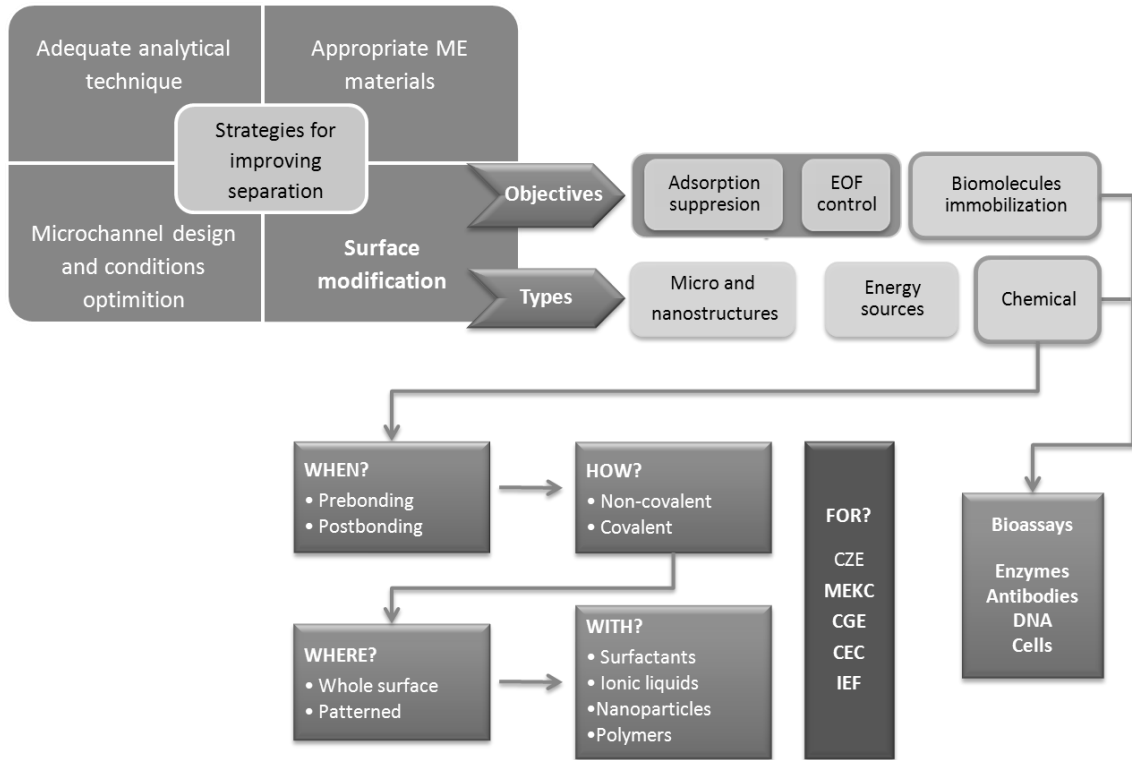


Figure 1. Classification of surface modification procedures according to diverse criteria.

2.5.2. Employment of energy sources

When dealing with surface modifications, two main options are possible: physical or chemical. It is known that exposing materials to various energy sources (i.e., oxygen plasmas, UV light, and corona discharges) can alter surface properties. Plasma is a mixture of electrons and ions with high energy. This modification employs gases such as oxygen, nitrogen, and hydrogen, which dissociate and react with the substrate surface, creating chemical functional groups. UV treatment can also be employed, with the advantage that it facilitates much deeper modification of the surface. On the other hand, chemical vapor deposition (CVD) is a chemical process used to produce a thin film on a substrate surface by means of the deposition of gaseous molecules, which react chemically on the surface. The sequence of events is typically sublimation, pyrolysis, and deposition. PDMS is the material in which these

treatments were mostly employed [66], exposure to oxygen plasma being, by far, the approach most often employed, as will be shown later in this chapter, in **Table 5**.

Surface modification of PDMS by Tesla coil oxidation can be utilized to yield a hydrophilic surface that is capable of possessing a significant zeta potential at high pH values. The Si-CH₃ groups on the PDMS surface can be modified through oxidation to Si-OH [74]. Three consequences can be envisaged. First, the surface is much more hydrophilic, enabling facile filling of the micron-sized channels with aqueous buffers. Second, the surface now closely resembles glass in terms of functionality (Si-OH) and, as a result, a strong EOF, very similar to glass, results at pH values above the pKa of the silanol group [75]. Third, the oxidized surface is able to form a permanent bond when placed in conformal contact with a similarly oxidized piece of PDMS. Nevertheless, the modification is only temporary because the hydrophilic surface begins to revert back to its original hydrophobic form, exhibiting a 75 % decrease in flow in less than 24 h. The process can be slowed somewhat by contacting with a buffer solution, but finally it reverts to its original form [76]. However, when the PDMS surface is derivatized with 3-aminopropyltriethylsilane (APTES) following oxidation, the modification is stable for more than 10 days [77].

The goal of this chapter, however, is to present another possibility for surface modification, namely by using chemical reagents. This does not mean that a choice has to be made between the two possibilities (physical or chemical modification) because in most cases (see **Table 5**) the physical treatment is employed as a pretreatment that prepares the surface for further chemical modification.

2.5.3. Chemical surface modification

There is a wide range of reports on the use of surface chemistry in order to add new functionalities. This would advance the introduction of more steps in the same device, which will approximate the concept of LOC devices. However, different objectives can be pursued with the addition of new functional groups. On the one hand, improvements in the separation in ME devices are one of the objectives, which normally is related to EOF control and elimination of analyte adsorption. This objective is the aim of this chapter and is considered in the following sections. However, on the other hand, high immobilization capacity and low nonspecific binding are aimed at for the development of bioassays. Summarizing, the purposes of modifying the surface of microfluidic devices fall into two main categories: improvement of the surface properties for normal functioning of the devices (this includes EOF control that greatly affects the separation efficiency and precision of analysis, control of the adsorption of

biological components, modification of the hydrophobic/hydrophilic character of some materials, etc.) and functionalization of the surface to tailor the device to a specific use [78]. In addition, in this section different considerations depending on when, where, or how the modification is made are discussed, in addition to the electrophoresis mode that is commonly employed.

Application to Bioassays. Surface chemistry procedures can be shared with those employed in bioassays such as arrays for DNA or protein determination [79]. In conventional solid-phase immunoassays (and bioassays in general), a long incubation time is a result of inefficient mass transport by molecular diffusion from the solution to the solid surface, although the immunoreaction itself is a rapid process [80]. The use of microfluidic devices is very appropriate for this type of analysis. However, because of the large surface-to-volume ratio of the microchannels, controlling the surface properties becomes one of the most critical issues in developing those assays. Conventional passive adsorption of bioreagents on the surface often causes protein denaturation and reduces functional sites or activities. Therefore, developing an efficient surface modification method to enhance the binding efficiency and activity is critical in bioassay development. Poly(ethylenimine) (PEI, MW 75,000 Da), which produces amine functionalization, allows binding of antibodies *via* glutaraldehyde interaction, with 10 times more active antibody bound to the surface. The results were superior to those obtained with other amino-bearing chemicals such as poly(allylamine hydrochloride) (PAH), hexamethylenediamine (HMD), and 1,3-diaminopropane (DAP). The amine-bearing polymers give a better response than small diamine molecules because the spacer function of polymers can preserve most of the biological activity of the bound protein molecules [81]. Antibodies directed toward human cardiac troponin I were immobilized on the internal surface of the PDMS channel on which a protein G layer that enhances proper orientation of the antibodies had been generated by silanization [82]. This was done by injection of 7-octenyltrichlorosilane and further oxidation of the vinyl groups into carboxylic groups. N-(3-Dimethylaminopropyl)-N-ethylcarbodiimide (EDC) and N-hydroxysulfosuccinimide (sulfo-NHS) were injected into the channel to activate the carboxyl groups and protein G was anchored via chemical reaction between its free amino groups and the NHS-activated carboxyl groups. However, not only PDMS is employed as a substrate material for immunoassay development, immobilization of antibodies on PMMA microchannels has also been effected using PEI containing

abundant NH_2 groups to immobilize the monoclonal antibodies covalently for the determination of α -fetoprotein (AFP) [83].

Combination of pillar arrays and grafting with hyperbranched polyglycerols (HPGs) on an amine-modified PDMS was applied for the selective capture of positively charged proteins (avidin). The charge density on grafted HPG was optimized to minimize the nonspecific protein adsorption and increase the selective capture [84].

Surface modifications can be performed with the aim of carrying out bioassays, and in this field not only immunoassays are considered but also DNA hybridization assays. In this case, the final objective is the immobilization of the affinity reagent. Chemical modification of PDMS by curing a mixture of undecylenic acid (UDA) in PDMS prepolymer on a gold-coated glass slide was performed. This gold slide had been previously pretreated with a self-assembled hydrophilic monolayer of 3-mercaptopropionic acid (MPA). During curing of UDA–PDMS, the hydrophilic UDA carboxyl moieties diffused toward the hydrophilic MPA carboxyl moieties on the gold surface. Once completely cured, the PDMS is peeled off the gold substrate, exposing the interfacial carboxyl groups, which are available for subsequent attachment of 50-amino-terminated DNA oligonucleotides via amide linkages [85]. Further, DNA extraction from samples can be performed by a procedure based on the electrostatic interaction between amine groups (from APTES) or 3-[2-(2-aminoethylamino)ethylamino]propyltrimethoxysilane (AEEA) on a solid support (silicon wafer with a microchannel that after functionalization is enclosed with PDMS) [86].

It is clear that for the development of bioassays, immobilization of reagents is often required. The absence of functional groups makes the immobilization of reactive coatings with excellent adhesion difficult when deposited in thin films. For this type of applications, glass is not very appropriate because of its intrinsic stiffness and its incompatibility with soft materials for making valves and actuators. Poly(*p*-xylylenecarboxylic acid pentafluorophenol ester-*co*-*p*-xylylene) (PPX-PPF) was deposited on the luminal surface of PDMS. The high chemical reactivity of their functional groups supported conversion with biological ligands, proteins, and cells [87]. PDMS microchannels with a poly(*N*-isopropylacrylamide) (PNIPAAm)-grafted surface were employed for cell-based assays. PNIPAAm is a type of thermoresponsive smart polymer that exhibits a reversible phase transition at around 32 °C (lower critical solution temperature, LCST). At temperatures below its LCST, the polymer chains swell and

become hydrophilic, whereas at temperatures above the chains collapse and become hydrophobic [88]. When PNIPAAm is grafted on to different substrates, cells can adhere and proliferate at temperatures above the LCST. The adhering cells can be detached from the surfaces by lowering the temperature to below the LCST without the help of trypsin digestion. The most attractive properties of PDMS are biological compatibility and gas permeability, and therefore it has been chosen for cell culture [89] and cell-based assays [90].

Proteolysis is a key process for protein sequencing in proteome research. High-quality alternatives for conventional in-solution digestion of proteins that is time consuming are needed. Immobilizing protease enzymes on the channel walls of microchips for further coupling to mass spectrometry (MS) produced a layer that is more stable and highly resistant to environmental changes. Moreover, it provides molecular-level interactions between the immobilized enzymes and the flowing protein substrates. Trypsin is a proteolytic enzyme that has been immobilized on the channel walls of microchips by sol-gel encapsulation [91], covalent linking [58], or layer-by-layer (LBL) procedures with multilayer assembly of chitosan and hyaluronic acid [92], or poly(diallyldimethylammonium chloride) (PDMA) and nanozeolite crystals [93]. In these cases, as in the majority, microchannel surface modification has been reported but special and interesting cases of a different type of ME-modifications can be found. Fibers made from various substances are versatile materials that can be employed as platforms for protein digestion. A piece of trypsin-immobilized glass fiber was inserted into the channel of a PMMA microchip to fabricate a core-changeable microfluidic bioreactor. The reactor could be regenerated by changing the core, which consisted of a piece of glass fiber and a layer of trypsin immobilized on a silica coating [94]. The reactor was prepared by a sol-gel method with tetraethoxysilane (TEOS) and APTES as precursors, offering a porous surface to accommodate trypsin. It was immobilized on the primary amino group-containing coating (from APTES) with the aid of glutaraldehyde. The original waste reservoir was cut off to leave the channel outlet for inserting the fiber core in such a way that 3mm protruded outside the channel outlet, facilitating its removal.

When is the surface modification made? It is said that the next generation of microchips will incorporate more diverse surface functionalities in already complex geometries, requiring advanced methods for patterning the internal surfaces of the microchannels. One of the issues that have to be taken into account is that the

modification of the microchannel surface is far less amenable to the patterning methods employed for planar surfaces. Two different approaches, prebonding and postbonding modification, are possible. The first one is effective for selected systems; however, in many cases the bonding conditions can damage the surface treatment. The second one has the advantage of using highly effective bonding methods. Moreover, modification can be carried out immediately prior to microchip use, avoiding aging of the surface chemistry in the time between fabrication and application [66]. This type of modification also circumvents potential alignment problems, where chemical patterns are required at specific locations within the microchannel network and offer the reuse of expensive or difficult-to-fabricate microfluidic devices by chemically stripping under flow. Postbonding modification methodologies such as laminar flow and capillarity, photolithography, use of microplasmas, and electrochemical biolithography have recently been reviewed [95]. In most of the cases commented upon here, postbonding procedures with introduction of reagents *via* flow through the channels, either by capillarity or by external pressure, and further reaction/adsorption at the channel walls are performed. Alternatively, and especially with covalent coatings, this is made in one of the plates that is further sealed with the other microchip plate.

Where does the modification takes place? Another aspect to be considered is the homogeneity of the modified microchannel surface. Most of the procedures achieved homogeneous modification but exclusive modification of discrete regions will be required in the near future, where microchannel walls are no longer simply guides for fluid flow but important instruments in the functionality of microchips. Here, greater spatial control over surface modification to perform more complex designs is needed in addition to the development of inexpensive polymers for disposable biochips [95]. In this case, it should be noted that prebonding patterning with inorganic materials (metals, metal oxides, etc.) can facilitate postbonding patterning of less robust materials (organic self-assembled monolayers, proteins, DNA, etc.). Metallic materials can act as electrodes that provide a suitable platform for postbonding surface biomodification by electrochemical methodologies [96,97]. Moreover, photopatterning of the channels by UV-mediated grafting is possible, either before assembling the microchip plates [98] or directly in the microchannel [99], as will be commented on in the section dedicated to polymer modifications.

How is the modification performed? In most of the reports and related reviews, modification is classified in dynamic and static or noncovalent and covalent coatings. The first is the easiest way for surface modification and usually surfaceactive or other components such as polymers or nanostructures are included in running buffers. Alternatively, they can be added to the sample reservoir or employed first in a preliminary treatment. Since a not very strongly adsorbed layer is formed on the wall surface, this is sometimes referred to as a pseudostationary phase (PSP). The benefit of this approach is that uncomplicated procedures are employed apart from the fact that the “one-time use” approach allows continuous regeneration and absence of a stationary phase carry-over effect. The dynamic coating therefore has the same basis of disposable devices, something simple that can be employed each time for improving the resolution. Among the aims of dynamic modifiers is to control/change the EOF, whose velocity is given by the equation [100]:

$$\mu_{eo} = (\epsilon_0 / 4 \pi \eta) E \xi$$

where ϵ_0 is the dielectric constant; η is the solution viscosity, E is the electric field strength in $V\text{ cm}^{-1}$, and ξ is the zeta potential that depends on the surface charge. Therefore, the dynamic modifier can act by altering the viscosity or the surface charge, both with effects on the EOF. Low cost and ease of performing procedures are achieved simply by physical adsorption of molecules on a surface. However, dynamic coatings are degraded with electrophoresis or cause problems when coupled with some types of detection such as MS [101]. Therefore, another possibility is a permanent or covalent coating that is generated when a chemical compound is covalently bound to functional groups of the surface. In this case, and by comparison with chromatographic methods, a stationary phase is created. This subject is one of the focuses of research because improving resolution is still among the problems to be solved in electrophoresis, and there are many papers related to capillary coatings and surface modifications in recent reviews on CE [102].

What electrophoresis mode is the modification made for? Referring to the electrophoretic modes, most of the treatments are performed for capillary zone electrophoresis (CZE) in microchips but treatments are also advantageous for other modes, such as isoelectric focusing (IEF). Immobilization of hydroxypropylcellulose (HPC) and poly(dimethylacrylamide-co-allyl glycidyl ether) (PDMAAGE) on glass and PDMS microchips demonstrated that a coating was needed to avoid pH gradient drift [103].

Both coatings were efficient on glass microchips, but only the second one allowed focusing of *pI* markers on PDMS microchips. A double coating using PDMA-AGE and methylcellulose (MC)–Tween-20 was employed for the separation of *b*-peptides in cerebrospinal fluid by gel electrophoresis in PDMS microchips [104].

Gel electrophoresis is one of the most commonly employed modes because of its applicability to DNA separation and new gels are continuously appearing in order to improve resolution, such as the cholesterol-bearing pullulan nanogels [105]. The formation of the gel is due to weak hydrophobic interactions between cholesterol molecules above 30 mg mL⁻¹ and can be easily deformed by external forces. Thus, the loading process of the nanogels into the microchannels becomes easier. Gel electrophoresis has frequently been combined with the use of surfactants (*e.g.*, sodium dodecyl sulfate polyacrylamide gel electrophoresis, SDS-PAGE), and also surfactants are the basis of the micellar electrokinetic chromatography (MEKC) mode, due to the formation of micelles that allows the separation of neutral molecules and the improvement for ionic analytes because of the differential interaction with micelles. Although surfactants will be considered in this chapter, these modes will not be exhaustively considered. Some special cases that refer to surface modification will be commented upon. Referring to the CE modes, electrochromatography is also sometimes involved where the use of stationary or PSP is concerned. Electrochromatography is a technique that combines the efficiency of electrophoresis with the selectivity of chromatography. In capillary electrochromatography (CEC), three different types are generally distinguished, based on the capillary column used: packed, open-tubular, or monolithic. Porous polymer monolithic materials, which emerged in the early 1990s [106], have become popular owing to their ease of preparation. The first syntheses of organic monoliths were carried out in glass chips [107], but different materials, such as cyclic olefin copolymers (COCs) that are compatible with a broad range of chemicals and solvents, can be employed. As an example, a lauryl methacrylate monolith was synthesized into a COC microdevice for reversed-phase electrochromatography [108]. A fourth type of CEC can also be distinguished, which uses a PSP, micelles being the first PSP to be used in the MEKC technique. Other macromolecular entities such as liposomes, proteins, cyclodextrins, dendrimers, and nanoparticles (NPs) can be employed. In this case, they can be considered as modifiers. The use of NPs will be particularly considered in this chapter. Frontiers are not rigid and therefore a PSP–CEC methodology with micelles can be considered MEKC or NP-PSP as a dynamic coating for CZE. In the same manner, a surface

modification for improving separation such as a static coating for CZE can be considered as a CEC. It depends on the focus: if the coating produces a differential interaction of the analytes, a CEC methodology can be considered; if the coating just modifies the surface for avoiding adsorption or controlling the EOF for improving resolution, a CZE mode with modifiers can be considered.

3. Chemical Modifiers

Chemical modifiers are a group of substances with varying properties such as size, charge, functionalities, and so on that affect the performance of electrophoresis, especially in the case of ME, where the area-to-volume ratio is very high. The use of organic solvents has been extended to the use of electrolyte solutions prepared from pure organic solvents or their mixtures in NACE [109]. Organic solvents can solubilize compounds hardly soluble in water and thus afford the possibility of separating such compounds by CE. Moreover, their physical and chemical properties can offer large changes in separation factor/resolution, analysis time, selectivity, and reduced electrophoretic currents. Therefore, changing organic solvents, usually amines (*e.g.*, diethanolamine) or alcohols (*e.g.*, methanol), which are the most common, or varying the proportions allows a simple tuning of separation.

Special consideration will be given to other types of modifiers: surfactants, ionic liquids, nanostructures, and polymers. Special modification procedures such as sol–gel protocols make modification possible with different types of chemical modifiers, but they are scarce. Sol–gel methods can be employed to fabricate PMMA electrophoresis microchips with a hydrophilic channel wall. TEOS is injected into the channel and is allowed to diffuse into the surface layer for 24 h. After removing the extra material, the channel is filled with acidic solution for 3 h, flushed with water, and maintained in an oven to obtain a sol–gel-modified PMMA microchip [110]. In this chapter, however, only the four types commented on at the beginning of the paragraph will be considered.

In **Fig. 2**, we present histograms with the number of publications in which surfactants, ionic liquids, and NPs appeared in relation to CE or ME in the period from January 2000 to April 2011. Several differences can be seen. First, the use of surfactants as modifiers is a well-established methodology. Even though a slight increase over the years can be noted, they have been employed from the beginning of the decade. Actually, SDS has long been used in well-known methodologies such as SDS-PAGE and MEKC. Further, there has been an increase in use in recent years, not only for CE but also for ME.

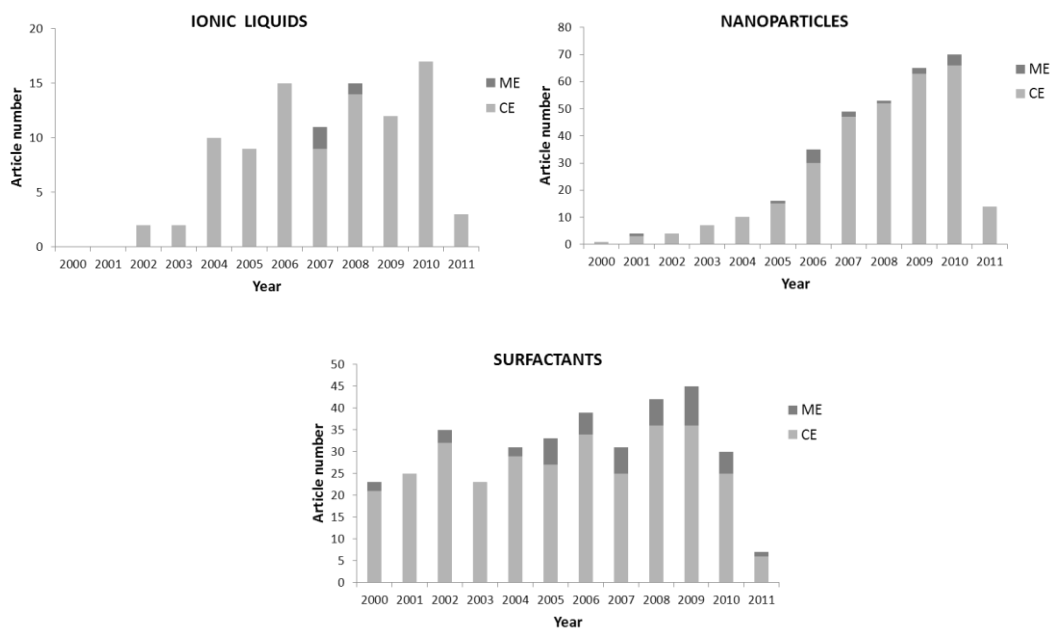


Figure 2. Number of publications in which surfactants, ionic liquids, and nanoparticles appeared related to CE or ME applications. ISI Web of Knowledge, April 2011.

The words “surfactants” and “capillary electrophoresis”/ “microchip electrophoresis” were employed for the Internet search. It should be noted that when “SDS” was employed instead of surfactants, for CE, the number of articles was at least doubled (*e.g.*, it changed from 21 to 42, from 27 to 53, or from 25 to 57 for the years 2000, 2005, and 2010, respectively). In the case of ME devices, the search was refined with the terms “SDS,” “CTAB,” “Triton X-100,” or “Tween 20” and the results were checked to avoid duplication. The search was also performed with “microchip capillary electrophoresis” for all the modifiers, since this term was more used at the beginning of the decade. The results were also cross-checked to avoid repetitions.

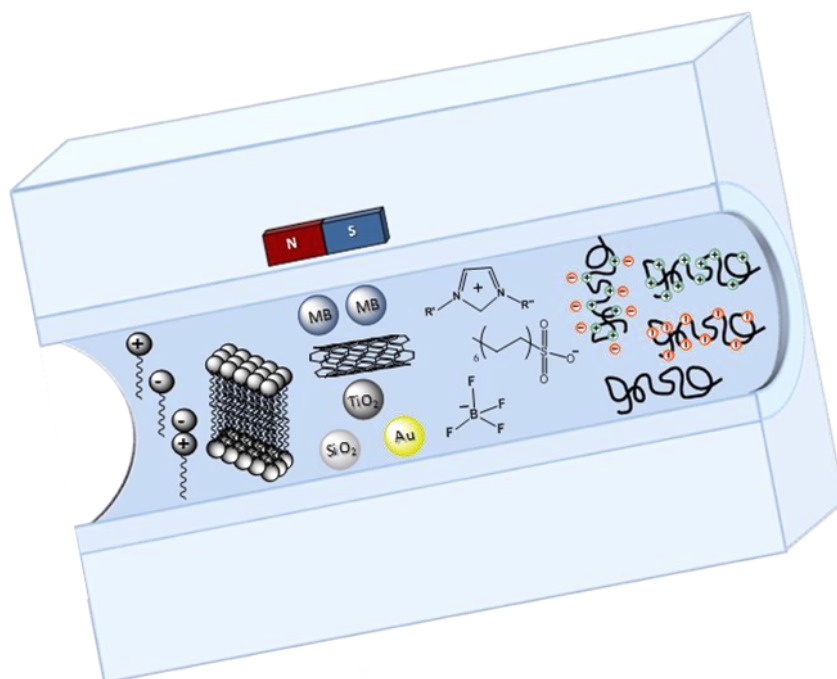
The case of ILs and NPs is totally different from that of surfactants. In both cases, the research in this field, in combination with CE, originated in 2002 and 2000, respectively, and an increase (continuous in the case of NPs) can be seen. The situation for ME is slightly different. In the case of NPs, the first work of the decade appears in 2001 and a continuous increase is seen from 2005 to date. However, in the case of ILs, first works appeared in 2007 and 2008, and no further research is reported to date. The words employed in the search were “ionic liquids” and “capillary electrophoresis”/“microchip electrophoresis” as well as “nanoparticles” and “capillary electrophoresis”/“microchip electrophoresis.” Refinement was made for ME with “background additive” for ILs and “nanotubes”/“nanostructures” for NPs.

Therefore, it can be concluded that surfactants are widely employed for electrophoresis methodologies and an increase in their use is expected. The field of application of ILs is still unexplored in ME, and in the case of NPs, an almost exponential increase is suspected. The number of publications is significant for 2010: the number of publications on NPs overtook that for surfactants. Moreover, new materials are continuously being incorporated (*e.g.*, graphene, NPs of smaller sizes, and new functionalizations) and future possibilities are still unknown.

In the following sections, these modifiers will be considered in more detail. It has to be taken into account that some procedures can employ more than one type of modifier. An explanatory scheme with the different types of modifiers is presented in **Fig. 3**, together with the classification of the modifiers that have been employed in ME. In further sections, each modifier will be considered in depth. This chapter does not try to provide exhaustive information, but explains the more representative strategies. Some more information can be found in the tables and in the reviews that are cited in the text.

3.1. Surfactants

Surfactants are considered among the small molecules that can be used as modifiers. It is known that the use of small molecules has some effect on the separation. Owing to the nonpolymeric nature of these additives, any physically adsorbed layer on the surface is likely to be fairly thin [63]. Salts, amines, and surfactants have been reported as additives for improving protein separations by capillary and chip electrophoresis [63]. Surfactant is an abbreviation for surface-active agent, which literally means “active on a surface.” The surface can be established between a solid and a liquid, between air and a liquid, or between two immiscible liquids. The primary property of a surfactant in a solution is that the concentration of the surfactant is higher on the surface than in the bulk of the liquid. Thus, the surfactant concentrates on the surface, where it is active. Surfactants consist of a hydrophilic group (anionic, cationic, nonionic or amphoteric) and a hydrophobic group, hydrocarbon chains in the majority and usually linear because of the demand for biodegradability (commonly between C10 and C16). The hydrophilic group determines the main differences between the majority of surfactants, the hydrophobic group being the largest part of the molecule. As noted earlier, one of the drawbacks of hydrophobic materials (*e.g.*, PDMS) is that they adsorb organic solvents and hydrophobic analytes due to their hydrophobic surface, causing fouling of the material and poor separation efficiency. Surfactant-based dynamic modification is a favorable method to avoid these adsorptions owing to its versatility and low cost.



- | | | | |
|----------------------|---|----------------------|--|
| Surfactants | <ul style="list-style-type: none"> - Anionic - Cationic - Zwitterionic - Nonionic - Phospholipid bilayer | Nanoparticles | <ul style="list-style-type: none"> - Carbon nanotubes - Titanium dioxide (TiO₂) - Silica (SiO₂) - Gold - Magnetic beads |
| Ionic liquids | <ul style="list-style-type: none"> - Cations { <ul style="list-style-type: none"> - Imidazolium - Anions { <ul style="list-style-type: none"> - BF₄⁻ - Dodecanesulfonate | Polymers | <ul style="list-style-type: none"> - Polyelectrolyte brushes - Cationic - Anionic - Neutral |

Figure 3. Scheme of the different types of modifiers that have been employed in combination with ME.

Surfactants can be classified according to their ionic (cationic, anionic, zwitterionic) or nonionic character, SDS (anionic) and cetyltrimethylammonium bromide (CTAB) (cationic) being the most commonly employed. Although usually a surfactant is associated with small molecules, nonionic polymers such as Tween 20 (polysorbate surfactant with three hydroxyl groups *per* molecule) and Triton X-100 (nonionic surfactant with a hydrophilic PEO group) are also widely employed. Other less common surfactants can be combined for the better performance of ME devices. n-Dodecyl b-D-maltoside (DDM) is an alkylpolyglucoside that adsorbs strongly on hydrophobic surfaces forming a monolayer, which causes the surface to become hydrophilic and nonionic, thus reducing the interaction between proteins and PDMS surface [111].

A review that considers the perspectives of surface treatment in electrophoresis and lab-on-chips [57] differentiates between thin and thick films when preparing coatings. The

most common method for the build-up of thin films is Langmuir films (Langmuir–Blodgett films by transferring the first to a solid substrate). They are prepared from amphiphilic molecules scattered on the surface of a liquid, in such a way that the hydrophilic headgroup positions at the water/film interface while the hydrophobic end group sticks out from the film/solid interface. These films are mostly bonded through weak hydrogen bonds and van der Waals interactions. Self-assembled monolayers (SAMs) relate to the formation of ordered molecular assemblies that are formed spontaneously by the adsorption of a surfactant with a specific affinity of its headgroup to a substrate [112]. Single-chain surfactants, such as those noted above, have been widely employed but, in recent years, double-chain surfactants, which are also called lipid or supported lipid bilayer membranes, have been increasingly employed. On the other hand, biomimicking phospholipid membranes and liposomes are utilized in many liquid chromatography (LC) and CE techniques, either as coatings or as carriers [113,114]. Lipids can group to form different aggregates: liposomes, micelles, bicelles, and discoidal micelles. Adding PEG (PEGylation) provides structural stabilization and also prevents protein adsorption on the lipid layer [115]. Phospholipid disks based on 1-palmitoyl-2-oleyl-sn-glycero-phosphatidylcholine and 1,2-distearoyl-sn-glycero-3-phosphoethanolamine-N-[methoxy-(polyethylene glycol)] with a molar mass of 3000 were employed as a dynamic coating for SU-8 microfluidic chips [116]. The effects on surface charge and nonspecific protein adsorption was compared with those of two common surfactants, anionic SDS and neutral Tween-20, employed as buffer additives. The effect on the EOF was more prominent than that of SDS and similar to that of Tween-20. This indicates that the neutral PEG chains are able to shield the negative charges of lipids, suggesting that the disks maintain their discoid form upon immobilization on microchannel surfaces. A similar shield against nonspecific adsorption was obtained.

A negatively charged phospholipid polymer biointerface containing 2-methacryloyloxyethylphosphorylcholine (MPC), n-butyl methacrylate (BMA), potassium 3-methacryloyloxypropylsulfonate (PMPS), and 3-methacryloxypropyltrimethoxysilane (MPTMSi) moieties was synthesized to introduce such phosphorylcholine segments and also surface charges on to a silica-based microchannel. Along with another uncharged copolymer, poly(MPC-co-MPTMSi), the regulation of the surface charge density can be realized by adjusting the initial concentrations, providing a feasible approach to controlling the EOF, especially in systems with biological applications requiring neutral buffer conditions [117].

In **Table 1**, ME studies that employed surfactants are reported. The type of surfactant, substrate material, analyte, type of detection, and some comments are included. As can be

deduced from the references, the rows follow a chronological order. It should be noted that of the ten oldest references, eight employed SDS, and of the most recent ten, only two used this surfactant. Referring to the material, initially most of the microchips in these studies were made of PDMS, later glass was the material of choice, and nowadays there is a coexistence of glass and polymers. Fluorescence is the most common principle of detection, followed by the use of electroanalytical methodologies (amperometry and conductometry).

Table 1. Studies related to ME with employment of surfactants

| Surfactants | ME Material | Analyte | Detection | Comments | Ref. |
|--|-----------------------|---|----------------------------------|---|------|
| Phospholipid disks | SU-8, PDMS, glass | BSA | Fluorescence | Reduce adsorption | 117 |
| Zwitterionic surfactants | PDMS | Perchlorate | Contact conductivity detection | Separate perchlorate from common water anions | 118 |
| SDS | PMMA | Proteins | LIF | 2D separation: SDS μ -CGE with μ -MEEKC | 119 |
| Tween-20 | PDMS | Peptides | Fluorescence | MGE | 104 |
| DTAC and DDM | PMMA | N-linked glycans | LIF | Reduce adsorption | 120 |
| Acid-labile surfactant and SDS | Glass | Proteins | Fluorescence | Surfactant effects on proteins separation | 121 |
| SDS | Glass | Small-chain aldehydes | Amperometry | Sensitive and rapid determination of harmful atmosphere | 122 |
| SDS | PDMS-glass | Biogenic amines | LIF | MEKC | 123 |
| SDS | Glass | Nitrate ester explosives | Amperometry | Multichannel microchip | 124 |
| Zwitterionic surfactant | Glass | PB-amines and amino acids | Fluorescence | MEKC | 125 |
| SDS + MeOH | Glass | Serotonin, tryptophan, propranolol, and acetaminophen | UVabsorbance and UV fluorescence | MEKC | 126 |
| Zwitterionic surfactant | PDMS | Atmospheric aerosol | Conductivity | MEKC | 127 |
| SDS | Glass | Lipoproteins | LIF | Rapid diagnostics | 128 |
| SDS | PMMA | Proteins | LIF | CGE + MEKC | 129 |
| SDS | Glass | Proteins | LIF | Size-based protein separation | 130 |
| SDS | Glass | Endotoxins | LIF | MGE | 131 |
| SDS | PMMA | Proteins | LED | MGE | 132 |
| SE ₈ S, SD ₁₀ S, SD ₁₂ S and ST ₁₄ S | PDMS | Phenols | PAD | Adsorption behavior | 133 |
| SDS + MeOH | Glass | Nitrated benzodiazepines | LIF | MEKC | 134 |
| SDS | Glass | Virus | LED | SEC | 135 |
| SDS | PDMS | NDA-amino acids | Fluorescence | Increased reproducibility | 136 |
| SDS + PAMAM | Glass | Cationic neurotransmitters | Amperometry | CZE | 137 |
| SDS | Glass | Rhodamine derivatives | LIF | MEKC | 138 |
| CTAB | Glass | Anionic species | Conductivity | Reverse the EOF | 139 |
| SDS | PDMS-PDMS, PDMS-glass | Neuropeptides | Fluorescence | On-chip electrokinetic sample stacking | 140 |
| Tween 20 | PDMS | Amino acids | Amperometry | Reduce adsorption | 141 |

| | | | | | |
|--------------------|------------|--|--------------|--|-----|
| SDS | PDMS | Amino acids | LIF | MEKC | 142 |
| SDS, PA, DOCh | PDMS | Glucose, penicillin, phenol, and homovanillic acid | PAD | Decrease analysis time and increase electrochemical response | 143 |
| CTAB | Glass | Inorganic arsenic | Fluorescence | Reverse the EOF | 144 |
| SDS | PDMS | Carbohydrates | iPAD | Improve separation and detector response | 145 |
| SDS | Glass | NBD-DL-amino acids | LIF | Enantiomeric separation | 146 |
| Triton X-100 | PDMS-glass | Rhodamine B | LIF | Reduce adsorption | 147 |
| SDS | PDMS | Glucose and glucosamine | PAD | Signal enhancement and flow stabilization | 148 |
| SDS + α -CD | PMMA | AAs | LIF | Serpentine MCE | 149 |
| SDS | Glass | Lipoproteins | LIF | Rapid diagnostics | 150 |
| SDS | PMMA | Proteins | Conductivity | MEKC | 151 |
| SDS | PDMS | | Fluorescence | CZE | 152 |
| SDS + γ -CD | Glass | FITC-amino acids | Fluorescence | MEKC | 153 |

CD, cyclodextrin; CGE, capillary gel electrophoresis; DTAC, n-dodecyltrimethylammonium chloride; iPAD, indirect pulsed amperometric detection; LED, light-emitting diodes; LIF, laser-induced fluorescence; mCGE, microcapillary gel electrophoresis; mMEEKC, microemulsion electrokinetic chromatography; PAD, pulsed amperometric detection; SD10S, sodium decyl sulfate; SDS (equivalent to SD12S), sodium dodecyl sulfate; SE8S, sodium 2-ethylhexyl sulfate; ST14S, sodium tetradecyl sulfate; SEC, size-exclusion chromatography.

3.2. Ionic liquids

Room-temperature ILs are compounds formed of organic (commonly nitrogen-containing) cations and inorganic or organic anions that are either liquid at room temperature or whose melting points are slightly higher than ambient temperature. Any salt with a melting point below 100 °C is considered to be an IL [154], whereas those with higher melting points are referred to as molten salts. Although ILs were first reported in 1914 [155], it was not until 2000 that they were widely exploited. Applications are increasing: from large potential window electrolytes in electrochemical devices, media for enzyme catalysis, solvents in organic synthesis or extraction processes to sensor layers or modifiers in analytical separations. Their application in analytical chemistry [156], especially in separating analytes [157], is merited because of their unique properties (hydrophobicity, water solubility, viscosity, conductivity, acidity, etc.). They can be tuned depending on the anions (usually chlorides, hexafluorophosphate, tetrafluoroborate, etc.) and cations (heterocyclic aromatic ions, quaternary ammonium, phosphonium, etc.). Since ILs are not used as pure solvents, but rather diluted in aqueous solutions, they are just salts, and therefore the influence of the cations and anions has to be considered, although too often the properties of the cations are taken as the properties of the IL itself [157].

In this context, ILs, initially based on tetraalkylammonium ions, have been employed as modifiers in CE. An excellent review on the combination of IL and CE [158] focuses on two

different approaches: application of CE for the analysis of ILs and application of ILs in CE. In the later context, ILs are considered for sample treatment before CE analysis or for CE resolution enhancement. The high capacity to interact/solvate analytes, the high tendency to be adsorbed on silanol groups of the capillary wall and change the EOF providing dynamic coatings, the change in the ionic strength, conductivity, and viscosity of the BGE, or the formation of a stationary (CEC) or PSP because of the capacity of some ILs to form micelles (MEKC) being some of the reasons for the improvement. Although ILs have been employed in combination with CE, their use in ME is very scarce (see Figure 6.2). Referring to CE, most of the studies employed imidazolium cations, 1-ethyl-3-methyl [159,160] as the most common followed by 1-butyl-3-methyl [161,162] substituted. (S)-(–)-2-Hydroxymethyl-1,1-dimethylpyrrolidinium was also employed as a cation [163]. In this case, there is suppression of the magnitude of the EOF and a gradual change in its direction. Therefore, this IL was employed as an alternative to cationic surfactants for the determination of tricyclic antidepressants.

Concerning the anions, most of them are BF_4^- apart from bis(trifluoromethanesulfonyl)imide (NTf₂) [164] or acetate, fluoroacetate, heptafluorobutanoate [109], or dodecyl sulfate [165]. ILs have been employed in NACE since alkylimidazolium- and alkylammonium-based salts are well soluble in organic solvents and can be successfully used as BGE components [109]. Different molecules such as nicotinic acid and structural isomers [160], anthraquinones [161], benzodiazepines [164], and the amino acids proline and hydroxyproline [165] have been separated. However, the differences between the materials employed in the two methodologies (CE and ME) make a thorough study necessary.

Only a few reports have appeared on ILs combined with ME devices and most of them were for the analysis of proteins and peptides. In **Table 2**, studies reported for IL combined with ME devices (glass, PDMS, and hybrid PDMS–glass) are presented. In all cases, the detection method was laser-induced fluorescence (LIF).

The effect of ILs used as supporting electrolytes was studied for Rhodamine B and fluorescently labeled streptavidin and IgGs. A hybrid coating with IL (1-ethyl-3-methylimidazolium tetrafluoroborate, EMIm BF_4) [which gave better results than BMIm BF_4 (1-butyl-3-methylimidazolium) tetrafluoroborate] and BMIm hexafluorophosphate (PF_6), which possess butyl radicals, and the nonionic surfactant Triton X-100, produced a more efficient modification [166]. This IL, which possesses high conductivity, low viscosity, miscibility with water, and good solvating properties, was also employed in combination with an anionic

surfactant (SDS) [167]. EMIm BF₄ was directly employed as the supporting electrolyte in a PDMS–glass microchip without adding other buffers to adjust its pH. The role of SDS is that cationic dyes (Pyronin Y in this case) can form weak fluorescent dimers with SDS, whereas when proteins are added to the dye–surfactant system, some dye dimers turn into monomers, resulting in fluorescence enhancement of the dye–surfactant system. On the other hand, IL was applied to overcome protein adsorption in the microchannels. Phosphate-buffered saline (PBS) and EMIm BF₄ were compared at similar concentrations and a lower background current and shorter migration time (due to an increase in the EOF) were achieved for the IL. It not only had the ability to separate hydrophobic analytes while maintaining an adequate background current, but also produced smaller Joule heating in the microchannels, which induced more rapid sample analysis and better reproducibility. The combination of IL and surfactant was designed in the same molecule, with the aim of combining the advantages of the two. In this way, 1-butyl-3-methylimidazolium dodecanesulfonate (BAS) was applied to microchip MEKC in PDMS material, obtaining an eightfold increase in the EOF [168].

Table 2. Studies Related to ME with Employment of Ionic Liquids

| Ionic Liquid | ME Material | Analyte | Detection | Comments | Ref. |
|--------------------------------------|-------------|---|-----------|--------------------------|------|
| BAS | PDMS | Cy3-extravidin and Cy3-IgG | LIF | MEKC | 166 |
| [EMIm]BF ₄ | PDMS | TRITC-IgG, Cy3-IgG, FITC-IgG | LIF | Studies with Rhodamine B | 167 |
| [EMIm]BF ₄ + Triton X-100 | PDMS-glass | BSA, bovine hemoglobine, cytochrome C and trypsin | LIF | Employment of SDS | 168 |
| [EMIm]BF ₄ | Glass | NBD-peptides | LIF | Chiral separation | 169 |

TRITC, tetramethyl rhodamine isothiocyanate; NBD, nucleotide-binding domain.

The most common IL (EMIm BF₄) exhibited great potential in the glass microchip electrophoretic separation of complex optical isomers such as peptides, when employed as the working electrolyte with chiral selectors included [169]. A chiral IL, (S)-[3-(chloro-2-hydroxypropyl) trimethylammonium] [bis((trifluoromethyl)sulfonyl) amide] was synthesized for use as both co-electrolyte and chiral selector [170], although it has not yet been employed in ME.

The influence of ILs on the separation of analytes with different ME materials has not been thoroughly studied as well as the influence of different ion compositions, including synthetic ILs. In **Fig. 4**, the electropherograms obtained for two model analytes, DA and EP, in a

native glass microchip and in a dynamically IL-coated glass ME are presented. The improvement in the separation is demonstrated through the baseline resolution of the peaks.

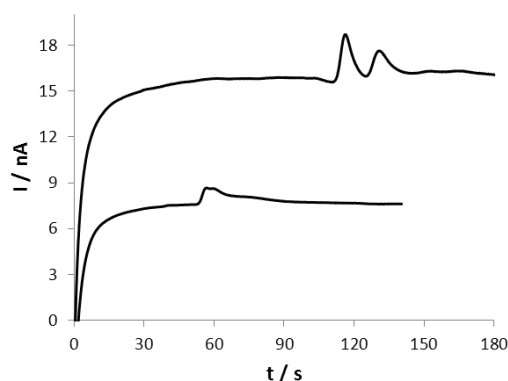


Figure 4. Electropherograms recorded in a solution of dopamine ($100 \mu\text{M}$) and epinephrine ($100 \mu\text{M}$): top curve, with IL; bottom curve, without IL. V_{sep} , 1500 V; V_{inj} , 500 V; t_{inj} , 1 s; working electrode (WE), Au wire, 100 μm diameter; E_d , 0.8V; ME material, soda-lime glass; L_{sep} , 55 mm; BGE, 25 mM MES-His, pH 5.5; IL (in case of use; 20 mM [BMIm] HSO_4^-); detection electrolyte, 0.1 M H_2SO_4 (Álvarez-Martos et al., unpublished results).

3.3. Nanoparticles

NPs are having a significant impact in many scientific fields with the advance and promotion of nanotechnology. They are particles with a size in the nanometer range, that is, up to 1000 nm, and due to their large surface-to-volume ratio they have been extensively studied in recent years in separation science. Therefore, NPs are also applied to capillary and microchip electrochromatography since they can be used as stationary phases or PSPs. NPs need to fulfill some important requirements to be suitable in PSP-CE: be able to form stable suspensions in a wide range of electrolytes, provide the desired selectivity in the interaction with electrolytes, be charged, and show equal velocity to prevent peak broadening, show small mass transfer resistance, not disturb detection, and be small so as to provide a high surface area to improve sample capacity [171]. The use of polymer, gold, and silica NPs in addition to fullerenes and carbon nanotubes (CNTs) in CE has been reviewed [172,173]. The first attempt to use NPs as PSPs in CEC was described in 1989 [174]. Even though they have many advantages, the main problem is the negative effect of NPs on UV-Vis detection due to the light-scattering properties of the NPs. Another difficulty in NP-based ME is the necessity to form stable suspensions in aqueous solutions, which often can be solved by dynamic or covalent modification of the NPs. Referring to protocols, they can be used as additives in the running buffer (PSPs) or they can act as modifiers adsorbed on the channel surface. In the

former case, they are suspended in the electrolyte solution and continuously pumped by the EOF.

In **Table 3**, studies related to the use of NPs in combination with ME are presented, indicating the analytes, detection system, and ME material employed.

Table 3. Studies Related to ME with Employment of Nanoparticles.

| Nanoparticles | ME Material | Analyte | Detection | Comments | Ref. |
|---|-------------|---|----------------------|---|------------|
| Porous liquid crystalline lipid-based NPs | COP | GFP-proteins | LIF | Reduce adsorption | 197 |
| Au | PDMS | FITC-labeled myoglobin | LIF | Reduce adsorption | 175 |
| Au | Glass | Endocrine disruptors | Amperometry | Improve separation and increase sensitivity | |
| Magnetic beads | PDMS | Peptides | LIF | Binding constants determination | 176 |
| Titanium dioxide (TiO ₂) | PDMS | Amino acids | Indirect amperometry | LBL assembly technique | 177 |
| SWCNTs | Glass | Proteins | Fluorescence | SWCNTs-PEG-acrylate hydrogel composite | 187 178 |
| Au | Glass | DNA | Amperometry | MGE | 179 |
| Au | PDMS | Dopamine, epinephrine, arginine and histidine | Amperometry | EOF-switchable MCE | 180 |
| Silica | PDMS | Neurotransmitters | Amperometry | LBL assembly technique | 181 |
| Au | PDMS | Neurotransmitters | Amperometry | LBL assembly technique | 190 |
| Au | PDMS | Neurotransmitters and pollutants | Amperometry | LBL assembly technique | 182 |
| PEGylated-latex | PMMA | dsDNA (10 bp to 2 kbp) | LED | Improved DNA separations | 183 |
| Au | Glass | Aminophenols | Amperometry | LBL assembly technique | 188 |
| Silica (SiO ₂) | PMMA | dsDNA (100 bp to 1.5 kbp) | LED | Improved DNA separations | 184 |

COP, cyclic olefin polymer.

A potential alternative for modifying the surface properties of PDMS is to use a sol-gel process to form nanometer sized silica particles throughout a polymerized PDMSmatrix. To form the particles, an alkoxysilane precursor such as tetraethyl orthosilicate (TEOS), which is soluble in the polymerized PDMS, is first hydrolyzed. Particles (~ 10 nm) are then formed through condensation of the hydrolyzed silanes. The condensation reaction is generally catalyzed using either an acid or a base. The process should result in the generation of permanent free silanol groups at the surface of the PDMS, thereby increasing the EOF and wettability. Particle formation in the bulk PDMS should also allow for irreversible sealing of

PDMS. The silanol groups on these particles should allow a wide range of surface modifications developed for glass to be used on these modified devices. This process has been extensively studied [185] and NPs have been characterized [186].

Although metallic NPs made of titanium dioxide have been reported for modifying a PDMS microfluidic channel surface by sequentially immobilizing PDDA and NPs by a layer-by-layer technique [187] (see the electropherograms in **Fig. 5**), gold NPs are without any doubt the most commonly employed. The first use of gold NPs (10 nm) was for the separation and amperometric detection of aminophenols [188]. Gold NPs form stable (red to purple) solutions with most buffer solutions used in electrophoresis. Owing to their sizes, ease of synthesis, and properties, they have been tested as additives in CE. The selectivity and efficiency increased compared with uncoated microchannels.

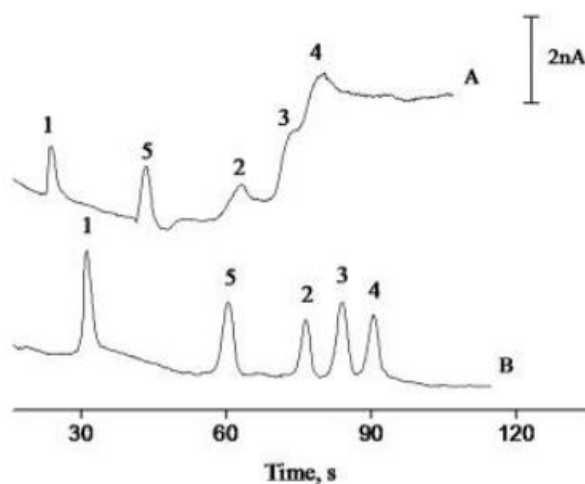


Figure 5. Electropherograms recorded for amino acids on (A) native, and (B) PDDA-TiO₂ NP-coated PDMS microchips. Experimental parameters: BGE, 5.0 mM, pH 9.2 STB; V_{inj} , 800 V; t_{inj} , 5 s; V_{sep} , 1200 V; E_d , 0 V. (1) Arginine; (2) phenylalanine; (3) serine; (4) threonine; (5) EOF. Reprinted from Ref. 187 with permission, © John Wiley & Sons, Inc.

Gold NPs can be synthesized *in situ* by infusing HAuCl₄ solution into channels and incubating at 37 °C for 48 h [189]. Once they have been formed, a stable bovine serum albumin (BSA) blocking layer can be prepared simply by incubation. The PDMS-AuNP-BSA-treated microchannel could successfully suppress protein adsorption, as demonstrated by the lack of fluorescence in a coated channel with incubated fluorescein isothiocyanate (FITC)-labeled myoglobin. Contact angle measurements revealed that the coated surface was hydrophilic.

Modification of the microchannel can be achieved by a layer-by-layer (LBL) assembly technique, employed for taking advantage of electrostatic interactions. Polyelectrolytes (PEs) are commonly employed since charges vary from one layer to the other. A simple procedure is usually employed: in this case, a PE was used as the first coating and then citrate-stabilized gold NPs were adsorbed [190]. The procedure is as simple as pumping the running buffer containing the PE through the microchip for polymer adsorption. Then, the microchip is flushed with the buffer and then with gold NP solution for a fixed time. Improvement in the separation of neurotransmitters that were detected amperometrically was achieved. Gold NPs were also employed as bifunctional linkers to immobilize cysteine on the surface. After coating a PDMS microchannel with PDDA, gold NPs were immobilized to chemisorbed cysteine *via* their –SH functionality. The unique feature of the chemisorbed amino acid is that, depending on the solution pH, the surface can have excess positive charge (low pH), no net charge (isoelectric point), or excess negative charge (high pH). As a result, the EOF can be switched by using running buffer with different pH [191].

Two different strategies were employed using LBL procedures for the separation of neurotransmitters and environmental pollutants: cationic PE (chitosan), gold NPs, and albumin in the first place, and lysozyme and albumin in the second place [182]. The adsorption properties of the microchip material (PDMS) were due to proteins. Therefore, adsorption of small molecules is avoided and separation improved. In this way, even when NPs are employed, the surface-active compounds are proteins. Gold NPs were also employed in MEKC that uses SDS as a micelle-forming agent for the separation of neutral analytes [192]. In this case, the purpose of the NPs is to provide additional interaction sites with which the solutes can interact. The presence of AuNPs in the running buffer can significantly affect the apparent mobility of the solute and also change the electroosmotic mobility of the running buffer.

Apart from small analytes, the use of NPs has been combined with DNA analysis. Gel electrophoresis sometimes caused trapping of the molecules. Gold NPs were immobilized following a more complicated procedure, consisting of a three-layer procedure: coating with PVP, PEO, and PEO–gold NPs (citrate stabilized) that produced a sharper peak profile and improvement in resolution [193]. Multilayer deposition minimized unspecific adsorption of NA [194].

Polymeric NPs can also be prepared. PEG-coated polystyrene latex NPs were prepared by polymerization of styrene in the presence of PEG. Improved separation is achieved when PEG is present on the NP surface. The smaller size gives the better the DNA separation when

mixed with hydroxypropylmethylcellulose buffer [195]. This conventional polymer was mixed with silica NPs, which are supposed to cause repulsion in DNA (polyanionic) and accelerate it, resulting in an increase in resolution and speed [196].

A lipid-based liquid crystalline NP suspension (average diameter 70 nm) was prepared by one-step procedure based on lipid self-assembly and applied to the separation of green fluorescent protein (GFP) mutants differing in only one amino acid [197]. An aqueous NP suspension was formed when soy phosphatidylcholine, glycerol dioleate, polysorbate 80, oleic acid, and ethanol were added to water and stirred for 48 h.

Magnetic beads (MBs) are a material with many possibilities in analytical chemistry. Magnetic particles offer an additional advantage over other solid surfaces and conventional particles: having embedded magnetic entities, they can be easily manipulated using permanent magnets or electromagnets, independently of normal microfluidic or biological processes [198]. The main advantage is the reusability, since magnetic particles are released by blocking/removing the magnetic field. Moreover, the configuration can easily be changed by functionalization. In most cases, they are used for performing bioassays [199], rather than for improving the separation. In this way, in-line extraction has been performed with C₁₈ functionalized magnetic particles (silica-coated iron oxide particles) on a disposable PMMA microfluidic device [200]. The use of magnetic NPs as obstacles in the channel by applying a magnetic field allows the separation of large dsDNAs [201]. The NP suspension becomes self-organized into a fixed array when a constant homogeneous magnetic field is applied.

Increasing developments in technology have produced carbon nanoparticles (CNPs). However, their use among the rest of NPs is not widespread, mainly where microchips are concerned. An overview of the use of CNPs as PSPs in electrokinetic chromatography (EKC) has been reported [202]. A variety of carbon nanostructures including fullerenes, nano-onions, nanodiamonds, nanotubes, nanohorns, peapods, nanofibers, and nanotube rings have been reported. CNTs are the carbon nanostructures most widely used recently in analytical chemistry [203,204], including their use as a separation carrier in CE [205]. Although Wiles and Abrahamson [206] observed a thick mat of fine fibers of graphite anodes with diameters ranging from 4 to 100 nm composed of graphitic layers with a hollow core, the discovery of CNTs was attributed to Iijima [207], who prepared carbon structures consisting of needle-like tubes, each needle comprising coaxial tubes of graphitic sheets. On each tube, the carbon-atom hexagons are arranged in a helical manner about the needle axis, resulting in high-aspect (length to diameter) ratio materials with outstanding electrical, mechanical, chemical, and

thermal properties. They can be present in different forms: multiple-walled carbon nanotubes (MWCNTs) (in “hollow-tube,” “herringbone,” or “bamboo” morphological variations) and single-walled carbon nanotubes (SWCNTs); metallic (armchair) and semiconducting (zigzag or chiral); closed- or open-ended CNTs; and different functionalizations are possible. Therefore, even when they have a very simple chemical composition and atomic-bond configuration, they exhibit the most extreme diversity in structure and in turn in properties and behavior.

Although some reports can be found on CE combining the use of CNTs and surfactants [208], or composites with polymers [209], its application in ME is still scarce. A special case is the use of CNTs (shortened carboxylic SWCNTs) that were bound after chemical oxidation under ultrasonication to BSA and used as a chiral detector for tryptophan [210]. The separation is based on the fact that BSA has different binding affinities to D- or L-tryptophan. This stationary phase was adsorbed taking advantage of the adsorption properties of proteins. Similarly to most of the cases related to modification by NPs, the detection system is amperometry.

ILs have been shown to have thermophysical properties that justify the replacement of several of the chemical processes now under exploitation because they can be considered as green solvents. Dissolving NPs (MWCNTs) in ILs forms “bucky gels” or ionanofluids, which have recently been shown to have thermal conductivity enhancements ranging from 5 % to 35 % for $[(\text{HMIIm}) \text{BF}_4]$, $[(\text{BMIm}) \text{PF}_6]$, $[(\text{HMIIm}) \text{PF}_6]$, $[(\text{BMIm}) \text{CF}_3\text{SO}_3]$, $[(\text{BMPyrr}) (\text{CF}_3\text{SO}_2)_2\text{N}]$ (1-hexyl-3-methylimidazolium, HMIIm; 1-butyl-3-methylpyrrolidinium, BMPyrr) with MWCNTs [211]. Considering that solid materials, namely metals or CNTs, have a thermal conductivity at room temperature several orders of magnitude higher than that of fluids, it has been shown that the thermal conductivity of fluids containing suspended particles could be significantly higher than that of the base fluids. The term nanofluid [212], in this case, designates a new class of heat transfer fluid formed by the dispersion of nanometer-sized solid particles, rods, or tubes in traditional heat transfer fluids. This is supposedly based on nanocluster formation. Combination with ME methodologies is a promising and unexplored methodology.

Multifunctional NPs are exciting nanomaterials with promising applications: (bio)sensing, (bio)assays, catalysis, and separations based on their magnetic, optical, and electrochemical properties [213]. In **Fig. 6**, a scheme of the possibilities of these NPs is shown.

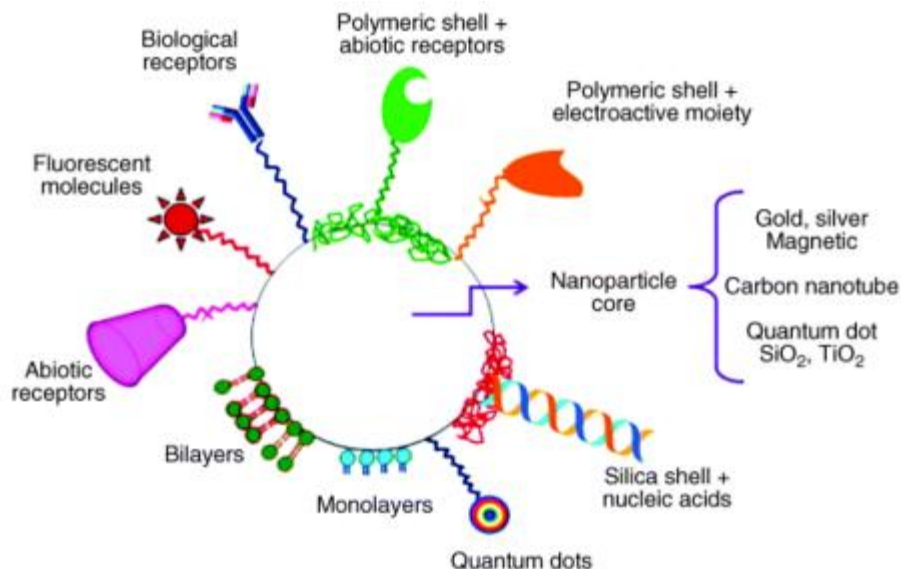


Figure 6. Multifunctional nanoparticles that schematized all the possibilities of use. Reprinted from Ref. 213 with permission from Elsevier.

3.4. Polymers

Polymers cover a type of molecules that are different in size, dispersity, charge, and so on, which is very appropriate for surface modification due to, among other features, its versatility. In this section, the more representative cases of different strategies will be presented. Some examples have already been commented on because they can be employed in combination with other types of chemical modifiers in order to improve jointly the characteristics of the analytical methodology. In many cases, polymers are applied as preconcentration matrices. The applications of monoliths and related porous polymer gels in microfluidic devices have been reviewed [214]. Monolithic columns can be formed within PMMA microchannels by *in situ* photopolymerization, for performing preconcentration through retention/elution mechanisms [215], and chambers for including monolithic disks were prepared at the junction between the injection and separation channels for adsorption and elution of catecholamines [216]. In many cases, they have been employed for improving resolution, as dynamic or static coatings. They have been mainly applied in combination with CZE methodologies, but they also improve microchip gel electrophoresis (MGE) (constituting the gel or the viscous solution), MEKC (accompanying the micellar medium or as a pretreatment), or even IEF methodologies.

Many polymers, commonly derived from cellulose, have been employed for improving separations, usually for DNA or protein analysis. DNA analysis has moved from the slow and labor-intensive slab gels to the fast and automated capillary arrays and, more recently, to the

even faster and potentially integrated microfluidic devices that can be fabricated for running several assays in parallel. Depending on the concentration and the molecular weight, the viscosity varies in addition to the pore size. Polymers can act as a sieving matrix and different macromolecule sizes can be separated. Surface modification of polymer microchips (PMMA and COC) with HPC dissolved in a matrix of the copolymer [poly(methyl methacrylate-8.5-methacrylic acid)] in a spin-coated thin film on the surface has been proposed [217]. On the other hand, linear polyacrylamide (LPA) [218] has been commonly employed as a sieving matrix, not only the concentration but also the molecular weight being important parameters in the resolution of DNA fragments (*e.g.*, differences are observed between a 4 % w/v >5.5 MDa LPA or a mixed system consisting of 3 % w/w 10 MDa LPA and 1 % w/w 50 kDa LPA). Easy handling for matrix preparation, loading into channels and replacement after runs, and consistency in batch quality are parameters that have to be taken into consideration. To suppress the EOF of plastic (polyolefinic) channels, a coating solution of polydimethylacrylamide–diethylacrylamide was filled to allow non-covalent coating before loading with a denaturing sieving matrix.

Table 4. Terms Employed in ME Surface Modification with Polymers.

| | | |
|----------------------|---|--|
| Layer-by-layer (LBL) | Formation of a film by depositing alternating layers of opposite charge | |
| Click chemistry | Usually, it is a reaction between a terminal alkyne and an organic azide to yield a triazole. It was given that name because of its reliability | |
| ATRP | A living radical polymerization that uses a metal catalyst, usually copper | |
| Grafting to | Consists in attaching a functionalized polymer to an active site on the surface | |
| Grafting from | A procedure according to which a polymerization initiator or a monomer is covalently bonded to the surface and then the polymer is conveniently grown from the initiator or the monomer | |

The first step to improve separation is the optimization of the instrumental conditions, mainly buffer pH, concentration, and composition, and also the separation voltage. When

separation is still not adequate, surface modification and polymers can be an alternative. In **Table 4**, some terms employed in surface modification with polymers are reported.

The use of additives as a dynamic coating is the first simple solution. Three major classes of dynamic coating modifiers, amines, surfactants, and neutral polymers, have been widely adopted in conventional CE [219]. This is mainly due to the possibility of forming hydrogen bonds through hydroxyl and amine groups and also hydrophobic interactions through hydrocarbon chains with the surface. Among candidate dynamic coating additives, amines and surfactants have attracted perhaps the greatest attention because very small amounts of such additives can significantly affect the EOF and suppress analyte interaction. Such minute amounts of surfactant do not alter the properties (pH and conductivity) of the BGE and therefore do not adversely affect the speed of separation. Amines such as ethylamine, diethylamine, triethylamine, and triethanolamine, and surfactants such as SDS, dodecyltrimethylammonium chloride (DTAC), and CTAB, did not show any observable effects on suppressing oligosaccharide adsorption under acidic or alkaline conditions [220]. In this case, also PA, well known for its excellent capillary wall coating and sieving properties in conventional CE, only very slightly reduced adsorption. Neutral polymers with hydroxyl groups such as PEG, hydroxyethylcellulose (HEC), hydroxypropylmethylcellulose (HPMC), and MC clearly suppressed adsorption and improved separation. Among them, MC is preferred because it gave a better performance and less tailing than HPC. The low molecular weight of HEC and the very small number of hydroxyl groups in PEG produced poorer separations. Therefore, as commented on before, molecular weight, hydrophilicity/hydrophobicity, and concentration of polymer are important parameters to be considered. In many cases, neutral polymers are chosen because they do not impart a charge to the surface to give extra EOF. Neutral polymers with polyhydroxyl groups such as PEG, HPMC, MC, and HEC have been employed together with amines and surfactants for the improvement of derivatized oligosaccharide separation on PMMA microchips. There are special cases where the alternatives have not been widely exploited for ME, for example, dendrimers. The first use of dendrimers as PSPs in CE separations was described in 1992. One of the important conclusions is that separation was influenced by the size and charge of the dendrimers and by the composition of the electrolyte [221]. In **Fig. 7**, electropherograms showing the improvement in the resolution of several neurotransmitters and cationic metabolites are shown.

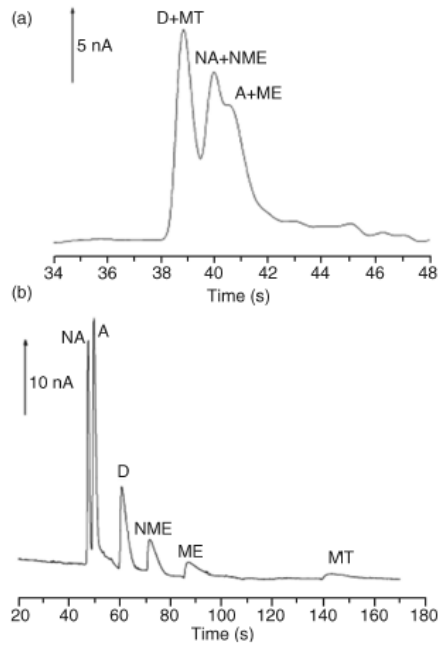


Figure 7. Electrophoretic separation of catecholamines and cationic metabolites on the microchip. BGE, 5 mM borate–phosphate buffer (pH 7) containing SDS and PAMAM dendrimer; V_{sep} , 3 kV; V_{inj} , 1 kV (3 s); Au electrode; E_d , 1400 mV. Reprinted from Ref. 137 with permission from Elsevier.

As commented on previously, polymeric coatings on solid surfaces can be performed following two main strategies: physisorption and covalent attachment. For polymer physisorption, a polymer or a block copolymer can be adsorbed *via* interaction of the polymer or one of the blocks with suitable surfaces. The technique of LBL has been developed as a versatile method to functionalize surfaces. The process is based on the sequential deposition of interactive polymers from their solutions in such a way that a film is formed by deposition of alternating layers of opposite charge.

Chitosan is a biopolymer derived from chitin, made primarily of repeating units of glucosamine, among which amino groups have been used in the immobilization of proteins and other molecules. Furthermore, chitosan is positively charged in mildly acidic aqueous solutions, and its charge density is high. Therefore, it can be used as a polycation in an LBL assembly system, on which various polyanions can be adsorbed [92].

PE coatings have an important effect on the velocity and direction of the EOF as well as on the separation efficiency for PDMS-ME. Successive multiple ionic layer coatings indicated that the EOF direction reversed with each additional deposited polymer layer (first anionic and then cationic or *vice versa*), but did not vary significantly with layer number or polymer structure [222]. The maximum separation efficiency was achieved for coatings of polybrene (cationic) and dextran sulfate (anionic) polymers after deposition of six layers. Complexation

between oppositely charged polyions occurs through electrostatic interactions and is a means to control the structure and order of assemblies.

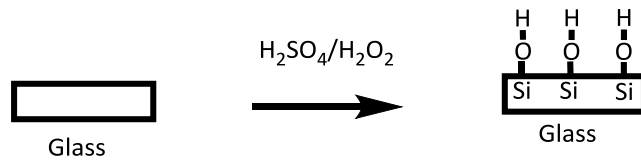
Another possibility is the generation of PE brushes. When long linear PE chains are grafted densely to a solid surface, a PE brush results [223]. One of the main features of PE brushes is the strong confinement of the counterions within the brush layer. There are large differences compared with monolayers of end-grafted uncharged macromolecules. Two classes of PE brushes are possible [223]: if strongly dissociating PE chains such as poly(styrenesulfonic acid) (PSS) are grafted to surfaces, a quenched PE brush results. The degree of dissociation of ionic monomer units within these systems is independent of the pH. On the other hand, an annealed PE brush is obtained if weak PEs such as poly(acrylic acid) (PAA) are affixed to surfaces. Here, the state of charging of the chains depends directly on the local pH, which depends both on pH and on the ionic strength of the solutions. In both cases, salt concentration is important.

For a covalent attachment, two approaches have been envisaged: “grafting to” or “grafting from.” According to the first, a functionalized polymer is attached to an active site on the surface; mostly the functional group is allocated at one of the polymer ends. In the second procedure, a monomer/polymerization initiator is covalently bonded to the surface and then the polymer is conveniently grown from the monomer/initiator.

The advantages of the “grafting to” procedure is that free polymers that are going to be attached to the surface by formation of a chemical bond between the end groups of the polymer and the solid [224] can be synthesized and characterized prior to attachment. Neutral brushes can be converted to PE brushes by chemical treatment, often requiring rough conditions. “Grafting from” techniques present a viable alternative for the synthesis of dense PE brushes [225]. A monolayer of initiators is attached to the surface of the solid substrate and a surface-initiated polymerization is started that is not hampered by kinetic or thermodynamic barriers. In principle, any chain reaction that leads to long polymer chains can be used to create brushes. Block copolymers consisting of polymers with hydrophobic and PE blocks can also be employed [226], in addition to grafting of several different functional polymers on to a solid substrate *via* functional end groups, which results in mixed polymerbrushes [227], *e.g.* PE and non-PE, and also two oppositely charged PEs are possible. Depending on the pH of the system, the charge of these brushes could be switched. PE block copolymers can be used to tune the nanostructure assembly by changing the charged block or the degree of ionization, adding salts, and changing the solution conditions [228].

Surface modification

Pretreatment



Anchorage of a molecule with a convenient end functional group

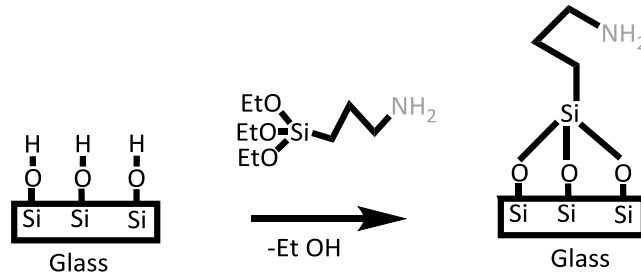
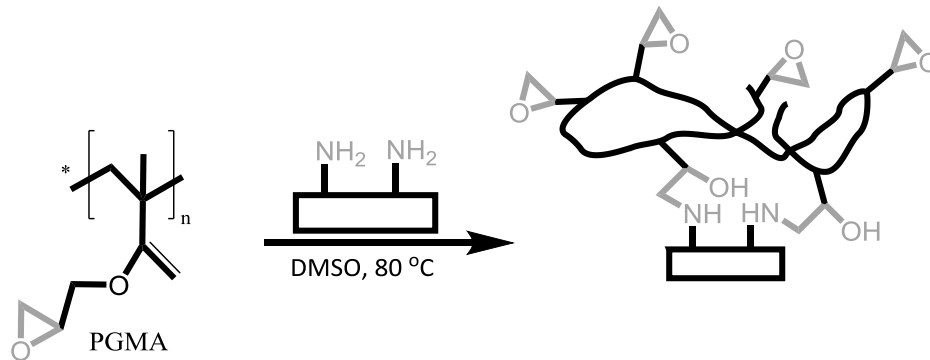
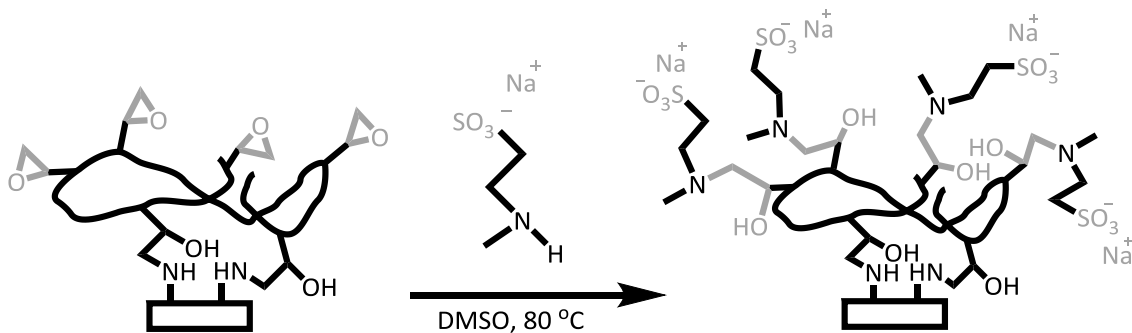
**Polymer grafted to****Functionalization of the polymer**

Figure 8. Successive steps for immobilization and functionalization of polymers on a microchip surface. Alonso-García et al. (unpublished results).

Some examples for both approaches are considered in the following paragraphs. Prebonding or postbonding procedures can be performed (see the section When Is the Surface

Modification Made?). If the latter is chosen, the most common procedure is introduction of the reagent solutions, with incubation there for a given time, or pumping them through the microchannel at a fixed flow rate. In both cases, washing the channel with deionized water (or another solvent such as ethanol depending on the functionalization and material of the channel) is carried out for a while. Long times are usually required, but they are decreased when flow is employed. Conditioning with the BGE is always mandatory.

Covalent modification can be performed in simple one step procedures or more complex approaches. An example of covalent immobilization is presented in **Fig. 8**. In this case, a glass microchannel is modified by a “grafting to” procedure. A pretreatment for enhancement of silanol groups is performed by immersion of the glass surface in a piranha solution [H_2O_2 (30 %)- H_2SO_4 (18 M) 1:3 v/v]. Then, the surface is covered with primary amines by reaction of the glass silanols with 3-aminopropyl(triethoxy)silane (APTES), $(\text{EtO})_3\text{SiCH}_2\text{CH}_2\text{CH}_2\text{NH}_2$, liberating EtOH. Later poly(glycidyl methacrylate) (PGMA) is immobilized on the glass surface by opening some of the epoxy rings in the polymer by the NH_2 groups previously anchored to the surface. Finally, the attached PGMA further reacts with the sodium salt of the methyltaurine, coating the surface with a negatively charged polymer (Alonso-García *et al.*, unpublished results).

In **Table 5**, the different steps for permanent modification of the ME surface with polymers are summarized. Although there are particular cases, a general procedure can be envisaged. Taking into account the objective, namely to anchor a polymer to a substrate, the steps can be divided into two. The first one consists in preparing the surface for receiving the (pre)polymer and can be subdivided into a pretreatment of the surface and later anchorage of a convenient molecule. The pretreatment aims to clean and activate the surface for later performing the immobilization of a molecule with an appropriate end functional group. The pretreatment, which can be chemical (piranha solution, basic solutions, etc.) or physical (UV irradiation, oxygen plasma, etc.), tries to generate active groups such as $-\text{Si}-\text{OH}$ groups in PDMS or $-\text{C}(\text{O})\text{OH}$ groups in PMMA. On the other hand, the pretreatment is very important because the oxidized surface must have enough surface silanols to allow a polymer film to be of sufficient density to protect the substrate from unspecific analyte adsorption.

Table 5. Studies related to covalent immobilization of polymers in ME.

| Surface Modification | | Bonded Polymer | | Analyte | Ref. | | |
|----------------------|---|--|---|---------|---|---------------------------------|-----|
| Substrate | Pretreatment, Generated Group | Group (Molecule Anchorage) | Graft to | | | Graft from | |
| PDMS | O ₂ plasma, Si—OH | —NH ₂ (APTES) | Oxidized Dextran | | Neurotransmitters, peptides, proteins | 238 | |
| | | —NH ₂ (APTES) | NSS-mPEG | | Amino acids | 101 | |
| | | —NH ₂ (APTES) | P(AAM-co-GMA), P(DAM-co-GMA), (PVP-g-GMA), (PVA-g-GMA) ^a | | | Peptides, proteins | 248 |
| | | —N ₃ (CPTCS, NaN ₃) | PEG-alkyne | | | Amino acids, proteins | 241 |
| | | Epoxy (GPTMS) | PEG-NH ₂ | | | Amino acids, proteins | 236 |
| | O ₂ plasma, generating Si—OH | —NH ₂ (APDMES) | PGA | | | Amino acids | 237 |
| | | (a) 3-Chloropropyltrichlorosilane | Alkyne-PEG | | | Proteins | 241 |
| | | (b) NaN ₃ for “click chemistry” | | | PA (ATRP) | Proteins | 252 |
| | | 1-Trichlorosilyl-2-(m,pchloromethylphenyl)ethane | | | | | |
| | | MPTS | | | PAAm ^b (NH ₄) ₂ SO ₅ | Protein | 229 |
| UV | Benzophenone ^c | | | | PAA, PA-g-PEG | Peptides | 99 |
| | | | | | AMPS, C ₁₈ -AMPS, PSS, VSA, PAA, StMA-AMPS | Peptides | 244 |
| | | | | | PAA, PAAm, etc. | Peptides | 55 |
| | | | | | PMMA-g-PEG (ATRP) | Amino acids, peptides, proteins | 249 |
| | | | | | PMMA-g-PEG (ATRP) | Amino acids, peptides, proteins | 246 |
| PMMA | Basic solution | | PEG-NH ₂ | | Amino acids, proteins | 235 | |
| | LiNHCH ₂ CH ₂ NH ₂ , UV, ethylenediamine (en), EDC | Methacrylic acid, EDC | | PA | DNA samples | 243 | |
| | O ₂ plasma, C(O)OH, C—OH | 2-Bromoisobutyryl bromide ^d | | | | | |
| TPE | UV radiation | 2-Bromoisobutyryl | HPMC or PVA | | DNA ladder | 230 | |
| | | | | PMMA-g- | Amino acids, | 231 | |

| | | | | | | |
|-------------------------|--|---|---|------------|-----------------------------------|-----|
| P(MMA- MAA) Glass | | bromide | HPC | PEG (ATRP) | peptides, proteins Proteins | 217 |
| | NaOH | MPTS | | PAA | DNA sequencing | 232 |
| | H ₂ O ₂ , NH ₃ , H ₂ O Acetone, isopropyl alcohol, and deionized water | MET ^d (a) Deposition of 11- Bromoundecyltrichlo rosilane (BUTS) (b) NaN ₃ in DMF for “click chemistry” | Alkyne (a) PAMAM (b) PEOX (c) PEI (d) PEG | PAAm | PCR products | 240 |

^aRemaining epoxy groups were blocked by 0.1M aminoethanol.

^bIn addition, methylcellulose was dynamically coated on the PAAm.

^cCerium(IV) catalyzed.

^dOther coating methods are described in this chapter.

3-CPTCS, chloropropyltrichlorosilane; VSA, poly(vinylsulfonic acid); PA, polyacrylamide (equivalent to PAAm); PA-g-PEG, polyacrylate-graft-polyethylene glycol; PCR, polymerase chain reaction; PMMA-g-PEG, poly(methylmethacrylate)-graft-poly(ethylene glycol); P(MMA-MAA), poly(methyl methacrylate-co-methacrylic acid); P(AAM-co-GMA), poly(acrylamide-co-glycidyl methacrylate); P(DAM-co-GMA), poly(dimethylacrylamide-co-glycidyl methacrylate); PVP-g-GMA, polyvinylpyrrolidone-graft-poly(glycidyl methacrylate); PVA-g-GMA, poly(vinyl alcohol)-graft-poly(glycidyl methacrylate); StMA-AMPS, poly(stearyl methacrylate-co-acrylamido-2-methyl-1-propanesulfonic acid); MET, 3-methacryloxypropyltrimethoxysilane (equivalent to MPTMSi and MPTS).

Concerning the immobilization of the functional molecule, this differs depending on the chosen conjugation procedure and can vary from amine, azide, epoxy, vinyl, carboxylate, hydroxyl, and so on. A different possibility is to anchor a polymerization initiator in case an atom transfer radical polymerization (ATRP) is performed. Since the possibilities vary depending on the material employed, classification is made taking into account the material: glass or polymer [PDMS, PMMA, or less common polymers such as P(GMA-MMA), P(MMA-MAA), or TPE].

The second step in the covalent immobilization of a polymeric modifier is bonding the polymer. As commented on earlier, two different approaches can be performed. A “grafting to” procedure involves the attachment of the polymer to the functional group in the substrate surface. Different polymers have been reported: dextran, PEG, PEI, and so on, or proteins, mainly depending on the analytes under separation. In many cases, polymers are also functionalized in order to perform the covalent bonding with the counterpart in the surface (*e.g.*, PE can be amine, alkyne, or NSS-functionalized).

The “grafting from” procedure is mainly executed by polymerization of a monomer that modifies the substrate surface or by the ATRP procedure. This is a controlled polymerization in which the polymer chains grow at a more constant rate than in traditional chain polymerization and their lengths remain very similar (very low polydispersity index). This is due to the use of a transition metal-based catalyst (usually copper) that provides an equilibrium

between active (propagating) and inactive (dormant) forms of the polymer, which suppresses side reactions. Many functional groups for use as monomer or initiator are possible.

Surface bonding of PEG or PEO is a common strategy for retarding the nonspecific adsorption of proteins and other biological species. PEG is an uncharged and nontoxic polymer. Proteins are macromolecules bearing hydrophobic, hydrophilic, and ionic chemical groups; they are complex natural organic PEs. There are several reasons for the adsorption resistance of PEO surfaces in water. It was proposed that polymer chains have the ability to extend into an aqueous medium and thus create a steric repulsion for other adsorbates [233] apart from the ability of ethylene oxide units to form helices [234]; much more hydrogen bonds are available resulting in a more hydrophilic surface. On the other hand, PEG is generally recognized as the benchmark for the resistance of nonspecific adsorption of proteins due to its biocompatibility, low toxicity, and excellent protein resistance. The hydroxyl group of PEG is readily modified to produce a functional end group. For the determination of anionic proteins, amino-terminal PEG is covalently immobilized by reaction between the acyl carbon of PMMA and the primary amino group in PEG-NH₂ dissolved in a basic aqueous solution [235]. In both cases, a one-step immobilization procedure is performed.

In a two-step grafting method, PEG-NH₂ was used for an environmentally friendly PDMS modification. The PDMS was epoxy functionalized through reaction of the silanol groups on the surface with 3-glycidoxypropyltrimethoxysilane (GPTMS). Significantly improved electrophoretic performance of the modified microchips, with a noticeable EOF suppression and resistance to nonspecific protein adsorption for more than 30 days, was obtained [236]. NSS-mPEG {O-[(N-succinimidyl)succinyl]-O'-methyl-poly(ethylene glycol)} was grafted on to an amine-functionalized (with APTES reagent) surface. In this way, hydrophilic polymer brushes were obtained on a PDMS microchannel for improvement of amino acid separation [101], as shown in **Fig. 9**.

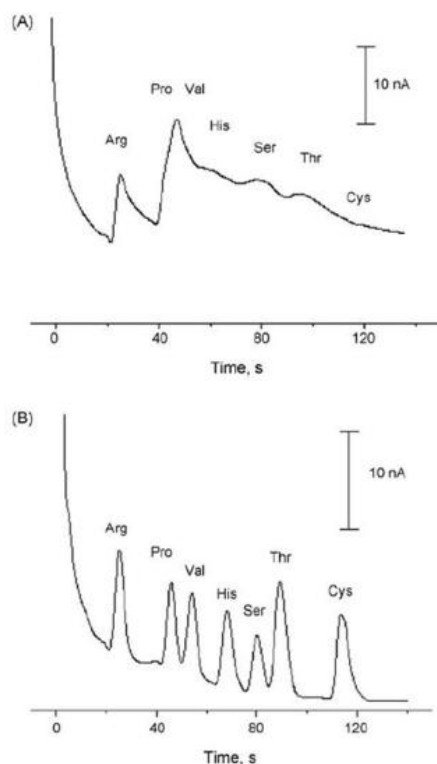


Figure 9. Electropherograms for amino acids: (a) on the native PDMS–PDMS microchip; (b) on the mPEG-coated PDMS–PDMS microchip. Conditions: BGE: 5.0 mM STB; Vinj: 600 V for 3 s; Vsep: 1600 V. Reprinted from Ref. 101 with permission from Elsevier.

Novel covalent strategies are being continuously developed. Although PEG is one of the more common polymers because of its hydrophilic characteristics, different polymers have been covalently grafted on microchip surfaces. Silanization with 3-aminopropyldimethylethoxysilane (APDMES) of a plasma oxidized PDMS surface produced amine groups on the surface. Further, amide bonds (through EDC and NHS) were formed with polyglutamic acid (PGA) [237] for the separation of four amino acid derivatives and homocysteine. Dextran, a glucose polymer, was selectively oxidized to aldehyde groups with sodium periodate and subsequently grafted on to amine-functionalized PDMS (through APTES reagent) *via* a Schiff base reaction (between an aldehyde and an amine producing an imine) [238]. The coated PDMS surface efficiently prevented biomolecules from adsorption and suppressed EOF. Improvements in the separation of different analytes are shown in **Fig. 10**.

When choosing a surface modification procedure, the total procedure has to be kept in mind: consumption of time, working conditions, and so on. For example, oxygen-free conditions that can be required for radical polymerization are difficult to handle during *in situ* modification of PDMS microchips. Moreover, nonpolar organic solvents can severely damage

the materials, similarly to what happens with high temperatures when polymeric microchips are employed. Special chemistries such as “click” chemistry are sometimes involved.

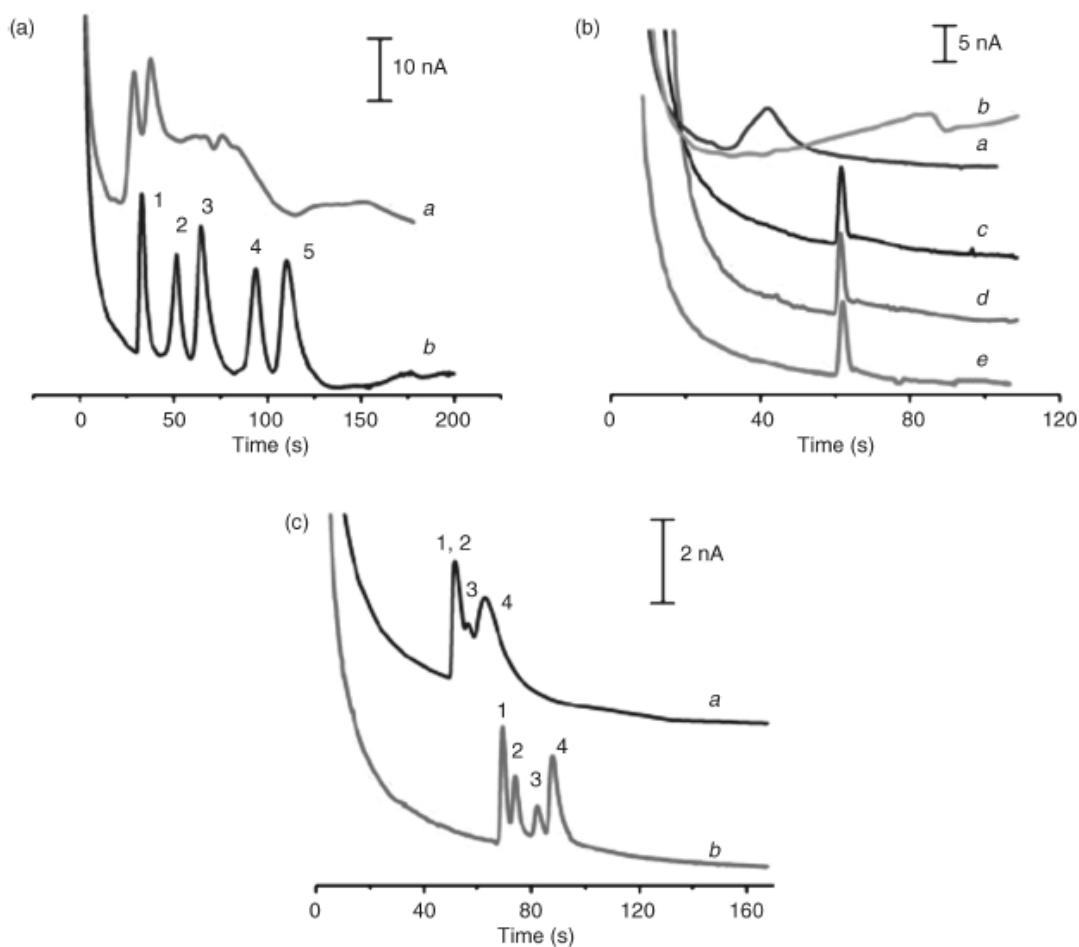


Figure 10. Electropherograms for peptides (a), protein (b), and neurotransmitters (c) on native and oxidized-dextran coated PDMS microchips. (a) (1) Thr–Arg–Lys; (2) Lys–Gly–Ser; (3) Ile–His–Pro; (4) Val–Ala–Ser; (5) Ile–Leu–Met. Conditions: BGE, 5.0 mM STB (pH 9.5); V_{inj} , +700 V for 3 s; V_{sep} , +1600 V; WE, copper microelectrode; E_d , +0.6 V. (b) Glucose oxidase (GOx); a, the first injection on the native PDMS microchip; b, the third injection on the native PDMS microchip; c–e, the first, third, and fifth injections on the coated PDMS microchip. Conditions: BGE, 30 mM NaOH; V_{inj} , +600 V for 3 s; V_{sep} , +1100 V; WE, copper microelectrode; E_d , +0.6 V. (c) a, on the native PDMS microchip; b, on the oxidized dextran-coated PDMS microchip; (1) 5-HT (5-hydroxytryptamine); (2) DA; (3) EP; (4) DBA (dobutamine). Conditions: BGE, 40 mM PB (pH 7.0); V_{inj} , +600 V for 3 s; V_{sep} , +1000 V; WE, single carbon fiber electrode; E_d , +1.40 V. Reprinted from Ref. 238 with permission from Elsevier.

“Click” chemistry is a type of highly efficient surface modification method with high specificity, nearly quantitative with mild ambient conditions in both organic and aqueous solutions, suitable for in situ reactions [239]. Among these, the copper-catalyzed Huisgen cycloaddition of alkynes and azides is considered particularly useful. Covalent attachment of preformed terminally functionalized linear and dendritic polymers [polyamidoamine (PAMAM), linear m-PEG, PEI, and poly(2-ethylloxazoline) (PEOX)] were synthesized with

terminal alkynes for “click” modification of glass microfluidic channels [240]. A “click” chemistry-based surface modification strategy was also developed for PDMS microchips to enhance the separation performance for both amino acids and proteins. Alkyne- PEG was synthesized by a conventional procedure and then “click” grafted to azido-PDMS. EOF regulation and stability of the modification were evident [241].

As can be seen in **Table 5**, proteins and peptides together with amino acids are the most common analytes. Most of the materials used in the production of analytical microchips have the inconvenience of the strong adsorption of hydrophobic molecules. Proteins are particularly prone to surface adsorption, and therefore strategies for obtaining hydrophilic microchannels are being continuously developed.

Recently, “grafting from” procedures have advanced considerably for the covalent immobilization of polymers. Immobilization of a monomer in an aminated PMMA surface [through either a chemical [242] (lithiated diamine) or photochemical (UV modification) procedure] was performed prior to surface coating with an LPA. The aminated surface is used to covalently anchor methacrylic acid, which was used as a scaffold to produce LPAs on the surface through radical polymerization of acrylamide. It was applied to single-base resolution of ssDNA [243].

In the more usual procedure, only disassembled channels could be coated by UV-mediated graft polymerization. Ce-catalyzed polymerization has also been reported [244]. In this case, vinylsulfonic acid, acrylic acid, 2-acrylamido-2-methylpropanesulfonic acid (AMPS), 4-styrenesulfonic acid, and stearyl methacrylate were used for successful modification of the surface of PDMS by cerium(IV)-catalyzed polymerization. AMPS-coated PDMS channels were shown to give a reproducible separation of a synthetic peptide mixture for over 1 month. Referring to UV-mediated polymerization, by preadsorbing a photoinitiator (benzophenone) on the surface (PDMS), the rate of polymer formation at the surface was greatly accelerated compared with that in solution. Thus, a gel did not form in the lumen of enclosed microchannels. After addition of a variety of monomer solutions [acrylic acid, poly(ethylene glycol), monomethoxyl acrylate, or poly(ethylene glycol) diacrylate] and illumination with UV light, a stable coating was produced. The placement of an opaque mask over a portion of the channel permitted photopatterning of the microchannels. By using an appropriate mixture of monomers combined with masks, it should be possible to fabricate PDMS devices with distinct surface properties in different regions or channels [99]. In this case, two different problems need to be solved at the same time: the difficulty in applying the coating in an intact

microchannel and the fact that many coatings that can be accomplished through the use of laminar flow are limited to patterning.

UV-mediated grafting has been applied but with channels that had to be assembled after coating [99]. When applied to an intact channel, it forms a gel rather than a surface coating. In addition, the small amount of free monomer within the channel is rapidly consumed by gel formation, leaving little to no monomer available for polymerization on the surface. The gel also restricts diffusion of any residual monomer to the surface of the channels. Unless the channel can be disassembled and reassembled, the gel forms a plug in the channel, restricting movement. By adsorbing the photoinitiator on the surface and removing free photoinitiator prior to graft polymerization, an accelerated rate of formation of the polymer on the surface relative to that in solution during the grafting step occurs.

On the other hand, the most common procedure for radical polymerization is ATRP, sometimes called surface initiated atom transfer radical polymerization (SI-ATRP), in which an initiator of the polymerization is anchored on the surface. This is one of the methods employed for covering surfaces with hydrophilic polymers on microchannel surfaces. Different from traditional radical polymerization, ATRP is a transition metal-catalyzed free-radical living polymerization method, which produces welldefined polymers. In this case, an initiator is anchored in the surface and then the monomer is polymerized. An example is the anchorage of 2-bromoisobutyryl bromide to the hydroxyl groups of oxidized PMMA, and polymerization of a PEG-functionalized monomer (methyl ethermethacrylate) [245].

The same initiator and monomer are employed with this procedure but using a surface-reactive acrylic polymer, PGMAMMA. The advantage of this approach is that this copolymer presents epoxy groups on the surface that can be activated by air plasma treatment, hydrolysis, or aminolysis [246]. Actually, tentacle-type polymer chains with epoxy groups were fabricated for open-tubular CEC but no test was made in ME format. The fabrication procedure of the stationary phase included pretreatment of the capillary inner wall, silanization, and glycidyl methacrylate (GMA)-grafted polymerization. The epoxy group-containing monomer GMA is the commonly used precursor monomer. The prepared GMA-grafted stationary phase could be easily modified with different chromatographic ligands by the ring-opening reaction of the epoxy groups [247]. A procedure for anchoring epoxy groups, following two different paths, copolymerization of GMA and acrylamide–dimethylacrylamide or graft polymerization of GMA on a pretreated, amine-functionalized (*via* APTES) PDMS microdevice, has been reported for resisting nonspecific protein adsorption [248]. It has to be pointed out that SU-8,

an epoxy-based polymer (glycidyl ether of bisphenol A), mainly used as a negative tone photoresist, is employed for ME fabrication (<http://www.micruxfluidic.com>) and shows promising possibilities for surface chemistry.

During the ATRP modification processes described earlier, the total surface of both plates was grafted with a PEG layer, which affected the thermal bonding strength of the resultant microchip. ATRP grafting is performed on the surfaces of top and bottom plates before bonding them together thermally to form the enclosed microchannels, but they can delaminate spontaneously during use, due to the weak bonding strength of the PEG-functionalized surfaces. Furthermore, the underlying substrate surface polymers were prevented from interacting because of the more hydrophilic PEG-functionalized surface layer. Modification of only the microchannel surface is also possible if the initiator is anchored on the whole surfaces of both plates before bonding them together to form the enclosed microchannel, instead of bonding before introducing initiator into the channels. In this way, the reaction is faster and more efficient, avoiding swelling and deforming the microchannel and also its clogging with precipitate generated in the reagent solutions. After thermal bonding of the plates, an aqueous solution containing monomer (PEG-MEMA), catalyst, and ligand, prepared in an oxygen-free environment, was pumped into the microchannels to perform the inchannel ATRP modification [249].

ATRP involves activation of the surface, immobilization of the initiator, and subsequent grafting of the chosen polymer. The length of polymer tethered to the initiator can be controlled readily. In-channel ATRP grafting of a thin film of PEG on the surface of TPE microchannels was performed using 2-bromoisobutyryl bromide as initiator. Immobilization occurred on TPE microdevices in a water free environment. Further, grafting solution (Cu, PEGMEMA) was pumped through the TPE microchannels at a sufficiently slow flow rate for the reaction conditions to be close enough still to allow ATRP functionalization. Since ATRP is performed after TPE microdevices have been bonded together, it does not interfere with device fabrication [250].

ATRP of acrylamide on PDMS tries to achieve a lasting hydrophilicity due to the growth of PA chains from oxidized PDMS surface. Their immiscibility ought to promote stability of the hydrophilic surface. A 20-fold improvement in resisting irreversible adsorption of lysozyme, compared with bare PDMS and a 10-fold improvement compared with bare glass was reported. Moreover, unlike oxidized PDMS, which reverts fully to being hydrophobic after 2 days, the surface treated by ATRP of acrylamide was shown to remain hydrophilic for at least 1

month [251]. Similarly, a thin PA layer on a PDMS microchannel surface was formed by ATRP by using 1-trichlorosilyl-2-(*m,p*-chloromethylphenyl) ethane as initiator [252]. Because of the hydrophilic nature of the PA-coated silica surface, the aqueous solution of reagents was able to fill the channels by capillary force within 0.5 h. This is very important because pressure must be used to fill hydrophobic channels with aqueous buffers and this is hampered by bubble formation due to the permeability of PDMS [253]. The surface can be oxidized to become somewhat hydrophilic due to surface silanol and carboxylic acid groups, allowing filling to occur by capillary action, but hydrophobicity can be recovered.

4. Conclusions

ME devices are extremely promising tools with many analytical possibilities and applications, but they are still under development. Important advances from their beginning in all the areas involved in ME—new materials, more appropriate designs, integration of different steps, improvement of detection methodologies, and so on—have been reported. However, modern analytical chemistry has important aims, such as the simultaneous determination of closely related analytes that are still a challenge. Therefore, there are wide research activities on ME resolution improvement. With this objective, the state of the device surface is of paramount importance and different methodologies have been reported for obtaining the most suitable one. Micro and nanostructuring, employment of energy sources, and chemical modification are reported methodologies. They can be combined and, in many cases, a physical treatment (oxygen plasma and UV radiation are among the most common) is employed as a means of conditioning the surface before a chemical modification is made. The main objective is to improve separation through control of the EOF and suppression of analyte adsorption, but a totally different one can be found in the development of bioassays.

Procedures have to consider when (before or after bonding the plates that constitute the microchip), where (in the whole surface or in discrete patterned locations), how (through covalent or noncovalent bonds), and which modifiers to use. Different modes of electrophoresis are available (CZE, MEKC, CGE, CEC, etc.).

Referring to chemical modifiers, the use of surfactants is well established. However, ILS and NPs are at the beginning of their application and further promising results are envisaged. The possibilities for polymers are wide, and therefore much research is found in this area. As in the case of the rest of the modifiers, a dynamic or permanent coating can be performed. The former is a very simple procedure but more unstable layers are obtained. Covalent coating

often requires organic solvents or high temperatures, and the procedures are more tedious. However, the possibilities are varied and very appropriate for nondisposable devices.

Consideration of the material is of paramount importance. Similarity among glass (microchip) and fused silica (capillaries) has made this material the first choice. Different materials are employed taking advantage of the possibilities of polymers and most of the modification strategies have been applied to polymeric materials, probably due to their more hydrophobic nature. However, one of the major drawbacks when developing modification chemistries is that the procedure employed for one particular type of polymer may not necessarily transfer to another substrate with the same degree of success [59]. Research is still needed and interesting options, many of them still unexplored, are available: surface tuning through the properties of block copolymers, use of branched molecules, patterning of surfaces, exploitation of the possibilities of ILs, application of new multifunctional NPs, and so on.

Surface chemistry is of great importance in ME, especially in highly miniaturized devices, due to the high surface area-to-volume ratio. With reduction of the size of the channels, the properties of channel walls are becoming probably more important than originally thought. The properties are commonly explained on the basis of the structures of the material employed, but some additives (heat stabilizers, plasticizers, antioxidants, UV stabilizers, etc.) can affect the surface of the microchannel and the effect has not been thoroughly studied. Moreover, although the surface science community has developed many protocols, they have not yet been exploited deeply. The field of surface chemistry is not yet well known by the analytical chemistry community, and multidisciplinary efforts have to continue in order to obtain real applications. Coated capillaries are commonly applied in CE and they are commercially available. However, in the case of ME, the basic research has to focus on commercial applications.

Acknowledgments

This work was supported by FICYT under project FC-11-PC10-30. Isabel Álvarez Martos thanks the MICINN for the award of a PhD grant (AP2008-04451).

REFERENCES

- [1] Ortner, H.M. (1992) *Fresen. J. Anal. Chem.* 343, 825–826.
- [2] Valcarcel, M. (1997) *Trends Anal. Chem.* 16, 124–131.
- [3] Manz, A., Graber, N., and Widmer, H.M. (1990) *Sens. Actuators B* 1, 244–248.
- [4] Vazquez, M., Frankenfeld, C., Coltro, W.K.T., Carrilho, E., Diamond, D., and Lunte, S.M. (2010) *Analyst* 135, 96–103.
- [5] Fernández-la-Villa, A., Pozo-Ayuso, D.F., and Castaño-Alvarez, M. (2010) *Electrophoresis* 31, 2641–2649.
- [6] Kovachev, N., Canals, A., and Escarpa, A. (2010) *Anal. Chem.* 82, 2925–2931.
- [7] Oita, I., Halewyck, H., Thys, B., Rombaut, B., van der Heyden, Y., and Mangelings, D. (2010) *Anal. Bioanal. Chem.* 398, 239–264.
- [8] Arora, A., Simone, G., Salieb-Beugelaar, G.B., Kim, J.T., and Manz, A. (2010) *Anal. Chem.* 82, 4830–4847.
- [9] Zubritsky, E. (2002) *Anal. Chem.* 74, 22A–26A.
- [10] Kraly, J.R., Jones, M.R., Gomez, D.G., Dickerson, J.A., Harwood, M.M., Eggertson, M., Paulson, T.G., Sanchez, C.A., Odze, R., Feng, Z., Reid, B.J., and Dovichi, N.J. (2006) *Anal. Chem.* 78, 5977–5986.
- [11] Kenyon, S.M., Meighan, M.M., and Hayes, M.A. (2011) *Electrophoresis* 32, 482–493.
- [12] Chandra, U., Swamy, B.E.K., Gilbert, O., and Sherigara, B.S. (2010) *Electrochim. Acta* 55, 7166–7174.
- [13] Ensafi, A.A., Rezaei, B., Zare, S.Z.M., and Taei, M. (2010) *Sens. Actuators B* 150, 321–329.
- [14] Kissinger, P.T. and Heineman, W.R. (1984) *Laboratory Techniques in Electroanalytical Chemistry*, 2nd ed., Marcel Dekker, New York.
- [15] Varenne, A. and Descroix, S. (2008) *Anal. Chim. Acta* 628, 9–23.
- [16] Scharwz, M.A. and Hauser, P.C. (2001) *J. Chromatogr. A* 198, 225–232
- [17] Nagl, S., Schulze, P., Ludwig, M., and Belder, D. (2009) *Electrophoresis* 30, 2765–2772.
- [18] Ward, T.J. and Ward, K.D. (2010) *Anal. Chem.* 82, 4712–4722.
- [19] Guihen, E., Hogan, A., and Glennon, J. (2009) *Chirality* 21, 292–298
- [20] Sun, X., Li, D., and Lee, M. (2009) *Anal. Chem.* 81, 6278–6284.
- [21] Qu, P., Lei, J., Ouyang, R., and Ju, H. (2009) *Anal. Chem.* 81, 9651–9656.
- [22] Weinberger, R. (2000) *Practical Capillary Electrophoresis*, Academic Press, San Diego, CA.
- [23] Bowen, A.L. and Martin, R.S. (2009) *Electrophoresis* 30, 3347–3354.
- [24] Zubritsky, E. (2000) *Anal. Chem.* 72, 687A–690A.
- [25] Ramsey, J.D., Jacobson, C.T., Culbertson, C.T., and Ramsey, J.M. (2003) *Anal. Chem.* 75, 3758–3764.

- [26] Li, M.W., Huynh, B.H., Hulvey, M.K., Lunte, S.M., and Martin, R.S. (2006) *Anal. Chem.* 78, 1042–1051.
- [27] Castaño-Álvarez, M., Fernández-la-Villa, A., Pozo-Ayuso, D. F., Fernández-Abedul, M.T., and Costa-García, A. (2009) *Electrophoresis* 30, 3372–3380.
- [28] Muck, A., Wang, J., Jacobs, M., Chen, G., Chatrathi, M.P., Jurka, V., Výborný, Z., Spillman, S.D., Sridharan, G., and Schoning, M.J. (2004) *Anal. Chem.* 76, 2290–2297.
- [29] Chen, Y., Zhang, L., and Chen, G. (2008) *Electrophoresis* 29, 1801–1814.
- [30] Wang, Y., Chen, H., He, Q., and Soper, S.A. (2008) *Electrophoresis* 29, 1881–1888.
- [31] Liu, A.-L., He, F.-Y., Hu, Y.-L., and Xia, X.-H. (2006) *Talanta* 68, 1303–1308.
- [32] Bai, X.X., Roussel, C., Jensen, H., and Girault, H.H. (2004) *Electrophoresis* 25, 931–935.
- [33] Kameoka, J., Craighead, H.G., Zhang, H., and Henion, J. (2001) *Anal. Chem.* 73, 1935–1941.
- [34] Stachowiak, T.B., Rohr, T., Hilder, E.F., Peterson, D.S., Yi, M., Svec, F., and Fréchet, J.M.J. (2003) *Electrophoresis* 24, 3689–3693.
- [35] Castaño-Álvarez, M., Fernández-Abedul, M.T., and Costa-García, A. (2005) *Electrophoresis* 26, 3160–3168.
- [36] Lee, J.N., Park, C., and Whitesides, G.M. (2003) *Anal. Chem.* 75, 6544–6554.
- [37] Vickers, J.A., Dressen, B.M., Weston, M.C., Boonsong, K., Chailapakul, O., Cropek, D.M., and Henry, C.S. (2007) *Electrophoresis* 28, 1123–1129.
- [38] Fiorini, G.S., Lorenz, R.M., Kuo, J.S., and Chiu, D.T. (2004) *Anal. Chem.* 76, 4697–4704.
- [39] Coltro, W.K.T., da Silva, J.A.F., da Silva, H.D.T., Richter, E. M., Burlan, R., Angnes, L., do Lago, C.L., Mazo, L.H., and Carrilho, E. (2004) *Electrophoresis* 25, 3832–3839.
- [40] Castaño-Álvarez, M., Fernández-Abedul, M.T., Costa-García, A., Agirregabiria, M., Fernández, L.J., Ruano-López, J.M., and Barredo-Presa, B. (2009) *Talanta* 80, 24–30.
- [41] Agirregabiria, M., Blanco, F.J., Berganzo, J., Fullaondo, A., Subyaga, A.M., Mayora, K., and Ruano-López, J.M. (2006) *Electrophoresis* 27, 3627–3634.
- [42] Piccin, E., Coltro, W.K.T., da Silva, J.A.F., Neto, S.C., Mazo, L. H., and Carrilho, E. (2007) *J. Chromatogr. A* 1173, 151–158.
- [43] Fercher, G., Haller, A., Smetan, W., and Vellekoop, M.J. (2010) *Analyst* 135, 965–970.
- [44] Martinez, A.W., Philipps, S.T., Whitesides, G.M., and Carrilho, E. (2010) *Anal. Chem.* 82, 3–10.
- [45] Silkanen, T., Aura, S., Heikkilä, L., Kotiaho, T., Franssila, S., and Kostianen, R. (2010) *Anal. Chem.* 82, 3874–3882.
- [46] Klasner, S.A., Metto, E.C., Roman, G.T., and Culbertson, C.T. (2009) *Langmuir* 25, 10390–10396.
- [47] Liu, J.K., Sun, X.F., and Lee, M.L. (2005) *Anal. Chem.* 77, 6280–6287.
- [48] Kim, P., Jeong, H.F., Khademhosseini, A., and Suh, K.Y. (2006) *Lab Chip* 6, 1432–1437.
- [49] Liu, J.K., Sun, X.F., and Lee, M.L. (2007) *Anal. Chem.* 79, 1926–1931.
- [50] Kim, M.-S., Cho, S., Il, Lee, K.-N., and Kim, Y.-K. (2005) *Sens. Actuators B* 107, 818–824.

- [51] Lacher, N.A., de Rooij, N.F., Verpoorte, E., and Lunte, S.M. (2003) *J. Chromatogr. A* 1004, 225–235.
- [52] Coltro, W.K.T., Lunte, S.M., and Carrilho, E. (2008) *Electrophoresis* 29, 4928–4937.
- [53] Sikanen, T., Heikkilä, L., Tuomikoski, S., Ketola, R.A., Kostianen, R., Franssila, S., and Kotiaho, T. (2007) *Anal. Chem.* 79, 6255–6263.
- [54] Duffy, D.C., McDonald, J.C., Schueller, O.J.A., and Whitesides, G.M. (1998) *Anal. Chem.* 70, 4974–4984.
- [55] Hu, S., Ren, X., Backman, M., Sims, C.E., Li, G.P., and Li, Allbritton, N. (2002) *Anal. Chem.* 74, 4117–4123.
- [56] Yu, H., He, F.-Y., Lu, Y., Hu, Y.-L., Zhong, H.-Y., and Xia, X.-H. (2008) *Talanta* 75, 43–48.
- [57] Pallandre, A., de Lambert, B., Attia, R., Jonas, A.M., and Viovy, J.-L. (2006) *Electrophoresis* 27, 584–610.
- [58] Fan, H.Z. and Chen, G. (2007) *Proteomics* 7, 3445–3449.
- [59] Belder, D. and Ludwig, M. (2003) *Electrophoresis* 24, 3595–3606.
- [60] Dolnik, V. (2004) *Electrophoresis* 25, 3589–3601.
- [61] Muck, A. and Svatos, A. (2007) *Talanta* 74, 333–341.
- [62] Makamba, H., Kim, J.H., Lim, K., Park, N., and Hahn, J.H. (2003) *Electrophoresis* 24, 3607–3619.
- [63] Doherty, W.A.S., Meagher, R.J., Albarghouthi, M.N., and Barron, A.E. (2003) *Electrophoresis* 24, 34–54.
- [64] Chen, Y., Zhang, L., and Chen, G. (2008) *Electrophoresis* 29, 1801–1814.
- [65] Liu, J. and Lee, M.L. (2006) *Electrophoresis* 27, 3533–3546.
- [66] Zhou, J., Ellis, A.V., and Voelcker, N.H. (2010) *Electrophoresis* 31, 2–16.
- [67] Kist, T.B.L. and Mandaji, M. (2004) *Electrophoresis* 25, 3492–3497.
- [68] Lu, Y., Hu, Y.-L., and Xia, X.-H. (2009) *Talanta* 79, 1270–1275.
- [69] Cao, H., Yu, Z., Wang, J., Tegenfeldt, J.O., Austin, R.H., Chen, E., Wu, W., and Chou, S.Y. (2002) *Appl. Phys. Lett.* 81, 174–176.
- [70] Chantiwas, R., Hupert, M.L., Pullagurla, S.R., Balamurugan, S., Tamarit-Lopez, J., Park, S., Datta, P., Goettert, J., Cho, Y. K., and Soper, S.A. (2010) *Lab Chip* 10, 3255–3264.
- [71] Kaji, N., Okamoto, Y., Tokeshi, M., and Baba, Y. (2010) *Chem. Soc. Rev.* 39, 948–956.
- [72] Li, H.Y., Dauriac, V., Thibert, V., Senechal, H., Peltre, G., Zhang, X.X., and Descroix, S. (2010) *Lab Chip* 10, 2597–2604.
- [73] Sano, T., Iguchi, N., Iida, K., Sakamoto, T., Baba, M., and Kawaura, H. (2003) *Appl. Phys. Lett.* 83, 4438–4440.
- [74] McDonald, J.C., Duffy, D.C., Anderson, J.R., Chiu, D.T., Wu, H., Schueller, O.J.A., and Whitesides, G.M. (2000) *Electrophoresis* 21, 27–40.

- [75] Wang, B., Abdulali-Kanji, Z., Dodwell, E., Horton, J.H., and Oleschuk, R.D. (2003) *Electrophoresis* 24, 1442–1450.
- [76] Murakami, T., Kuroda, S., and Osawa, Z. (1998) *J. Colloid Interface Sci.* 202, 37–44.
- [77] Wang, B., Chen, L., Abdulali-Kanji, Z., Horton, J.H., and Oleschuk, R.D. (2003) *Langmuir* 19, 9792–9798.
- [78] Jones, B.J. and Hayes, M.A. (2006) Henry, C.S. (ed.) *Microchip Capillary Electrophoresis, Methods and Protocols*, Humana Press, Totowa, NJ, pp. 49–56.
- [79] Preininger, C, Sauer, U., Kern, W., and Dayteg, J. (2004) *Anal. Chem.* 76, 6130–6136.
- [80] Rossier, J.S. and Girault, H.H. (2001) *Lab Chip* 1, 153–157.
- [81] Bai, Y., Koh, C.G., Boreman, M., Juang, Y.-J., Tang, I.-C., Lee, L.J., and Yang, S.-T. (2006) *Langmuir* 22, 9458–9467.
- [82] Ko, S., Kim, B., Jo, S.-S., Oh, S.Y., and Park, J.-K. (2007) *Biosens. Bioelectron.* 23, 51–59.
- [83] Liu, Y., Wang, H., Huang, J., Yang, J., Liu, B., and Yang, P. (2009) *Anal. Chim. Acta* 650, 77–82.
- [84] Yen, P.-Y., Rossi, N.A.A., Kizhkkedathu, J.N., and Mu, C.A. (2010) *Microfluid. Nanofluid.* 9, 199–209.
- [85] Zhou, J.W., Voelcker, N.H., and Ellis, A.V. (2010) *Biomicrofluidics* 4, 046504.
- [86] Nakagawa, T., Tanaka, T., Niwa, D., Osaka, T., Takeyama, H., and Matsunaga, T. (2005) *J. Biotechnol.* 116, 105–111.
- [87] Lahann, J., Balcells, M., Lu, H., Rodon, T., Jensen, K.F., and Langer, R. (2003) *Anal. Chem.* 75, 2117–2122.
- [88] Gil, E.S. and Hudson, S.A. (2004) *Prog. Polym. Sci.* 29, 1173–1222.
- [89] Dai, W., Zheng, Y., Luo, K.Q., and Wu, H. (2010) *Biomicrofluidics* 4, 024101.
- [90] Ye, N.N., Win, J.H., Shi, W.W., Liu, X., and Lin, B.C. (2007) *Lab Chip* 7, 1696–1704.
- [91] Qu, H.Y., Wang, H.T., Huang, Y., Zhong, W., Lu, H.J., Kong, J.L., Yang, P.Y., and Liu, B.H. (2004) *Anal. Chem.* 76, 6426–6433.
- [92] Liu, Y., Lu, H., Zhong, W., Song, P., Kong, J., Yang, P., Girault, H.H., and Liu, B. (2006) *Anal. Chem.* 78, 801–808.
- [93] Ji, J., Zhang, Y., Zhou, X., Kong, J., Tang, Y., and Liu, B. (2008) *Anal. Chem.* 80, 2457–2463.
- [94] Liu, T., Wang, S., and Chen, G. (2009) *Talanta* 77, 1767–1773.
- [95] Priest, C. (2010) *Biomicrofluidics* 4, 032206.
- [96] Luo, X., Lewandowski, A.T., Yi, H., Payne, G.F., Ghodssi, R., Bentley, W.E., and Rubloff, G.W. (2008) *Lab Chip* 8, 420–430.
- [97] Kaji, H., Hashimoto, M., and Nishizawa, M. (2006) *Anal. Chem.* 78, 5469–5473.
- [98] Hu, S., Ren, X., Bachman, M., Sims, C.E., Li, G.P., and Allbritton, N.L. (2003) *Electrophoresis* 24, 3679–3688.

- [99] Hu, S., Ren, X., Bachman, M., Sims, C.E., Li, G.P., and Allbritton, N.L. (2004) *Anal. Chem.* 76, 1865–1870.
- [100] Camilleri, P. (1998) *Capillary Electrophoresis, Theory and Practice*, 2nd ed., CRC Press, Boca Raton, FL, p. 103.
- [101] Wang, A.-J., Feng, J.-J., and Fan, J. (2008) *J. Chromatogr. A* 1192, 173–179.
- [102] Frost, N.W., Jing, M., and Bowser, M.T. (2010) *Anal. Chem.* 82, 4682–4698.
- [103] Poitevin, M., Shakalisava, Y., Miserere, S., Peltre, G., Viovy, J.L., and Descroix, S. (2009) *Electrophoresis* 30, 4256–4263.
- [104] Mohamadi, M.R., Svobodova, Z., Verpillot, R., Esselmann, H., Wiltfang, J., Otto, M., Taverna, M., Bilkova, Z., and Viovy, J.L. (2010) *Anal. Chem.* 82, 7611–7617.
- [105] Kondo, K., Kaji, N., Toita, S., Okamoto, Y., Tokeshi, M., Akiyoshi, K., and Baba, Y. (2010) *Biomicrofluidics* 4, 032210.
- [106] Hjerten, S., Kiao, J.-L., and Zhang, R. (1989) *J. Chromatogr. A* 473, 273–275.
- [107] Ngola, S.M., Fintschenko, Y., Choi, W.Y., and Shepodd, T.J. (2001) *Anal. Chem.* 73, 849–856.
- [108] Landner, Y., Crétier, G., and Faure, K. (2010) *J. Chromatogr. A* 1217, 8001–8008.
- [109] Vaher, M. and Kohel, M. (2005) *J. Chromatogr. A* 1068, 83–88.
- [110] Chen, G., Xu, X.J., Lin, J.Y.H., and Wang, J. (2007) *Chem. Eur. J.* 13, 6461–6467.
- [111] Wang, H., Wang, D., Wang, J., Wang, H., Gu, J., Han, Ch., Jin, Q., Xu, B., He, Ch., Cao, L., Wang, Y., and Zhao, J. (2009) *J. Chromatogr. A* 1216, 6343–6347.
- [112] Schreiber, F. (2000) *Prog. Surf. Sci.* 65, 151–256.
- [113] Wiedmer, S.K., Jussila, M.S., and Riekkola, M.L. (2004) *Trends Anal. Chem.* 23, 562–582.
- [114] Gomez-Hens, A. and Fernandez-Romero, J.M. (2006) *Trends Anal. Chem.* 25, 167–178.
- [115] Vermette, P. and Meagher, L. (2003) *Colloids Surf. B* 28, 153–198.
- [116] Sikanen, T., Wiedmer, S.K., Heikkilä, L., Franssila, S., Kostianen, R., and Kotiaho, T. (2010) *Electrophoresis* 31, 2566–2574.
- [117] Xu, Y., Takai, M., Konno, T., and Ishihara, K. (2007) *Lab Chip* 7, 199–206.
- [118] Gertsch, J.C., Noblitt, S.D., Cropek, D.M., and Henry, C.S. (2010) *Anal. Chem.* 82, 3426–3429.
- [119] Osiri, J.K., Shadpour, H., and Soper, S.A. (2010) *Anal. Bioanal. Chem.* 398, 489–498.
- [120] Dang, F., Hasegawa, T., Biju, V., Ishikawa, M., Kaji, N., Yasui, T., and Baba, Y. (2009) *Langmuir* 25, 9296–9301.
- [121] Root, B.E., Zhang, B., and Barron, A.E. (2009) *Electrophoresis* 30, 2117–2122.
- [122] Dossi, N., Susmel, S., Toniolo, R., Pizzariello, A., and Bontempelli, G. (2009) *Electrophoresis* 30, 3465–3471.
- [123] Shi, M., Huang, Y., Li, X.T., and Zhao, S.L. (2009) *Chromatographia* 70, 1651–1657.
- [124] Piccin, E., Dossi, N., Cagan, A., Carrilho, E., and Wang, J. (2009) *Analyst* 134, 528–532.

- [125] Chiesl, T.N., Chu, W.K., Stockton, A.M., Amashukeli, X., Gruthaner, F., and Mathies, R.A. (2009) *Anal. Chem.* 81, 2537–2544.
- [126] Ohlsson, P.D., Ordeig, O., Mogensen, K.B., and Kutter, J.P. (2009) *Electrophoresis* 30, 4172–4178.
- [127] Noblitt, S.D., Schwandner, F.M., Hering, S.V., Collet, J.L., Jr., and Henry, C.S. (2009) *J. Chromatogr. A* 1216, 1503–1510.
- [128] Wang, H., Wang, H.M., Jin, Q.H., Cong, H., Zhuang, G.S., Zhao, J.L., Sun, C.L., Song, H.W., and Wang, W. (2008) *Electrophoresis* 29, 1932–1941.
- [129] Osiri, J.K., Shadpour, H., Park, S., Snowden, B.C., Chen, Z. Y., and Soper, S.A. (2008) *Electrophoresis* 29, 4984–4992.
- [130] Okada, H., Kaji, N., Tokeshi, M., and Baba, Y. (2008) *Electrophoresis* 29, 2533–2538.
- [131] Kilár, A., Farkas, V., Kovács, K., Kocsis, B., and Kilár, F. (2008) *Electrophoresis* 29, 1713–1722.
- [132] Okada, H., Kaji, N., Tokeshi, M., and Baba, Y. (2008) *Anal. Sci.* 24, 321–325.
- [133] Ding, Y., Mora, M.F., Merrill, G.N., and Garcia, C.D. (2007) *Analyst* 132, 997–1004.
- [134] Bishop, S.C., Lerch, M., and McCord, B.R. (2007) *J. Chromatogr. A* 1154, 481–484.
- [135] Kolivoska, V., Weiss, V.U., Kremser, L., Gas, B., Blaas, D., and Kenndler, E. (2007) *Electrophoresis* 28, 4734–4740.
- [136] Li, M.W. and Martin, R.S. (2007) *Electrophoresis* 28, 2478–2488.
- [137] Vlcková, M. and Schwarz, M.A. (2007) *J. Chromatogr. A* 1142, 214–221.
- [138] Sueyoshi, K., Nagai, H., Wakida, S., Nishii, J., Kitagawa, F., and Otsuka, K. (2006) *Meas. Sci. Technol.* 17, 3154–3161.
- [139] Vrouwe, E.X., Luttge, R., Olthuis, W., and van der Berg, A. (2006) *J. Chromatogr. A* 1102, 287–293.
- [140] Mourzina, Y., Kalyagin, D., Steffen, A., and Offenhäusser, A. (2006) *Talanta* 70, 489–498.
- [141] Wang, A.J., Xu, J.J., and Chen, H.Y. (2006) *Anal. Chim. Acta* 569, 188–194.
- [142] Roman, G.T., McDaniel, K., and Culbertson, C.T. (2006) *Analyst* 131, 194–201.
- [143] García, C.D., Dressen, B.M., Henderson, A., and Henry, C.S. (2005) *Electrophoresis* 26, 703–709
- [144] Li, F., Wang, D.D., Yan, X.P., Su, R.G., and Lin, J.M. (2005) *J. Chromatogr. A* 1081, 232–237.
- [145] García, C.D. and Henry, C.S. (2005) *Electroanalysis* 17, 223–230.
- [146] Nakajima, H., Kawata, K., Shen, H., Nakagama, T., and Uchiyama, K. (2005) *Anal. Sci.* 21, 67–71.
- [147] Kang, J., Yan, J., Liu, J., Qiu, H., Yin, X.B., Yang, X., and Wang, E. (2005) *Talanta* 66, 1018–1024.
- [148] García, C.D. and Henry, C.S. (2003) *Anal. Chem.* 75, 4778–4783.
- [149] Charvátová, J., Deyl, Z., Klevar, M., Miksík, I., and Eckhardt, A. (2004) *J. Chromatogr. B* 800, 83–89.

- [150] Ceriotti, L., Shibata, T., Folmer, B., Weiller, B.H., Roberts, M.A., de Rooij, N.F., and Verpoorte, E. (2002) *Electrophoresis* 23, 3615–3622.
- [151] Galloway, M., Stryjewski, W., Henry, A., Ford, S.M., Llopis, S., McCarley, R.L., and Soper, S.A. (2002) *Anal. Chem.* 74, 2407–2415.
- [152] Ocvirk, G., Munroe, M., Tang, T., Oleschuk, R., Westra, K., and Harrison, D.J. (2000) *Electrophoresis* 21, 107–115.
- [153] Rodríguez, I., Jin, L.J., and Li, S.F. (2000) *Electrophoresis* 21, 211–219.
- [154] Anderson, J.L., Armstrong, D.W., Wei, G.T. (2006) *Anal. Chem.* 78, 2892–2902.
- [155] Walden, P. (1914) *Bull. Acad. Sci. St. Petersburg* 405–422
- [156] Liu, J.-f., Jönsson, J.A., and Jiang, G.-B. (2005) *Trends Anal. Chem.* 24, 20–27.
- [157] Berthod, A., Ruiz-Angel, M., and Carda-Broch, S. (2008) *J. Chromatogr. A* 1184, 6–18.
- [158] López-Pastor, M., Simonet, B.M., Lendl, B., and Valcárcel, M. (2008) *Electrophoresis* 29, 94–107.
- [159] Jiang, T.-F., Gu, Y.-L., Liang, B., Li, J.-B., Shi, Y.-P., and Ou, Q.-Y. (2003) *Anal. Chim. Acta* 479, 249–254.
- [160] Marszatt, M.P., Markuszewski, M.J., and Kaliszan, R. (2006) *J. Pharm. Biomed. Anal.* 41, 329–332.
- [161] Tian, K., Wang, Y., Chen, Y., Chen, X., and Hu, Z. (2007) *Talanta* 72, 587–593.
- [162] Corradini, D., Nicoletti, I., and Bonn, G.K. (2009) *Electrophoresis* 30, 1969–1976.
- [163] Maier, V., Horakova, J., Petr, J., Drahonovsky, D., and Sevcik, J. (2006) *J. Chromatogr. A* 1103, 337–343.
- [164] Su, H.-L., Kao, W.-C., Lin, K.-W., Lee, C.-y., and Hsieh, Y.-Z. (2010) *J. Chromatogr. A* 1217, 2973–2979.
- [165] Xu, Y.H., Fang, L.Y., and Wang, E.K. (2009) *Electrophoresis* 30, 365–371.
- [166] Xu, Y.H., Jiang, H., and Wang, E.K. (2007) *Electrophoresis* 28, 4597–4605.
- [167] Xu, Y., Li, J., and Wang, E. (2008) *Electrophoresis* 29, 1852–1858.
- [168] Xu, Y.H., Li, J., and Wang, E.K. (2008) *J. Chromatogr. A* 1207, 175–180.
- [169] Zen, H.-L., Shen, H., Nakagama, T., and Uchiyama, K. (2007) *Electrophoresis* 28, 4590–4596.
- [170] Tran, C.D. and Mejac, I. (2008) *J. Chromatogr. A* 1204, 204–209.
- [171] Göttlicher, B. and B€eachmann, K. (1997) *J. Chromatogr. A* 780, 63–73.
- [172] Nilsson, C. and Nilsson, S. (2006) *Electrophoresis* 27, 76–83.
- [173] Nilsson, C., Birnbaum, S., and Nilsson, S. (2007) *J. Chromatogr. A* 1168, 212–224.
- [174] Wallingford, R.A. and Ewing, A.G. (1989) *Adv. Chromatogr.* 29, 1–76.
- [175] Fan, D.H., Yuan, S.W., and Shen, Y.M. (2010) *Colloids Surf. B* 75, 608–611.
- [176] Noh, H.B., Lee, K.S., Lim, B.S., Kim, S.J., and Shim, Y.B. (2010) *Electrophoresis* 31, 3053–3060.

- [177] Liu, X.J. and Gomez, F. (2009) *Anal. Bioanal. Chem.* 393, 615–621.
- [178] Makamba, H., Huang, J.W., Chen, H.H., and Chen, S.H. (2008) *Electrophoresis* 29, 2458–2465.
- [179] Wang, W., Zhao, L., Zhou, F., Zhu, J.J., and Zhang, J.R. (2007) *Talanta* 73, 534–539.
- [180] Wang, W., Zhao, L., Zhang, J.R., Wang, X.M., Zhu, J.J., and Chen, H.Y. (2006) *J. Chromatogr. A* 1136, 111–117.
- [181] Wang, A.J., Xu, J.J., and Chen, H.Y. (2006) *J. Chromatogr. A* 1107, 257–264.
- [182] Wang, A.J., Xu, J.J., and Chen, H.Y. (2006) *J. Chromatogr. A* 1107, 257–264.
- [183] Tabuchi, M., Katsuyama, Y., Nogami, K., Nagata, H., Wakuda, K., Fujimoto, M., Nagasaki, Y., Yoshikawa, K., Kataoka, K., and Baba, Y. (2005) *Lab Chip* 5, 199–204.
- [184] Ohno, T., Matsuda, T., Suzuki, H., and Fujimoto, M. (2006) *Adv. Powder Technol.* 17, 167–179.
- [185] Mark, J.E., Jiang, C.-Y., and Tang, M.-Y. (1984) *Macromolecules* 17, 2613–2616.
- [186] Roman, G.T., Hlaus, T., Bass, K.J., Seelhammer, T.G., and Culbertson, C.T. (2005) *Anal. Chem.* 77, 1414–1422.
- [187] Qiu, J.-D., Wang, L., Liang, R.-P., and Wang, J.-W. (2009) *Electrophoresis* 30, 3472–3479.
- [188] Pumera, M., Wang, J., Grushka, W., and Polsky, R. (2001) *Anal. Chem.* 73, 5625–5628.
- [189] Fan, D.H., Yuan, S.W., and Shen, Y.M. (2010) *Colloids Surf. B Biointerfaces* 75, 608–611.
- [190] Wang, A.J., Xu, J.J., Zhang, W., and Chen, H.Y. (2006) *Talanta* 69, 210–215.
- [191] Wang, W., Zhao, L., Zhou, F., Zhu, J.-J., and Zhang, J.-R. (2007) *Talanta* 73, 534–539.
- [192] Noh, H.B., Lee, K.S., Lim, B.S., Kim, S.J., and Shim, Y.B. (2010) *Electrophoresis* 31, 3053–3060.
- [193] Lin, Y.W., Huang, M.J., and Chang, H.T. (2003) *J. Chromatogr. A* 1014, 47–55.
- [194] Lin, Y.W. and Chang, H.T. (2005) *J. Chromatogr. A* 1073, 191–199.
- [195] Tabuchi, M., Ueda, M., Kaji, N., Yamasaki, Y., Nagasaki, Y., Yoshikawa, K., Kataoka, K., and Baba, Y. (2004) *Nat. Biotechnol.* 22, 337–340.
- [196] Tabuchi, M., Katsuyama, Y., Nogami, K., Nagata, H., Wakuda, K., Fujimoto, M., Nagasaki, Y., Yoshikawa, K., Kataoka, K., and Baba, Y. (2005) *Lab Chip* 5, 199–204.
- [197] Ohlsson, P., Ordeig, O., Nilsson, C., Harwigsson, I., Kutter, J.P., and Nilsson, S. (2010) *Electrophoresis* 31, 3696–3702.
- [198] Pamme, N. (2006) *Lab Chip* 6, 24–38.
- [199] Ambrosi, A., Guix, A.M., and Merkoci, A. (2011) *Electrophoresis* 32, 861–869.
- [200] Tnnico, Y.H. and Remcho, V.T. (2010) *Electrophoresis* 31, 2548–2557.
- [201] Doyle, P.S., Bibette, J., Bancaud, A., and Viovy, J.L. (2002) *Science* 295, 2237–2237.
- [202] Moliner-Martinez, Y., C_ardenas, S., Simonet, B.M., and Valcarcel, M. (2009) *Electrophoresis* 30, 169–175.
- [203] Fernández-Abedul, M.T. and Costa-García, A. (2008) *Anal. Bioanal. Chem.* 390, 293–298.
- [204] Trojanowicz, M. (2006) *Trends Anal. Chem.* 25, 480–489.

- [205] Wang, Z., Luo, G., Chen, J., Xiao, S., and Wang, Y. (2003) *Electrophoresis* 24, 4181–4188.
- [206] Wiles, P.G. and Abrahamson, J. (1978) *Carbon* 16, 341–349.
- [207] Iijima, S. (1991) *Nature* 354, 56–58.
- [208] Cao, J., Dun, W.L., and Qu, H.B. (2011) *Electrophoresis* 32, 408–413.
- [209] Chen, J.L. and Hsieh, K.H. (2010) *Electrophoresis* 31, 3937–3948.
- [210] Weng, X.X., Bi, H.Y., Liu, B.H., and Kong, J.L. (2006) *Electrophoresis* 27, 3129–3135.
- [211] Nieto de Castro, C.A., Lourenco, M.J.V., Ribeiro, A.P.C., Langa, E., Vieira, S.I.C., Goodrich, P., and Hardacre, C. (2010) *J. Chem. Eng. Data* 55, 653–661.
- [212] Choi, S.U.S., Zhang, Z.G., and Keblinski, P. (1995) Siginer, D.A. and Wang, H.P. (eds), *Developments and Applications of Non-Newtonian Flows*, ASME, New York, FED-Vol. 231/MD-Vol. 66 pp. 99–105
- [213] de Dios, A.S. and Díaz-García, M.E. (2010) *Anal. Chim. Acta* 666, 1–22.
- [214] Vázquez, M. and Paull, B. (2010) *Anal. Chim. Acta* 668, 100
- [215] Yang, W.C., Sun, X.H., Pan, T., and Woolley, A.T. (2008) *Electrophoresis* 29, 3429–3435.
- [216] Cakal, C., Ferrance, J.P., Landers, J.P., and Caglar, P. (2010) *Anal. Bioanal. Chem.* 398, 1909–1917.
- [217] Sun, X., Weichun, Y., Yanli, G., and Woolley, A.T. (2009) *Lab Chip* 9, 949–953.
- [218] Shi, Y.N. and Anderson, R.C. (2003) *Electrophoresis* 24, 3371–3377.
- [219] Righetti, P.G., Gelfi, C., Verzola, B., and Castelletti, L. (2001) *Electrophoresis* 22, 603–611.
- [220] Dang, F., Zhang, L., Hagiwara, H., Mishina, Y., and Baba, Y. (2003) *Electrophoresis* 24, 714–721.
- [221] Tanaka, N., Tanigawa, T., Hosoya, K., Kimata, K., Araki, T., and Terabe, S. (1992) *Chem. Lett.* 959–962.
- [222] Boonsong, K., Caulum, M.M., Dressen, B.M., Chailapakul, O., Cropek, D.M., and Henry, C.S. (2008) *Electrophoresis* 29, 3128–3134.
- [223] Ballauff, M. and Borisov, O. (2006) *Curr. Opin. Colloid Interface Sci.* 11, 316–323.
- [224] Rühle, J., Ballauff, M., Biesalski, M., Dziezok, P., Gröhn, F., and Johannsmann, D. (2004) *Adv. Polym. Sci.* 165, 79–150.
- [225] Rucker, O. and Rühle, J. (1998) *Macromolecules* 31, 592–601.
- [226] Förster, S., Hermsdorf, N., Böttcher, C., and Lindner, P. (2002) *Macromolecules* 35, 4096–4105.
- [227] Houbenov, N., Minko, S., and Stamm, M. (2003) *Macromolecules* 36, 5897–5901.
- [228] Hales, K. and Pochan, D.J. (2006) *Curr. Opin. Colloid Interface Sci.* 11, 330–336.
- [229] Wang, Y.-C., Choi, M.H., and Han, J. (2004) *Anal. Chem.* 76, 4426–4431.
- [230] Shah, J.J., Geist, J., Locascio, L.E., Gaitan, M., Rao, M.V., and Vreeland, W.N. (2006) *Electrophoresis* 27, 3788–3796.

- [231] Woolley, A.T. and Mathies, R.A. (1995) *Anal. Chem.* 67, 3676–3680.
- [232] Munro, N.J., Huhmer, A.F.R., and Landers, J.P. (2001) *Anal. Chem.* 73, 1784–1794.
- [233] Lee, J.H., Kopeckova, P., Zhang, J., Kopecek, J., and Andrade, J.D. (1988) *Polym. Mater. Sci. Eng.* 59, 234.
- [234] Halperin, A. and Leckband, D.E. (2000) *C.R. Acad. Sci. Paris (Ser. IV Phys. Astrophys.)* 1, 1171–1178.
- [235] Kitagawa, F., Kubota, K., Sueyoshi, K., and Otsuka, K. (2010) *J. Pharm. Biomed. Anal.* 53, 1272–1277.
- [236] Zhang, Z.W., Feng, X.J., Luo, Q.M., and Liu, B.F. (2009) *Electrophoresis* 30, 3174–3180.
- [237] Miyaki, K., Zeng, H.-L., Nakagama, T., and Uchiyama, K. (2007) *J. Chromatogr. A* 1166, 201–206.
- [238] Feng, J.-J., Wang, A.-A., Fan, J., Xu, J.-J., and Chen, H.-Y. (2010) *Anal. Chim. Acta* 658, 75–80.
- [239] Kolb, H.C., Finn, M.G., and Sharpless, K.B. (2001) *Angew. Chem. Int. Ed.* 40, 2004–2021.
- [240] Prakash, S., Long, T.M., Selby, J.C., Moore, J.S., and Shannon, M.A. (2007) *Anal. Chem.* 79, 1661–1667.
- [241] Zhang, Z.W., Feng, X.J., Xu, F., Liu, X., and Liu, B.F. (2010) *Electrophoresis* 31, 3129–3136.
- [242] Henry, A.C., Tutt, T.J., Galloway, M., Davidson, Y.Y., McWhorter, C.S., Soper, S.A., and McCarley, R.L. (2000) *Anal. Chem.* 72, 5331–5337.
- [243] Llopis, S.L., Osiri, J., and Soper, S.A. (2007) *Electrophoresis* 28, 984–993.
- [244] Slentz, B.W., Penner, N.A., and Regnier, F.W. (2002) *J. Chromatogr. A* 948, 225–233.
- [245] Liu, J., Pan, T., Woolley, A.T., and Lee, M.L. (2004) *Anal. Chem.* 76, 6948–6955.
- [246] Sun, X., Liu, J., and Lee, M.L. (2008) *Anal. Chem.* 80, 856–863.
- [247] Xu, L. and Sun, Y. (2008) *Electrophoresis* 29, 880–888.
- [248] Wu, D., Zhao, B., Dai, Z., Qin, J., and Lin, B. (2006) *Lab Chip* 6, 942–947.
- [249] Sun, X., Liu, J., and Lee, M.L. (2008) *Electrophoresis* 29, 2760–2767.
- [250] Pan, T., Fiorini, G.S., Chiu, D.T., and Woolley, A.T. (2007) *Electrophoresis* 28, 2904–2911.
- [251] Xiao, D., Zhang, H., and Wirth, M. (2002) *Langmuir* 18, 9971–9976.
- [252] Xiao, D., Le, T.V., and Wirth, M.J. (2004) *Anal. Chem.* 76, 2055–2061.
- [253] Hagg, M.B. (2000) *J. Membr. Sci.* 170, 173–190.

Article 1

*Poly (acrylic acid) Microchannel Modification
for the Enhanced Resolution of Catecholamines
Microchip Electrophoresis with Electrochemical
Detection*

Anal. Chim. Acta 724 (2012) 136-143.



Poly (acrylic acid) Microchannel Modification for the Enhanced Resolution of Catecholamines Microchip Electrophoresis with Electrochemical Detection

Isabel Álvarez-Martos^a, M. Teresa Fernández-Abedul^a, Adela Anillo^b, José Luis G. Fierro^c,
Francisco Javier García Alonso^b, Agustín Costa-García^{a*}

^a*Departamento de Química Física y Analítica, Universidad de Oviedo, Asturias, Spain*

^b*Departamento de Química Orgánica e Inorgánica, Universidad de Oviedo, Asturias, Spain*

^c*Instituto de Catálisis y Petroleoquímica, CSIC, Madrid, Spain*

ABSTRACT

A new modification of glass electrophoresis microchips based on poly (acrylic) acid immobilization has been performed. It is based on the reaction of PAA with an amine functionalized surface, obtained through the bifunctional reagent 3-aminopropyl triethoxysilane. Parameters affecting all the three steps involved: surface activation, silanization and polymer immobilization were optimized employing soda-lime glass plates. Characterization by SEM and XPS was carried out. Application of the modified microchips to the separation of a model system: dopamine (D), epinephrine (E) and norepinephrine (NE), that on the other hand are of high clinical relevance was performed employing amperometric detection. Modification is necessary for obtaining partial resolution of all the three analytes in a microchip with an effective separation length of 30 mm. Situation changes from no resolution (R_s) at all (only one peak was achieved for the mixture) to a partial resolution (R_s D–NE and R_s NE–E are 0.25 and 0.24 respectively). Microchips with 60 mm of separation channel were also modified, implying this procedure a resolution enhancement (R_s of 0.49 and 0.28 for D–NE and NE–E respectively), even when methanol is employed as organic modifier (R_s values of 0.70 (D–NE) and 0.66 (NE–E) for a 3% MeOH).

1. Introduction

The employment of flow systems had produced an important advance in Analytical Chemistry, since many methodologies that were performed in discrete steps could be automated. The next breakthrough in technology was the manipulation of fluids in channels with dimensions of tens of micrometres, namely, microfluidics. It has emerged as a distinct new field, nowadays with approximately 4000 new microfluidics papers published. However, it is still at an early stage in which refers to product commercialization [1]. Analytical methodologies are taking advantage of this area and microchip electrophoresis (ME) is an example. CE has demonstrated to be a robust technique with relevance in research of paramount importance [2] and an invaluable help to pathologists and doctors in the evaluation of patients status [3].

Neurotransmitters have been chosen several times as model system in analytical techniques because of their clinical relevance [4,5]. Thus, abnormal level of neurotransmitters (dopamine (D), norepinephrine (NE) and epinephrine (E) among them) has been linked to a wide range of disorders such as Parkinson's [6], Alzheimer's [7], cocaine addiction [8] or hypertension. D and E have been the most widely employed in order to check the efficiency of different procedures [9,10], obtaining in these cases resolution values from 0.58 to 1.44 depending on the pH value.

Fluorescent detection has been employed for catecholamines detection, but apart from some works based on native fluorescence measurement [11], derivatization chemistries are usually required for obtaining adequate sensitivity [12]. However, electrochemical detection (ED) has been combined with CE for the determination of these compounds due to their adequate electrochemical behavior. They are easily converted to quinones by electrochemical oxidation without prior derivatization [13,14]. Resolution of peaks by means of voltammetric techniques is commonly performed through electrode modification. Polymeric films with electrocatalytic activity have been combined with carbon electrodes for the voltammetric resolution of dopamine [15] or epinephrine [16] in the presence of ascorbic and uric acids. Chemometric techniques have been employed in combination with fast-scan cyclic voltammetry for the resolution of D, E and NE, substances with overlapped cyclic voltammograms [17]. To distinguish between chemical species that are involved in diffusion-controlled, e.g. one-electron electrolysis processes, it is required that E° 's differ by at least 0.118 V [18], and therefore combination with separation techniques is usually required.

Apart from intrinsic characteristics, ED fits well with miniaturisation, which in the case of catecholamines is almost mandatory for *in vivo* analysis, where portable instruments are preferable. Dopamine and/or epinephrine have been determined employing different electrochemical strategies and microchip materials (PDMS [19,20], glass [21-23], PDMS/glass [24,25]) together with other analytes. A recent study [26] reveals the importance of the material in the resolution of peaks. D and E were separated in PDMS, Topas and SU-8 microchips meanwhile in glass microchips only one peak was achieved. Glass, however, is a robust material that has demonstrated an adequate performance with other analytes as well as an appropriate durability. Microchip design is also important and the length of the channels has to be taken into consideration. It has been shown that resolution in free zone electrophoresis is directly proportional to the square root of separation length [27]. Therefore, increasing the separation channel length will lead to an increase in resolution between closely eluting analytes. Nevertheless, the microfabrication procedure is not usually conceived for very long microchips due to the equipment employed (UV irradiation or laser equipment, spin-coaters, etc.). Consequently, the increase in length can be made through serpentine microchannels with incorporated turns. An 8-cm separation channel was employed for the separation of NE, E and D [28]. However, it has to be beard in mind that this design increases analyte dispersion [29] and requires an optimized design [30]. The effect of surface microstructures on the separation efficiency in glass ME has been evaluated for the model system D-E [9] obtaining a relative resolution (R_s') of 2-2.5 depending on the % of microstructures. Most of the works employ capillary zone electrophoresis but resolution between D, NE and E by MEKC using SDS and borate has been reported [31].

In this context, development of robust and time resistant coating that modify electrophoretic behaviour of structurally related analytes, is of paramount importance. Therefore, D, NE and E with close pK_a s values and similar structures (which makes difficult their resolution) were chosen for the development of this work. Separation of catecholamines is reported all along the pH range, i.e at 10 mM boric buffer pH 9.2 [24], 10 mM phosphate buffer 7.4 [9], 50 mM MES-20 mM phosphate buffer pH 6.5 [21], 30 mM TES buffer pH 5.77 [20] or 50 mM phosphate buffer pH 2.5 [10].

Depending on the type of interaction, coatings can be classified into two different groups: dynamic or static. Dynamic coatings are only adsorbed on capillary walls; meanwhile the second ones are covalently bound to capillary surface. The main reasons for surface properties manipulation of the microchannel *via* coatings are minimization of analyte adsorption and also resolution improvement [32-35]. Developments in the preparation of both

wall coatings for ME of different materials have been reviewed [36,37]. Most of the modification strategies have been applied to polymeric materials [38,39], probably due to their more hydrophobic nature. Scarce works are reported for glass microchips: cationic polymer coatings [40] or single wall carbon nanotubes with soft hydrogel polymers [41] are some examples. Permanent coatings are often regarded as the most effective way for surface modification because they are stable, insoluble and no regeneration is needed. Since glass microchips can be considered durable devices, a permanent coating seems very adequate. Moreover, surface chemistry known from CE can often be transferred to glass MEs. Surface modification commonly occurs through silanol groups and cationic, neutral or anionic layers are possible. Poly (acrylic acid) (PAA) is a polymer that generates carboxylate groups and therefore, negative charges can be produced. Polymerization of acrylic acid was initiated by exposure of a benzophenone-implanted PDMS to UV radiation with a thin aqueous layer of acrylic acid [42]. Bioanalytical applications based on cell and protein immobilization through carboxyl groups were demonstrated. Although there are studies on the temperature influence on the adsorption mechanism of anionic PAA on silica surfaces [43], there is no any reference to its use on glass microchips.

In this paper a covalent polymeric coating with PAA is proposed, due to its chemical robustness compared to other surface modification methods. In order to get a stable and homogeneous coating, the procedure is firstly performed and optimised on glass plates. This is the first time, to the best of our knowledge, that this coating is employed on glass microchips. To evaluate the PAA influence on separation, analytes of similar structure (D, NE and E) with high clinical significance, were chosen as model system, trying to improve their separation, employing amperometric gold electrode end-channel detection for their detection.

2. Experimental

2.1. Reagents

Hydrogen peroxide (30%), methanol, ethanol, isopropanol, ammonia (25%), sulphuric (95-97%) and acetic acid were purchased from Merck (Darmstadt, Germany).

3-aminopropyl triethoxysilane (APTES), poly (acrylic acid) (PAA)(Mw ~1800 D), N,N-dimethylformamide (DMF), dichloromethane, toluene, dopamine (D), norepinephrine (NE), epinephrine (E), boric acid (99.5%), hydrofluoric acid (48%), 2-(N-morpholino)-ethane sulfonic acid (MES), tris(hydroxymethyl)aminomethane (Tris), histidine (His), sodium hydroxide and sodium citrate were obtained from Sigma-Aldrich (Madrid, Spain).

Catecholamines solutions were prepared daily in the running buffer and protected from light. All solutions were filtered through nylon syringe filters (Cameo 30 N, 0.1 μm , 30 mm) obtained from Osmonics (Minnetonka, MN, USA).

Britton-Robinson buffer was prepared by mixing H_3BO_3 , H_3PO_4 and AcH (in 0.04 M concentrations) and adjusting the pH with NaOH.

Water was purified employing a Milli-Q direct-Q system from Millipore (Bedford, MA, USA). All other reagents were of analytical reagent grade. The rest of volumetric material was of analytical reagent grade.

2.2. Materials and instrumentation

Soda-lime glass microchips were purchased from MicruX Fluidic (Oviedo, Spain). They consisted of a plate (48 mm x 16 mm) of 1 mm thickness containing a 30 or 60 mm longitudinal separation channel of 30 μm depth and 100 μm width. The injection cross (single-channel design) is formed by intersection of the separation channel with a shorter channel (10 mm) of identical cross sectional dimensions. Micropipette tips were cut to obtain 1 cm long pieces with a diameter of 0.5 cm at the top. Holes of 2 mm diameter that act as reservoirs are situated at the ends of the channels. They were attached concentrically to the chip holes with Araldite (Vantico, Basel, Switzerland) forming reservoirs of approximately 150 μL in volume.

Two high-voltage power supplies (HVPS, MJ series) with a maximum voltage of + 5000 V from Glassman High Voltage (High Bridge, NJ, USA) were employed. A Faraday cage was used to house the microchip in order to minimize electrical interference. High-voltage electrodes consist of 0.3 mm diameter platinum wires (Sigma-Aldrich, Madrid, Spain).

The amperometric detector was situated in the waste reservoir with a three electrode configuration. The reference and counter electrodes were coupled in a 250 μL micropipette tip that was introduced in the detection reservoir to perform the measurements. The reference electrode consisted of an anodized silver wire (Goodfellow, Huntingdon, UK) introduced in a tip through a rubber syringe piston. The tip was filled with saturated KCl solution and contained a low-resistance liquid junction. The platinum wire that acted as auxiliary electrode was fixed with insulating tape. A 100 μm diameter gold wire (Sigma-Aldrich) was employed as working electrode in an end-channel configuration [25]. Since the channel outlet was at the end side of the glass substrate while the cover plate was longer, hole for detection reservoir was not necessary. The gold wire electrode is coupled to a piece of adhesive tape to allow easier handling. It was placed on the cover plate and aligned at the outlet of the separation

channel with the aid of a microscope (MA722 model, Swift Optics, USA). The electrode was fixed over the cover plate with epoxy resin (Araldit) and the adhesive tape. Finally, a copper cable was fixed to gold wire with a conducting silver epoxy resin (CW2400, RS Components, UK) for electrical connection.

Amperometric detection was performed with an Autolab PGSTAT 10 (ECO Chemie, The Netherlands) bipotentiostat interfaced to a computer system and controlled by Autolab GPES 4.9 version for Windows 98.

Photoelectron spectra (XPS) were obtained with a VG Escalab 200R spectrometer equipped with a hemispherical electron analyser (pass energy of 50 eV) and a Mg K α ($h\nu = 1254.6$ eV, 1 eV = 1.6302×10^{-19} J) X-ray source, powered at 120 W. The kinetic energies of photoelectrons were measured using a hemispherical electron analyser working in the constant pass energy mode. The background pressure in the analysis chamber was kept below 2×10^{-8} mbar during data acquisition. The XPS data signals were taken at increments of 0.1 eV with dwell times of 50 ms. Binding energies were calibrated relative to the C 1s peak at 284.8 eV. High resolution spectra envelopes were obtained by curve fitting synthetic peak components using the software "XPS peak". The raw data were used with no preliminary smoothing. Symmetric Gaussian-Lorentzian product functions were used to approximate the line shapes of the fitting components. Atomic ratios were computed from experimental intensity ratios and normalized by atomic sensitivity factors [44].

A JEOL JSM-6100 scanning electron microscope (Japan) was used to characterize the glass plates.

2.3. Electrophoretic procedure

Prior to electrophoresis, microchips were initially rinsed for 15 min with 0.1 M NaOH for unmodified ME and 0.01 M NaOH for PAA-modified ME and then with the running buffer for 20 min. Washing was made with the aid of a simple vacuum system and reservoirs were filled with the running buffer solution. The detection potential is applied for baseline stabilization and afterwards, reservoir C (see **Fig.1** in **Supplementary Data**) is filled with the sample solution. Unpinched injections were performed by applying the desired voltage between sample (C) and detection (B, grounded) reservoirs. Separation was carried out by applying the corresponding voltage to the running buffer reservoir (A) with the detection reservoir (B) grounded. Then, the electropherogram is recorded. All experiments were performed at room

temperature. For overnight or prolonged storage, microchips are stored at room temperature filled with Milli-Q water and covered with Parafilm (Sigma-Aldrich).

2.4. Functionalization with PAA

2.4.1. Glass slides

Initially 7 mm x 7 mm x 1 mm glass plates were sonicated in water containing a commercial detergent for 15 min. After rinsing with deionized water, they were further sonicated for 15 min in ethanol and then for 30 min in a freshly prepared piranha solution {H₂SO₄ (18 M) / H₂O₂ (30 vol), 3:1 (v/v)}. Subsequently, they were rinsed thoroughly with deionized water and dried under vacuum for 10 min. Next, the slides were immediately introduced under nitrogen in a toluene solution of 3-aminopropyltriethoxysilane (20 % in volume) and heated at 40 °C for 4.5 h. After that, they were sonicated twice in CH₂Cl₂ for 10 min and dried under vacuum at 100 °C for 1 h. Finally, the glass slides were immersed under nitrogen in a solution of poly (acrylic acid) (Mw ~ 1800 D) in DMF (0.01 g.mL⁻¹), heated at 140 °C for 24 h, sonicated 10 min in methanol and kept under vacuum.

2.4.2. Microchannel surface of ME

The process was basically the same used for the glass plate surfaces (see Section 2.4.1), but taking into account the special characteristics of the microchip. Thus, the solutions were introduced into the microchannel via vacuum and in the reactions carried out along the process the microchip was immersed into the corresponding solution to avoid evaporations from the microchannel.

2.4.3. Safety considerations

Piranha solution is extremely corrosive and highly toxic. Contact can lead to very serious and permanent damage to the skin, eyes or mouth.

The contact with hydrofluoric acid (liquid or vapor) causes severe burns and possible irreversible eye damage. It may be fatal if it is absorbed through the skin, inhaled or ingested. It causes severe burns with delayed tissue destruction.

High-voltage power supplies should be handled with extreme care to avoid electrical shock.

3. Results and Discussion

A microchannel with homogeneous surface is essential for further development of adequate analytical methodologies. Obtaining quality coatings is therefore relevant for improving the analytical performance of microchips [36]. In this case, optimization of the PAA modification procedure was carefully performed on soda-lime glass plates and once characterized; it was translated to microchannel surface.

3.1. PAA immobilization on soda-lime glass surfaces

The surface of glass contains, similarly to fused silica (capillary electrophoresis material) silanol groups. The density of Si-OH groups on the fused silica surface is about $4.5 \text{ silanols mm}^{-2}$ and is smaller than theoretical $7.8 \text{ groups mm}^{-2}$ [45]. In glass, one would expect a lower silanol density. Still, the presence of Si-OH groups on the surface of a glass makes the reaction with silanol the first choice for its modification. Different glass surfaces are commercially available, namely Soda-lime and borosilicates. The main difference is silicon and alkaline / alkaline earth metals as well as boron content. Soda lime has a smaller content of silica (<75 %) than i.e. Borofloat (75-81 %) or Pyrex (80 %). This makes it easier to etch, increasing the etching rate [46], which is important in microchip manufacturing.

In this case, soda lime glass substrates were covered with PAA adapting and optimizing procedures earlier described in the literature [47]. The process took place in three steps, creation of silanol groups (**Fig. 1A**), silanization (**Fig. 1B**) and attachment of PAA to surface by amide bond formation (**Fig. 1C**).

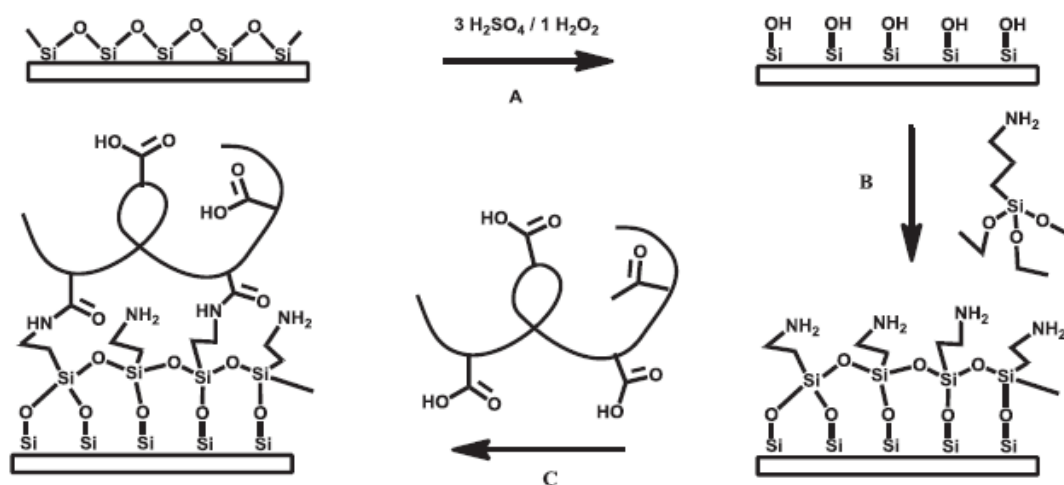


Figure 1. Steps in the glass surface modification: formation of silanol groups (A), coating the glass surface with amine groups (B), and immobilization of PAA on the surface (C).

Before starting the modification, the faces of the plates to be modified were marked with a diamond pencil. The formation of silanol groups on the surface was achieved by immersing the glass slides in a piranha acid solution and sonicating them for 30 min. Previously, the glass plates were sonicated 15 min in water with soap and then other 15 min in ethanol. Other alternatives cited in the literature for the creation of Si-OH groups on the glass surface, namely the use of an aqueous solution of HF (10 %) [48] or basic piranha {NH₃ (13.4 M)/H₂O₂ (30 vol), 3:1 (v/v)} [47] did not work properly. It has been reported [49] that heating under vacuum after activation should increase the number of silanol groups on the surface. With this aim, heating the plates overnight at 80 °C under vacuum was checked. However, less and more heterogeneous polymer distribution was observed.

In the second step the surface was covered with amine groups by reacting the silanols with the difunctional molecules of APTES under nitrogen in dry toluene, a procedure called silanization. The process depends directly on the following parameters: time between activation and silanization steps, APTES concentration, reaction time, presence of water in the silanization solution and subsequent thermal curing [47,49-55]. Reaction conditions were adjusted and the effects of these parameters were evaluated. The first observation that could be done was that the silanization reaction should be carried out immediately after the activation step, as far as a delay in the procedure has proved to be unfavorable. No polymer was observed in micrographs obtained by SEM when the surface activation occurred the day before. Moreover, the effect of APTES concentration (20 and 33 %) on polymer distribution was evaluated. Higher heterogeneity, probably due to formation of aggregates and less ordered layers [54], was found for the 33 % APTES. More uniform layers with a higher content of primary amines are obtained at lower concentrations [50]. A 20 % APTES concentration was chosen for further modifications. On the other hand, reaction time (4.5 and 48 h) was evaluated, concluding that long reaction times (48 h) produced a more heterogeneous distribution, because APTES multilayer formation with less accessible primary amines can occur [55]. Therefore, 4.5 h was chosen for further work. Another critical parameter studied in this work was the water content [0, 0.1 and 1 % (v/v)] in the silanization solution. In the two first cases, homogeneous distribution of PAA was encountered meanwhile no polymer was found in the third case. This can be due to the fact that large amounts of water lead to APTES molecules polymerization on the substrate surface, avoiding subsequent PAA immobilization [48,51,52]. Finally, thermal curing under vacuum (35 °C for 2 h [47] and 100 °C for 1 h [54]) after silanization reaction was checked. The second option, in which there is an increase in the number of primary amine available on the surface [54], was chosen.

PAA was later covalently linked onto the glass plates by the formation of an amide bond between some of the carboxylic groups of the macromolecules and the amine moieties of the silanized surface. The condensation reaction was carried out in dry DMF at 140 °C for 24 h releasing minute amounts of water which did not seem to play any important role. Two different concentrations were checked: 0.01 and 0.05 g mL⁻¹. Homogeneous distribution was obtained in both cases and 0.01 g mL⁻¹ was chosen for further microchip modification.

As seen in previous paragraphs, the whole process was followed by SEM. The attachment of PAA was checked by comparing the elemental analysis of two surface dots; one covered with the polymer the other not, being the carbon and oxygen percentages significantly higher in the first (9.06 vs. 1.68 in %C and 12.98 vs. 10.37 in %O respectively). Furthermore, every modification of the procedure was tested comparing the distribution of the polymer spots on the glass surface. Finally, the procedure described in the experimental part was confirmed to be confident by obtaining reproducible micrographs. In **Fig. 2**, SEM images corresponding to four glass slides modified in different days following the procedure described in *Section 2* are shown. The bright spots correspond to PAA immobilized on the glass surface and indicate an adequate precision of the procedure. Even when the whole surface is not coated, the polymer density along the glass surface is similar. Reaction blanks demonstrated that there is no modification when APTES or PAA are not present.

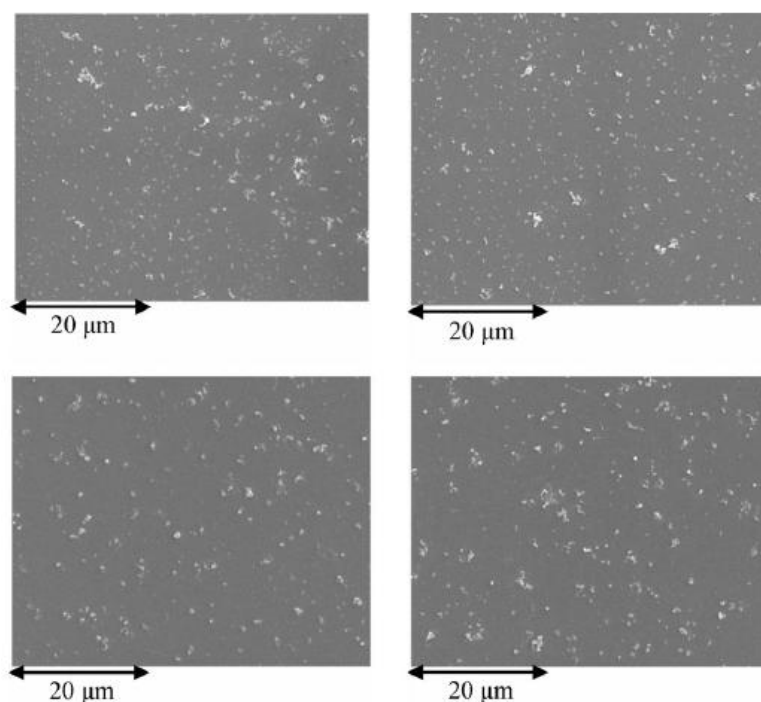


Figure 2. SEM images of the PAA coating obtained following the protocol described in *Section 2* for soda-lime glass slides, in four different days.

Further evidence of the success of functionalization comes from XPS measurements. This technique allows quantifying the surface composition and gives relevant information about functional groups. In this case, two glass slides (A and B) were simultaneously modified and characterized. **Fig. 3** shows the C 1s core-level spectra of sample A. The C 1s peak was deconvoluted into three different components. The most intense peak, at 284.8 eV, is assigned to sp^3 C-atoms, bonded either to hydrogen or carbon, in the polymeric structure. The less intense component at 286.2 eV has been usually attributed to sp^3 C-atoms single bonded to nitrogen (C-N) [56] and the components at 288.1 eV to C=O and -COO species [57]. It is likely that the component 286.2 eV also contains a certain contribution of C-O bonds coming from surface contamination because the binding energy of C-O and C-N is very close. Support to this possibility is provided by SEM analyses of the polymer free-surface which showed some carbon contamination. From the relative intensities of the C 1s components it appears that there are no significant changes between both samples. The O 1s core-level spectra have also been curve-resolved with two components, one at 531.9 eV assigned to C=O groups [56] and a second one at 533.2 eV assigned to C-O groups [57]. Finally, the N 1s spectra display two components at 399.8 and 401.3 eV which belong to free amine groups linked to C-atoms (H_2N-C) [58-60] and to amide bridges ($-NH-C=O$) groups [61], respectively. The presence of certain proportion of protonated NH_2^+ species whose N 1s binding energy falls somewhere around 401.3 eV, cannot be ruled out.

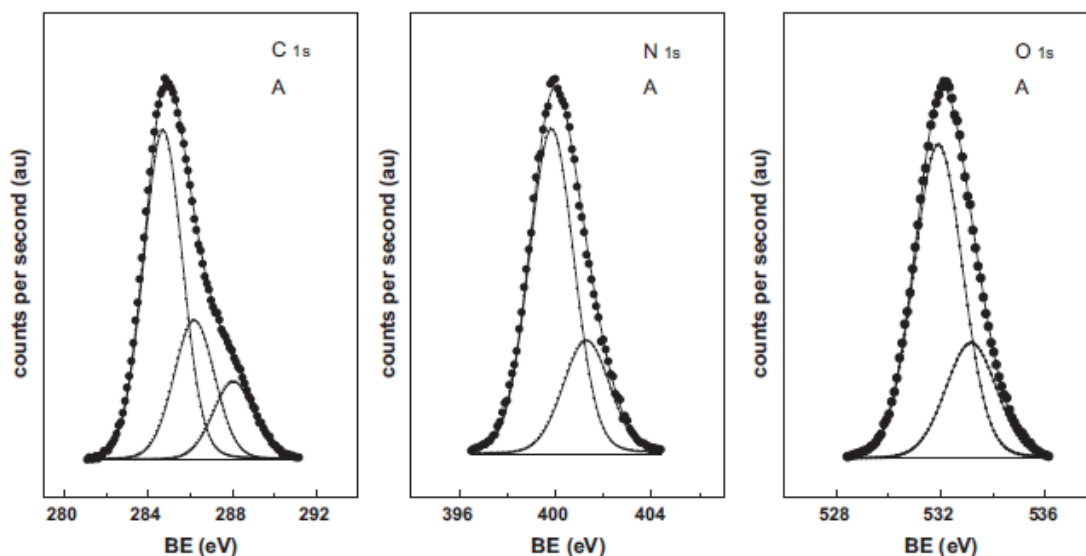


Figure 3. C 1s, N 1s and O 1s deconvoluted bands of XPS spectra corresponding to a PAA-modified glass plate surface.

The N/C atomic ratios were also calculated (**Table 1**). These were computed from peak intensity ratios normalized by atomic sensitivity factors [44]. The values of N/C are compiled in **Table 1** for the two samples, A (N/C = $0.123 \times 0.27/0.15$) and B (N/C = $0.113 \times 0.27/0.1$), respectively. These values are very close to nominal value (0.26). In addition, no attempt has been made to calculate the O/C ratios because uncertainty arising from surface contamination and also from the contribution of Si-O bonds of the uncovered substrate whose binding energy signal falls just at 532.8 eV where the signal of C-O peak appears. In this table, the values for the C 1s, N 1s and O 1s deconvoluted peaks are reported for both samples, showing the good precision of the measurements.

Table 1. Binding energies (eV) and surface atomic ratios for A and B samples.

| Sample | C1s | N1s | O1s | N/C at |
|--------|------------|------------|------------|--------|
| A | 284.8 (59) | | | 0.221 |
| | 286.2 (26) | 399.8 (73) | 531.9 (72) | |
| | 288.1 (15) | 401.3 (27) | 533.2 (28) | |
| B | 284.8 (60) | | | 0.203 |
| | 286.3 (25) | 399.9 (73) | 531.9 (78) | |
| | 288.3 (15) | 401.5 (27) | 533.3 (22) | |

Once the procedure was optimized in soda-lime glass plates, translation to microchip was performed. All the three steps were carried out: activation, silanization with APTES and immobilization of PAA. The procedure was followed rigorously, but in this case, microchannel's filling was done with the aid of vacuum and MEs were immersed in the solutions for avoiding evaporation.

3.2. Evaluation of catecholamines separation on MEs

Microchips with two different separation lengths (30 and 60 mm) were employed. The electric field strengths were 214 V cm^{-1} and 231 V cm^{-1} for separation voltages of +750 (30 mm ME) and +1500 V (60 mm ME) respectively. The injection voltage was +500 V in both cases. The chosen potential of detection was +1.2 and +0.8 V respectively for pH 5.5 and pH 9.0. These were chosen based on results obtained by cyclic voltammetry and previous works [21,24].

3.2.1. Preliminary studies on unmodified MEs

In an unmodified glass microchip and in order to expose the maximum number of silanol groups on the silica surface, the microchannels are initially rinsed with 0.1 M NaOH and then with the corresponding running buffer for equilibration. With the aim of determining the optimum conditions, measurements in different running buffer solutions have been

performed. Adjusting pH is a dominant factor in separation on unmodified MEs [10], but the concentration and composition affects also the separation. All the three catecholamines are electroactive in all the range of pHs (assayed by cyclic voltammetry in 0.1 M Britton-Robinson buffer and 0.1 M H₂SO₄). Peak current increases with decreasing pH meanwhile the oxidation process moves to more positive potentials.

Since the Si-C bond is unstable at extreme pH, 25 mM MES-His pH 5.5 and 25 mM boric acid-NaOH pH 9.0 were initially chosen for evaluation. Apart from the microchip material and the analyte electroactivity it has also to be taken into account the stability of the tested analytes during the operation conditions. In the case of catecholamines, they become oxidised with time and, therefore, fresh solutions are prepared daily. This process is favoured at alkaline pH, which is observable by the appearance of a brownish colour. In the case of boric-Tris buffer pH 9.0, this occurs in less than 2 min, meanwhile by changing the composition to boric-NaOH, catecholamine solutions are stable during the workday.

The electropherograms were recorded individually for 1mM solutions of the three catecholamines. The migration order was D, NE and E, and the difference in the migration times (t_m) was 1.1 s for the couple D-NE and 3.6 s for NE and E, when MES-His buffer is employed. In the case of the boric acid-NaOH buffer, the t_m window is 1.0 s in both cases, for D-NE and NE-E. The migration time for D changes from 21.6 to 89.5 s from one buffer to the other. Catecholamines are cationic at pH 5.5 meanwhile less positive charges are present at pH 9.0 and therefore, longer t_m can be expected. Complexation with borate ions has also to be taken into account [31,62]. The small t_m window makes difficult the separation and when they are injected as a mixture (500 μ M concentration in each), only one peak is observed in both buffers ($t_m = 22.7$ s with $i_p = 22.2$ nA for MES-His and $t_m = 90.6$ s with $i_p = 9.88$ nA for boric-NaOH buffer). Since no baseline separation is observed at any buffer solution pH, MES-His was chosen for the remainder of the work because in this buffer more intense and slightly resolved peaks are observed.

In order to obtain catecholamine resolution, a longer ME is needed. A microchip with double separation length is then employed. In this case the separation voltage is doubled (+1500 V) in order to maintain the electric field, meanwhile the injection potential is maintained to +500 V and applied for 0.3 s. In **Fig. 4A (a)**, the electropherogram obtained for a 500 μ M (in each) mixture is shown. Partial resolution is obtained in this case. The migration time increases to 98.6, 103.8 and 109.1 s for D, NE and E respectively, with Rs equal to 0.33 for D-NE and 0.25 for NE-E.

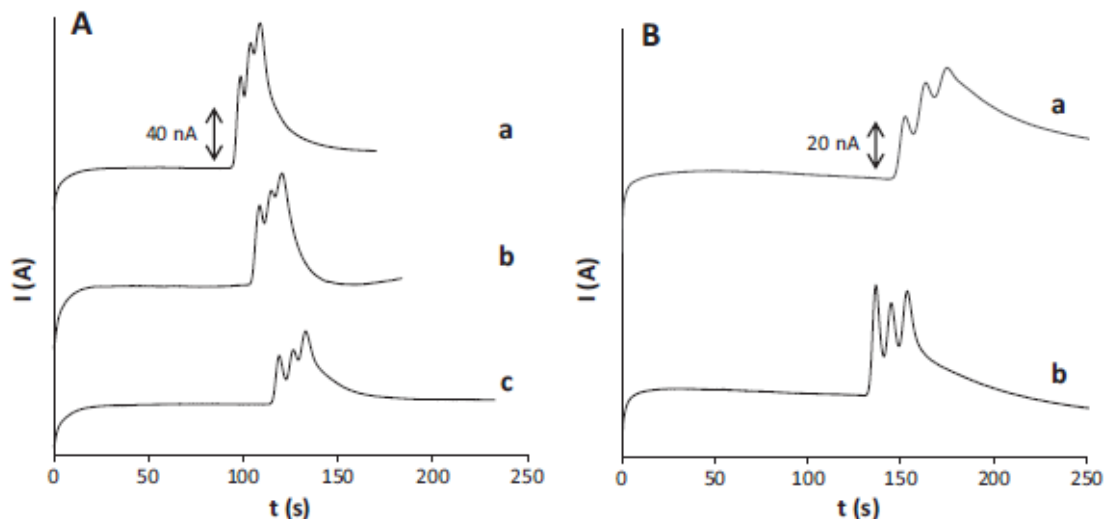


Figure 4. Electropherograms recorded for a mixture of D, NE and E ($100 \mu\text{M}$ each) (A) in an unmodified ME with (a) 0 %, (b) 5 % and (c) 10 % of methanol and, (B) in a PAA-modified ME with (a) 0% and (b) 3% of methanol. Conditions: 25 mM MES–His buffer at pH 5.5, effective separation length 60 mm, $t_{inj} = 0.3$ s, $V_{inj} = +500$ V, $V_{sep} = +1500$ V and $E_d = +1.1$ V (vs. Ag/AgCl).

The addition of organic solvents, commonly methanol, to the buffer can improve the selectivity, efficiency and resolution of CE [63]. Methanol changes the viscosity and the polarity of the solutions and then, EOF changes are expected. MeOH is usually added as a dynamic modifier of the running buffer and can also be added to the sample solution. In this way, methanol was added to MES–His buffer in a 5% concentration. However, gold electrode becomes oxidized and degrades with time when methanol passes continuously through the electrode. It is known that gold present anodic processes that are favoured in the presence of complexing agents. In our case, high voltages (above +1.2 V in this medium) or long times of methanol contact produces dissolution of gold. Then, methanol was only added as a sample additive. This is also advantageous from the point of view of stability of analyte solutions that usually increases with the percentage of methanol. **Fig. 4A (b)** and **4A (c)** show the electropherograms obtained by adding at the mixture of catecholamines ($100 \mu\text{M}$ each) a 5 and 10 % of methanol respectively. Longest migration times are obtained for increasing methanol concentration (t_m moves to 118.8, 126.3 and 133.1 s for D, NE and E respectively) due to an EOF reduction [63,64] as well as a decrease in peak intensity probably to the strong solvation capability of MeOH [65]. Moreover, the presence of MeOH leads to sharper and better resolved peaks (R_s obtained employing a 10 % of MeOH is 0.57 for D–NE and 0.39 for NE–E). This may be due to a stacking caused by organic solvent addition (only in the sample) by a difference in solutions viscosity [66].

3.3. Effect of the PAA coating

The inner environment of the microchannel is the main factor which affects the electroosmotic flow. Separation efficiency depends on the surface properties of the interior wall of separation microchannels, so in order to obtain a more effective separation; the microchannel was coated with PAA. This polymer coating was selected because it is commercially available at low molecular weight (which could be of paramount importance inside the channel). Moreover, it can act as a polyelectrolyte at high pH and as a not-charged polymer brush in neutral or acid media.

A covalent approach was chosen for the modification due to the durability of glass microchips. Moreover, a simple procedure in which channels are filled with reagents under vacuum without needing nitrogen atmosphere and immediately immersed in the reaction solutions under nitrogen is performed.

In the modified microchip (PAA-ME), the pretreatment was made with 0.01 M NaOH for 5 min instead of 0.1 M due to the stability of siloxane bond. Before recording electropherograms, equilibration with the running buffer was made. As in the unmodified microchip, two different separation lengths were checked. In both cases, partial resolution was obtained. Migration times increase in both cases when compared with those obtained in unmodified microchips (*i.e.* t_m for D, NE and E for 30 mm PAA-ME are 66.5, 73.7 and 82 s respectively; values for 60 mm are reported in **Table 2**). Taking into account the microchip dimensions, the electroosmotic velocity varies from $(2.88 \pm 0.04) \times 10^{-1} \text{ cm s}^{-1}$ (unmodified-ME) to $(8.45 \pm 0.02) \times 10^{-2} \text{ cm s}^{-1}$ (modified-ME). Thus, the mobility due to the EOF is $(1.34 \pm 0.02) \times 10^{-3} \text{ cm}^2 \text{ V}^{-1} \text{ s}^{-1}$ (unmodified-ME) to $(3.94 \pm 0.08) \times 10^{-4} \text{ cm}^2 \text{ V}^{-1} \text{ s}^{-1}$ (modified-ME). The plate number in both MEs was calculated too, as $5.54 \times (t_m/w_{0.5})^2$, where $w_{0.5}$ is the half-height width. Highest separation efficiencies were obtained for modified-MEs as can be deduced from the values of the plates m^{-1} : $(3.7 \pm 0.6) \times 10^4$, $(1.2 \pm 0.6) \times 10^4$ and $(0.7 \pm 0.2) \times 10^4$ for D, NE and E respectively in unmodified-ME and $(7 \pm 1) \times 10^4$, $(2.5 \pm 0.5) \times 10^4$ and $(1.9 \pm 0.7) \times 10^4$ for D, NE and E respectively, in modified-ME. In the short microchip the modification changes the situation from no resolution at all (only one peak was achieved for the mixture) to a partial resolution (R_s D-NE and R_s NE-E are 0.25 ± 0.05 and 0.24 ± 0.06 respectively). Clear increase in the migration time is noticed in both PAA coated microchips (30 and 60 mm) due to the significant decrease in the EOF. Generation of negative charges coming from carboxylates, the main ionisable groups, and interaction with cationic analytes have to be considered. It has also to be taken into account that although acrylic acid has a pK_a of 4.3, an increase of this value,

resulting from polymerization, can be observed [62]. As shown in **Fig. 4**, a slight improvement in catecholamines separation is observed when unmodified and modified MEs without employment of dynamic modifiers are compared (**Fig. 4A (a)** and **4B (a)** respectively).

Repeatability of t_m in PAA-MEs was proven by successive injections of 500 μM dopamine solution. The relative standard deviation (RSD) for four successive measurements was 1.6 %. The reproducibility of the coating with time was evaluated too, obtaining a RSD of 2.0 % and 3.9 % for dopamine measurements done over 3 days and 3 months respectively (always for three injections). In these cases, ME was stored with Milli-Q water at 4 °C and reservoirs are covered with Parafilm in order to avoid evaporation.

The effect of MeOH was also studied for modified microchips. **Fig. 4B** shows the electropherograms obtained in a PAA-ME microchip with 60 mm separation length and with an addition of a 3 % of MeOH to the sample solution. Resolution values for D-NE and NE-E can be seen in **Fig. 5**. Although peak intensity decreases with methanol addition, it leads to narrower and better resolved peaks when compared with those obtained for direct injection of the mixture in the PAA-ME. It has to be noted that such effects had been observed previously when MeOH was employed in unmodified-MEs. Best results in terms of resolution are obtained for a MeOH concentration of 3 %. The precision of Rs in the PAA-ME was checked, obtaining a RSD of 5.5 and 10.1 % (D-NE and NE-E respectively) without organic modifier and a RSD of 7.2 and 6.8 % (D-NE and NE-E respectively) for a 3 % of MeOH. The employment of higher methanol proportion (10 %) did not make any improvement. Migration time moved to higher values and peak intensity decreased without enhancement of Rs (0.5 ± 0.1 and 0.32 ± 0.09 for D-NE and NE-E respectively).

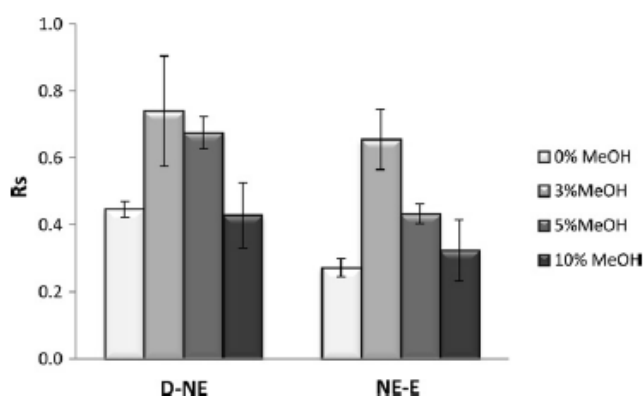


Figure 5. Resolution values for D-NE and NE-E obtained in a PAA-ME (60 mm separation channel) with a solution 100 μM in each analyte and different additions of methanol (25 mM MES-His, pH 5.5).

Recent works on ME with fluorescent detection reported also partial resolution for D, NE and E in a borofloat glass microchip. In this case a 100 mM phosphate buffer with a 25 % of n-propanol was employed [11].

4. Conclusions

A simple and accurate procedure for the modification with poly (acrylic acid) of the microchannel surface of soda-lime glass microchips has been proposed. It consists on the functionalization of the surface with amine groups and the reaction of these with the carboxylate groups of the polymer. Optimization and characterization has been performed on glass plates. Silanization conditions were adjusted. Activation of the plates prior to silanization proved to be a critical step. In the microchannel modification, reagent evaporation is avoided and microchannel filling can be performed without nitrogen atmosphere.

A reproducible method of glass microchips modification was achieved; this opens the possibility of other polymers immobilization, allowing introducing a wide variety of different functional groups in the separation microchannel. Moreover, this coating can be applied not only to the separation of analytes with similar structures, but also to bioassays through biomolecule immobilization by their carboxyl groups.

In a 30 mm separation length microchip, modification is needed for obtaining a partial resolution of catecholamines. An increase of the separation length as well as methanol addition to the sample solution improves the resolution. In a 60 mm separation length microchip, resolution is also improved by modification.

Supplementary Data



Figure 1. Scheme of the ME employed including the separation (A-B) and injection (C-D) voltage values.

Acknowledgements

This work has been supported by FICYT under projects IB08-108C2 and IB08-108C3. Isabel Álvarez-Martos thanks the MICINN for the award of a PhD grant (AP2008-04451).

REFERENCES

- [1] G.M. Whitesides, *Nature* 442 (2006) 368-373.
- [2] E. Zubritsky, *Anal. Chem.* 74 (2002) 22A-26A.
- [3] J.R. Kraly, M.R. Jones, D.G. Gomez, J.A. Dickerson, M.M. Harwood, M. Eggertson, T.G. Paulson, C.A. Sanchez, R. Odze, Z. Feng, B.J. Reid, N.J. Dovichi, *Anal. Chem.* 78 (2006) 5977-5986.
- [4] M. Tsunoda, *Anal. Bioanal. Chem.* 386 (2006) 506-514.
- [5] M. Perry, Q. Li, R.T. Kennedy, *Anal. Chim. Acta* 653 (2009) 1-22.
- [6] M. Ebadi, S. Sharma, S. Shavali, H.E.L. Refaey, *J. Neurosci. Res.* 67 (2002) 285-289.
- [7] C. Bruhlmann, F. Ooms, P.A. Carrupt, B. Testa, M. Catto, F. Leonetti, C. Altomare, A. Carotti, *J. Med. Chem.* 44 (2001) 3195-3198.
- [8] S.K. Lunsford, H. Choi, J. Stinson, A. Yeary, D.D. Dionysiou, *Talanta* 73 (2007) 172-177.
- [9] Y. Lu, Y.-L. Hu, X.-H. Xia, *Talanta* 79 (2009) 1270-1275.
- [10] H. Yu, F.-Y. He, Y. Lu, Y.-L. Hu, H.-Y. Zhong, X.-H. Xia, *Talanta* 75 (2008) 43-48.
- [11] C. Cakal, J.P. Ferrance, J.P. Landers, P. Caglar, *Anal. Bioanal. Chem.* 398 (2010) 1909-1917.
- [12] N. Zhang, H.S. Zhang, H. Wang, *Electrophoresis* 30 (2009) 2258-2265.
- [13] A. Sánchez Arribas, E. Bermejo, M. Chicharro, A. Zapardiel, G.L. Luque, N.F. Rerreyra, G. Rivas, *Anal. Chim. Acta* 596 (2007) 183-194.
- [14] V. Qaiserova-Mocko, M. Novotny, L.S. Schaefer, G.D. Fink, G.M. Swain, *Electrophoresis* 29 (2008) 441-447.
- [15] U. Chandra, B.E.K. Swamy, O. Gilbert, B.S. Sherigara, *Electrochim. Acta* 55 (2010) 7166-7174.
- [16] A.A. Ensafi, B. Rezaei, S.Z.M. Zare, M. Taei, *Sens. Actuators B* 150 (2010) 321-329.
- [17] M.L.A.V. Heien, M.A. Johnson, R.M. Wightamn, *Anal. Chem.* 76 (2004) 5697-5704.
- [18] P.T. Kissinger, W.R. Heineman, *Laboratory Techniques in Electroanalytical Chemistry*, 2nd ed., Marcel Dekker, Inc, New York, 1984.
- [19] N.A. Lacher, S.M. Lunte, R.S. Martin, *Anal. Chem.* 76 (2004) 2482-2491.
- [20] Y. Ding, A. Ayon, C.D. García, C.D. Anal. Chim. Acta 584 (2007) 244-251.
- [21] M.A. Schwarz, B. Galliker, K. Fluri, T. Kappes, P.C. Hauser, *Analyst* 126 (2001) 147-151.
- [22] M. Castaño-Álvarez, A. Fernández-la-Villa, D.F. Pozo-Ayuso, M.T. Fernández-Abedul, A. Costa-García, *Electrophoresis* 30 (2009) 3372-3380.
- [23] R.G. Wu, C.S. Yang, C.K. Lian, C.C. Cheing, F.G. Tseng, *Electrophoresis* 30 (2009) 2523-2531.
- [24] A.A. Dawoud, T. Kawaguchi, R. Jankowiak, *Electrochem. Comm.* 9 (2007) 1536-1541.

- [25] D.F. Pozo-Ayuso, M. Castaño-Álvarez, A. Fernández-la-Villa, M. García-Granda, M.T. Fernández-Abedul, A. Costa-García, J. Rodríguez-García, *J. Chromatogr. A* 1180 (2008) 193-202.
- [26] M. Castaño-Álvarez, D.F. Pozo-Ayuso, A. Fernández-la-Villa, M.T. Fernández-Abedul, A. Costa-García, *Electrophoresis* (submitted for publication).
- [27] R. Weinberger, *Practical Capillary Electrophoresis*. Academic Press; San Diego, 2000.
- [28] A.L. Bowen, R.S. Martin, *Electrophoresis* 30 (2009) 3347-3354.
- [29] E. Zubritsky, *Anal. Chem.* 72 (2000) 687A-690A.
- [30] J.D. Ramsey, C.T. Jacobson, C.T. Culbertson, J.M. Ramsey, *Anal. Chem.* 75 (2003) 3758-3764.
- [31] M. Vlckova, M.A. Schwarz, *J. Chromatogr. A* 1142 (2007) 214-221.
- [32] J. Zhou, H. Yan, K. Ren, W. Dai, H. Wu, *Anal. Chem.* 81 (2009) 6627-6632.
- [33] J.J. Feng, A.J. Wang, J. Fan, J.J. Xu, H.Y. Chen, *Anal. Chim. Acta* 658 (2010) 75-80.
- [34] A.J. Wang, J.J. Feng, J. Fan, *J. Chromatogr. A* 1192 (2008) 173-179.
- [35] T. Sikanen, S.K. Wiedmer, L. Heikkila, S. Franssila, R. Kostianen, T. Kotiaho, *Electrophoresis* 31 (2010) 2566-2574.
- [36] D. Belder, M. Ludwig, *Electrophoresis* 24 (2003) 3595-606.
- [37] V. Dolnik, *Electrophoresis* 25 (2004) 3589-3601.
- [38] A. Muck, A. Svatos, *Talanta* 74 (2007) 333-341.
- [39] Q. Guan, A.D. Noblitt, C.S. Henry, *Electrophoresis* 33 (2012) 379-387.
- [40] X. Liu, D. Erickson, D. Li, U.J. Krull, *Anal. Chim. Acta* 507 (2004) 55-62.
- [41] H. Makamba, J.W. Huang, H.H. Chen, S.H. Chen, *Electrophoresis* 29 (2008) 2458-2465.
- [42] Y.L. Wang, H.H. Lai, M. Bachman, C.E. Sims, G.P. Li, N.L. Allbritton, *Anal. Chem.* 77 (2005) 7539-7546.
- [43] M. Wisniewska, *J. Thermal Anal. Calorimetry* 101 (2010) 753-760.
- [44] C.D. Wagner, L.E. Davis, M.V. Zeller, J.A. Taylor, R.H. Raymond, L.H. Gale, *Surf. Interface Anal.* 3 (1981) 211-225.
- [45] K.R. Iller, *The Chemistry of Silica*, J. Wiley & Sons, New York, 1979.
- [46] M. Castaño-Álvarez, D.F. Pozo-Ayuso, M. García-Granda, M.T. Fernández-Abedul, J. Rodríguez-García, A. Costa-García, *Sens. Actuators B* 130 (2008) 436-448.
- [47] H. Zengin, J.A. Siddiqui, R.M. Ottenbrite, *Polym. Adv. Technol.* 19 (2008) 105-113.
- [48] N. Graf, E. Yegen, A. Lippitz, D. Treu, T. Wirth, W.E.S. Unger, *Surf. Interface Anal.* 40 (2008) 180-183.
- [49] T. Kovalchuk, H. Sfihi, L. Kostenko, V. Zaitsev, J. Fraissard, *J. Colloid Interface Sci.* 302 (2006) 214-219.
- [50] J. Kim, P. Seidler, L.S. Wan, C. Fill, *J. Colloid Interface Sci.* 329 (2009) 114-119.
- [51] L.D. White, C.P. Tripp, *J. Colloid Interface Sci.* 232 (2000) 400-407.

- [52] C.M. Halliwell, A.E.G. Cass, *Anal. Chem.* 73 (2001) 2476-2483.
- [53] M. Qin, S. Hou, L.-K. Wang, X.-Z. Feng, R. Wang, Y.-L. Yang, C. Wang, L. Yu, B. Shao, M.-Q. Qiao, *Colloids Surf. B Biointerf.* 60 (2007) 243-249.
- [54] F. Zhang, M.P. Srinivasan, *Langmuir* 20 (2004) 2309-2314.
- [55] J.A. Howarter, J.P. Youngblood, *Langmuir* 22 (2006) 1142-1147.
- [56] D. Briggs, G. Beamson, *Anal. Chem.* 65 (1993) 1517-1523.
- [57] T.I.T. Okpalugo, P. Papakonstantinou, H. Murphy, J. McLaughlin, N. Brown, *Carbon* 43 (2005) 153-161.
- [58] Y. Lin, A.M. Rao, B. Sadanadan, E.A. Kenik, Y.P. Sun, *J. Phys. Chem. B* 106 (2002) 1294-1296.
- [59] N. Graf, E. Yegen, T. Gross, A. Lippitz, W. Weigel, S. Krakert, A. Terfort, W.E.S. Unger, *Surface Sci.* 603 (2009) 2849-2860.
- [60] C. Tarducci, E.J. Kinmond, J.P.S. Badyal, S.A. Brewer, C. Willis, *Chem. Mater.* 12 (2000) 1884-1889.
- [61] T. Ramanathan, F.T. Fisher, R.S. Ruoff, L.C. Brinson, *Chem. Mater.* 17 (2005) 1290-1295.
- [62] J.-L. Chen, T.-L. Lu, Y.-C. Lin, *Electrophoresis* 31 (2010) 3217-3226.
- [63] Y. Hui, X. Li, X. Chen, *J. Chromatogr. A* 1218 (2011) 5858-5866.
- [64] S.C. Bishop, M. Lerch, B.R. McCord, *J. Chromatogr. A* 1154 (2007) 481-484.
- [65] E. Bosch, P. Bou, H. Allemann, M. Roses, *Anal. Chem.* 68 (1996) 3651-3657.
- [66] H.-Y. Huang, W.-L. Liu, B. Singco, S.-H. Hsieh, Y.-H. Shih, *J. Chromatogr. A* 1218 (2011) 7663-7669.

Article 2

*Ionic Liquids as Modifiers for Glass and
SU-8 Electrochemical Microfluidic Chips*

Sens. Actuators B: Chem. 188 (2013) 837-846



Ionic liquids as modifiers for glass and SU-8 electrochemical microfluidic chips

Isabel Álvarez-Martos^a, Francisco Javier García Alonso^b, Adela Anillo^b, Pilar Arias-Abrodo^a,
María Dolores Gutiérrez-Álvarez^a, Agustín Costa-García^a, M. Teresa Fernández-Abedul^{a*}

^a*Departamento de Química Física y Analítica, Universidad de Oviedo, Asturias, Spain*

^b*Departamento de Química Orgánica e Inorgánica, Universidad de Oviedo, Asturias, Spain*

ABSTRACT

Ionic liquids have been attracting attention as background additives to improve separations in the last years. This work reports about the use of four ionic liquids (ILs) 1-butyl-4-methylpyridiniumtetrafluoroborate (BMPyBF₄), 1-butyl-3-methylimidazolium tetrafluoroborate (BMIMBF₄), 1-butyl-3-methylimidazolium hydrogen sulfate (BMIMHSO₄) and 1-ethyl-3-methylimidazolium methyl sulfate (EMIMMeSO₄) as dynamic modifiers in glass and SU-8 microchip electrophoresis (ME). The influence of varying pH values and ILs concentration on the detection system was investigated. Moreover, ionic liquids with different cations and counterions were evaluated as background additives choosing two catecholamines (dopamine, DA and epinephrine, E) as model analytes. Dynamic modification with ILs proved to be necessary to obtain enhanced mixture separation in both 30 mm glass and SU-8 MEs. Good precision in terms of migration times and resolution was obtained for both kinds of MEs when ILs were employed. In addition, baseline resolution with good reproducibility over time (RSD values of 0.5% and 0.8% for migration times in one experiment and three days, respectively) was achieved in glass MEs with 60 mm effective separation length.

1. Introduction

Ionic liquids (ILs) can be described as salts with melting points below 100 °C, which in solution, are composed exclusively of ions [1,2] (commonly imidazolium or pyridinium organic cations and PF_6^- and BF_4^- anions [3]). Due to their unique properties, they have been widely used in organic chemistry [4-6] over the years. More recently, they have started to attract interest in analytical chemistry [7], with widespread applications in separation techniques such as gas or liquid chromatography and capillary electrophoresis (CE) [8], and most recently, in microchip electrophoresis (ME) [9].

They started to be used in CE to provide dynamic coatings due to their ability to be adsorbed on the silanol groups of the capillary wall [10]. Furthermore, they are capable of changing the conductivity and viscosity of the background electrolyte, which allows changes in the electroosmotic velocity, helping to improve resolution [11]. In principle, the IL cation has the most important influence since it can not only interact with the analyte, but also with the capillary wall [12,13]. Ionic liquids can be employed as static [14] or dynamic [15] coatings, with the latter being particularly interesting due to its versatility and simplicity (additives to the background electrolyte) compared to covalent coatings, which are more time consuming. Thus, ILs-based CE has been applied mainly to the analysis of inorganic cations [16] and anions [17], as well as to analytes of clinical interest [18].

Microchip electrophoresis has become a powerful and effective analytical tool in the last years [19,20] due to this unique features [21] and the general trend towards miniaturization. The success of microchip electrophoresis depends not only on a suitable fabrication material, but also on the choice of an adequate detection system. In their early stage, glass and quartz substrates were the main materials employed in MEs fabrication [22]; however, in recent years, with the advancement in fabrication technologies, low cost disposable microfluidic devices made from materials such as polymers (e.g. poly(dimethylsiloxane) (PDMS) [23], poly(methylmethacrylate) (PMMA) [24], cyclo-olefinic polymers (COP) [25], SU-8 [26], etc.) or even paper [27] have been explored as more versatile alternatives. Fluorescence, electrochemistry and mass spectroscopy (MS) are the most currently employed detection methods in MEs [18,19]. Fluorescence and MS require bulky instrumentation that compromises the benefits of miniaturization and portability. Therefore, electrochemical detection (ED) is the most suitable detection technique for these devices [28-30] due to its high sensitivity, inherent miniaturization, compatibility with microfabrication techniques and low cost.

Catecholamines such as dopamine (DA), norepinephrine (NE) and epinephrine (E) are organic compounds consisting of dihydroxyphenyl and amine moieties, which play an important role as disease markers. In the past, they have mainly been detected by HPLC and CE [31], but nowadays an increasing number of publications reporting catecholamine separation by microchip electrophoresis has been observed. Thus, different strategies for various materials such as glass (monolithic disks [32], sodium dodecyl sulfate (SDS) with dendrimers in the background electrolyte [33] or surface microstructures [34]), polydimethylsiloxane (PDMS)/glass (layer-by-layer coating of poly(diallyldimethylammonium chloride) (PDDA) and glucose oxidase (GOx) [35], serpentine separation channel [36] or zwitterionic surfactants in background electrolyte [37]) were reported in literature to improve the separation of catecholamine mixtures.

In this context and since ILs as a background additive can lead to an improvement in separation, this work is aimed to the use of ionic liquids as an alternative strategy to enhance the resolution of analytes with similar structures in ME-ED. Two catecholamines, DA and E, were selected as model analytes for this study because they have similar structures and are electroactive molecules, and can thus be detected without prior derivatization procedures.

To our knowledge only some works in the bibliography report about the employment of ionic liquids in catecholamines determination, mainly for enhancing separation in reversed-phase high-performance liquid chromatography (RP-HPLC) [38,39] or improving the electrochemical response by employing IL-modified working electrodes [40,41]. On the other hand, only three groups have used imidazolium-based ionic liquids in microchip electrophoresis. Firstly, Wootton *et al.* employ ILs Joule heating as an effective method of controlling temperatures with high precision and accuracy [42]. Secondly, since surfactants were not efficient enough for suppressing proteins adsorption in PDMS/glass MEs, Wang *et al.* investigated the effect of combining ILs and surfactants as background additives [43]. They evaluated 1-butyl-3-methylimidazolium tetrafluoroborate (BMIMBF₄) and 1-ethyl-3-methylimidazolium tetrafluoroborate (EMIMBF₄) with an anionic surfactant (SDS) as supporting electrolytes to determine closely related narcotic drugs [44] and to establish a fluorescence label-free protein detection method [45]. Afterwards, they synthesized a new hybrid IL (1-butyl-3-methylimidazolium dodecanesulfonate) which employed as background additive to obtain better resolution, higher fluorescence peaks and well-separated proteins mixture [46]. Finally, Uchiyama *et al.* employed EMIMBF₄ together with cyclodextrines as the working electrolyte and applied them to optical peptide isomers separation in glass microchip electrophoresis [47].

In this work, four commercially available ILs [1-butyl-4-methylpyridinium tetrafluoroborate (BMPyBF₄), 1-butyl-3-methylimidazolium tetrafluoroborate (BMIMBF₄), 1-butyl-3-methylimidazolium hydrogen sulfate (BMIMHSO₄) and 1-ethyl-3-methylimidazolium methyl sulfate (EMIMMeSO₄)] were evaluated as background additives to buffer solution. To evaluate their influence on migration times and resolution, DA and E were selected as model analytes. Two kinds of microchip electrophoresis materials, glass and SU-8/Pyrex, with different properties were tested. To the best of our knowledge there are no publications reporting the employment of these proposed ILs in glass MEs except for BMIMBF₄. SU-8 is a negative photoresist that has recently been used as a microchip electrophoresis material [48-50] and at present, no work investigating the employment of ILs on this kind of microchip has been reported.

2. Materials and Methods

2.1. Reagents

The ionic liquids: 1-butyl-3-methylimidazolium hydrogen sulfate ($\geq 95\%$, BMIMHSO₄), 1-butyl-3-methylimidazolium tetrafluoroborate ($\geq 97\%$, BMIMBF₄), 1-ethyl-3-methylimidazolium methyl sulfate ($\geq 98\%$, EMIM MeSO₄), 1-butyl-4-methylpyridinium tetrafluoroborate ($\geq 97\%$, BMPyBF₄) as well as the neurotransmitters: dopamine (DA), norepinephrine (NE) and epinephrine (E) and the reagents for buffer preparation: 2-(N-morpholino)-ethane sulfonic acid (MES), histidine (His), boric acid (99.5%) and sodium hydroxide were purchased from Sigma-Aldrich (St. Louis, MO, USA). Acetic and sulphuric (95-97%) acids were obtained from Merck (Darmstadt, Germany).

Catecholamine solutions were prepared daily in the running buffer and protected from light. All solutions were filtered through Nylon syringe filters (Cameo 30 N, 0.1 μm , 30 mm) acquired from Osmonics (Minnetonka, MN, USA).

Britton-Robinson buffer solutions were prepared by mixing together boric, phosphoric and acetic acid (0.04M in each) and fixing the pH with NaOH.

Water was purified employing a Milli-Q directQS system from Millipore (Bedford, MA, USA). All other reagents were of analytical reagent grade.

2.2. Materials and instrumentation

Micropipettes, 0.250 and 1.0 mL tips, as well as 1.5 mL tubes were obtained from Eppendorf (Hamburg, Germany).

Single-channel microchips employed in the development of this work (Soda-lime glass and SU-8 / Pyrex) were purchased from MicruX Technologies (Asturias, Spain). As displays **Fig. 1** for both cases, the injection cross was formed by intersection of separation and injection (10 mm) channels.

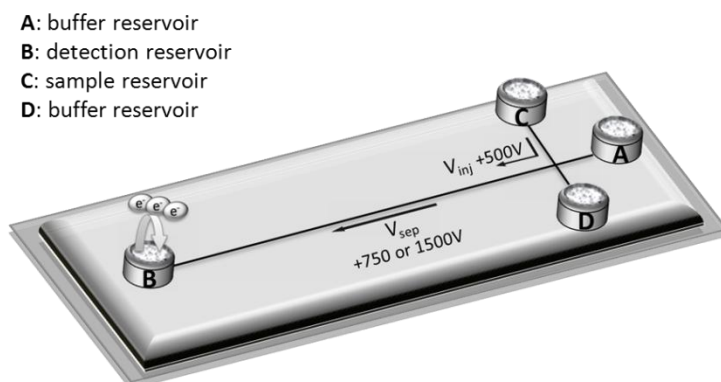


Figure 1. Schematic representation of the ME employed in the accomplishment of this work, including the separation (A for buffer solution and B for the electrochemical detection) and the injection reservoirs (C for the sample and D for buffer solution). An unpinched format (C-B) is employed to perform the sample injection.

The Soda-lime glass microchip consists of a plate (48 x 16 x 1 mm) containing a separation channel of 35 or 65 mm length, 30 μm depth and 90 μm width, whereas the SU-8 / Pyrex microchips were supported on a plate (38 x 13 x 0.75 mm) containing a separation channel of 35 mm length, 20 μm depth and 50 μm width. In both cases, access holes of 2 mm diameter are situated at the end of the separation and injection channels. Micropipette tips were cut to obtain 1 cm long pieces with a diameter of 0.5 cm that were concentrically attached to microchip electrophoresis access holes with Araldite (Vantico, Basel, Switzerland) acting as reservoirs of 150 μL volume. Microchips were housed in a Faraday cage in order to minimize electrical interferences.

The electrochemical detection (amperometry) system consisted of three electrodes (working, reference and counter) at the outlet of the separation channel. To perform the measurements in both types of microchips, reference (RE) and counter (CE) electrodes were homemade in a 250 μL micropipette tip. The RE consisted of an anodized silver wire (Goodfellow, Huntingdon, UK) introduced into a tip using a rubber syringe piston. The tip was

then filled with saturated KCl solution containing a low-resistance liquid junction. The platinum wire (250 μm diameter) that acted as the CE was fixed with insulating tape to the micropipette tip. A 100 μm diameter platinum wire (Goodfellow, Huntingdon, UK) and 100 μm wide platinum thin-film were employed as working electrodes (WE) in glass and SU-8 / Pyrex MEs respectively. In both cases, a copper cable was fixed to the WE with a conducting silver epoxy resin (CW2400, RS Components, UK) for electrical connection. In the case of the platinum wire, the WE was aligned at the outlet of the separation channel with the aid of a microscope (MA722 model, Swift Optics, USA). The electrode was fixed over the cover plate with adhesive tape and epoxy resin (Araldite).

Screen-printed electrodes of carbon (SPCEs), gold (AuSPEs, cured at low temperature) and platinum (PtSPEs) employed for cyclic voltammetry studies were purchased from DropSens (Asturias, Spain). Although all three electrodes (working, reference and auxiliary) were screen-printed on the card, measurements were performed employing external reference (Ag/AgCl/saturated KCl) and counter (Pt wire) electrodes, similar to those employed in MEs, in order to make the measurements more comparable with those obtained by ME-ED. It should be noted that all the SPEs employed during this work are disks of the same area (12.6 mm^2).

Amperometry and cyclic voltammetry detection were performed with an Autolab PGSTAT 10 (ECO Chemie, The Netherlands) bipotentiostat interfaced to a computer system and controlled by Autolab GPES 4.9 version for Windows 98.

2.3. Electrochemical measurements

A 40 μL aliquot of the corresponding solution was deposited onto the working area of the screen-printed electrode and cyclic voltammetry measurements were performed by scanning the potential between - 0.8 and + 1.2 V.

For amperometric measurements, a constant detection potential (E_d) of + 0.8 V was applied to the working electrode (situated at the end of the separation channel). After baseline stabilization, injection of the analyte solution was performed and the corresponding electropherogram was recorded.

In all cases anodic peak intensities (I_{pa}) were measured employing GPES software and drawing the tangent between the point where the anodic current begins to rise and the switching point.

2.4. Electrophoresis procedure

Two high-voltage power supplies (HVPS, MJ series) with a maximum voltage of + 5000 V from Glassman High Voltage (High Bridge, NJ, USA) were employed to perform the electrophoresis procedure. Platinum wires of 300 μm diameter (Sigma-Aldrich, Madrid, Spain) connected by alligator clips to the HVPS were employed as high-voltage electrodes.

Microchip channels were conditioned by rinsing with 0.1 M NaOH for 15 min and then with the running buffer for 20 min. The washings were performed by filling the reservoirs with the corresponding solutions and with the aid of a simple vacuum system. All the reservoirs, except the detection reservoir (B), were filled with the corresponding buffer solution while 0.1 M H_2SO_4 was employed for the detection. Unpinched injections (**Fig. 1**) were performed by applying the desired voltage (+ 500 V) between the sample (C) and detection (grounded) reservoirs. Separation was carried out by applying the corresponding voltages (+ 750 V and + 1500 V for 30 and 60 mm MEs respectively) between the buffer (A) and detection reservoirs (B). The running buffer was 25 mM MES-His with a pH of 5.5 and in cases where the buffer solution contained ILs, the buffer was prepared by mixing the corresponding IL (20 mM) and MES (25 mM) and fixing the pH to 5.5 using His. Dopamine and epinephrine (100 μM) were chosen as model analytes to study how IL affects their separation. All experiments were performed at room temperature.

2.5. electroosmotic flow (EOF) measurement

One of the methods employed for EOF measurement is current monitoring [51]. In this case, replacement of the buffer solution by a more diluted solution produces a decrease in the electrophoretic current. Taking into consideration that with the instrumentation employed is not possible to record current with time, a neutral electroactive marker (hydroquinone, HQ) has been chosen [52].

The microchannel and all the reservoirs were filled with buffer solution and a +750 V voltage was applied to the ends of the separation channel (depicted as A and B in **Fig. 1**) until baseline stabilization. Then, the buffer solution in A was changed to 50 μM HQ solution and the separation voltage was applied again. When the solution with the neutral marker (HQ), which eluted with EOF, displaces the running buffer an increase in the recorded current due to its oxidation on the working electrode was observed. A plateau is obtained when the rate of the electronic transference of HQ equals that of the mass transport to the electrode. Thus, the electroosmotic velocity is calculated as the ratio between the separation channel length and

the appearance time of HQ. Once a constant current was obtained, the HQ solution was changed back to buffer solution, which when is reintroduced in the microchannel produces a decrease in the HQ signal at the same time as before. This behavior could be explained because when the buffer solution starts to be flown into the microchannel (initially filled with HQ solution as a result of EOF measurement) the hydroquinone begins to be displaced, until it reaches the appearance time where HQ disappears completely and in consequence its electrochemical signal. However, when a solution containing DA and HQ is introduced, two successive plateaus are attained. This is explained by the different migration times, appearing first the cationic specie (DA) and then the neutral one (HQ). Moreover, in this case when the buffer solution is reintroduced in the microchannel the signal decrease occurs also in two steps (experimental data shown in *section 3.2.1*). This procedure was repeated four times.

3. Results and Discussion

The employment of ionic liquids as additives in microchip electrophoresis for improving the separation of dopamine and epinephrine is considered in this section. Since the employment of different types of ionic liquids has been reported in literature for enhancing electrochemical signals (hydrogen electrochemical oxidation on platinum electrode anion [53] or dopamine, adrenaline and dobutamine processes on carbon paste electrodes with graphite powder dispersed in different ILs [58]) the electrochemical behavior of dopamine is studied here in media containing ILs of different compositions and concentrations.

3.1. Electrochemical detection

In order to optimize the detection medium for the catecholamine (dopamine in this case), the buffer solution, pH and composition (including IL addition) were varied, while the corresponding voltammetric signals were recorded. Notice that screen-printed electrodes were chosen for the electrochemical characterization in order to evaluate the effect of ILs addition on the electrochemical signal, keeping the same electrode characteristics in terms of area and design. To establish the optimal working pH, cyclic voltammograms were performed on screen-printed carbon, gold and platinum electrodes (SPCE, AuSPE and PtSPE respectively) in Britton-Robinson buffers with pH values between 3 and 9, as well as in 0.1M H₂SO₄. **Fig. 2** shows the effect of pH variation on dopamine cyclic voltammograms on the three kinds of SPEs studied on this work.

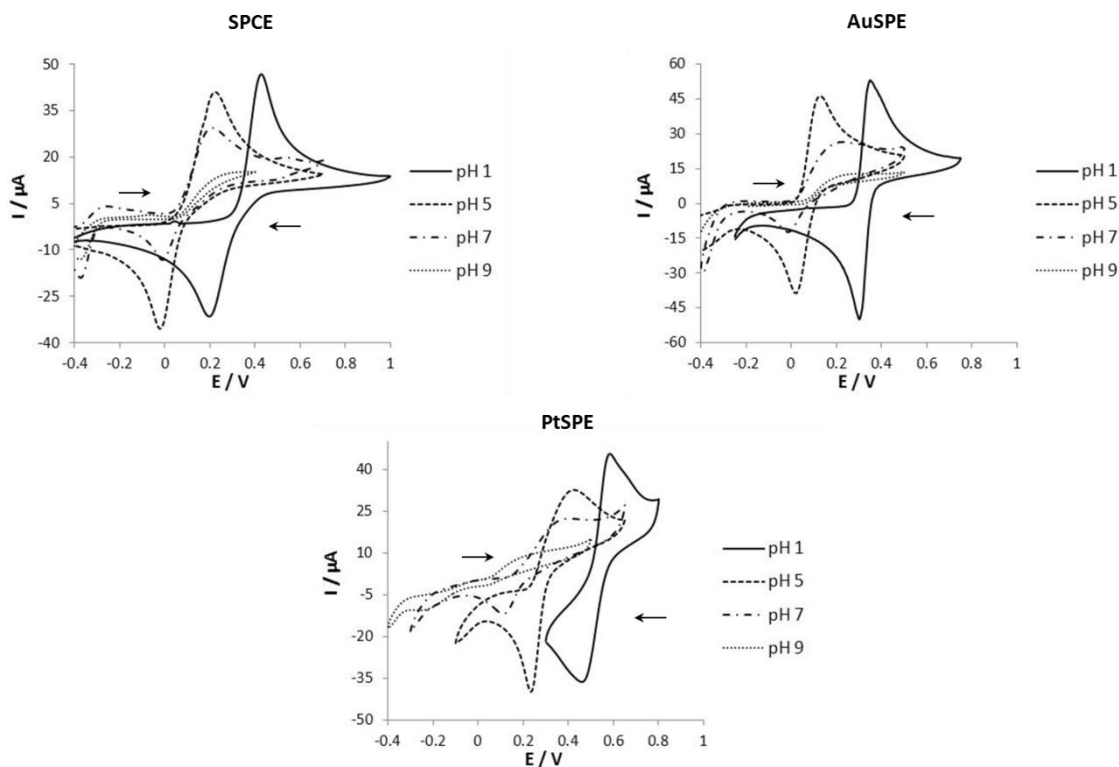


Figure 2. Cyclic voltammograms of 1 mM DA at different pHs on carbon, gold and platinum screen printed electrodes.

It should be noted that similar behavior in terms of peak intensities variation and oxidation potentials movement were observed regardless of the nature of the WE. Firstly, a decrease of both anodic (I_{pa}) and cathodic (I_{pc}) peak intensities were noted with increasing pH (**Table 1**), while the electrochemical activity disappears at pH 9. This demonstrates that the electrochemical process of DA is unfavorable at basic pHs, probably due to the auto-oxidation of catecholamines at alkaline pH [54]. On the other hand, when pH varies from 1 to 5, significant displacement towards lower peak potentials, anodic (from 0.44 ± 0.02 to 0.20 ± 0.02 , 0.38 ± 0.04 to 0.14 ± 0.03 and 0.578 ± 0.003 to 0.402 ± 0.005 V for SPCE, AuSPE and PtSPE respectively) and cathodic, could be observed, remaining almost constant with subsequent pH increases. Taking into account that the oxidation mechanism of the DA phenol group into a quinone compound implies a two electron / two proton transfer process, the changes in the anodic peak potential may be explained by the fact that increasing the H^+ concentration of the medium, disfavors oxidation and higher potentials are then necessary [55]. Moreover, the peak potential separation [$\Delta E = \text{anodic peak potential } (E_{pa}) - \text{cathodic peak potential } (E_{pc})$] of 0.26 ± 0.04 , 0.11 ± 0.08 and 0.100 ± 0.001 V observed for DA at pH 1 on SPCE, AuSPE and PtSPE respectively were greater than the value of 0.03V ($0.059 \text{ V} / 2 e^-$) expected for a reversible system, suggesting a quasi-reversible dopamine redox process. As also summarizes **Table 1**, SPCE shows more reversible processes with increasing pH, while on the contrary AuSPE and

PtSPE exhibit less reversibility with increasing pH. Furthermore, another remarkable fact is the appearance of a second peak for DA cathodic process at -0.4 V (pH 7) on the SPCE, which is explained by the possibility that DA can undergo a 1,4 Michael addition when its amine group is deprotonated. Thus, it could be deduced that pH 7 buffer solution leads to a deprotonation of the amine group and promotes that the DA molecule can undergo a cyclization reaction, resulting in a form called dopamineochrome whose processes appear at different potential [56,57].

Table 1. Anodic peak potentials (E_{pa}), ΔE (calculated as the difference between E_{pa} and E_{pc}), anodic peak intensities (I_{pa}) and cathodic peak intensities (I_{pc}) obtained for DA at different pHs in screen-printed electrodes of carbon, gold and platinum. Conditions as in Fig. 2.

| | | E_{pa} / V | $\Delta E / V$ | $I_{pa} / \mu A$ | $I_{pc} / \mu A$ |
|-------------|-------|-------------------|-------------------|------------------|------------------|
| pH 1 | SPCE | 0.44 ± 0.02 | 0.26 ± 0.04 | 41 ± 2 | 30 ± 1 |
| | AuSPE | 0.38 ± 0.04 | 0.11 ± 0.08 | 47 ± 4 | 55 ± 1 |
| | PtSPE | 0.578 ± 0.003 | 0.100 ± 0.001 | 42 ± 3 | 34 ± 2 |
| pH 5 | SPCE | 0.20 ± 0.02 | 0.19 ± 0.02 | 31 ± 4 | 29 ± 1 |
| | AuSPE | 0.14 ± 0.03 | 0.13 ± 0.04 | 31 ± 2 | 32 ± 3 |
| | PtSPE | 0.402 ± 0.005 | 0.166 ± 0.005 | 24 ± 1 | 28.2 ± 0.1 |
| pH 7 | SPCE | 0.24 ± 0.03 | 0.105 ± 0.005 | 17 ± 3 | 13.7 ± 0.2 |
| | AuSPE | 0.20 ± 0.04 | 0.20 ± 0.05 | 14 ± 3 | 12.1 ± 0.1 |
| | PtSPE | 0.344 ± 0.005 | 0.223 ± 0.006 | 10 ± 1 | 13 ± 1 |

As a complementary study and choosing SPCE and pH 1 as the best pH for catecholamine detection, the effect of medium composition on cyclic voltammograms was tested by employing three different acid solutions: H_2SO_4 , HNO_3 and $HClO_4$ (data not shown). In this case, no significant differences in anodic peak intensities ($44 \pm 2 \mu A$) or potentials ($0.40 \pm 0.03 V$) were observed in dopamine CVs and therefore, sulfuric acid will continue being used. Finally, the influence of H_2SO_4 concentration was also evaluated from 0.01 to 1 M (data not shown). In the same way than before similar I_{pa} ($42 \pm 2 \mu A$) and E_{pa} ($0.41 \pm 0.02 V$) were also obtained in this study and therefore pH 1 (0.1M H_2SO_4) was chosen as the best medium for DA detection.

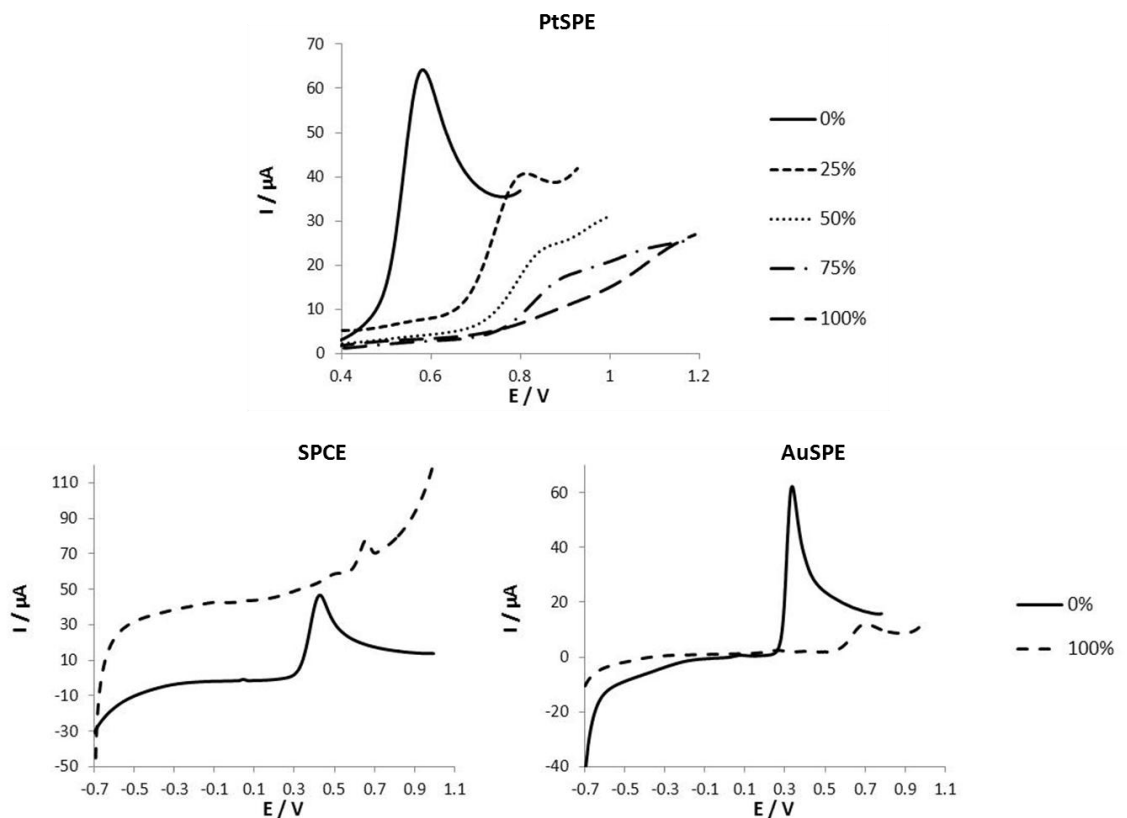


Figure 3. Effect of ILs on the DA oxidation process at platinum, carbon and gold screen printed electrodes. Conditions: scan rate of 100 mVs^{-1} .

Since the choice of an adequate ionic liquid (IL) could lead to increased analytical signals and in turn, to improved sensitivities for dopamine and epinephrine detection [58], the addition of different ILs in the detection medium was tested. Three imidazolium-based ionic liquids (BMIMBF_4 , BMIMHSO_4 and EMIMMeSO_4) were added to the detection medium in different proportions and the electrochemical behavior was evaluated. In all cases, cyclic voltammograms were recorded vs. $\text{Ag}/\text{AgCl}/\text{saturated KCl}$, at a scan rate of 0.1 Vs^{-1} in a 1 mM dopamine solution. Focusing on the oxidation process, **Fig. 3** illustrates the influence of increasing the amount of BMIMHSO_4 on the DA signal recorded on PtSPE, SPCE and AuSPE. The first remarkable fact when ILs are employed in the electrochemical detection medium is that E_{pa} values increase compared with those obtained in $0.1 \text{ M H}_2\text{SO}_4$ (i.e from 0.44 ± 0.02 to 0.46 ± 0.03 , 0.38 ± 0.04 to 0.54 ± 0.04 and 0.578 ± 0.003 to 0.844 ± 0.004 for SPCE, AuSPE and PtSPE respectively), where it remains almost constant for successive additions of IL. Although, reached a 100% of IL DA peak disappears in case of PtSPE or be shifted to a little more positive potentials in case of SPCE and AuSPE. From the data comprised in **Table 2**, it can be derived that this movement does not depend on the ionic liquid nature; due to E_{pa} values are almost similar for all the ILs. Therefore, this movement of oxidation potentials in ILs to more positive values indicates a strong interaction between dopamine and IL, hindering electron transfer

[59]. It is also worth noting that there is a significant decrease in DA I_{pa} for increasing amounts of ILs. Choosing PtSPE and BMIMHSO₄ as a representative example, I_{pa} decreases from 50 ± 3 (without IL) to $19.4 \pm 0.2 \mu\text{A}$ (25% of IL), 8.8 ± 0.7 (50% of IL), 5.2 ± 0.1 (75% of IL) and, no signal for a 100% of IL.

Table 2. Anodic peak potentials (E_{pa}) obtained for DA in 0.1 M H₂SO₄ solution with different percentages of BMIMBF₄, BMIMHSO₄ and EMIMMeSO₄ in screen-printed electrodes of carbon, gold and platinum.

| | | E_{pa} / V | | |
|-----------------------------|--------|---------------------|-----------------|-------------------|
| | | SPCE | AuSPE | PtSPE |
| BMIMBF₄ | 25-75% | 0.46 ± 0.03 | 0.54 ± 0.04 | 0.844 ± 0.004 |
| | 100% | 0.65 ± 0.04 | 0.75 ± 0.05 | - |
| BMIMHSO₄ | 25-75% | 0.45 ± 0.05 | 0.62 ± 0.07 | 0.84 ± 0.04 |
| | 100% | 0.52 ± 0.02 | 0.74 ± 0.02 | - |
| EMIMMeSO₄ | 25-75% | 0.46 ± 0.02 | 0.64 ± 0.05 | 0.78 ± 0.04 |
| | 100% | 0.56 ± 0.03 | 0.76 ± 0.03 | - |

Similar behavior was observed in all of the electrode surfaces for the three imidazolium-based ILs (**Fig. 4**). It should be noted that in the case of metallic electrodes, a higher I_{pa} is obtained and the decrease of the DA signal is usually more pronounced when compared to carbon electrodes. Thus, in the case of BMIMBF₄, the addition of 25% of ionic liquid in the detection buffer produces a decrease of 77% in the signal obtained for PtSPE. However, under the same conditions, the signal decrease in AuSPE is lower, with only a 31% variation. Whereas, in the case of SPCE, after 75% of IL was added into the detection medium, the signal decreased from 41 ± 2 to $32 \pm 1 \mu\text{A}$. Finally and, as it can also be seen in **Fig. 4**, there are no significant differences in peak intensities for BMIMBF₄ percentages between 25 and 75%. The most remarkable fact when the anion was changed by HSO₄⁻ is that while SPCE and PtSPE behaved similarly as before, AuSPE undergoes a significant signal intensity reduction. What is more, when 25% of BMIMHSO₄ was added to the detection medium a 20%, 61% and 62% dopamine signal decrease was observed for carbon, gold and platinum surfaces respectively. Finally, when the butyl cation is changed by an ethyl group and the anion is MeSO₄⁻, the behavior for a 25% addition of IL on the platinum and gold electrodes was similar (55 and 60% decreases, respectively), meanwhile, the signal for the carbon electrodes decreased 24%. For all of the ionic liquids employed in the detection medium at 100%, the signal decreased significantly and almost disappears on the platinum electrodes, which means that charge

transference is unfavorable. In view of the results, the viscosity of ILs has a strong influence on the mass transport properties of the solution, which is a major drawback in electrochemical studies. This could be explained because the diffusion coefficient of the electroactive specie in ILs solutions commonly is inversely proportional to the viscosity in agreement with the Stokes-Einstein equation [59] and, peak intensity is proportional to the square root of the diffusion coefficient. Thus, increasing the amount of IL, and therefore the solution viscosity, leads to lower diffusion coefficients which results in lower DA signal intensity. Taking into account that higher intensities were obtained for electrodes without IL addition and by employing different detection and separation solutions in microchip electrophoresis [60,61], 0.1 M H₂SO₄ was selected as the best choice to perform the detection in this study. Moreover, taking into account that dopamine oxidation process occurs at about +0.5 V, detection potential (E_d) of the working electrode in MEs was fixed at +0.8 V to ensure D oxidation.

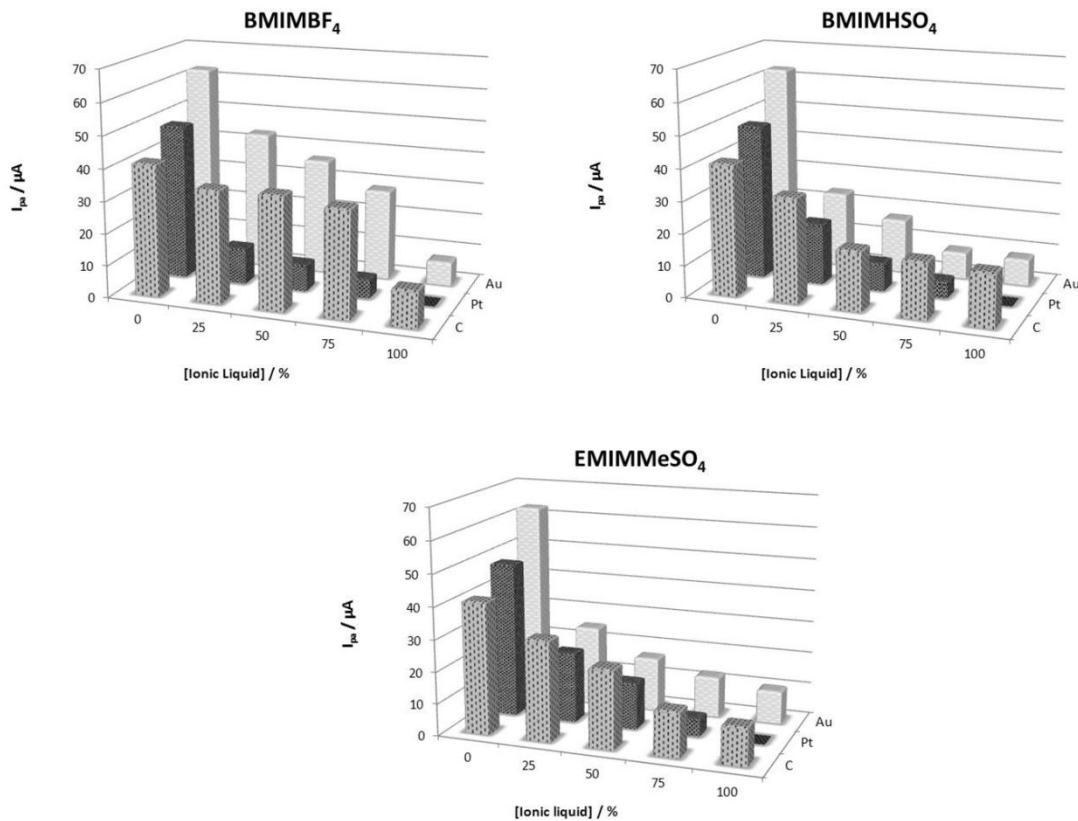


Figure 4. Influence of ionic liquids (BMIMBF₄, BMIMHSO₄ and EMIMMeSO₄) in dopamine (DA) oxidation peak varying the proportions IL:H₂SO₄ in screen-printed electrodes of different materials.

3.2. Effect of ILs as running buffer additives

3.2.1. SU-8/Pyrex MEs

Ionic liquids were chosen as background additives for the accomplishment of this work, because of their high density (about 1.2 g/mL at 20 °C), low ionic conductivity and different pHs (varying from about pH 5 for BMIMBF₄ and BMPyBF₄ to around pH 1 for BMIMHSO₄ and EMIMMeSO₄). The influence of the cation (BMPy⁺ and BMIM⁺ with the same counterion) and the anion (BF₄⁻ and HSO₄⁻ with the same cation) or both in the case of EMIM MeSO₄, on DA and E migration times (t_m), electroosmotic flow (EOF) and resolution was studied. According to previous work, 25mM MES-His pH 5.5 was employed as the optimal buffer solution for DA and E separation [62].

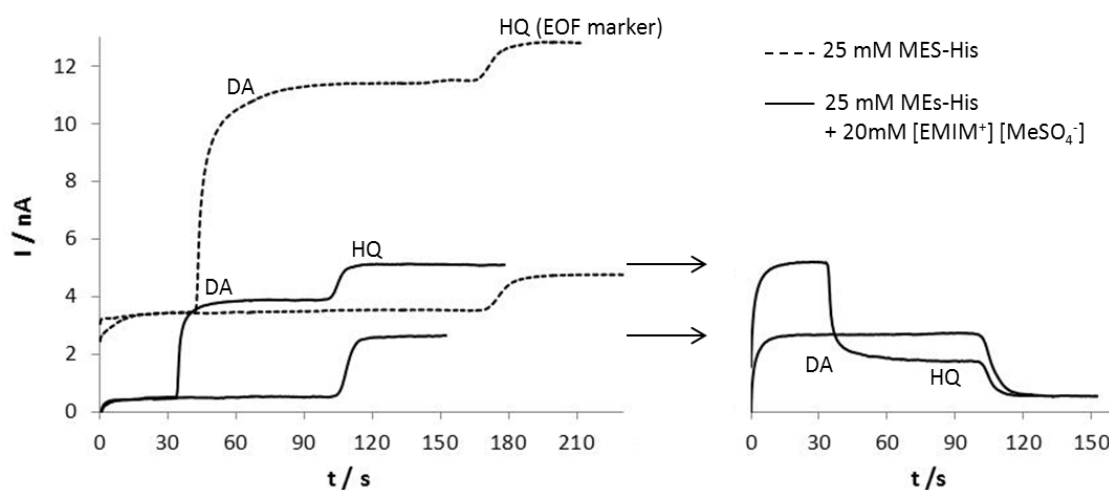


Figure 5. EOF measurements in 50 μ M HQ solution (EOF marker) and a mixture (50 μ M in each) of DA and HQ in both MES-His and MES-His with 20 mM of EMIMMeSO₄ buffer solutions.

Fig. 5 shows the electropherograms recorded for 50 μ M HQ (EOF marker) and a mixture of DA and HQ (50 μ M each) both of them in the buffer solution (MES-His) and in buffer solution with 20mM EMIMMeSO₄. The same behavior was found in both cases, when the buffer solution of the microchannel is displaced by the one that contains HQ or both D and HQ, an increase in the current due to oxidation could be observed (**Fig. 5 at left**). Note that, previously observed dopamine signal is less intense in the presence of IL. Afterwards, when the solution containing HQ or both DA and HQ, is displaced by buffer solution, a proportional decrease in the signal could be seen (**Fig. 5 at right**). On the other hand, it should be noted that while a substantial increase in EOF is achieved in presence of EMIMMeSO₄, dopamine migration times undergo minimal displacement. This suggests the possibility of interactions between DA and IL, leading to lower decreased migration times compared to those expected according to changes

in EOF. Taking into account the microchip electrophoresis dimensions, the mobility due to the EOF has been calculated and included in **Table 3**.

Table 3. Electroosmotic flow values for 25 mM MES-His buffer solution and buffer solution with 20 mM of BMPyBF₄, BMIMBF₄, BMIMHSO₄ and EMIMMeSO₄. Conditions as in Fig. 5.

| | EOF (x 10 ⁻⁵ cm ² V ⁻¹ s ⁻¹) |
|---|---|
| 25 mM MES-His | 9.9 ± 0.1 |
| 25 mM MES-His + 20 mM BMPyBF ₄ | 1.6 ± 0.1 |
| 25 mM MES-His + 20 mM BMIMBF ₄ | 1.3 ± 0.1 |
| 25 mM MES-His + 20 mM BMIMHSO ₄ | 1.20 ± 0.03 |
| 25 mM MES-His + 20 mM EMIMMeSO ₄ | 1.612 ± 0.005 |

The electropherograms recorded for a mixture of DA (100µM) and E (100µM) in MES-His buffer solution without ionic liquids and with a 20mM concentration of them are displayed in **Fig. 6a**. Firstly, based on Δt calculation included in **Table 4** it should be noted that, when ILs were employed as a background additive in the buffer solution, narrower peaks were observed when compared to those obtained in MES-His buffer. On the other hand, a strong influence in terms of DA and E separation efficiency is observed for ILs with different cations (BMPy⁺ and BMIM⁺) with the same counterion (BF₄⁻). However, the influence of anions (BF₄⁻ and HSO₄⁻) with the same cation (BMIM⁺) is not as marked. More similar migration times (t_m) with wider peaks for HSO₄⁻ were obtained. The effect of EMIMMeSO₄ is more similar to that of BMPyBF₄, but with a lower peak resolution. Therefore, the presence of ionic liquid with respect to the MES-His buffer solution results in lower catecholamine t_m (**Table 4**) and consequently, slightly higher mobilities of dopamine, varying from $(3.30 \pm 0.03) \times 10^{-4} \text{ cm}^2\text{V}^{-1}\text{s}^{-1}$ (buffer solution) to $(4.8 \pm 0.2) \times 10^{-4}$, $(3.49 \pm 0.06) \times 10^{-4}$, $(3.87 \pm 0.05) \times 10^{-4}$ and $(4.94 \pm 0.08) \times 10^{-4} \text{ cm}^2\text{V}^{-1}\text{s}^{-1}$ (for BMPyBF₄, BMIMBF₄, BMIMHSO₄ and EMIMMeSO₄ respectively). The EOF variation depends on the ionic liquid employed (using the same concentrations), which may be attributable to differences in the ion association constants [12,63]. In all of the cases, peaks were identified by adding E to the mixture sample, being observed an increase of the intensity in the peak with higher migration time. Repeatability in terms of migration times (t_m) and peak intensity (I_p) were demonstrated by four consecutive injections of the mixture. The t_m relative standard deviation (RSD) values vary from 0.3% to 1.7% and from 0.5% to 1.8% for DA and E respectively. Slightly higher values of RSD are obtained for I_{pa} , varying from 0.6% to 4.7% and from 3.1% to 14.2% for DA and E respectively.

Table 4. Migration times (t_m), peak intensities (I_p), relative standard deviations (RSD), resolution values (R_s) and, Δt (calculated as the difference between disappearance time and appearance time) obtained for a DA and E mixture in SU-8 / Pyrex ME with different buffers based on 25mM MES-His pH 5.5. Conditions as in Fig. 6a.

| | SU-8/ Pyrex-ME (L_{sep} 3cm) | | | | | |
|---------------------------------------|---------------------------------|---------------|-------------|---------------|------------------------|-------------|
| | Dopamine | | Epinephrine | | $\Delta t = t_d - t_a$ | R_s |
| | t_m / s | I_{pa} / nA | t_m / s | I_{pa} / nA | | |
| MES-His | 49.5 ± 0.4 | 2.5 ± 0.04 | 55.1 ± 0.3 | 1.6 ± 0.04 | 30 ± 1 | 0.30 ± 0.02 |
| MES-His + 20 mM BMPyBF ₄ | 34.5 ± 0.2 | 2.26 ± 0.05 | 37.4 ± 0.3 | 0.89 ± 0.05 | 9.0 ± 0.8 | 0.27 ± 0.03 |
| MES-His + 20 mM BMIMBF ₄ | 46.8 ± 0.8 | 1.47 ± 0.07 | 51.5 ± 0.9 | 0.42 ± 0.04 | 9.7 ± 0.6 | 0.46 ± 0.04 |
| MES-His + 20 mM BMIMHSO ₄ | 40.9 ± 0.4 | 1.4 ± 0.2 | 50.7 ± 0.4 | 0.8 ± 0.1 | 18.6 ± 0.3 | 0.70 ± 0.04 |
| MES-His + 20 mM EMIMMeSO ₄ | 35.8 ± 0.1 | 2.23 ± 0.01 | 38.5 ± 0.2 | 0.8 ± 0.1 | 7.7 ± 0.3 | 0.27 ± 0.01 |

When the IL is removed from the running buffer, the electropherogram becomes the original, with a reproducibility of 9% (RSD) for the t_m of a DA and E mixture (100 μ M of each). This was calculated from measurements performed in MES-His buffer solution after the corresponding measurement in buffer with IL. As noted previously, there is a strong influence of the IL cation in catecholamine resolution (R_s) (**Table 4**), obtaining better separation efficiency when ILs with BMIM⁺ were employed. Reproducibility in terms of resolution was also evaluated by three successive injections of the mixture, obtaining RSD values of 3.3, 10.1, 8.6, 5.4 and 2.5% for BMPyBF₄, BMIMBF₄, BMIMHSO₄ and EMIMMeSO₄ respectively. From these results, it can be concluded that BMIMHSO₄ employed as an additive in the buffer solution leads to a slight improvement of the catecholamine peak resolution.

3.2.2. Glass MEs

Another material with different properties than those of SU-8 / Pyrex was selected to evaluate ILs as a background additive. In order to compare the results obtained in both cases, the same effective separation length (3 cm), detection potential (+ 0.8 V), separation (+ 750 V) and injection (+ 500 V) voltages were selected. In this case, electropherograms recorded for a DA and E mixture (500 μ M of each) in MES-His buffer solution and buffer solution with 20 mM of BMPyBF₄ and BMIMBF₄, there was no peak resolution (data not show). However, the addition of 20mM of BMIMHSO₄ and EMIMMeSO₄ changes the situation, leading to more separated peaks. In glass MEs, the addition of IL does not significantly modify catecholamine migration times. This was proven by successive injections of DA in the different buffers,

obtaining migration time values of 45.2 ± 0.3 , 50.8 ± 0.4 , 50.4 ± 0.3 , 55.3 ± 0.8 and 48.2 ± 0.6 s, and consequently mobilities of $(3.10 \pm 0.02) \times 10^{-4}$, $(2.76 \pm 0.02) \times 10^{-4}$, $(2.78 \pm 0.01) \times 10^{-4}$, $(2.53 \pm 0.04) \times 10^{-4}$, $(2.90 \pm 0.03) \times 10^{-4} \text{ cm}^2\text{V}^{-1}\text{s}^{-1}$ in MES-His and MES-His modified with 20 mM BMPyBF₄, BMIMHSO₄, BMIMBF₄ and EMIMMeSO₄, respectively. The influence of IL concentration on catecholamine separation was evaluated as well. Selecting BMIMHSO₄ as the optimal background additive, working electrolytes with 10, 20 and 30mM of BMIMHSO₄ were tested. Only one peak is observed for the 10 and 30mM concentrations; the noise level increased significantly for 30mM.

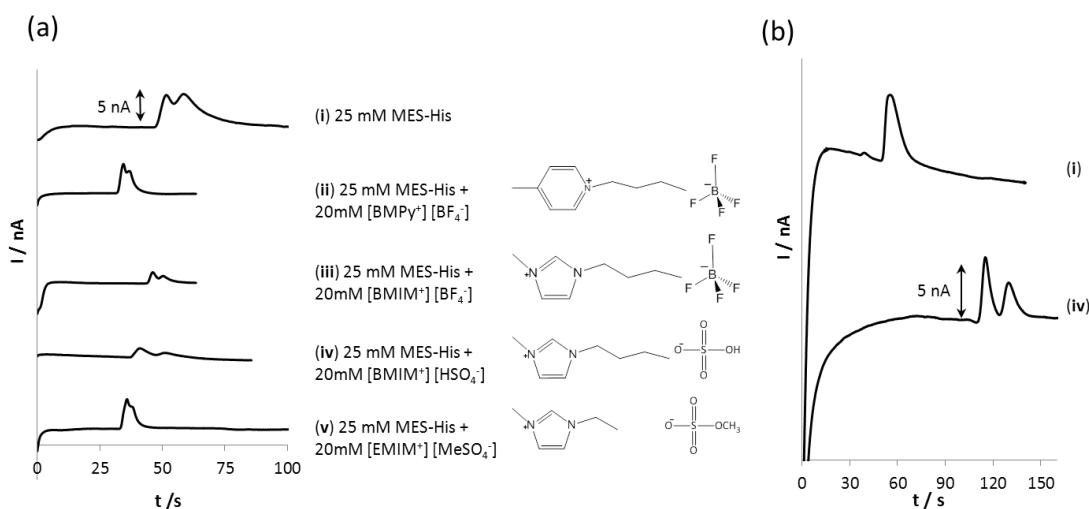


Figure 6. (a) Electropherograms recorded in SU-8/Pyrex ME for a mixture of DA and E ($100 \mu\text{M}$ each) and structures of the ILs employed all along the work. Conditions: separation length: 35 mm, $t_{inj} = 0.5$ s, $V_{inj} = +500$ V, $V_{sep} = +750$ V and $E_d = +0.8$ V (vs. Ag/AgCl). (b) Electropherograms recorded in glass ME for a mixture of DA and E ($500 \mu\text{M}$ each). Conditions: separation length: 65 mm, $t_{inj} = 0.5$ s, $V_{inj} = +500$ V, $V_{sep} = +1500$ V and $E_d = +0.8$ V (vs. Ag/AgCl). The buffers were in all cases: 25 mM MES-His pH 5.5 (i) and this with 20 mM of BMPyBF₄ (ii), BMIMBF₄ (iii), BMIMHSO₄ (iv) and EMIMMeSO₄ (v).

Since higher concentrations did not increase the resolution, the length of the glass microchip electrophoresis separation channel was doubled (60 mm). To maintain the electric field constant, the separation voltage (+1500 V) was also doubled; meanwhile, injection voltage and detection potential were maintained. In **Fig. 6b** the electropherograms obtained for a $500 \mu\text{M}$ mixture of DA and E in MES-His buffer solution and MES-His with 20 mM BMIMHSO₄ are shown. When BMIMHSO₄ was employed as the background additive, baseline resolution is achieved; nevertheless, in buffer solution without IL, only one peak is observed. Also an increase in DA and E migration times (from 55.8 ± 0.5 s in MES-His solution to 115.5 ± 0.5 s and 130.0 ± 0.6 s for DA and E respectively in the buffer with 20mM BMIMHSO₄) was observed. This might be due to a decrease in the EOF that changes from $(1.88 \pm 0.2) \times 10^{-4} \text{ cm}^2\text{V}^{-1}\text{s}^{-1}$ (without BMIMHSO₄) to $(1.31 \pm 0.01) \times 10^{-4} \text{ cm}^2\text{V}^{-1}\text{s}^{-1}$ (with 20mM BMIMHSO₄). The

decrease in the catecholamine migration times and also in their mobilities, from $(4.66 \pm 0.03) \times 10^{-4} \text{ cm}^2\text{V}^{-1}\text{s}^{-1}$ without IL, to $(2.22 \pm 0.05) \times 10^{-4}$ and $(2.00 \pm 0.09) \times 10^{-4} \text{ cm}^2\text{V}^{-1}\text{s}^{-1}$ for DA and E respectively, may be due to the fact that imidazolium cations can be adsorbed on the microchannel walls, and their aromatic group can associate with the phenolic group of DA and E by π - π interaction [12]. Therefore, a pseudostationary phase can be formed and the catecholamine interaction results in longer t_m . In this case, it is clear that IL as a background additive leads to sharper and more resolved peaks (R_s of 1.08 ± 0.07). Repeatability in terms of resolution was studied by four successive injections of a 500 μM mixture, obtaining a RSD of 0.6%.

Reproducibility of t_m was also evaluated, for one experiment, three days and one month (always with three dopamine injections), obtaining RSD values of 0.5, 0.8 and 11% over these time windows. Moreover, high separation efficiencies were obtained for DA and E when MES-His with 20mM of IL was employed, obtaining plate numbers of 41000 ± 3000 and $21000 \pm 4000 \text{ plates.m}^{-1}$ for DA and E respectively.

Finally, since the baseline resolution was obtained, another catecholamine with a similar structure (norepinephrine, NE) was included in the mixture. Migration order, determined by spiking on the mixture sample, was DA, NE and then E. In this case, slightly resolved peaks with R_s of 0.43 ± 0.07 and 0.33 ± 0.05 for DA-NE and NE-E were obtained, with a repeatability of 15%.

4. Conclusions

In the present work a fast and simple dynamic modification with ionic liquids has been proposed for improving catecholamine (DA and E) separation. ILs with different cations and anions were tested in both SU-8 / Pyrex and glass MEs and it was found that an addition of 20 mM BMIMHSO₄ was the optimal background additive. Moreover, the separation mechanism involves molecular interactions between ionic liquids and catecholamines. The employment of BMIMHSO₄ in 60mm effective length - glass microchip electrophoresis leads to DA and E baseline separation. Good precision and reproducibility in terms of migration times and resolution were obtained, which indicated that this method has an excellent potential application to improve separation of similar structure analytes.

Acknowledgments

This work has been supported by MICINN under project CTQ2011-25814 and by the Asturias Government with funds from PCTI 2006-2009, cofinanced with FEDER funds (Programa Operativo FEDER del Principado de Asturias 2007-2013) under project FC-11-PC10-30. Isabel Álvarez-Martos thanks the MICINN for the award of a PhD grant (AP2008-04451).

REFERENCES

- [1] R.M. Barrer, The viscosity of pure liquids. II . Polymerised ionic melts, *Transactions of the Faraday Society* 39 (1943) 59-66.
- [2] J.H. Davis, Task-specific ionic liquids, *Chemistry Letters* 33 (2004) 1072-1077.
- [3] D. Han, K.H. Row, Recent applications of ionic liquids in separation technology, *Molecules* 15 (2010) 2405-2426.
- [4] J. Pavlinac, M. Zupan, K.K. Laali, S. Stavber, Halogenation of organic compounds in ionic liquids, *Tetrahedron* 65 (2009) 5625-5662.
- [5] K. Wilpiszewska, T. Szychaj, Ionic liquids: media for starch dissolution, plasticization and modification, *Carbohydrate Polymers* 86 (2011) 424-428.
- [6] M.A.P. Martins, C.P. Frizzo, D.N. Moreira, N. Zanatta, H.G. Bonaccorso, Ionic liquids in heterocyclic synthesis, *Chemical Reviews* 108 (2008) 2015-2050.
- [7] P. Sun, D.W. Armstrong, Ionic liquids in analytical chemistry, *Analytica Chimica Acta* 661 (2010) 1-16.
- [8] A. Berthod, M.J. Ruiz-Ángel, S. Carda-Broch, Ionic liquids in separation techniques, *Journal of Chromatography A* 1184 (2008) 6-18.
- [9] Y. Xu, E. Wang, Ionic liquids used in and analyzed by capillary and microchip electrophoresis, *Journal of Chromatography A*, 1216 (2009) 4817-4823.
- [10] A. Varenne, S. Descroix, Recent strategies to improve resolution in capillary electrophoresis-a review, *Analytica Chimica Acta* 628 (2008) 9-23.
- [11] M. López-Pastor, B.M. Simonet, B. Lendl, M. Valcárcel, Ionic liquids and CE combination, *Electrophoresis* 29 (2008) 94-107.
- [12] E.G. Yanes, S.R. Gratz, M.J. Baldwin, A.E. Robison, A.M. Stalcup, Capillary electrophoretic application of 1-alkyl-e-methylimidazolium-based ionic liquids, *Analytical Chemistry* 73 (2001) 3838-3844.
- [13] L. Yu, W. Qin, S.F.Y. Li, Ionic liquids as additives for separation of benzoic acid and chlorophenoxy acid herbicides by capillary electrophoresis, *Analytica Chimica Acta* 547 (2005) 165-171.
- [14] M. Borissova, M. Vaher, M. Koel, M. Kaljurand, Capillary zone electrophoresis on chemically bonded imidazolium based salts, *Journal of Chromatography A* 1160 (2007) 320-325.

- [15] T-F. Jiang, Y-L. Gu, B. Liang, J-B. Li, Y-P. Shi, Q-Y. Ou, Dynamically coating the capillary with 1-alkyl-3-methylimidazolium-based ionic liquids for separation of basic proteins by capillary electrophoresis, *Analytica Chimica Acta* 479 (2003) 249-254.
- [16] N. Mofaddel, H. Krajian, D. Villemin, P.L. Desbène, New ionic liquids for inorganic cations analysis by capillary electrophoresis: 2-hydroxy-N,N,N-trimethyl-1-phenylethanaminium bis (trifluoromethylsulfonyl)imide (phenylcholineNTf₂), *Analytical and Bioanalytical Chemistry* 393 (2009) 1545-1554.
- [17] H.B. Mo, L.Y. Zhu, W.J. Xu, Use of 1-alkyl-3-methylimidazolium-based ionic liquids as background electrolytes in capillary electrophoresis for the analysis of inorganic anions, *Journal of Separation Science* 31 (2008) 2470-2475.
- [18] F. Shang, E. Guihen, J.D. Glennon, Recent advances in miniaturization-the role of microchip electrophoresis in clinical analysis, *Electrophoresis* 33 (2012) 105-116.
- [19] A Arora, G. Simone, G.B. Salieb-Beugelaar, J.T. Kim, A. Manz, Latest developments in micro total analysis systems, *Analytical Chemistry* 82 (2010) 4830-4847.
- [20] J.L. Felhofer, L. Blanes, C.D. García, Recent developments in instrumentation for capillary electrophoresis and microchip-capillary electrophoresis, *Electrophoresis* 31 (2010) 2469-2486.
- [21] M.C. Breadmore, Capillary and microchip electrophoresis: challenging the common conceptions, *Journal of Chromatogr. A* 1221 (2012) 42-55.
- [22] E. Verpoorte, N.F. de Rooij, Microfluidics meets MEMS, *Proceedings of the IEEE* 91 (2003) 930-953.
- [23] J.A. Vickers, M.M. Caulum, C.S. Henry, Generation of hydrophilic poly(dimethylsiloxane) for high-performance microchip electrophoresis, *Analytical Chemistry* 78 (2006) 7446-7452.
- [24] J. Wang, M. Pumera, M.P. Chatrathi, A. Escarpa, R. Konrad, A. Griebel, W. Dorner, H. Lowe, Towards disposable lab-on-a-chip: Poly(methylmethacrylate) microchip electrophoresis device with electrochemical detection, *Electrophoresis* 23 (2002) 596-601.
- [25] M. Castaño-Álvarez, M.T. Fernández-Abedul, A. Costa-García, Poly(methylmethacrylate) and Topas capillary electrophoresis microchip performance with electrochemical detection, *Electrophoresis* 26 (2005) 3160-3168.
- [26] M. Castaño-Álvarez, M.T. Fernández-Abedul, A. Costa-García, M. Agirregabiria, L.J. Fernández, J.M. Ruano-López, B. Barredo-Presa, Fabrication of SU-8 based microchip electrophoresis with integrated electrochemical detection for neurotransmitters, *Talanta* 80 (2009) 24-30.
- [27] A.W. Martinez, S.T. Phillips, E. Carrilho, G. Whitesides, Diagnostics for the developing world: microfluidic paper-based analytical devices, *Analytical Chemistry* 82 (2010) 3-10.
- [28] J. Wang, electrochemical detection for microscale analytical systems: a review, *Talanta* 56 (2002) 223-231.
- [29] C.D. García, C.S. Henry, Coupling capillary electrophoresis and pulsed electrochemical detection, *Electroanalysis* 17 (2005) 1125-1131.
- [30] M. Trojanowicz, Recent developments in electrochemical flow detections-a review, *Analytica Chimica Acta* 653 (2009) 36-58.

- [31] R.P.H. Nikolajsen, A.M. Hansen, Analytical methods for determining urinary catecholamines in healthy subjects, *Analytica Chimica Acta* 449 (2001) 1-15.
- [32] C. Cakal, J.P. Ferrance, J.P. Landers, P. Caglar, development of a micro-total analysis system (μ -TAS) for the determination of catecholamines, *Analytical and Bioanalytical Chemistry* 398 (2010) 1909-1917.
- [33] M. Vlckova, M.A. Schwarz, Determination of cationic neurotransmitters and metabolites in brain homogenates by microchip electrophoresis and carbon nanotube-modified amperometry, *Journal of Chromatography A* 1142 (2007) 214-221.
- [34] Y. Lu, Y.-L. Hu, X.-H. Xia, Effect of surface microstructures on the separation efficiency of neurotransmitters on a direct-printed capillary electrophoresis microchip, *Talanta* 79 (2009) 1270-1275.
- [35] A.-J. Wang, J.-J. Xu, H.-Y. Chen, Enhanced microchip electrophoresis of neurotransmitters on glucose oxidase modified poly(dimethylsiloxane) microfluidic devices, *Electroanalysis* 19 (2007) 674-680.
- [36] A.L. Bowen, R.S. Martin, Integration of serpentine channels for microchip electrophoresis with palladium decoupler and electrochemical detection, *Electrophoresis* 30 (2009) 3347-3354.
- [37] Q. Guan, S.D. Noblitt, C.S. Henry, Electrophoretic separations in poly(dimethylsiloxane) microchips using a mixture of ionic and zwitterionic surfactants, *Electrophoresis* 33 (2012) 379-387.
- [38] W.Z. Zhang, L.J. He, Y.L. Gu, X. Liu, S.X. Jiang, Effect of ionic liquids as mobile phase additives on retention of catecholamines in reversed-phase high-performance liquid chromatography, *Analytical Letters* 36 (2003) 827-838.
- [39] X.H. Xiao, L. Zhao, X. Liu, S.X. Jiang, Ionic liquids as additives in high performance liquid chromatography analysis of amines and the interaction mechanism of ionic liquids, *Analytica Chimica Acta* 519 (2004) 207-211.
- [40] D.S. Silvester, Recent advances in the use of ionic liquids for electrochemical sensing, *Analyst* 136 (2011) 4871-4882.
- [41] K. Jackowska, P. Kryszynski, New trends in the electrochemical sensing of dopamine, *Analytical and Bioanalytical Chemistry* 405 (2013) 3753-3771.
- [42] A.J. de Mello, M. Habgood, N.L. Lancaster, T. Welton, R.C.R. Wootton, Precise temperature control in microfluidic devices using Joule heating of ionic liquids, *Lab on a Chip* 4 (2004) 417-419.
- [43] Y. Xu, H. Jiang, E. Wang, Ionic liquid-assisted PDMS microchannel modification for efficiently resolving fluorescent dye and protein adsorption, *Electrophoresis* 28 (2007) 4597-4605.
- [44] Y. Du, E.K. Wang. Separation and detection of narcotic drugs on a microchip using micellar electrokinetic chromatography and electrochemiluminescence, *Electroanalysis* 20 (2008) 643-647.
- [45] Y.H. Xu, J. Li, E. Wang, Sensitive, label-free protein assay using 1-ethyl-3-methylimidazolium tetrafluoroborate-supported microchip electrophoresis with laser-induced fluorescence detection, *Electrophoresis* 29 (2008) 1852-1858.

- [46] Y. Xu, J. Li, E. Wang, Microchip micellar electrokinetic chromatography based on one functionalized ionic liquid and its excellent performance on proteins separation, *Journal of Chromatography A* 1207 (2008) 175-180.
- [47] H-L. Zeng, H. Shen, T. Nakagama, K. Echiyama, property of ionic liquid in electrophoresis and its application in chiral separation on microchips, *Electrophoresis* 28 (2007) 4590-4596.
- [48] T. Sikanen, S.K. Wiedmer, L. Heikkila, S. Franssila, R. Kostainen, T. Kotiaho, Dynamic coating of SU-8 microfluidic chips with phospholipid disks, *Electrophoresis*. 31 (2010) 2566-2574.
- [49] N. Nordman, T. Sikanen, M.-E. Moilanen, S. Aura, T. Kotiaho, S. Franssila, R. Kostainen, Rapid and sensitive drug metabolism studies by SU-8 microchip capillary electrophoresis-electrospray ionization mass spectrometry, *Journal of Chromatography A*. 1218 (2011) 739-745.
- [50] A. Fernández-la-Villa, V. Bertrand-Serrador, D. F. Pozo-Ayuso, M. Castaño-Álvarez, Fast and reliable urine analysis using a portable platform based on microfluidic electrophoresis chips with electrochemical detection, *Analytical Methods*. 5 (2013) 1494-1501.
- [51] X. Huang, M.J. Gordon, R.N. Zare, Current-monitoring method for measuring the electroosmotic flow-rate in capillary electrophoresis, *Analytical Chemistry* 60 (1988) 1837-1838.
- [52] C. Schwer, E. Kenndler, electrophoresis in fused-silica capillaries-the influence of organic solvents on the electroosmotic velocity and the zeta-potential, *Analytical Chemistry* 63 (1991) 1801-1807.
- [53] D.S. Silvester, K.R. Ward, L. Aldous, C. Hardacre, R.G. Compton, The electrochemical oxidation of hydrogen at activated platinum electrodes in room temperature ionic liquids as solvents, *Journal of Electroanalytical Chemistry* 618 (2008) 53-60.
- [54] T. Mori, T. Ishii, M. Akagawa, Y. Nakamura, T. Nakayama, Covalent binding of tea catechins to protein thiols: the relationship between stability and electrophilic reactivity, *Bioscience Biotechnology and Biochemistry* 74 (2010) 2451-2456.
- [55] Y. Lin, Z. Zhang, L. Zhao, X. Wang, P. Yu, L. Su, L. Mao, A non-oxidative electrochemical approach to online measurements of dopamine release through laccase-catalyzed oxidation and intramolecular cyclization of dopamine, *Biosensors and Bioelectronics* 25 (2010) 1350-1355.
- [56] J. Wang, L. Wang, Y. Wang, W. Yang, L. Jiang, E. Wang, Effect of buffer capacity on electrochemical behavior of dopamine and ascorbic acid, *Journal of Electroanalytical Chemistry* 601 (2012) 107-111.
- [57] M.D. Hawley, S.V. Tatawawadi, S. Piekarski, R.N. Adams, Electrochemical Studies of the oxidation pathways of catecholamines, *Journal of the American chemical Society* 89 (1967) 447-450.
- [58] D.V. Chernyshov, N.V. Shvedene, E.R. Antipova, I.V. Pletnev, Ionic liquid-based miniature electrochemical sensors for voltammetric determination of catecholamines, *Analytica Chimica Acta* 621 (2008) 178-184.
- [59] P. Hapiot, C. Lagrost, Electrochemical reactivity in room-temperature ionic liquids, *Chemical Reviews* 108 (2008) 2238-2264.

- [60] M Scampicchio, J. Wang, S. Mannino, M.P. Chatrathi, Microchip capillary electrophoresis with amperometric detection for rapid separation and detection of phenolic acids, *Journal of Chromatography A* 1049 (2004) 189-194.
- [61] M.P. Godoy-Caballero, M.I. Acedo-Valenzuela, T. Galeano-Díaz, A. Costa-García, M.T. Fernández-Abedul, Microchip electrophoresis with amperometric detection for a novel determination of phenolic compounds in olive oil, *Analyst* 137 (2012) 5153-5160.
- [62] I. Álvarez-Martos, M.T. Fernández-Abedul, A. Anillo, J.L.G. Fierro, F.J. García Alonso, A. Costa-García, Poly(acrylic acid) microchannel modification for the enhanced resolution of catecholamines microchip electrophoresis with electrochemical detection, *Analytica Chimica Acta* 724 (2012) 136-143.
- [63] M.T. Glaceran, L. Puignou, M.J. Diez, Comparison of different electroosmotic flow modifiers in the analysis of inorganic anions by capillary electrophoresis, *Journal of Chromatography A* 732 (1996) 167-174.

Biographies

Isabel Álvarez-Martos obtained her B.Sc. degree in 2009 with the work "Polymer modification of microchip electrophoresis: influence in catecholamines resolution". One year later she has obtained her MSc. entitled "Microchip electrophoresis microchannel modification". Her research is focused on the employment of electrochemical microfluidic devices (electrophoresis and paper), their modification (static and dynamic) with polymers and ionic liquids and the enhancement of their electrochemical properties, based on the employment of grown carbon nanotubes (disordered and forest).

Francisco Javier García Alonso was graduated (1977) and received his PhD (1982) in Inorganic Chemistry at the University of Valladolid (Spain). In the same year he moved to the University of Oviedo (Spain) where he was promoted to Titular (Associate Professor) in 1987 and later to Catedrático (full Professor) in 2009. He spent one and half year at the University of Würzburg (Germany) (1982-1985) and one year at Southern Methodist University in Dallas, Texas, (1991-1992). He has been dedicated successively to Organometallic Chemistry (Manganese Carbonyls Compounds with Prof. V. Riera and Rhodium Vinylidenes Complexes with Prof. H. Werner) and Inorganic Polymers, {Poly(methylphenylphosphazenes) with Prof. Patty Wisian-Neilson and Poly(spirophosphazenes) with Prof. G. A. Carriedo}. At the present, he is interested in Nanostructured Copolymers and Functionalization of Surfaces with different kind of polymers.

Adela Anillo obtained her Ph.D. in Chemistry in 1986 at the University of Oviedo, Spain. Since 1999 she has been working as Associate Professor in Inorganic Chemistry at the University of Oviedo. Her current research interests include both the synthesis and characterization of functionalized polymers for coating the surface of miniaturized analytical devices (e.g. microchips) used in the electrochemical detection of clinically interesting biomolecules and also the preparation of organometallic species for acting as labeling systems on electrochemical biosensors. A. Anillo also collaborates with a physics research group in the preparation of nanostructured copolymer films.

Pilar Arias Abrodo received her PhD in Chemistry in 1984 from the University of Oviedo (Spain) and is working as a Professor in Analytical Chemistry at the University of Oviedo since

1988. Her areas of interest are related with the characterization of the aromatic profile of Asturian apple juices employed in cider production by solid-phase microextraction (SPME) followed by fast gas chromatography (Fast GC), using commercial and new synthetic polymeric ionic liquids as stationary phases as well as fiber coatings.

María Dolores Gutiérrez Álvarez obtained her PhD in Chemistry at the University of Oviedo in 1980, where she has been working as a Professor of Analytical Chemistry since 1987. Her research involves the synthesis of new ionic liquids and compounds derived from polymeric ionic liquid and their applications as sorbent coatings in micro extraction techniques and as stationary phases in gas chromatography. Moreover, her research deals with obtaining graphene materials of different characteristics by chemical reduction procedures and its potential applications.

Agustín Costa-García obtained his B.Sc. degree in Chemistry, focus on Analytical Chemistry, in 1974 (University of Oviedo) and the Ph.D. in chemistry in 1977 (University of Oviedo). Since February 2000 he is Professor in Analytical Chemistry (University of Oviedo). He leads the Immunoanalytical Research Group of the University of Oviedo and has been supervisor of several research projects developed at the electrochemistry laboratories of the Department of Physical and Analytical Chemistry of the University of Oviedo. Nowadays his research is focused on the development of nanostructured electrodic surfaces and its use as transducers for electrochemical immunosensors and genosensors employing electrochemical labels.

María Teresa Fernández-Abedul received her PhD in Chemistry in 1995 at the University of Oviedo, Spain. Since 2002 is working as Associate Professor in Analytical Chemistry at the University of Oviedo. Her current research interests are the development of immunosensors and genosensors employing nanostructured transducers as well as the development of miniaturized analytical devices (microchip electrophoresis and paper microfluidic devices) for the sensitive electrochemical detection of analytes of interest, even those non-electroactive through adequate electroactive labeling systems.

Article 3

*Poly(glycidyl methacrylate) Derivatives
as Modifiers in Microfluidic Devices for the
Improvement of Catecholamines Separation
(considering for publication)*



Considering for Publication



Poly(glycidyl methacrylate) Derivatives as Modifiers in Microfluidic Devices for the Improvement of Catecholamines Separation

Isabel Álvarez-Martos^a, Rebeca Alonso-Bartolomé^a, Verónica Mulas Hernández^b, Francisco Javier García Alonso^b, Adela Anillo^b, Agustín Costa-García^a, M. Teresa Fernández-Abedul^{a*}

^a*Departamento de Química Física y Analítica, Universidad de Oviedo, Asturias, Spain*

^b*Departamento de Química Orgánica e Inorgánica, Universidad de Oviedo, Asturias, Spain*

ABSTRACT

In this paper, we report the synthesis of three different types of water soluble Poly(glycidyl methacrylate) (PGMA) derivatives. Thermal properties of the resulting polymers were determined by thermal gravimetric analysis (TGA) and differential scanning calorimetry (DSC), and their structures were intensively characterized by infrared (IR), ¹H-NMR and ¹³C-NMR. Finally, they were used as dynamic modifiers of SU-8/Pyrex[®] microfluidic chips for improving separation efficiency. Several important variables, including separation voltage, detection potential, polymer concentration and pH were assessed and optimized in order to achieve the separation of three catecholamines (dopamine, DA, norepinephrine, NE, and epinephrine, E). Under the optimum conditions, baseline separation of target analytes (Rs values of 1.3 ± 0.1 and 1.58 ± 0.03 for DA-NE and NE-E respectively) was achieved within 3 min. Moreover, the coating shows an excellent stability throughout time, with relative standard deviation in terms of migration times less than 3 % (n=10).

1. Introduction

The desire of controlling the properties of microfluidic walls has motivated both experimental and theoretical studies dealing with polymer modified surfaces¹⁻³ to reduce analyte adsorption⁴, suppress the electroosmotic flow (EOF)⁵, or even for manipulating fluid transport through the microchannels, known as “electroosmotic valving”⁶. These variations in transport properties may be caused by changes in microchannel effective size, physicochemical properties or fluids viscosity². There are a large number of polymer modification strategies^{7,8} mainly, *via* the so-called “dynamic coatings” or “static coatings”^{9,10}, employing different methods like silanization¹¹, sol-gel chemistry¹², chemical vapor deposition (CVD)¹³, layer-by-layer (LBL)¹⁴ or grafting (“grafting to”, “grafting from” or “grafting through”)^{10,15-17}. Given their simplicity, dynamic modifications are the easiest way of changing microchannel properties, either by adding the modifier to the buffer solution or by rinsing with it before measuring.

The search of a general procedure for modifying the microchannel surface is also a challenge, due to the huge variety of materials employed nowadays in the fabrication of microfluidic devices (glass, quartz, poly(dimethylsiloxane), poly(methylmethacrylate), poly(ethylene terephthalate), poly(carbonate), SU-8....)^{18,19}. Particular attention deserves photoresists like SU-8 (negative epoxy-based photoresist), which has attracted the attention in the last years for being one of the best materials for microfluidic devices fabrication²⁰⁻²². It provides some important characteristics like good chemical biocompatibility, nontoxicity, high mechanical and thermal stability, fabrication of high aspect ratio structures (by standard UV lithography) at low cost, or the lower voltages needed due to the lower Young’s modulus. In spite of these advantages, the main problem with SU-8 could be its hydrophobic moieties, which could lead to a surface fouling problem caused by analyte adsorption, hindering its immediate use without any surface modification. Therefore, it is of key importance to find a surface polymer modification method that allows modulating the electroosmotic flow in order to obtain high efficient and reproducible separations.

Poly(glycidyl methacrylate) (PGMA) is a polymer that can be functionalized in very different ways because of the extraordinary versatility of the epoxy group chemistry. Thus, PGMA oxirane rings have been hydrolyzed by strong acids^{23,24} or bases²⁵ under mild conditions yielding diols, without breaking the ester bond linkage (the resulting alcohols could be later oxidized with KMnO_4 , to give carboxylic groups²⁶). Under more severe conditions, the PGMA epoxy groups have been opened by bases²⁷ or acids²⁸, but initiating then a crosslinking

polymerization. Carboxylic acids have also been added to this group, opening the oxirane ring²⁹; furthermore in the case of 2-Bromo-2-methylpropionic acid, the α -Bromoester moiety has been used later as initiator for atom transfer radical polymerization (ATRP)³⁰. In a similar way, phosphoric acid³¹, sodium hydrogensulfite³², thioalcohols³³ and amines^{34,35} have been incorporated to the epoxy group. Particularly, biomolecules possessing amine groups (enzymes^{31,36}, proteins³⁷ or DNA³⁸) can be immobilized upon PGMA polymer. Primary amines once incorporated to a first epoxy group, may open later a second epoxy group, originating inter- and intra-molecular crosslinking³⁹. On the other hand, after the introduction of the amine molecule in the oxirane ring it can be easily protonated yielding to a cationic polyelectrolyte⁴⁰.

We decided to functionalize the poly(glycidyl methacrylate) (PGMA) with three secondary amines to obtain water soluble polymers wide different charged, with neutral, anionic and cationic nature. We choose secondary amines to avoid the already mentioned cross-coupling reactions observed in the reactions of PGMA with primary amines^{39,41}. The selected amines were N-methyl-D-glucamine (NMG) to prepare a neutral polymer with many alcohol groups, N-methyltaurine sodium salt (NMT) to obtain a polymer with pendant anionic sulfonate groups, and piperidine (PPD) to synthesize a polymer that could be transformed into a polycationic polymer after methylation with MeI. Dibenzylamine (DBA) was also chosen due to its bulkiness thus, the resulting polymer should be easily detected by the UV detector in the gel permeation chromatography apparatus (GPC).

Some of the polymers prepared, and several reactions studied in this work have been cited in the literature, but the resultant polymers were poorly characterized and the reactions were not fully explored. Thus, a poly(glycidyl methacrylate-N-methyl-D-glucamine) was synthesized by radical polymerization of the glycidyl methacrylate-N-methyl-D-glucamine monomer, however the resulting polymer was not characterized⁴². There are other reactions of PGMA copolymer resins⁴³⁻⁴⁶ or PGMA attached to a membrane⁴⁷ with *N*-metil-(*D*)-glucamina, which have been described in the bibliography, but again poorly characterized (only Infrared (IR) or eventually Photoelectron Spectra (XPS) techniques have been employed). In the same way, the reaction of PGMA with piperidine has been mentioned⁴⁸, although only GPC data and ¹H-NMR spectrum of the resultant polymer are given. Reactions with dibenzylamine have been also mentioned, but the efficiency in oxirane ring opening was only about 35%⁴⁹. Until now it has not been reported any reaction between PGMA and N-methyltaurine sodium salt. There are only several references describing the epoxy ring

opening of PGMA previously attached to different substrates by taurine sodium salt⁵⁰⁻⁵³, being the resulting derivatives ill characterized.

Catecholamines, including dopamine (DA), norepinephrine (NE), and epinephrine (E), are one of the most studied neuroactive compounds as they are involved in nervous and endocrine systems⁵⁴. This fact makes that a lot of efforts have been recently focused not only to improve their sensitivity⁵⁵, but also to improve their separation efficiency⁵⁶⁻⁵⁹. Throughout bibliography several polymer surface modifications have been proposed⁶⁰⁻⁶², although to our knowledge this is the first time that the PGMA derivatives described in this manuscript are employed with this aim.

In this work, the reactions of PGMA with four different secondary amines (NMG, NMT, PPD and DBA) have been studied in detail and the resultant polymers properly characterized. Later, two of them (those obtained with NMG and NMT), and a cationic derivative of a third one (that with piperidine) were evaluated as modifiers onto SU-8/Pyrex[®] microchips to improve the separation efficiency of a catecholamines mixture (analytes difficult to separate because of their close structures, **Figure S1**). A simple and versatile procedure for microfluidic devices modification has been proposed. Moreover, the surface modification was capable of maintain its properties throughout its use, and the employment of sample stacking technique enabled the baseline separation of the mixture.

2. Experimental

2.1. Reagents

Poly(glycidyl methacrylate), PGMA, was prepared by free radical polymerization as described previously⁶³. The anhydrous solvents, glycidyl methacrylate, methyl iodide and the amines N-Methyl-D-glucamine, piperidine and dibencylamine were used as purchased from Sigma-Aldrich (Madrid, Spain). N-methyltaurine sodium salt was purchased from Alfa Aesar (Karlsruhe, Germany).

Catecholamines [dopamine (DA), norepinephrine (NE) and epinephrine (E)], reagents for buffer preparation [2-(N-morpholino)-ethane sulfonic acid (MES) and histidine (His)] and sodium hydroxide (NaOH) were purchased from Sigma-Aldrich (Madrid, Spain). Moreover, catecholamine solutions were freshly prepared all days in the buffer solution and protected from light. In all cases solutions were filtered through Nylon syringe filters (Cameo 30 N, 0.1 μm , 30 mm) obtained from Osmonics (Minnetonka, MN, USA).

Water was purified employing a Milli-Q direct QS system from Millipore (Bedford, MA, USA). All other reagents were of analytical reagent grade.

2.2. Materials and instrumentation

The infrared (IR) spectra were recorded with a Perkin–Elmer FT Paragon 1000 spectrometer in KBr. Nuclear magnetic resonance (NMR) spectra were recorded on Bruker AV400 instrument, using CDCl_3 , or D_2O as solvents. ^1H and $^{13}\text{C}\{^1\text{H}\}$ NMR are given in δ relative to TMS. C, H, N analyses were performed with an Elementar Vario Macro microanalyzer with a TCD detector. GPC were measured with Perkin–Elmer equipment with a Model LC 250 pump, a Model LC 290 UV, and a Model LC 30 refractive index detector. The samples were eluted with 0.1 wt% of tetra-*n*-butylammonium bromide in THF through Perkin–Elmer PLGel (Guard, 10^5 , 10^4 and 10^3\AA) at 30 °C. Approximate molecular weight calibration was obtained using narrow molecular weight distribution polystyrene standards. Electrospray ionization mass spectrum was obtained using an Agilent MSDG 1946B model. Glass transition temperature (T_g) values were measured with a Mettler Toledo 822 differential scanning calorimeter. Thermal gravimetric analysis (TGA) was performed on a Mettler Toledo TGA/SDTA 51 instrument. The polymer samples were heated at a rate of 10 °C/min from ambient temperature to 1000 °C under constant flow of nitrogen (50 $\mu\text{L}/\text{min}$).

Micropipettes, 0.250 and 1.0 mL tips, as well as 1.5 mL tubes were obtained from Eppendorf (Hamburg, Germany).

SU-8/Pyrex® single-channel microchips used through this work were acquired from MicruX Technologies (Oviedo, Spain). As exhibits **Figure 1** they consist on a SU-8 photoresist which contains a separation channel of 35 mm length, 20 μm depth and 50 μm width supported on a glass plate (38 x 13 x 0.75 mm). A cross is formed by the intersection of separation and injection (10 mm) channels, and at the end of each one holes of 2 mm diameter have been drilled. Moreover micropipette tips, which act as solution reservoirs, were cut into 1 cm long pieces (0.5 cm diameter) and subsequently adhered to these holes using Araldite (Vantico, Basel, Switzerland) with a final volume of approximately 150 μL . The purchased microchips have three electrodes (working, reference and counter) at the end of the separation channel for the electrochemical detection. It should be noted that in all cases for the electrochemical measurements, microchips have been housed in a Faraday cage in order to minimize electrical interferences. In the accomplishment of this work reference (RE) and counter (CE) electrodes were homemade in a micropipette tip as described in previous works⁶⁴.

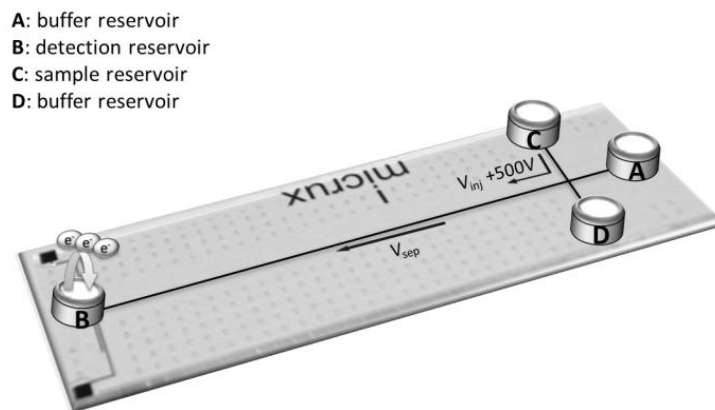


Figure 1. Schematic representation of the microfluidic chip employed in the accomplishment of this work, including the separation (A for buffer solution and B for the electrochemical detection) and the injection reservoirs (C for the sample and D for buffer solution). An unpinched injection (C-B) is employed to perform the sample injection.

Electrochemical measurements (amperometry) were performed with an Autolab PGSTAT 10 (ECO Chemie, The Netherlands) bipotentiostat interfaced to a computer system and controlled by Autolab GPES 4.9 version for Windows 98.

2.3. Electrophoresis procedure

Electrophoresis separations were performed employing two high-voltage power supplies (HVPS, MJ series) with a maximum voltage of + 5000 V purchased from Glassman High Voltage (High Bridge, NJ, USA). Moreover, platinum wires (300 μm diameter) bought from Sigma-Aldrich (Madrid, Spain) and connected by alligator clips to the HVPS operated as high-voltage electrodes.

In all cases microchip channels were preconditioned by rinsing them, with the aid of a vacuum system, first with 0.1 M NaOH (15 min) and then with the buffer solution (20 min). At the end of this washing step all reservoirs were filled with the buffer solution (25 mM MES-His). Unpinched injections (**Figure 1**) were done by applying the desired injection voltage ($V_{\text{inj}} = + 500 \text{ V}$) between the sample (C) and grounded detection (B) reservoirs. In other way, separation was carried out by applying the appropriate separation voltage (V_{sep}) between buffer (A) and detection (B) reservoirs. When polymer dynamic modification was performed, buffer solution containing an adequate concentration of PGMA was introduced through the microchannel and stopped for 40 min. After a washing step with the buffer solution (without polymer) for 10 min, microchannels were then filled with the buffer solution.

Dopamine and epinephrine (100 μM) were chosen as model analytes and, their resolution values (R_s) were calculated as $R_s = 2(t_{m2} - t_{m1}) / (W_1 + W_2)$ where t_{m1} and t_{m2} are the

migration times of both species and W_1 and W_2 are their corresponding base peak widths. All experiments were performed at room temperature.

For Electroosmotic Flow (EOF) measurements there are two main methods widely reported in the bibliography: current monitoring⁶⁵ or neutral marker⁶⁶. In this work, EOF was measured employing a previously reported method⁶⁴ with a neutral electroactive molecule (hydroquinone, HQ) as EOF marker.

2.4. Poly(glycidyl methacrylate) synthesis and characterization

2.4.1. Preparation of $[CH_2-C(CH_3)-C(O)-O-CH_2-CH(OH)-CH_2-N(CH_3)-CH_2-CH(OH)]_n$ (1)

N-Methyl-(*D*)-Glucamine (5.5 g, 28.1 mmol) was added to a solution of PGMA (0.4 g, 2.81 mmol) in DMSO (10 mL), the mixture was then heated 22 h at 80 °C under N_2 . The solution was then poured portion-wise with a Pasteur pipette into 2-propanol (200 mL). The white precipitate was washed with 2-propanol (2 x 30 mL) and Et_2O (3 x 30 mL) and dried under vacuum. Afterwards, the crude polymer was dialyzed against distilled water to eliminate the amine excess using a 7000 mol.-wt.-cutoff (MWCO) cassette, changing the external water each 12 h (8 times). The water was evaporated and the polymer dried under vacuum at 40 °C for 3 days.

2.4.2. Reaction of PGMA with *N*-Methyltaurine sodium salt. Obtention of $[CH_2-C(CH_3)-C(O)-O-CH_2-CH(OH)-CH_2-N(CH_3)-CH_2-CH_2-SO_3^- Na^+]_n$ (2a) and $[CH_2-C(CH_3)-C(O)-O-CH_2-C(CH_2OH)H-N(CH_3)-CH_2-CH_2-SO_3^- Na^+]_n$ (2b) as an isomer mixture.

N-Methyltaurine sodium salt (0.68 g, 4.22 mmol) was added to a solution of PGMA (0.4 g, 2.81 mmol) in DMSO (12 mL), the mixture was then heated 22 h at 60 °C under N_2 . The solution was then poured into 2-propanol (200 mL). The white precipitate was washed with 2-propanol (2 x 30 mL) and Et_2O (3 x 30 mL) and dried under vacuum. Afterwards, the crude polymer was dialyzed against distilled water to eliminate the amine excess using a 7000 mol.-wt.-cutoff (MWCO) cassette, changing the external water each 12 h (7 times). The water was evaporated and the polymer dried under vacuum at 40 °C for 3 days.

2.4.3. Preparation of $[CH_2-C(CH_3)-C(O)-O-CH_2-CH(OH)-CH_2-N-CH_2CH_2CH_2CH_2CH_2]_n$ (3)

Piperidine (5.6 mL, 56.3 mmol) was added under N₂ to a suspension of PGMA (0.8 g, 5.63 mmol) in butanone (8 mL), refluxing the mixture (80 °C) for 25 h. The resulting light yellow solution was poured into petroleum ether (200 mL) to give a white polymer. Then the solid was reprecipitated from butanone/petroleum ether (six times). The final product was dried under vacuum for 3 days at room temperature.

2.4.4. Reaction of PGMA with dibencylamine. Obtention of: $\{CH_2-C(CH_3)-C(O)-O-CH_2-CH(OH)-CH_2-N[CH_2(C_6H_5)]_2\}_n$ (4)

Dibencylamine (5.4 mL, 28.1 mmol) was added to a solution of PGMA (0.4 g, 2.81 mmol) in butanone (6 mL), and the mixture was refluxed under N₂ for 22 h. Then the solution was poured on petroleum ether (200 mL) and the resulting polymer was reprecipitated from butanone / petroleum ether three times. The solid was dried under vacuum for 3 days at room temperature.

2.4.5. Preparation of $[CH_2-C(CH_3)-C(O)-O-CH_2-CH(OH)-CH_2-N(CH_3)-CH_2CH_2CH_2CH_2CH_2]^+_n I^-$ (5).

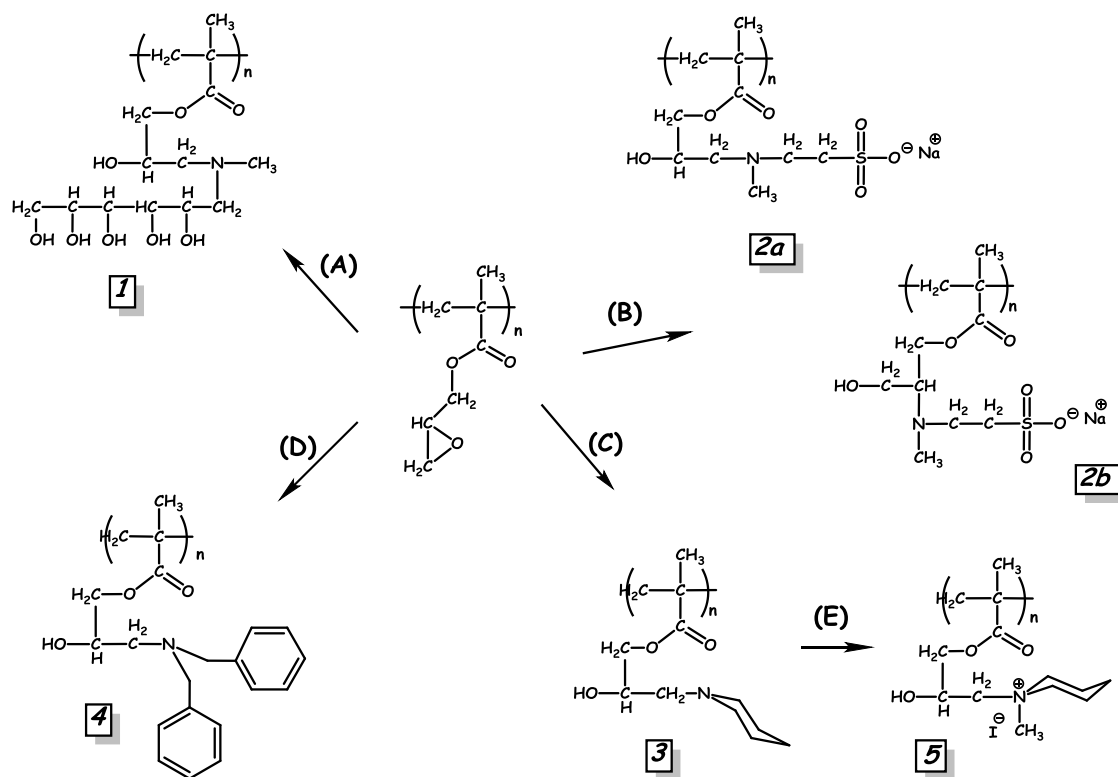
Methyl iodide, CH₃I (1.1 mL, 17.6 mmol) was added to a solution of polymer **3** (0.4 g, 1.76 mmol) in THF (4 mL), and the mixture was refluxed under N₂ for 14 h, using water at 3 °C as circulating liquid in the reflux condenser. Along the reaction time a continuous formation of a white solid was observed. The solvent and the excess of methyl iodide were evaporated to dryness. Afterwards, the polyelectrolyte was washed under N₂ with THF (5 mL) four times. Finally the product was dried under vacuum for 3 days at room temperature.

3. Results and Discussion

3.1. Synthesis and characterization of the polymers

The reaction of poly(glycidyl methacrylate) with the secondary amines used in this work led to the oxirane ring opening with a concomitant formation of an alcohol and a carbon-nitrogen bond (**Scheme 1**), as evidenced the spectroscopic and analytical data of the resulting polymers (see supporting information). However, depending on steric hindrance around the amine nitrogen, the reactions differed markedly. Using N-Methyl-(D)-Glucamine or piperidine a single product was obtained while, in case of the less steric crowding (N-Methyltaurine sodium

salt) two isomers were formed. The reaction with the bulky dibenzylamine was almost completed using a 10/1 amine/PGMA ratio in refluxing butanone for 24 h, but tiny amounts of starting material remained unaltered.



Scheme 1. Reactivity of PGMA with different amines: *N*-methyl-(*D*)-glucamine (**1**), *N*-methyltaurine sodium salt (**2a** and **2b**), piperidine (**3**), and dibenzylamine (**4**), as well as the subsequent methylation of polymer **3** with methyl iodide (**5**).

The IR spectra of polymers **1** and **2** shows that bands at 907 and 848 cm^{-1} , corresponding to the epoxy ring of the starting polymer, have disappeared. In the IR spectrum of polymer **3** there exists a peak at 905 cm^{-1} of very low intensity, but not any peak is observed at 850 cm^{-1} . However, in the case of **4** the presence of two very small peaks at 912 and 854 cm^{-1} suggested that the reaction between PGMA and dibenzylamine has not been finished. Furthermore, its DEPT-135 $^\circ$ (^{13}C -NMR) spectrum evidenced that this bulky amine was not able to open all PGMA epoxy rings; in fact, it showed tiny but clear signals at 49 ppm (CH) and at 44.6 ppm (CH_2), the chemical shifts owing to the two oxirane carbons of the starting PGMA. It is noteworthy that in a previous attempt to prepare the same polymer only 35 % of the epoxy rings had been opened⁴⁹.

On the other hand, the IR spectra of the polymers **1-4** showed intense and very broad bands in the 3300-3450 cm^{-1} region corresponding to the OH stretching. In addition, the polymers **1** and **2** exhibited a weak band around 1650 cm^{-1} indicating the presence of H_2O ,

which is in accordance with the 2-3% weight loss around 100 °C shown in their TGA thermograms. In fact, polymers **1** and **2** are hygroscopic and they retained some water even after being dried several days under vacuum (eventually the polymers could have absorbed some water during the samples handling, because the infrared spectrometer is outside the dry box). The intensity of 3300-3400 cm^{-1} broad bands supports the formation of alcohol groups. Furthermore, a strong absorption around 1080 cm^{-1} , attributable to a C-O stretching of the COH group, was detected in the infrared spectra of **1**, **3** and **4** (in the spectrum of **2** that signal is hidden by a very broad and very strong band centered at 1167 cm^{-1}).

Strong absorptions around 1730, 1265 and 1160 cm^{-1} were also noticed from the IR spectra of these polymers, corresponding to the presence of an ester carbonyl group. The first band is due to C=O stretching, and the other two to $\text{C}_{\text{sp}^2}\text{OC}$ stretching.

It is expected that the alkyl-sulfonate group (R-SO_3) exhibits in its spectrum four absorption bands at wave numbers close to those strong peaks shown in the IR spectrum of the N-Methyltaurine sodium salt, namely at 1192, 1055, 614 and 530 cm^{-1} . However in the spectrum of **2** the first two bands were hidden by the strong band centered at 1167 cm^{-1} , an absorption already mentioned, but the other two were detected at 606 and 527 cm^{-1} .

Regarding the ^{13}C -NMR spectra of the PGMA and secondary amines reaction products, the most relevant feature was a collection of small peaks that appeared beside a series of strong signals in case of N-Methyltaurine sodium salt, which is illustrated in **Figure 2** (at left).

The peaks of low intensity suggested the presence of minute amounts of a second isomer. In this sense, it should be noticed that there exist four signals in the spectrum, those at 73.6, 60.4, 64.9, and 58.2 ppm, that could be assigned to the carbons that were part of the former epoxy ring in the starting PGMA. Therefore, it could be safely assumed that the N-Methyltaurine sodium salt has attacked the two carbons of the oxirane ring, generating in this way the two isomers (**2a** and **2b**) whose structures are shown in **Figure 2** (at right). Furthermore, the peaks of small intensity at 73.6 and 60.4 ppm could be attributed to carbons 16 and 17 indicating that the minor isomer was the result of the amine attack at the more crowded carbon of the epoxy ring. The rest of the signals in the Figure due to both isomers were also assigned (see later).

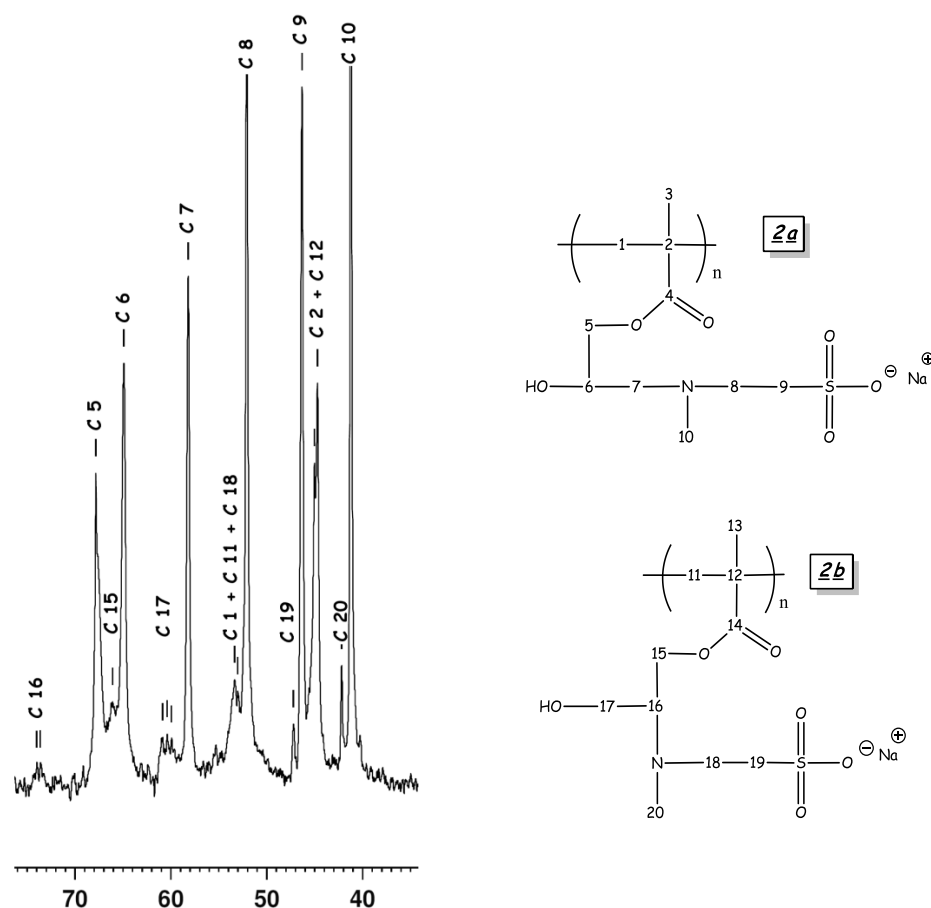


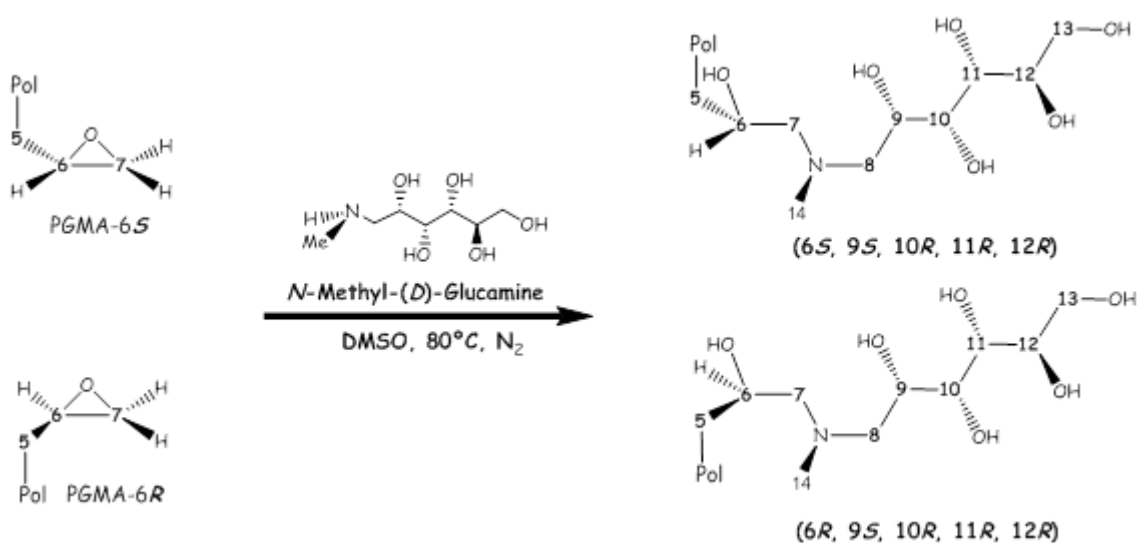
Figure 2. ^{13}C -NMR spectrum (in the region of 30-80 ppm) for the reaction product between poly(glycidyl methacrylate) and *N*-methyltaurine sodium salt (left), and the structure of the resulting regioisomers (right).

Carbon atoms placed in the PGMA main chain undergo a chemical shift values, and those close to it, remained unaltered in the obtained derivatives, although the fine structure of many of these signals, due to these polymers tacticity⁶⁷, was notably simplified in the spectra we have recorded, probably because the measurements were made at room temperature²³.

Carbon atoms signals of the former epoxy ring appeared downfield from that of the parent polymer (independent of the used solvent), as a consequence of the epoxy ring opening (**Table S1**).

The rest of polymers **1-4** signals that appeared in the ^{13}C -NMR spectra were those attributable to the attacking amine. In case of **3** and **4** they were easily assigned taking into account their intensity and the spectrum of both *N*-Methyl-Piperidine⁶⁸ and *N*-Methyl-Dibenzylamine⁶⁹.

The ^{13}C -NMR spectrum of polymer **1** showed split signals for carbon 11 (69.1 and 69.7 ppm) and 14 (42.7 and 42.4 ppm), and appreciable broad peaks for carbons 5 (68.2 ppm), 6 (66.0 ppm) and 7 (60.2 ppm) - the last partially mixed with the signal corresponding to carbon 8 - evidencing the presence of diastereoisomeric repeating units in the polymer **1**. In fact, the starting polymer PGMA contained pairs of enantiomeric repeating units, as it was prepared using a racemic mixture of glycidyl methacrylate (GMA) monomers. Therefore, in its reaction with the enantiomeric pure amine *N*-Methyl-(*D*)-glucamine, diastereoisomeric repeating units should be observed in the resulting polymer **1** (Scheme 2).



Scheme 2. Reaction of poly(glycidyl methacrylate) with *N*-methyl-(*D*)-glucamine, resulting in the formation of the polymer **1**, which contains two diastereoisomeric repeating units.

On the other hand, the ^1H -NMR spectra of polymers **1-4** were less informative. Signals attributable to protons located in the main chain or near to it appeared at chemical shift values close to those of the parent polymer⁷⁰. The rest of signals were tentatively assigned taking into account the predictions of the software incorporated in the program ChemDraw Ultra 12.0, the ^1H -NMR spectra of the corresponding free amines, and in case of polymers **2a** and **2b** employing a ^1H - ^{13}C correlation spectrum (see NMR data in SI).

It is noteworthy that the ^1H -NMR spectrum of a concentrated solution of the isolated product **4** enabled the detection of tiny peaks at 4.2, 3.2, and 2.7 ppm caused by protons around the epoxy ring of the starting polymer⁷⁰.

The reaction of polymer **3** with MeI in refluxing THF led to the formation of the polycation (**5**). Pendant piperidine group's methylation of the starting polymer was complete, and the resulting polymer contains a positive charge in every repeating unit. Electrospray mass

spectrum exhibited an intense peak at 242 Daltons, and no other peaks of significant intensity at higher values. The proposed formulation was also supported by spectroscopic and analytical data.

In fact, in the NMR spectrum of **5** in D₂O only the chemical shifts of signals corresponding to atoms in the main chain are coincident with those of the starting polymer **3**. The main changes are the presence of new signals due to the methyl group bonded to the piperidine N atom at 49.5 ppm (¹³C-NMR) and at 3.22 ppm (¹H-NMR), and the chemical shifts modifications of peaks attributable to the piperidine ring atoms and to the CH₂ group close to it (**Table S2**). Other minor changes are included in the experimental data collected in the supporting information.

The most relevant feature in the infrared spectrum of **5** is a broad absorption of medium intensity at 1628 cm⁻¹, due to the presence of water. This is explained because of polymer hygroscopic nature, which makes difficult to obtain it completely dried.

Thermal properties of PGMA derivatives, studied by TGA and DSC calorimetry, are illustrated in **Table 1**. All polymers were decomposed mainly in two steps around 300 and 400 °C. However TGA curves of the hygroscopic polymers, namely those containing hygroscopic pendant moieties (**1**, **2**, and **5**), exhibited also an initial weight loss (3 %) at ca. 100 °C, corresponding to the retained water. In case of **1** and **2** another small weight loss was detected at 560 and 745 °C respectively. The residues left after 1000 °C were always small, but insignificant in the case of **3** and **5**.

Table 1. Experimental data obtained from thermal gravimetric analysis (TGA) and differential scanning calorimetry (DSC) of polymers **1-4**.

| Polymer | T (°C) / Weight loss (%) | | | Residue at 1000 °C | T _g (°C) | |
|----------|--------------------------|----------------|--------------|--------------------|---------------------|-----|
| PGMA | 255 / 42 | 365 / 51 | | 7 | 72 | |
| 1 | 100 / 2 | 300 / 43 | 415 / 39.5 | 560 / 6.5 | 9 | 58 |
| 2 | 100 / 3 | 285 / 33 | 400-420 / 38 | 745 / 5.5 | 20.5 | 113 |
| 3 | | 268-322 / 57.5 | 419 / 38.5 | | 4 | 68 |
| 5 | 100 / 3 | 270 / 46 | 400 / 50 | | 1 | 180 |
| 4 | | 350 / 69 | 425 / 19.5 | | 11.5 | 51 |

Glass transition temperature values of polymers containing ionic species in the lateral chains (113 °C for **2**, and 130 °C for **5**) were higher than that of the starting PGMA (72 °C) whereas, these values for the other polymers were almost similar (68 °C for **3**), or a little bit lower (58 °C for **1** and 51 °C for **4**).

Finally, the molecular weight of **4** (Mw: 680 000; IPD: 1.45) was found to be higher than that of the starting polymer (Mw: 110 000, IPD: 3.99), measured under the same conditions, but using IR detector (in the later) instead UV detector (in the former). That means that no breaks were observed along the main chain when PGMA reacted with secondary amines under the used conditions.

3.2. Catecholamine separation on SU-8 MEs

3.2.1. Optimization of electrophoresis parameters for unmodified MEs

Parameters like separation voltage (V_{sep}), detection potential (E_d) and running buffer composition determine the behavior of microfluidic devices. Thus, the electrochemical response and, in consequence the resolution (R_s), defined as the separation achieved between analytes, are going to be directly related with these parameters. To establish the optimal working conditions of the SU-8 microchip, dopamine (DA) and epinephrine (E), with close chemical structures, were chosen as model analytes.

Firstly, the effect of separation voltage in both migration time (t_m) and R_s has been studied employing a mixture 100 μ M of DA and E. As expected, increasing the V_{sep} from + 400 to + 750 V leads to a linear decrease in migration times (**Figure 3A**) of both analytes (from 108 ± 2 and 117 ± 3 to 57 ± 1 and 63 ± 1 s for DA and E respectively), and also, to an increase in R_s values from 0.17 ± 0.02 to 0.342 ± 0.007 (**Figure 3B**). This behavior is explained because faster migration leads to smaller analytes dispersion through the microchannel, resulting in narrower peaks, until the voltage is increased above + 700 V where R_s was gradually reduced^{71,72}.

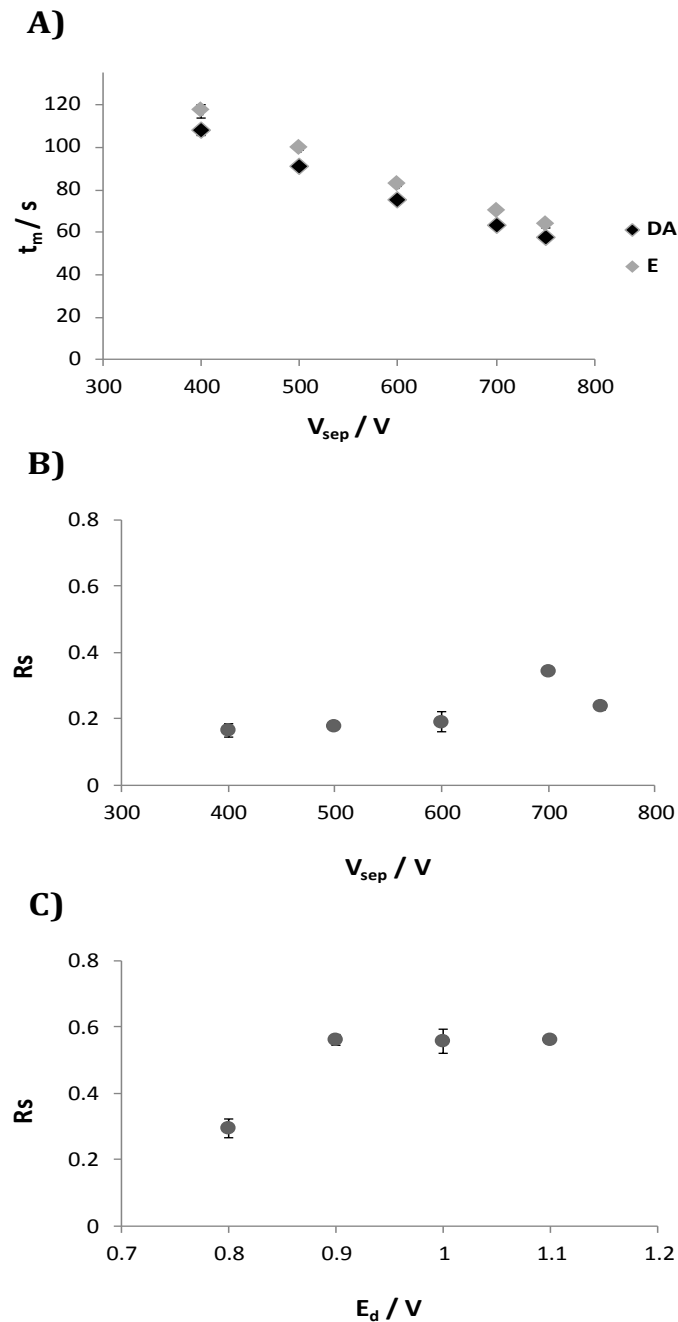


Figure 3. Influence of: **A)** V_{sep} in t_m , **B)** V_{sep} in R_s [conditions: 25 mM MES-His pH 5.7, $V_{inj} = + 500$ V for 1 s, $E_d = + 0.8$ V (vs. Ag/AgCl)] and, **C)** E_d in R_s [conditions: 25 mM MES-His pH 5.5, $V_{inj} = + 500$ V for 1 s, $V_{sep} = + 750$ V]. In all cases a mixture of DA and E (100 μ M each) on SU-8/Pyrex[®] ME was employed.

On the other hand, it has been reported that the detection potential (E_d) also influences the separation between peaks⁷³, so the second parameter to be evaluated was the effect of E_d in R_s (**Figure 3C**); in this case while the raise in detection potential from + 0.8 V to + 0.9 V implies an improvement in R_s (from 0.29 ± 0.03 to 0.56 ± 0.02), no further increase was observed for higher E_d . Moreover, too high detection potentials are not desirable because they could induce the formation of hydrogen bubbles at the electrode surface, resulting in higher noise levels. Finally, the effect of the buffer solution pH in the electrophoretic separation,

which strongly influences the mobility of analytes by modifying EOF velocity and molecule's charge, has been also assessed. The buffer composition consisted of MES-His due to previous studies developed in our group^{72,74}, showing that it is one of the best for catecholamines separation. Thereby, different pH values ranging from 5.5 to 6.5 were tested. These pHs have been mainly delimited by the MES useful pH range. It should be said that slight variations in this pH range did not induce strong changes in R_s (comprised between 0.51 ± 0.01 and 0.65 ± 0.01), being the lower values those that come from pHs above 5.7. Therefore, a V_{sep} of + 700 V, an E_d of + 0.9 V and a 25 mM MES-His running buffer solution pH 5.5 were selected for DA and E separation on SU-8/Pyrex[®] ME.

3.2.2. PGMA derivatives as modifiers of SU-8/Pyrex[®] microchip electrophoresis

One of the main factors involved in separation efficiency is the microchannel's surface properties⁷⁵. Thus, by modifying the inner walls with molecules containing different functional groups, more effective separations than in the native microchip could be achieved. With this purpose, in the development of this work PGMA derivatives have been proposed as new surface modifiers.

Firstly, with the aim of obtaining a more durable coating a covalent approach was checked, following a three steps protocol (glass activation, silanization and "grafting to" polymer immobilization) previously optimized in our group¹¹. With this aim polymer **2** was chosen, and two parameters involved in its immobilization on the pre-aminated glass surface were optimized: the choice of the solvent and the polymer optimal concentration. Thus, the solvent in which the reaction was performed proved to be a critical parameter in the amount of PGMA immobilized on the surface. **Figure 4** shows scanning electron microscopy (SEM) photographs of surfaces obtained after carried out the reaction with polymer **2** dissolved in tetrahydrofuran (THF), toluene, 2-butanone, and dimethylsulfoxide (DMSO). As it can be noticed in case of THF no polymer attached on the surface was observed, which is explained by the dipole-dipole interactions established between THF and the amine groups present on the surface⁷⁶. Among all studied solvents, DMSO was chosen as ideal, considering that is the one that provides the most homogeneous coating. Moreover, different polymer concentrations were also checked obtaining in all cases good surface coatings. A value of 0.001 g mL^{-1} was chosen to perform the microfluidic device modification. The small dimensions of the microchannel are incompatible with higher levels of polymer, leading to their obstruction. Nevertheless, some problems (originated by the high molecular weight of this polymer) appeared when this coating was employed for electrophoretic measurements (even for 0.001

g mL⁻¹ concentration), being the main one bubbles formation. This makes that measures were irreproducible, and in consequence another alternative based on a dynamic modification approach was proposed.

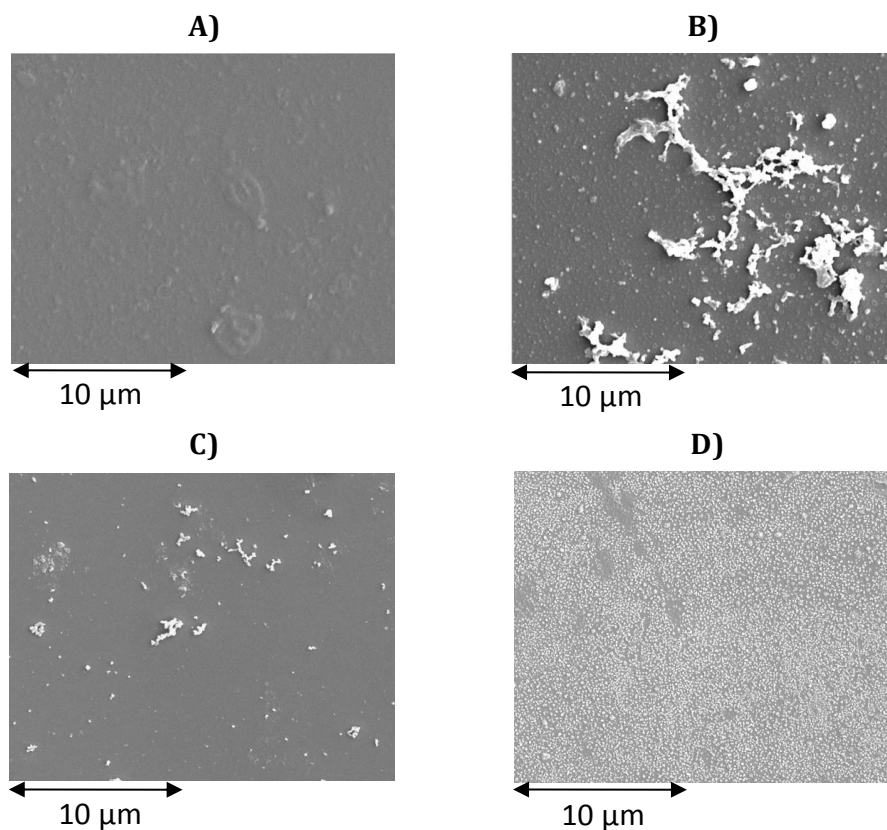


Figure 4. SEM images of 0.010 g mL⁻¹ PGMA coating obtained in four different organic media, **A)** THF at 40 °C 24 h, **B)** toluene at 60 °C 24 h, **C)** 2-butanone at 80 °C 24 h and **D)** DMSO at 80 °C 24 h.

Another strategy for improving efficiency in microfluidic devices is the dynamic modification of the inner walls. This strategy is particularly attractive because of its simplicity, versatility, and its ability to overcome the above problems arisen with the static coating. In this case, the effect of three of the previously synthesized PGMA derivatives with neutral (**1**), cationic (**5**) and anionic (**2**) nature as potential modifiers (included in the buffer solution or adsorbed on capillary walls) was evaluated. In this work, polymers with different nature were studied because it is known that the electroosmotic flow, EOF (involved in analytes separation efficiency) is a surface driven phenomenon and, therefore depends on microchannel charge distribution⁷⁷.

It should be said that when these polymers were part of the buffer solution a lot of noise was recorded, especially in case of anionic and cationic polymers, making impossible to see any dopamine or epinephrine signals. This effect is explained by the increase in the medium

conductivity^{78,79} due to the high charge of both polymers, leading to a detachment of the working electrode. Therefore, this is not suitable for its employment in microfluidic devices with electrochemical detection and, in consequence the adsorption strategy was chosen as best alternative.

The first parameter in being optimized was the type of polymer (neutral, anionic or cationic) that results in the best separation efficiency. With this purpose polymers were adsorbed on the inner wall surface. Thus, microchannels were filled with the buffer solution containing a concentration of 0.025 % of anionic, cationic or neutral PGMA derivatives for 30 min, after which microchannels were rinsed with the buffer solution without additives for 15 min. The results obtained in this study were very different depending on polymer nature. While the measure with the cationic was not possible, the anionic did not improve at all the separation, and the neutral enhanced considerably the separation efficiency between dopamine and epinephrine.

In view of this previous study, the neutral polymer was chosen as the most promising for catecholamines separation improvement. Therefore, further studies in order to find the optimum concentration and pH, which provide the best separation efficiency between dopamine and epinephrine, were made. Using the previously optimized working conditions (25 mm MEs-His pH 5.5, $V_{sep} = + 700$ V and $E_d = + 0.9$ V), a range of polymer concentrations comprised between 0.025 and 1 % were evaluated. As illustrates **Figure 5**, the bare microchip could not separate efficiently dopamine and epinephrine whereas, with the neutral polymer adsorbed on the surface this situation changes, obtaining a baseline resolved peaks. Furthermore, increasing concentrations of polymer causes that the separation between DA and E ($\Delta t = t_m E - t_m DA$) go up from 6.2 ± 0.6 s (for bare microchip) to 18.0 ± 0.3 , 29.5 ± 0.2 and 32.3 ± 0.7 s (for 0.025, 0.05 and 0.075 % concentrations of neutral polymer respectively). It is noteworthy that reached the 0.05 % concentration, subsequent growth did not bring an appreciable increase in Δt , hence this concentration was taken as the smaller that brings the best separation between analytes. Moreover, as discussed in the above section (for the bare microchip) the difference in terms of resolution for pHs comprised between 5.5 and 5.7 was not substantial, so both were tested in the polymer coated ME. In this case the behavior of electropherograms was not as expected and, slightly higher Δt values were obtained for pH 5.7 (40.0 ± 0.2 s) than for 5.5 (29.5 ± 0.2 s). Therefore, pH 5.7 and 0.05 % of neutral polymer, were taken as the best conditions to achieve a baseline resolved peaks of dopamine and epinephrine.

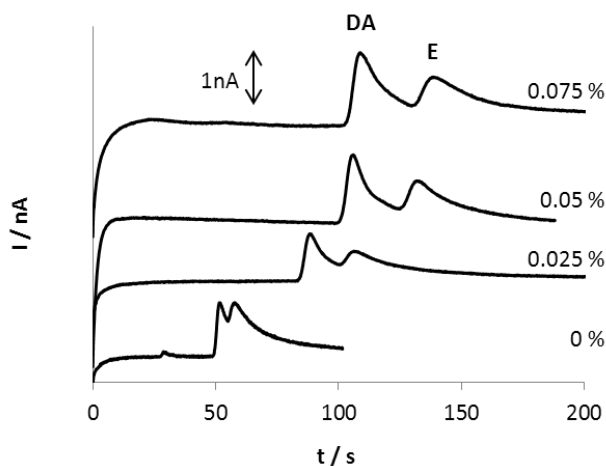


Figure 5. Electropherograms recorded in SU-8/Pyrex® microchip with different polymer **1** concentration for a mixture of DA and E ($100 \mu\text{M}$ each). Conditions: separation length: 35 mm, $t_{inj} = 1$ s, $V_{inj} = +500$ V, $V_{sep} = +700$ V, $E_d = +0.9$ V (vs. Ag/AgCl) and 25 mM MES-His buffer solution at pH 5.5.

Under this optimized conditions (pH 5.7 and 0.05 % of PGMA), the influence of the polymer surface modification in the electroosmotic flow (EOF) was studied. Thus, it was observed a substantial decrease in its value, from $(2.0 \pm 0.1) \times 10^{-4}$ to $(0.81 \pm 0.04) \times 10^{-4} \text{ cm}^2 \text{ V}^{-1} \text{ s}^{-1}$ for bare and modified microchips respectively, indicating that the polymer was effectively adsorbed on the microchannel surface. Moreover, as it can be seen in **Figure 5**, the catecholamine's migration times were also influenced by the polymeric modifier, being higher in the modified microchip (111.4 ± 0.1 and 141.6 ± 0.2 s for DA and E respectively) than in the bare one (53.2 ± 0.3 and 59.3 ± 0.5 s for DA and E respectively). This suggests the possibility of interactions between catecholamines and the alcohol groups of the neutral polymer. This behavior is especially favorable for the separation of analytes with similar structures that have also nearly the same migration times⁸⁰.

To test the potential of the proposed polymeric modification, another catecholamine (norepinephrine, NE) with a closely related structure to DA and E was added to the mixture. Electropherograms achieved for this three catecholamines mixture in the bare microfluidic chip and in the modified are shown in **Figure 6A**. It should be noted that, while in the bare microchip the mixture is slightly resolved (R_s values of 0.22 ± 0.02 and 0.21 ± 0.01 for DA-NE and NE-E respectively) when the polymer was adsorbed on inner walls better resolution of the mixture was obtained with R_s values of 0.72 ± 0.02 and 0.66 ± 0.06 for DA-NE and NE-E respectively. Finally, sample stacking that is a widely known strategy (in which heterogeneous electrolyte solutions are employed, and so sample is in a low conductivity matrix making ions migrate from the low to the high conductivity region) for achieving increased separation efficiencies⁸¹ was applied. This strategy really improved analytes separation, as displays **Figure**

6A, leading to baseline resolved peaks with R_s values of 1.3 ± 0.1 and 1.58 ± 0.03 for DA-NE and NE-E respectively.

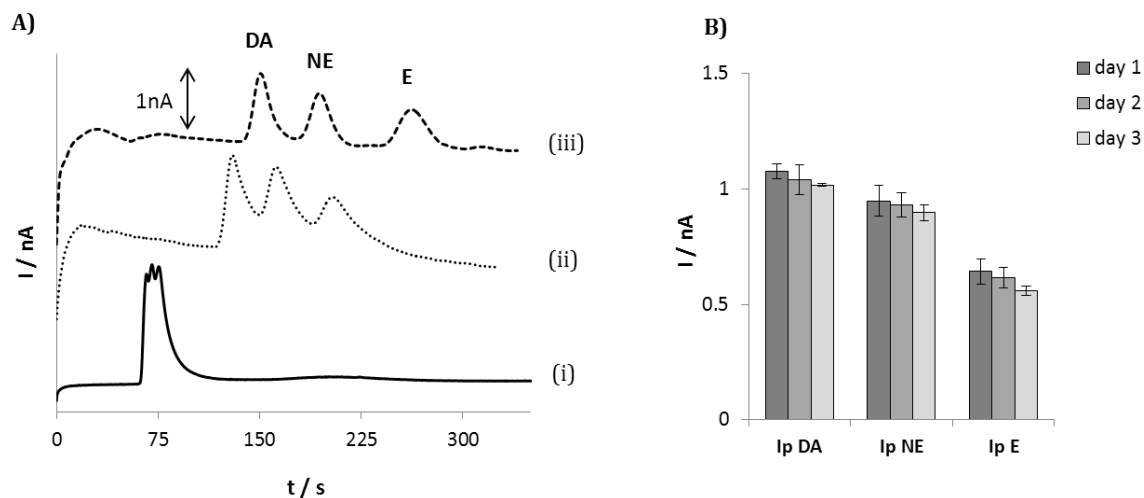


Figure 6. A) Electropherograms recorded in (i) bare microchip and, neutral polymer modified microchip: (ii) without and (iii) with sample stacking. **B)** Peak intensity values, obtained in a modified microchip for three different days. Conditions: DA, NE and E mixture ($100 \mu\text{M}$ each), separation length: 35 mm, $t_{inj} = 1$ s, $V_{inj} = +500$ V, $V_{sep} = +700$ V, $E_d = +0.9$ V (vs. Ag/AgCl), and 25 mM MES-His buffer solution at pH 5.7.

For successive measurements in the same microchip, a good stability of the polymer modification were achieved, with relative standard deviations (RSD) under 3 % for migration times and 7 % for both peak intensities and R_s values ($n = 10$). Moreover, the inter-day reproducibility (measures performed in 3 different days with the same microchip) was also good, with RSD values around 3 % for migration times and similar peak intensities as displays **Figure 6B**.

4. Conclusions

The reaction between PGMA and secondary amines, results to be dependent on the steric hindrance around the amine nitrogen. Meanwhile, only the less steric crowded amine was able to attack the two carbons of the epoxy ring, the more bulky one could not open all the oxirane rings of the starting polymer. In any case, the nucleophile attack is predominant on the less congested carbon atom in the epoxy ring. Polymers containing pendant hygroscopic moieties (**1**, **2**, and **5**) are themselves hygroscopic, which should be taken into account in order to be stored properly.

The present work also describes a simple and efficient method for the surface modification of SU-8/Pyrex[®] microfluidic devices using a new home-made polymer. This is the

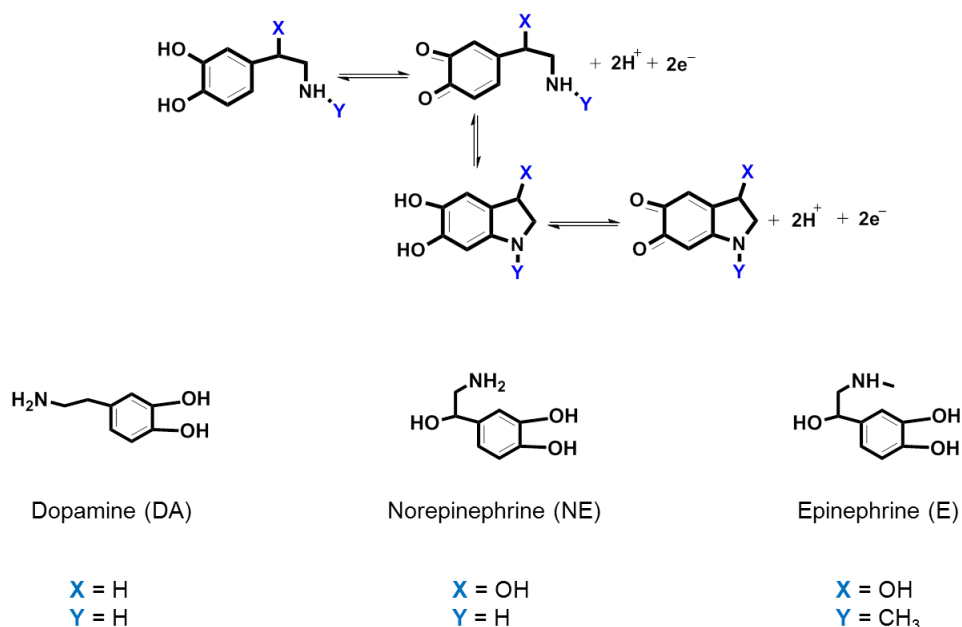
first time that these PGMA derivatives were used as additives in the buffer solution. The studies described through this manuscript show important advantages: (i) the microfluidic device can be easily modified in a short time (about one hour), (ii) the proposed modification procedure proved to be reproducible (RSD values lower than 7 % for migration times, peak intensities, and Rs), (iii) the modified microfluidic device shows an excellent separation performance for challenging compounds, such as those with very similar structures (Rs values of 1.3 ± 0.1 and 1.58 ± 0.03 for DA-NE and NE-E respectively), and (iv) this opens the opportunity of generating surfaces with completely different properties (anionic, cationic and neutral) depending on the nature of the polymer immobilized.

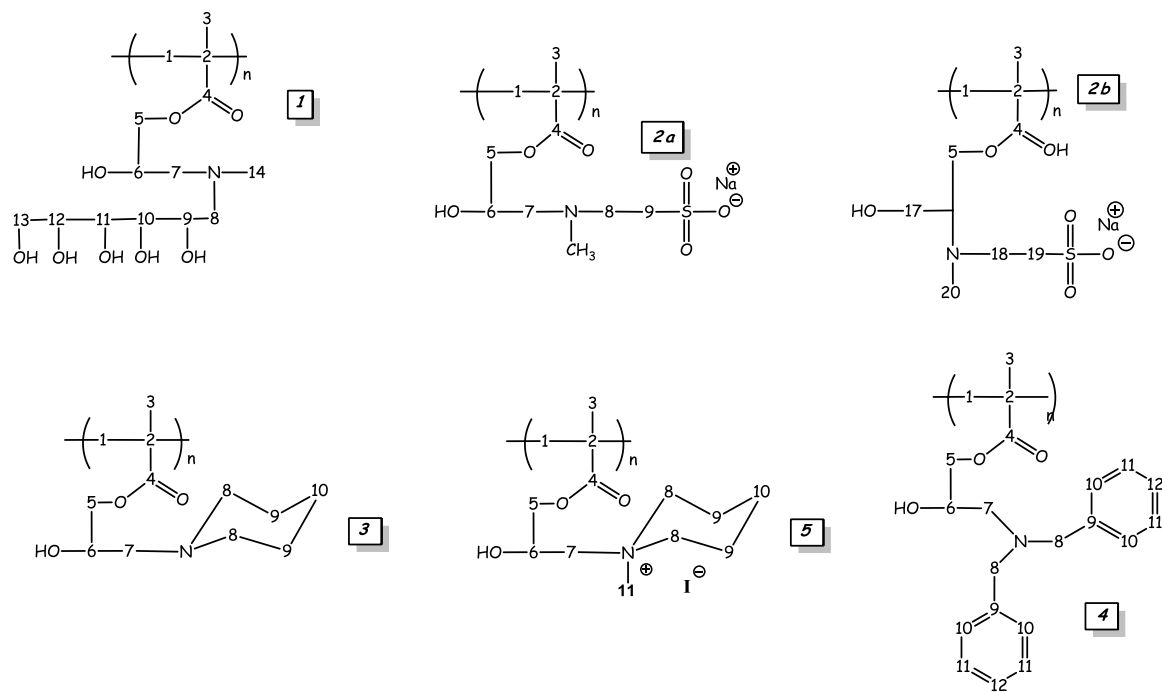
Acknowledgments

This work has been supported by MICINN under project CTQ2011-25814. Isabel Álvarez-Martos thanks the MICINN for the award of a PhD grant (AP2008-04451).

Supporting Information

Figure S1. Catecholamines electrochemical process and their structures.



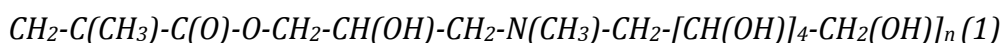
Experimental data from the polymer synthesis.**Figure S2.** Polymer structures and numbering of their carbon atoms. Protons bonded to carbon atoms are identified with the same number as its carbon atom.**Table S1.** ^{13}C -NMR peaks due to carbon atoms 6 and 7 of the polymers 1-4.

| Polymer | Solvent | δ (ppm) C6 | δ (ppm) C7 |
|-----------|----------------------|--------------------|-------------------|
| PGMA | CDCl_3 | 49.0 / 48.9 / 48.7 | 43.8 |
| 1 | D_2O | 66.0 | 60.2 |
| 2a | D_2O | 64.9 | 58.2 |
| 2b | D_2O | 73.6 | 60.4 |
| 3 | CDCl_3 | 64.8 | 61.2 |
| 4 | CDCl_3 | 65.7 | 55.9 |

Table S2: Principal alterations in the chemical shifts of the signals corresponding to the piperidine atoms (8, 9, and 10), and the CH₂ group close to it (7) after methylation of **3**. For numeration see Figure S2.

| | ¹³ C-NMR data for 3 | ¹³ C-NMR data for 5 | ¹ H-NMR data for 3 | ¹ H-NMR data for 5 |
|------------|-----------------------------------|-----------------------------------|----------------------------------|----------------------------------|
| C7 | 61.2 | 62.4 | 2.57 | 3.48 |
| C8 | 54.8 | 63.2 | 2.36 | 3.57 |
| C9 | 26.1 | 19.9 | 1.60 | 1.90 |
| C10 | 24.3 | 20.5 | 1.47 | 1.67 |

Spectroscopic, NMR, and thermal data of the obtained polymers



Yield 0.8 g, (88%). Anal. Calc. for C₁₄H₂₇NO₈ (337.4): C, 49.8; H, 8.1; N, 4.2. Found: C, 49.0; H, 9.2; N, 4.2%.

IR (KBr, cm⁻¹): 3390 (vs, v br ν_{OH}), 2945 (vs, ν_{CH}), 1725 (vs, ν_{C=O}) 1653 (w, δ_{H₂O}), 1456 (s), 1406 (s), 1332 (s), 1273 (s, ν_{CO} ester), 1252 (s), 1159 (vs, ν_{CO} ester), 1081 (vs, ν_{CO} alcohol), 1040 (vs), 969 (m) 940 (m), 877 (m), 748 (m) 579 (v br, s). ¹³C-NMR (D₂O)(δ/ppm): 179.7, 179.5, 178.8 (C₄); 71.5, 71.3, 71.1 (C₉, C₁₀, C₁₂); 69.1, 69.7 (C₁₁); 68.2 (C₅); 66.0 (C₆); 62.9 (C₁₃); 60.2 (C₇); 59.9 (C₈); 53.7 (C₁); 45.0, 44.7 (C₂); 42.7, 42.4 (C₁₄); 18.6, 16.6 (C₃). ¹H-NMR (D₂O)(δ/ppm): 4.05 (H₅), 3.90 (H₅, H₆); 3.80, 3.75, 3.70, 3.62, 3.61 (H₉, H₁₀, H₁₁, H₁₂, H₁₃); 2.60 (H₇, H₈); 2.32 (H₁₄); 1.90 (H₁); 1.01, 0.86 (H₃).

TGA: -2 % (80 °C), -43% (300 °C), -39.5% (415 °C), -6.5% (560 °C). Residue at 1000 °C: 9 %.

Tg (DSC from 0 to 200 °C) = 58 °C.

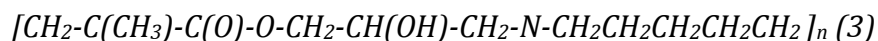
$[\text{CH}_2\text{-C}(\text{CH}_3)\text{-C}(\text{O})\text{-O-CH}_2\text{-CH}(\text{OH})\text{-CH}_2\text{-N}(\text{CH}_3)\text{-CH}_2\text{-CH}_2\text{-SO}_3^- \text{Na}^+]_n$ (2a) and
 $[\text{CH}_2\text{-C}(\text{CH}_3)\text{-C}(\text{O})\text{-O-CH}_2\text{-C}(\text{CH}_2\text{OH})\text{H-N}(\text{CH}_3)\text{-CH}_2\text{-CH}_2\text{-SO}_3^- \text{Na}^+]_n$ (2b) as an
 isomer mixture.

Yield 0.6 g, (70%). Anal. Calc. for C₁₀H₁₈NO₆SNa (303.31): C, 39.6; H, 6.0; N, 4.6; S, 10.6. Found: C, 41.8; H, 6.0; N, 4.5 S, 8.3. %. IR (KBr, cm⁻¹): 3441 (v br, vs, ν_{OH}), 2999 (s, ν_{CH}), 2953 (s, ν_{CH}), 2852 (m, ν_{CH}), 1727 (s, ν_{C=O}), 1653 (m, δ_{H₂O}), 1471 (s), 1387 (m), 1273 (s, ν_{CO} ester), 1167

(vs, ν_{CO} ester), 1038 (vs, SO_3^-), 964,2 (m) 935 (m), 861 (w), 797 (w), 743 (s), 606 (s, SO_3^-), 527 (s, SO_3^-) ^{13}C -NMR (D_2O)(δ /ppm): 179.3, 178.8 (C_4+C_{14}); 73.6 (C_{16}); 67.8 (C_5); 66.1(C_{15}) 64.9 (C_6); 60.4 (C_{17}); 58.2 (C_7); 53.4 ($\text{C}_1+\text{C}_{11}+\text{C}_{18}$); 52.1(C_8); 47.2 (C_{19}); 46.3(C_9) ; 45.0, 44.7 (C_2+C_{12}); 42.2 (C_{20}); 41.2 (C_{10}); 18.6, 16.7 (C_3+C_{13}). ^1H - NMR (D_2O)(δ /ppm): 4.20-3.90 ($\text{H}_5, \text{H}_6, \text{H}_{15}, \text{H}_{16}$); 3.15 ($\text{H}_8 + \text{H}_9 + \text{H}_{18} + \text{H}_{19}$); 2.83 ($\text{H}_8 + \text{H}_7 + \text{H}_{17}$); 2.50 (H_{10}); 2.30 (H_{20}); 1.90 (H_1+H_{11}); 1.01, 0.84 (H_3+H_{13}).

TGA: -3 % (100 °C), -33% (285 °C), -38% (400, 420 °C), -5.5% (745 °C). Residue at 1000 °C: 20.5 %.

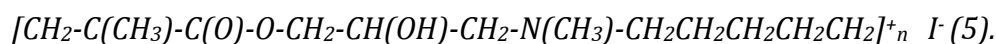
Tg (DSC from 0 to 113 °C) = 58 °C.



Yield 1.04 g, (81%). Anal. Calc. for $\text{C}_{12}\text{H}_{21}\text{NO}_3$ (227.30): C, 63.4; H, 9.3; N, 6.2; Found: C, 60.1; H, 8.6; N, 5.9 %. IR (KBr, cm^{-1}): IR (KBr, cm^{-1}): 3446 (vs, ν_{OH}), 2936 (vs, ν_{CH}), 2854 (s, ν_{CH}), 2803 (s, ν_{CH}), 1733 (vs, $\nu_{\text{C=O}}$), 1470 (s), 1456 (s), 1388 (m), 1355 (m), 1325 (m), 1302 (m), 1270 (s, ν_{CO} ester), 1158 (vs, ν_{CO} ester), 1120 (s), 1081 (sh, ν_{CO} alcohol), 1062 (m), 1038 (m), 997 (m), 964 (w), 935 (w), 905,3 (w), 862 (m), 782 (m), 748 (w), 660 (vw), 557 (w), 513 (w), 474 (w). ^{13}C -NMR (CDCl_3)(δ /ppm): 177.7, 177.4, 176.8 (C_4); 67.7 (C_5); 64.8 (C_6); 61.2 (C_7); 54.8 (C_8); 53.4 (C_1); 45.2, 44.8 (C_2); 26.1 (C_9); 24.3 (C_{10}); 18.7, 16.9 (C_3). ^1H NMR (CDCl_3)(δ /ppm):3.96, 3.88, (H_5, H_6); 2.57, (H_7); 2.36 (H_8); 1.94, 1.86 (H_1); 1.60 (H_9); 1.47 (H_{10}); 1.08, 0.93 (H_3).

TGA: -57.5 % (268, 322 °C), -38.5 % (419 °C). Residue at 1000 °C: 4 %.

DSC: Tg = 68 °C.



Yield 0.53 g, (81%). Anal. Calc. for $\text{C}_{13}\text{H}_{24}\text{NO}_3\text{I}$ (369.24): C, 42.3; H, 6.6; N, 3.8; Found: C, 40.6; H, 6.4; N, 3.7 %. IR (KBr, cm^{-1}): 3419 (vs, ν_{OH}), 2962 (s, ν_{CH}), 2871,1 (m, ν_{CH}), 2018 (v br, vw), 1725 (vs, $\nu_{\text{C=O}}$), 1623 (w, $\delta_{\text{H}_2\text{O}}$), 1472 (s), 1450 (s), 1387 (m), 1363 (w), 1328 (w), 1265 (s, ν_{CO} ester), 1244 (s), 1158 (vs, ν_{CO} ester), 1118 (s), 1084 (m, ν_{CO} alcohol), 1057 (m), 1031 (m), 993 (m), 959 (m), 938 (m), 920 (m), 900 (m), 867 (w), 835 (vw), 788 (vw), 747 (w), 570 (m), 502 (m), 474 (m). ^{13}C NMR (D_2O)(δ /ppm):179.2, 178.1 (C_4); 67.8 (C_5); 64.6 (C_6); 63.2 (C_8); 62.4 (C_7); 53.4 (C_1); 49.5 (C_{11}); 44.8 (C_2); 20.5 (C_{10}); 19.9 (C_9); 17.8 (C_3). ^1H NMR (D_2O)(δ /ppm):4.65 (H_5); 4.08 (H_5+H_6); 3.57 (H_8); 3.48 (H_7); 3.22 (H_{11}); 1.90 (H_1+H_9); 1.67 (H_{10}); 1.07, 0.89 (H_3).

TGA: -49 % (270 °C), -50 % (400 °C). Residue at 1000 °C: 1 %.

Tg (DSC from 0 to 200 °C) = 180 °C.

Reaction of PGMA with dibencylamine. Obtention of: $\{CH_2-C(CH_3)-C(O)-O-CH_2-CH(OH)-CH_2-N[CH_2(C_6H_5)]_2\}_n$ (4)

Yield 0.8 g, (83%). Anal. Calc. for $C_{13}H_{24}NO_3$ (339.43): C, 74.3; H, 7.4; N, 4.1; Found: C, 74.5; H, 7.6; N, 4.0 %. IR (KBr, cm^{-1}): 3466 (s, ν_{OH}), 3085 (m, ν_{ArH}), 3062 (s, ν_{ArH}), 3027 (s, ν_{ArH}), 2940 (s, ν_{CalkH}), 2906 (sh, ν_{CalkH}), 2830 (s, ν_{CalkH}), 2807 (s, ν_{CalkH}), 1954 (vw) 1870 (vw) 1812 (vw) (aromatic combination bands) 1731,7 (vs, $\nu_{C=O}$), 1602 (w, $\nu_{CC\ arom}$), 1585 (w, $\nu_{CC\ arom}$), 1495 (vs) 1453 (vs), 1371 (s), 1321 (m) 1262 (vs, $\nu_{CO\ ester}$), 1246 (vs) 1156 (vs, $\nu_{CO\ ester}$), 1074 (vs, $\nu_{CO\ alcohol}$), 1028 (s), 970 (s), 935 (m), 912 (m), 876 (w), 854 (w), 820 (w) 749 (vs, $\delta_{Ar-H\ out\ of\ plane}$) 699,1 (vs) 614,0 (w) 473,7 (m). ^{13}C NMR ($CDCl_3$)(δ/ppm): 177.6, 177.3, 176.7 (C_4); 138.5 (C_{ipso}); 129.1 (C_{orto}); 128.5 (C_{meta}); 127.3 (C_{para}); 67.6 (C_5); 65.7 (C_6); 58.5 (C_8); 55.9 (C_7); 54.0 (C_1); 45.2, 44.8 (C_2); 19.0, 17.2 (C_3). 1H NMR ($CDCl_3$)(δ/ppm): 7.28 ($H_{orto}+H_{para}$); 7.21 (H_{meta}); 3.93 (H_5); 3.71 (H_6, H_8); 3.47 (H_8'); 2.54, 2.45 (H_7, H_7'); 1.76 (H_1); 0.98, 0.86 (H_3).

TGA: -69 % (350 °C), -19.5 % (425 °C). Residue at 1000 °C: 11.5 %.

Mw(GPC) 680 000 (Mw/Mn = 1). Tg (DSC from 0 to 200 °C) =51 °C.

REFERENCES

- (1) Hickey, O.A.; Holm, C.; Harden, J.L.; Slater, G.W. *Macromolecules* **2011**, *44*, 9455-9463.
- (2) Cao, Q.; Zuo, C.; Li, L.; Yang, Y.; Li, N. *Microfluid. Nanofluid.* **2011**, *10*, 977-990.
- (3) Qiao, R.; He, P. *Langmuir* **2007**, *23*, 5810-5816.
- (4) Catai, J.R.; Tervahauta, H.A.; de Jong, G.J.; Somsen, G.W. *J. Chromatogr. A* **2005**, *1083*, 185-192.
- (5) Doherty, E.A.S.; Meagher, R.J.; Albarghouthi, M.N.; Barron, A.E. *Electrophoresis* **2003**, *24*, 34-54.
- (6) Dutta, D.; Ramsey, J.M. *Lab on a Chip* **2011**, *11*, 3081-3088.
- (7) Fernández-Abedul, M.T.; Álvarez-Martos, I.; García Alonso, F.J.; Costa-García, A. *Capillary Electrophoresis and Microchip Capillary Electrophoresis: Principles, Applications, and Limitations*, García, C.D.; Chumbimuni-Torres, K.Y.; Carrilho, E., Eds.; John Wiley & Sons, Inc, 2013; Chap. 6, p 95.
- (8) Barbier, V.; Viovy, J.-L. *Curr. Opin. Biotech.* **2003**, *14*, 51-57.
- (9) Salim, M.; McArthur, S.L.; Vaidyanathan, S.; Wright, P.C. *Mol. Biosyst.* **2011**, *7*, 101-115.
- (10) Wong, I.; Ho, C.-M. *Microfluid. Nanofluid.* **2009**, *7*, 291-306.
- (11) Álvarez-Martos, I.; Fernández-Abedul, M.T.; Anillo, A.; Fierro, J.L.G.; García Alonso, F.J.; Costa-García, A. *Anal. Chim. Acta* **2012**, *724*, 136-143.
- (12) Bhattarai, N.; Ramay, H.R.; Gunn, J.; Matsen, F.A.; Zhang, M. *J. Control. Release* **2005**, *103*, 609-624.
- (13) Le, N.C.H.; Gubala, V.; Gandhiraman, R.P.; Daniels, S.; Williams, D.E. *Langmuir* **2011**, *27*, 9043-9051.
- (14) DeRocher, J.P.; Mao, P.; Han, J.; Rubner, M.F.; Cohen, R.E. *Macromolecules* **2010**, *43*, 2430-2437.
- (15) Kitsara, M.; Ducrée, J. *J. Micromech. Microeng.* **2013**, *23*, 033001.
- (16) He, M.; Zeng, Y.; Jemere, A.B.; Harrison, D.J. *J. Chromatogr. A* **2012**, *1241*, 112-116.
- (17) Li, Z.; Zhang, K.; Ma, J.; Chong, C.; Wooley, K. L.; *J. Polym Sci A, Polym Chem*, **2009**, *47*, 5557-5563.
- (18) Belder, D.; Ludwig, M. *Electrophoresis* **2003**, *24*, 3595-3606.
- (19) Dolnik, V. *Electrophoresis* **2004**, *25*, 3589-3601.
- (20) Liu, C. *Adv. Mater.* **2007**, *19*, 3783-3790.
- (21) Abgrall, P.; Conedera, V.; Camon, H.; Gue, A.-M.; Nguyen, N.-T. *Electrophoresis* **2007**, *28*, 4539-4551.
- (22) del Campo, A.; Greiner, C. *J. Micromech. Microeng.* **2007**, *17*, R81-R95.
- (23) Kenawy, E.R. *Polym.-Plast. Technol. Eng.* **2001**, *40*, 437-450.
- (24) Jonsson, M.; Nyström, D.; Nordin, O.; Malmström, E. *Eur. Polym. J.* **2009**, *45*, 2374-2382.
- (25) Padeste, C.; Farquet, P.; Potzner, C.; Solak, H.H. *J. Biomat. Sci-Polym. E.* **2006**, *17*, 1285-1300.
- (26) Horák, D.; Rittich, B.; Španová, A. *J. Magn. Magn. Mater.* **2007**, *311*, 249-254.

- (27) Edmondson, S.; Huck, W.T.S. *Adv. Mater.* **2004**, *16*, 1327-1331.
- (28) Fukuda, T.; Kohara, N.; Onogi, Y.; Inagaki, H. *J. Appl. Polym. Sci.* **1991**, *43*, 2201-2205.
- (29) Soto-Cantu, E.; Lokitz, B.S.; Hinestrosa, J.P.; Deodhar, C.; Messman, J.M.; Ankner, J.F.; Kilbey, S.M. *Langmuir* **2011**, *27*, 5986-5996.
- (30) Yu, W.H.; Kang, E.T.; Neoh, K.G. *Langmuir* **2005**, *21*, 450-456.
- (31) Xu, F.J.; Cai, Q.J.; Li, Y.L.; Kang, E.T.; Neoh, K.G. *Biomacromolecules* **2005**, *6*, 1012-1020.
- (32) Bondar, Y.; Kim, H.J.; Yoon, S.H.; Lim, Y.J. *React. Funct. Polym.* **2004**, *58*, 43-51.
- (33) Xu, Y.; Yuan, J.; Müller, A.H.E. *Polymer* **2009**, *50*, 5933-5939.
- (34) Xu, F.J.; Zhu, Y.; Chai, M.Y.; Liu, F.S. *Acta Biomater.* **2011**, *7*, 3131-3140.
- (35) Xu, J.; Gleason, K.K. *Chem. Mater.* **2010**, *22*, 1732-1738.
- (36) Huang, J.; Li, X.; Zheng, Y.; Zhang, Y.; Zhao, R.; Gao, X.; Yan, H. *Macromol. Biosci.* **2008**, *8*, 508-515.
- (37) Huang, J.; Han, B.; Yue, W.; Yan, H. *J. Mater. Chem.* **2007**, *17*, 3812-3818.
- (38) Lin, D.J.; Lin, D.T.; Young, T.H.; Chen, T.C.; Chang, H.H.; Cheng, L.P. *J. Biomat. Sci-Polym. E.* **2009**, *20*, 1943-1959.
- (39) Edmondson, S.; Huck, W.T.S. *J. Mater. Chem.* **2004**, *14*, 730-734.
- (40) Anirudhan, T.S.; Jalajamony, S.; Divya, L. *Ind. Eng. Chem. Res.* **2009**, *48*, 2118-2124.
- (41) Comrie, J.E.; Huck, W.T.S. *Langmuir* **2007**, *23*, 1569-1576.
- (42) Sánchez, J.; Rivas, B. L.; Nazar, E.; Bryjak, M.; Kabay, N. *J. Appl. Polym. Sci.* **2013** DOI: 10.1002/APP38851
- (43) Qi, T.; Sonoda, A.; Makita, Y.; Kanoh, H.; Ooi, K.; Hirotsu, T. *Ind. Eng. Chem. Res.* **2002**, *41*, 133-138.
- (44) Wang, L.; Qi, T.; Gao, Z.; Zhang, Y.; Chu, J. *React. Funct. Polym.* **2007**, *67*, 202-209.
- (45) Samatya, S.; Kabay, N.; Tuncel, A. *React. Funct. Polym.* **2010**, *70*, 555-562.
- (46) Wei, Y.T.; Zheng, Y.M.; Chen, J.P. *J. Colloid Interf. Sci.* **2011**, *356*, 234-239.
- (47) Wei, Y.T.; Zheng, Y.M.; Chen, J.P. *Langmuir* **2011**, *27*, 6018-6025.
- (48) Benaglia, M.; Alberti, ; Giorgini, L.; Magnoni, F.; Tozzi, S. *Polym. Chem.* **2013**, *4*, 124-132.
- (49) McEwan, K. A.; Slavin, S.; Tunnah, E.; Haddleton, D. M. *Polym. Chem.*, **2013**, *4*, 2608-2614
- (50) Miyoshi, K.; Saito, K.; Shiraishi, T.; Sugo, T. *J. Membrane Sci.* **2005**, *264*, 97-103.
- (51) Iwanade, A.; Umeno, D.; Saito, K.; Sugo, T. *Biotechnol. Prog.* **2007**, *23*, 1425-1430.
- (52) Barbey, R.; Klok, H.A. *Langmuir* **2010**, *26*, 18219-18230.
- (53) Zillillah, Tan, G.W.; Li, Z. *Green Chem.* **2012**, *14*, 3077-3086.
- (54) Calabresi, P.; Mercuri, N.B.; Sancesario, G.; Bernardi, G. *Brain* **1993**, *116*, 433-452.
- (55) Jackowska, K.; Kryszynski, P. *Anal. Bioanal. Chem.* **2013**, *405*, 3753-3771.

- (56) Li, H.-F.; Cai, Z.W.; Lin, J.-M. *Anal. Chim. Acta* **2006**, *565*, 183-189.
- (57) Lapainis, T.; Sweedler, J.V. *J. Chromatogr. A* **2008**, *1184*, 144-158.
- (58) Zhao, J.; Zhang, Q.; Yang, H.; Tu, Y. *Biomicrofluidics* **2011**, *5*, 34104-341049.
- (59) Guan, Q.; Noblitt, S.D.; Henry, C.S. *Electrophoresis* **2012**, *33*, 2875-2883.
- (60) Liu, Y.; Fanguy, J.C.; Bledsoe, J.M.; Henry, C.S. *Anal. Chem.* **2000**, *72*, 5939-5944.
- (61) Wang, A.-J.; Feng, J.-J.; Dong, W.-J.; Lu, Y.-H.; Li, Z.-H.; Riekkola, M.-L. *J. Chromatogr. A* **2010**, *1217*, 5130-5136.
- (62) Faure, K.; Bias, M.; Yassine, O.; Delaunay, N.; Cretier, G.; Albert, M.; Rocca, J.L. *Electrophoresis* **2007**, *28*, 1668-1673.
- (63) Çelik, S.Ü.; Bozkurt, A. *Eur. Polym. J.* **2008**, *44*, 213-218.
- (64) Álvarez-Martos, I.; García Alonso, F.J.; Anillo, A.; Arias-Abrodo, P.; Gutiérrez-Álvarez, M.D.; Costa-García, A.; Fernández-Abedul, M.T. *Sensor. Actuat. B-Chem.* **2013**, *188*, 837-846.
- (65) Huang, X.; Gordon, M.J.; Zare, R.N. *Anal. Chem.* **1988**, *60*, 1837-1838.
- (66) Dearie, H.S.; Spikmans, V.; Smith, N.W.; Moffatt, F.; Wren, S.A.C.; Evans, K.P. *J. Chromatogr. A* **2001**, *929*, 123-131.
- (67) Dhal, P.K.; Babu, G.N.; Steigel, A. *Polymer* **1989**, *30*, 1530-1535.
- (68) Beguin, C.G.; Deschamps, M.N.; Boubel, V.; Delpuech, J.J. *Org. Magn. Reson.* **1978**, *11*, 418-423.
- (69) Zhao, Y.; Foo, S.W.; Saito, S. *Angew. Chem. Int. Ed.* **2011**, *50*, 3006-3009.
- (70) Espinosa, M.H.; del Toro, P.J.O.; Silva, D.Z. *Polymer* **2001**, *42*, 3393-3397.
- (71) Dasgupta, P.K.; Kar, S. *Anal. Chim. Acta* **1999**, *394*, 1-12.
- (72) Castaño-Álvarez, M.; Fernández-Abedul, M.T.; Costa-García, A.; Agirregabiria, M.; Fernández, L.J.; Ruano-López, J.M.; Barredo-Presa, B. *Talanta* **2009**, *80*, 24-30.
- (73) Vilela, D.; Garoz, J.; Colina, A.; González, M.C.; Escarpa, A. *Anal. Chem.* **2012**, *84*, 10838-10844.
- (74) Castaño-Álvarez, M.; PhD Thesis, University of Oviedo, 2008.
- (75) Lucy, C.A.; MacDonald, A.M.; Gulcev, M.D. *J. Chromatogr. A* **2008**, *1184*, 81-105.
- (76) Raman, V.I.; Palmese, G.R. *Macromolecules* **2005**, *38*, 6923-6930.
- (77) Yasui, T.; Kaji, N.; Mohamadi, M.R.; Okamoto, Y.; Tokeshi, M.; Horiike, Y.; Baba, Y. *ACSNano* **2011**, *5*, 7775-7780.
- (78) Jouyban, A.; Kenndler, E. *Electrophoresis* **2006**, *27*, 992-1005.
- (79) Persat, A.; Chambers, R.D.; Santiago, J.G. *Lab. Chip* **2009**, *9*, 2437-2453.
- (80) Zhao, J.; Zhang, Q.; Yang, H.; Tu, Y. *Biomicrofluidics* **2011**, *5*, 034104-034109.
- (81) Perlati, B.; Carrilho, E.; Aguiar, F.A. . In *Capillary Electrophoresis and Microchip Capillary Electrophoresis: Principles, Applications, and Limitations*, 1st ed.; García, C.D., Chumbimuni-Torres, K.Y., Carrilho, E., Eds.; John Wiley & Sons, Inc., 2013; Chap. 2, p 23.

CHAPTER 2: SENSITIVITY IMPROVEMENT

2.1 Background

2.2 Research & Development:

- ▣ **Article 4:** Manufacture of Carbon Microelectrodes by Laser Lithography for Electrochemical Detection.
 - ▣ **Article 5:** Electrochemical Properties of Spaghetti and Forest like Carbon Nanotubes Grown on Glass Substrates.
-

2.1. Background

Background

Another critical parameter involved in the achievement of a high throughput microchip electrophoresis is the development of a selective and sensitive integrated amperometric detection system. This is particularly important when target analytes require extremely low detection limits. Catecholamines belong to that kind of compounds (present in the sample at very low concentrations) with significant differences in their concentration ranges (micromolar to nanomolar) depending on the matrix (urine, blood, plasma ...) [115].

The **approaches to achieve improved sensitivities** could be classified in two main groups (i) improve the detectability by label conjugates or (ii) improve the electron transfer by acting on the transducer surface. In electrochemistry the most employed labels are enzymes, electroactive molecules and nanomaterials. However, the last ones provide some important advantages when they are compared with the other labels like higher stability and lower prices. Despite the fact that the first strategy is a very interesting approach, in this work we are going to emphasize the improvement of the electron transfer properties by changing the transducer properties employing nanomaterials.

Carbon-based materials have been widely used in electroanalysis due to their advantages such as low cost, chemical inertness, wide potential window (compared with metals), good electron transfer kinetics and low background currents. Its importance is evidenced also by the large number of carbon varieties usually employed in the design of electrochemical detectors (glassy carbon, pyrolytic graphite, carbon ink, carbon paste and carbon fiber). Thus, by combining the advantages of both carbon and nanomaterials, carbon-based nanomaterials represent a promising tool for improving sensitivity in electrochemistry. Focusing on carbon-based nanomaterials it should be said that during the last decade there has been an ongoing interest in carbon nanotubes, motivated mainly by their chemical compatibility with biomolecules at the same time that they possess a strong electrocatalytic activity for a wide range of compounds.

One of the mayor challenges for the preparation of **carbon nanotubes** based electrodes is how to incorporate them into the electrode. These preparation methods could be classified in two main groups:

¹ W.H.A. de Jong, E.G.E. de Vries, I.P. Kema. Clin. Biochem. 44 (2011) 95-103.

- The first and most commonly used is by **modifying conventional electrodes**, mainly by dispersion (obtained by mixing carbon nanotubes and solvents in absence or in presence of dispersing agents). However, it is difficult to obtain a homogeneous dispersion (especially in water), the chemical treatment required can degrade them and, solvents can change carbon nanotubes electrochemical behavior.
- For employing carbon nanotubes as electrode material is essential to preserve their properties. Thus, a second approach based on the **growth of carbon nanotubes on a solid substrate** was proposed. This strategy is particularly attractive because it can overcome dispersion problems and provide a good surface attachment.

On the other hand, the advantages of the electrochemical techniques are widely known but, one of the most prominent comes from its capability of miniaturization allowing an easy integration into microfluidic chips. Moreover, it offers extraordinary properties in micro- and nano- scales that arise from the electrode dimensions (in the range of tens of micrometers or below). At this scale, the mass transport and electron transfer kinetics at the electrode surface are significantly enhanced leading to reduced capacitive current (improving signal-to-noise ratios) and faster response times (allowing high spatial and temporal resolution). The only disadvantage of microelectrodes is the difficulty in measuring low currents. Nevertheless, this problem can be overcome by fabricating an array, so that current signals from multiple microelectrodes can be added together to make a large enough signal. If the individual electrodes are spaced enough from one another, the currents from each individual electrode are additive and non-interfering.

Therefore, the main objectives of this chapter could be summarized in:

- ▣ Design and fabrication of carbon ink microelectrode arrays with the aim of enhancing the electrochemical response compared with conventional carbon ink electrodes (**Article 4**).
- ▣ Improve these electrochemical properties by employing carbon-based nanomaterials, specially grown carbon nanotubes. Thus, this aim could be classified in two sub-objectives:
 - Investigate the electrochemical response of the grown carbon nanotubes (non-oriented and oriented) by cyclic voltammetry and

chronoamperometry in order to determine the growth conditions that lead to the best electrochemical and analytical features (**Article 5**). This study allows us to obtain a more detailed understanding of the surface behavior prior to employ it in an array configuration.

- Design and fabrication of grown carbon nanotubes array in order to achieve improved limits of detection compared with the ones obtained in large area electrodes, being capable to reach the ones required for catecholamines analysis.

This Chapter 2 contains one published paper (reformatted to a word file), and also a paper which is being considered for publication.

2.2. Research & Development

Article 4

*Manufacture of Carbon Microelectrodes by
Laser Lithography for Electrochemical Detection*

*J. Micro/Nanolith. MEMS MOEMS 10 (2011)
043013-1.*



Manufacture of Carbon Microelectrodes by Laser Lithography for Electrochemical Detection

Silvino Antuña^a, Adrián Fernández^a, Isabel Álvarez^b, M. Teresa Fernández^b, Agustín Costa^b, Miguel García^c, María Rodríguez^d, José Rodríguez^a

^a*Physics Department, University of Oviedo, Spain*

^b*Physical and Analytical Chemistry Department, University of Oviedo, Spain*

^c*ETH, Zürich, Switzerland*

^d*Energy Department, University of Oviedo, Spain*

ABSTRACT

Carbon microelectrodes have been implemented as sensing phases in order to improve the efficiency of the electrochemical sensing in capillary electrophoresis microchips. Surface and embedded carbon microelectrodes were fabricated on glassy substrates using a laser lithography technique. Both types of microelectrodes were successfully verified and, in the case of embedded microelectrodes, are proving to be an excellent alternative to increase the sensitivity of biosensors based on capillary electrophoresis.

1. Introduction

Miniaturization, automation, and simplification of analytical systems is a scientific challenge in constant development and has led to the emergence of so-called micrototal analysis systems (μ TAS) or lab-on-a-chip. It has been described that a large number of these systems, but probably the most popular today, are the capillary electrophoresis microchips. Initially, the laser-induced fluorescence [1] was the most used technique due to its high sensitivity and its simplicity to focus the laser in the microchannels. Nowadays, a new promising alternative is the electrochemical detection due to its high sensitivity, selectivity, inherent miniaturization, portability, low cost, and its compatibility with microfabrication techniques used in the microchips manufacturing process [2-4]. Amperometric detection, since its introduction in capillary electrophoresis microchips by Woolley et al. in 1998 [5], has been the most used method in electrochemical detection. In this line of work, it has been described as three configurations, depending on the position of the working electrodes, in order to use electrochemical detection with a capillary electrophoresis system [6,7]: “end-channel,” “in-channel,” and “off-channel.”

One important issue is the material used to build the electrode. There are a variety of possibilities from carbon in its different forms (fiber [8], paste [9], ink [10], glassy carbon [11], or diamond [12]) to metals (gold [13-15], platinum [16,17], copper, silver, or palladium [18,19]).

Carbon electrodes are widely used due to its low overpotential and noise, little surface poisoning, and wide range of potentials. The possibility of using carbon electrodes in different ways allows a greater versatility in terms of their integration into microchips. Currently, in general, the microchips can only get fully integrated as working electrodes if external auxiliary and reference electrodes are used with them. However, in order to approach the concept of μ TAS, all electrodes (working, reference, auxiliary, and voltage) should be fully integrated into the microchip without using external components.

Focused on improving the efficiency of electrochemical sensing in capillary electrophoresis microchips performed on vitreous, crystalline, and polymeric substrates, the possibility of designing, manufacturing, and evaluating a sensor phase consisting of carbon microelectrodes has been raised. Currently, in the framework of scientific collaboration with the Laboratory of Immuno-electroanalysis at University of Oviedo and the company MicruX Fluidic [20], we have initiated the design and manufacture of two configurations of carbon

microelectrodes [5]. The first is a configuration where the electrodes are located on the substrate surface (surface electrodes). In the second proposal, the electrodes are accommodated in the substrate itself (embedded electrodes). Both proposals require the prior manufacture of masks done by laser lithography. These masks contain the pattern of electrodes to implement which are transferred to a microchip via a photolithographic process. The carbon microelectrodes were tested in the Immulectroanalysis Laboratory at the University of Oviedo. In all cases, and especially the embedded configuration, the microelectrodes have shown an excellent behavior when they were used as a sensing phase.

2. Manufacturing Process

2.1. Mask Fabrication

To perform a more complete and comprehensive study, and in order to improve the quality of the microelectrodes, they have been fabricated and tested with various positive and negative photoresists in the manufacturing process. So, two masks with the pattern will be used, each one with each type of photoresist. We will denote our masks as positive and negative, according to the type of photoresist we have used.

The manufacturing process of the first of the masks, the positive mask, must be conducted through two different photolithographic processes that are outlined in **Fig. 1 (A)**. These processes are performed on a soda-lime substrate that has been cleaned in a clean room. In the second step, a 200 nm thick aluminum layer is deposited by evaporation (Emitech K950X). Then, a positive photoresist layer is deposited on the glass substrate by spin-coating (WS-400A-6NPP Laurell Technologies Corp). The sample is submitted to a photolithographic process, through a laser writing system depicted in **Fig. 1 (B)**. An Nd:yttrium–aluminum–garnet (YAG) laser working at $\lambda = 465$ nm is accompanied by a Fabry–Pérot interferometer to ensure horizontal movement of the micropositioning stages. A shutter allows starting and stopping the writing process in accordance with the geometry of the mask. All functions are controlled by a computer: the design of the geometry, dimensions of the mask, shutter on/off states, and micropositioning speed. With this equipment, an array of lines is written in the photoresist. **Fig. 2 (A)** shows an image of a mask with an array of 5 μm wide lines, spaced 15 μm . Currently, we are optimizing this photolithography process with different types of positive photoresists such as S1813, SPR220, or AZ4562.

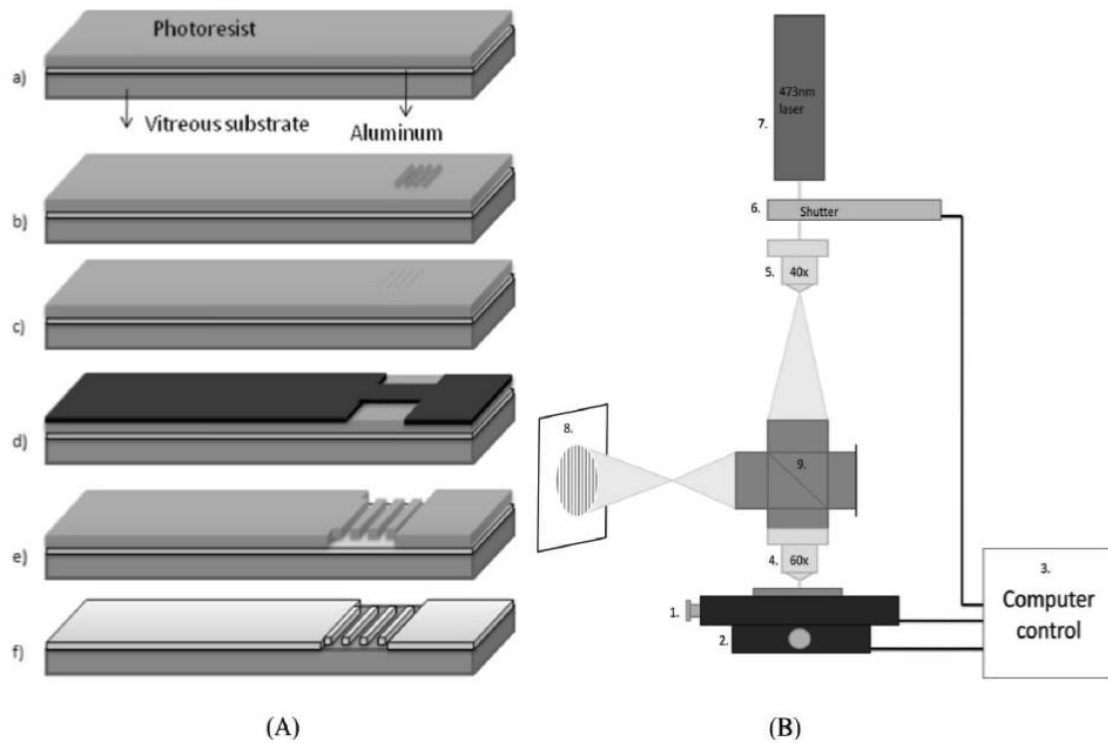


Figure 1. (A) Photolithographic process: a) Aluminium and photoresist deposition. b) Laser writing. c) First photoresist reveal. d) UV isolation through a film. e) Second reveal. f) Aluminium etching and photoresist elimination: final positive mask. (B) Laser writing system: 1) First micropositioner (x axis). 2) Second micropositioner (y axis). 3) Computer control. 4) 60× objective. 5) 40× objective. 6) Shutter. 7) Nd:YAG laser. 8) Interference pattern. 9) Fabry-Pérot interferometer.

Once the laser writing process is finished, the reveal of the photosensitized part is carried out. To implement the broad areas of connection on both ends of the sensing microelectrodes, a UV isolation through a film is performed and then revealed again. Finally, the sample is dipped in a solution of $\text{H}_3\text{PO}_4:\text{HCl}:\text{H}_2\text{O}$ (17:1:2). This solution attacks the aluminum selectively and the remaining photoresist is eliminated with acetone. **Fig. 2 (B)** shows an Al mask fabricated according with the described procedure.

This Al master mask will be used for the fabrication of a new mask which will be used to manufacture the microelectrodes with a negative photoresist.

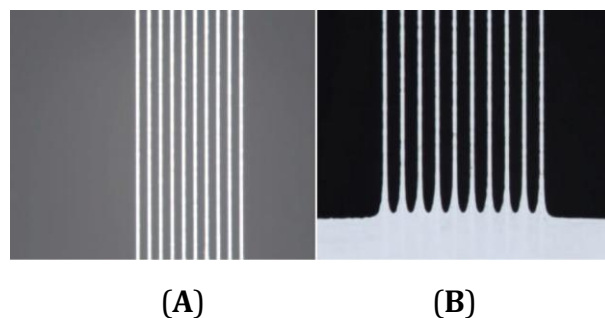


Figure 2. (A) Photograph of the upper side of the array of lines with a mask of 10 microchannels with a magnification of 200 \times . (B) Photograph of the final mask with a magnification of 200 \times .

Regarding with the negative masks, the manufacturing process is very similar to the one used for positive mask implementation. In this case, after cleaning a soda-lime glass in a clean room, a thin layer of aluminum (200 nm thickness) is also deposited by evaporation. By using the spin-coating technique, a layer of negative photoresist (AZ nLOF 2070 in this work) is deposited and a soft bake is performed. The substrate is exposed to UV sunlight and then a post-exposure bake is made for cross-linking the photoresist. This process causes the photoresist to be more stable and ready to be revealed. The last steps after development are similar to the previous case. The mask is dipped in a solution $\text{H}_3\text{PO}_4:\text{HCl}:\text{H}_2\text{O}$ (17:1:2) to attack the aluminum selectively and, finally, the photoresist is eliminated with acetone to leave the mask ready to be used.

2.2. Materials

For the production of all microelectrodes, we have used as a substrate a soda-lime glass, whose physical properties are well known [21]. For carbon deposition on the glass substrate, different materials and techniques have been tested and applied, such as a homogeneous mixture of phenolic resin and graphite, carbon rod evaporation, and a commercial carbon solution called Aquadag E [22] diluted in water.

Carbon microelectrodes have two crucial parameters to be good candidates to be used as a sensing phase [5] in capillary electrophoresis microchips. The first is low electrical resistance which is related to the signal obtained from the sensor. The second one is high grip on the substrate glassy surface which allows the reusability of the system.

During the study of the materials, we have developed and applied evaporation deposition techniques using carbon rods. This method has been proved to be ineffective due to the difficulty of depositing carbon layers thicker than 1 μm . These evaporated nanometric

layers show an extremely high electrical resistance and a very low grip on the substrate glassy surface, so they have been excluded from the study.

We found good results with the addition of small amounts of carbonaceous substances which can act as binders, in this case, mixing Aquadag and phenolic resin and doing cure cycles. After mixing the two components, the resulting substance was heated in a reducing atmosphere of N_2 , during 22 h at $550^\circ C$. This heat treatment not only dramatically improves the electric conductivity but also significantly increases the grip on the glass substrate. Highly promising carbon microelectrodes were obtained following the described procedure.

2.3. Microelectrodes

Both microelectrodes proposals are sketched in **Fig. 3**. The fabrication process begins with the deposition of the photoresist on the glass by spin-coating. As we will see in the results, a positive photoresist was chosen for surface microelectrodes and a negative photoresist was chosen for embedded microelectrodes. Next is the UV light exposure using the respective mask. It is performed in both cases to transfer the pattern of the microelectrodes. The development of the photosensitized photoresist is the next stage.

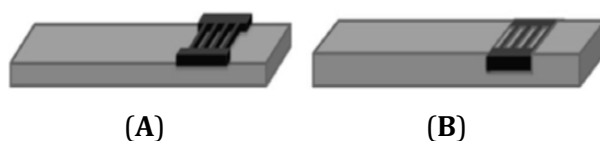


Figure 3. Carbon microelectrodes: (A) surface and (B) embedded.

Once the photoresist was revealed, we have two alternatives depending on the type of electrodes we want to implement: focusing on surface microelectrodes it is now time to inject the carbon on the revealed area. Once the carbon was injected, a lift-off process [23] is done to finish it.

Regarding with the embedded electrodes, and before injecting the carbon solution, a soda lime glass etching must be performed. For this purpose two different alternatives have been studied: the first of them, wet etching [24], is a technique which is already optimized in our laboratory [16], and the other one, dry etching [25], is a process which requires a reactive ion etching system. It is currently being developed by the authors. Finally, carbon is deposited and, in the last step, a surface polishing is performed in the sample.

3. Results

3.1. Surface Microelectrodes

The best results of manufacturing surface microelectrodes have been obtained with evaporation of carbon rods. **Fig. 4** shows one of the tests for this design. An intensive labwork was done to optimize the manufacturing process of this type of microelectrode in order to achieve a minimum width of 10 μm arrays. However, as stated before, this method was discarded due to not getting a sufficient grip on the glass and a low electrical resistance.

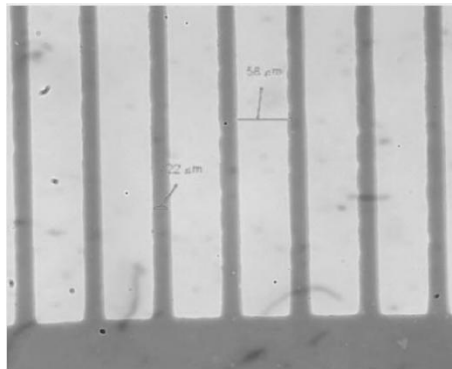


Figure 4. Photograph (top view) of the surface microelectrode with a magnification of 200 \times .

Good results with superficial carbon microelectrodes have been achieved when a negative photoresist was used. When the carbon solution Aquadag E was deposited by brushing to build these microelectrodes, lower electrical resistance microelectrodes have been achieved. However, when they were tested as a sensing phase, the results were not successful due to the fact that the microelectrodes show a weak grip to the surface.

3.2. Embedded microelectrodes

The first task in these microelectrodes was the glass etching. **Fig. 5 (A)** shows the geometry of the array of lines etched into the glass by wet etching. The complete array has been measured with a profilometer. **Fig. 5 (B)** shows a top view of the microelectrode before filling it. The second task was how to fill the microelectrodes. Taking into account the study done with surface microelectrodes, carbon evaporation was discarded. Injection of carbon dissolution with a brush was the chosen method. In the first test, made with positive photoresist, these types of microelectrodes were very irregular. When they were tested, they failed due to the fact that the microelectrodes show a huge electrical resistance (about tens of $\text{k}\Omega$) for being a sensor phase.

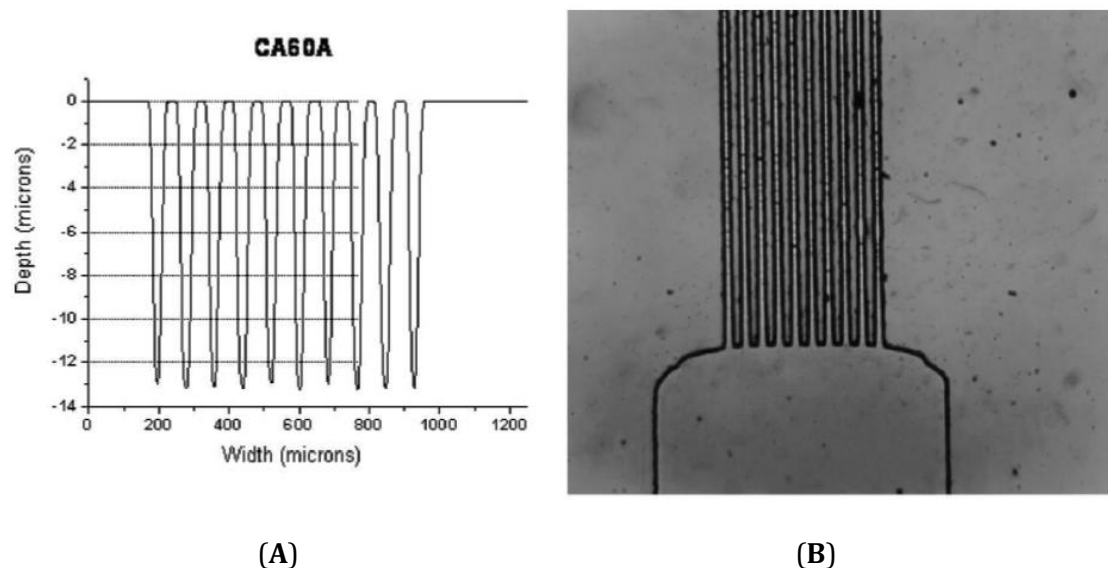


Figure 5. (A) Measurements of the array of lines etched in glass obtained with a profilometer. (B) Photography (top view) of the etching glass with a 40 \times magnification.

Recently, much better results were obtained when using a negative photoresist. **Fig. 6** shows two photographs of the top view of two carbon microelectrodes whose manufacturing process has been completed. These microelectrodes have more regular channels which let us achieve narrower channels. Its electrical resistance has been reduced to a few hundred ohms by the study of a carbon curing cycle. These latest prototypes of microelectrodes have been tested by the Immunoanalysis Laboratory to check their quality and efficiency. The results have been positive and they are shown in **Fig. 7**.

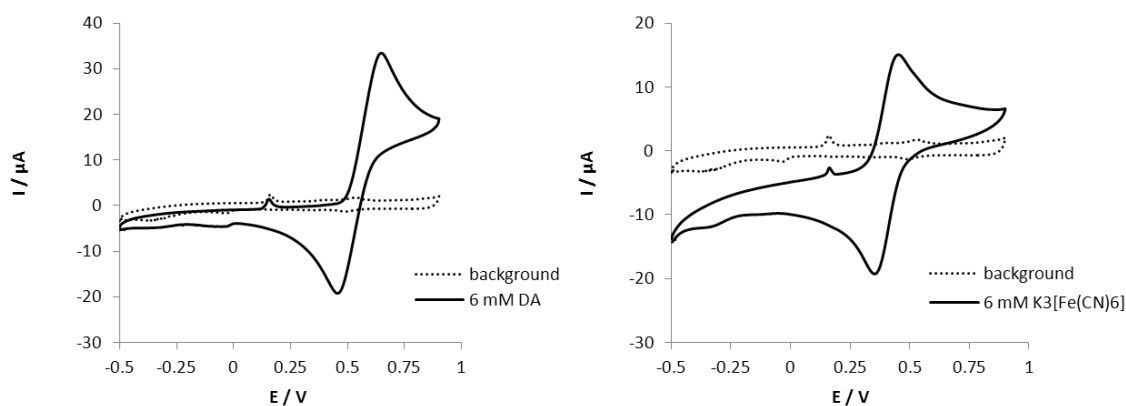


Figure 7. Cyclic Voltammograms obtained in a carbon microelectrode array for dopamine and potassium ferricyanide with a scan rate of 0.025 Vs^{-1} .

From the cyclic voltammograms display in **Fig. 7**, we can see that carbon embedded microelectrodes designed and manufactured in our laboratory show good performance as a sensor with an excellent reproducibility between drops (**Fig. 8**).

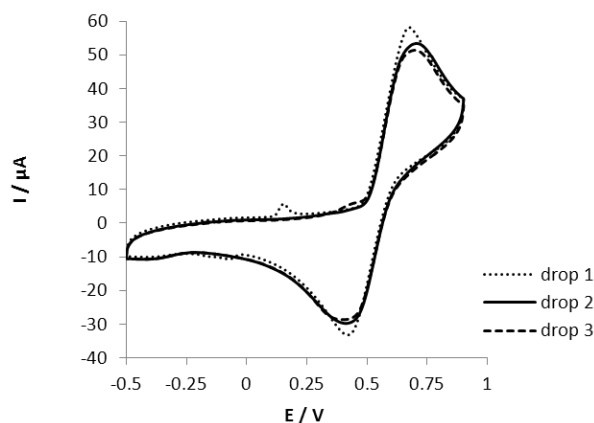


Figure 8. *Reproducibility inter-drop. Cyclic Voltammograms obtained for dopamine with a scan rate of 0.1 Vs^{-1} .*

4. Conclusions

A laser lithography technique was implemented and applied for manufacturing integrated carbon microelectrodes as a sensing stage in capillary electrophoresis microchips. Surface and embedded microelectrodes for electrochemical sensing were fabricated and investigated. The best results were obtained with embedded microelectrodes in a sodalim glass and by using the negative photoresist AZ nLOF 207 during the laser lithography process. Carbon dissolution Aquadag E with distilled water (1:1) with 1% of phenolic resist are the materials with which the carbon microelectrodes show the best performance. Carbon deposited by using brushing techniques and cured at 300°C offers the best solution. The carbon microelectrodes have been tested and have shown their functionality as a sensing phase. These microelectrodes are currently under active development in order to improve their sensing properties. Further improvements are focused in achieving a better grip to the substrate. To achieve that goal, new carbon solutions are under study as well as deposition techniques of carbon nanotubes. To date, the first tests have shown good behavior.

Acknowledgments

This work was supported by Grant BP09-007 "Severo Ochoa" from FICYT (Principado de Asturias, Spain) and MICINN (AP2008-04451).

REFERENCES

- [1] M. E. Johnson and J. P. Landers, "Fundamentals and practice for ultrasensitive laser-induced fluorescence detection in microanalytical systems," *Electrophoresis* 25, 3513–3527 (2004).
- [2] M. Pumera, A. Merkoci, and S. Alegret, "New materials for electrochemical sensing VII. Microfluidic chip platforms," *Trends Anal. Chem.* 25, 219–235 (2006).
- [3] J. Wang, "Electrochemical detection for capillary electrophoresis microchips: A review," *Electroanalysis* 17, 1133–1140 (2005).
- [4] F. M. Matysik, "Miniaturization of electroanalytical systems," *Anal. Bioanal. Chem.* 375(1), 33–35 (2003).
- [5] A. T. Woolley, K. Lao, A. N. Glazer, and R. A. Mathies, "Capillary electrophoresis chips with integrated electrochemical detection," *Anal. Chem.* 70(4), 684–688 (1998).
- [6] W. R. Vandaveer IV, S. A. Pasas, R. S. Martin, and S. M. Lunte, "Recent developments in amperometric detection for microchip capillary electrophoresis," *Electrophoresis* 23, 3667–3677 (2002).
- [7] W. R. Vandaveer IV, S. A. Pasas-Farmer, D. J. Fischer, C. N. Frankenfeld, and S. M. Lunte, "Recent developments in electrochemical detection for microchip capillary electrophoresis," *Electrophoresis* 25, 3528–3549 (2004).
- [8] D. M. Osbourn and C. E. Lunte, "On-column electrochemical detection for microchip capillary electrophoresis," *Anal. Chem.* 75, 2710–2714 (2003).
- [9] R. S. Martin, A. J. Gawron, B. A. Fogarty, F. B. Regan, E. Dempsey, and S. M. Lunte, "Carbon paste-based electrochemical detectors for microchip capillary electrophoresis/electrochemistry," *Analyst* 126, 277–280 (2001).
- [10] T.-K. Lim, H. Ohta, and T. Matsunaga, "Microfabricated on-chip-type electrochemical flow immunoassay system for the detection of histamine released in whole blood samples," *Anal. Chem.* 75, 3316–3321 (2003).
- [11] J. Wang, G. Chen, A. Mick, Jr., D. Shin, and A. Fujishima, "Microchip capillary electrophoresis with a boron-doped diamond electrode for rapid separation and detection of purines," *J. Chromatogr. A* 1022, 207–212 (2004).
- [12] G. Chen and J. Wang, "Fast and simple sample introduction for capillary electrophoresis microsystems," *Analyst* 129, 507–511 (2004).
- [13] C. D. Garcia and C. S. Henry, "Direct detection of renal function markers using microchip CE with pulsed electrochemical detection," *Analyst* 129, 579–584 (2004).
- [14] C. D. Garcia and C. S. Henry, "Enhanced determination of glucose by microchip electrophoresis with pulsed amperometric detection," *Anal. Chim. Acta.* 508, 1–9 (2004).
- [15] M. Castaño-Álvarez, M. T. Fernández-Abedul, and A. Costa-García, "Electroactive intercalators for DNA analysis on microchip electrophoresis," *Electrophoresis* 28, 4679–4689 (2007).

- [16] M. Castaño-Álvarez, M. T. Fernández-Abedul, and A. Costa-García, “Poly(methylmethacrylate) and Topas capillary electrophoresis microchips performance with electrochemical detection,” *Electrophoresis* 26, 3160–3168 (2005).
- [17] N. A. Lacher, S.M. Lunte, and R. S.Martin, “Development of a microfabricated palladium decoupler/electrochemical detector for microchip capillary electrophoresis using a hybrid glass/poly(dimethylsiloxane) device,” *Anal. Chem.* 76, 2482–2491 (2004).
- [18] R. Wilke and S. Büttgenbach, “A micromachined capillary electrophoresis chip with fully integrated electrodes for separation and electrochemical detection,” *Biosens. Bioelectron.* 19, 149–153 (2003).
- [19] J. Wang, G. Chen, M. P. Chatrathi, and M. Musameh, “CE microchips with carbon-nanotube electrochemical detectors,” *Anal. Chem.* 76, 298–302 (2004).
- [20] <http://www.micruxfluidic.com>.
- [21] R. A. Synowickilow, B. D. Johsa, and A. C.Martina, “Optical properties of soda-lime float glass from spectroscopic ellipsometry,” *Thin Solid Films* 519(9), 2907–2913 (2011).
- [22] <http://www.laddresearch.com/tds/60785tds.pdf>.
- [23] X. Xia, H. Yang, Yi. Sun, Z. Wang, L. Wang, Z. Cui, and C. Gu, “Fabrication of terahertz metamaterials using S1813/LOR stack by liftoff,” *Microelectron. Eng.* 85, 1433–1436 (2008).
- [24] M. Castaño-Álvarez, D. F. Pozo Ayuso, M. García Granda, M. Teresa Fernández-Abedul, J. Rodríguez, and A. Costa-García, “Critical points in the fabrication of microfluidic devices on glass substrates,” *Sens. Actuators B* 130(1), 436–448 (2008).
- [25] J. H. Park, N.-E. Lee, J. Lee, J. S. Park, and H. D. Park, “Deep dry etching of borosilicate glass using SF₆ and SF₆/Ar inductively coupled plasmas,” *Microelectron. Eng.* 82, 119–128 (2005).

Article 5

*Electrochemical Properties of Spaghetti and
Forest like Carbon Nanotubes Grown on Glass
Substrates*

(considering for publication)



Considering for Publication



Electrochemical Properties of Spaghetti and Forest like Carbon Nanotubes Grown on Glass Substrates

Isabel Álvarez-Martos^a, Adrián Fernández-Gavela^b, Jose Rodríguez-García^b, Nuria Campos-Alfaraz^c, A. Belén García-Delgado^c, David Gómez-Plaza^c, Agustín Costa-García^a, M. Teresa Fernández-Abedul^{*a}

^a*Departamento de Química Física y Analítica, Universidad de Oviedo, Asturias, Spain*

^b*Departamentode Física, Universidad de Oviedo, Asturias, Spain*

^d*Energy area, ITMA materials technology*

ABSTRACT

Carbon nanotubes (CNTs) have been widely used in many fields of chemical analysis to achieve more sensitive detection systems. In this work, we performed fundamental studies on grown or bottom-up fabricated MWCNTs (both non-oriented and oriented configurations), showing how variables like orientation, density, underlayer deposition, or synthesis time strongly determine their behavior (physical, electrochemical and analytical) as transducers. The electrochemical performance of these surfaces was demonstrated by cyclic voltammetry and chronoamperometry of dopamine (DA) solutions in 0.1 M H₂SO₄. The carbon nanotubes surfaces pre-treated with 1 M HNO₃ lead to increased signals, sensitivity and enhanced limits of detection (LOD). The grown working electrodes (WE) were reproducible and stable over the time. The peak variations gave RSD values of 8, 4 and 3% for high-density spaghetti-like and ITO or Al underlayered forest-like MWCNTs grown for 30 min, respectively. This study highlighted the importance of controlling the synthesis variables to achieve better analytical parameters.

1. Introduction

Nowadays there is a strong demand in many fields of chemical analysis to produce highly selective and sensitive detection systems [1]. As a consequence of their large surface-to-volume ratios, nano-structured materials have been widely used to favor electron transfer processes, resulting in improved sensitivities [2]. Special attention deserves carbon-based materials and particularly carbon nanotubes (CNTs) [3]. They have been the focus of intensive research due to their unique properties [4] and particularly their strong electrocatalytic activity, which makes carbon nanotubes extremely attractive for developing highly sensitive electrode surfaces [5-7].

Carbon nanotubes have often been integrated onto electrode surfaces as modifiers [8-11], frequently by random dispersions obtained by mixing them with solvents in absence or in presence of dispersing agents [12-15]. However, it is difficult to obtain a homogeneous dispersion (especially in water) [12] and the chemical treatment required to obtain it can degrade them. To use carbon nanotubes as electrode material is essential to preserve and take advantage of their properties [16]. With this aim, several efforts have been focused on increasing the control over nanotubes distribution, not only by modification of the electrode surface [17,18] but also by direct growth from the substrate [19-21]. This latter strategy is particularly attractive because it can overcome problems related with the dispersion process and provide a good surface attachment. The grown carbon nanotubes can be classified in two main groups: non-oriented (spaghetti-like or disordered) and oriented (forest-like or vertically-aligned carbon nanotubes, VACNTs) [22] and they have been grown not only onto metallic [19,23,24] and carbon [5,25,26] materials, but also on surfaces electrically isolated, such as silicon [27].

Many synthesis techniques have been described in the literature [20,28] in order to obtain low cost processes with high control over the structure, orientation and length of the produced CNTs. However, the most critical parameter in the resulting CNTs and thus, in their properties, is the choice of an adequate catalyst. They usually are transition metals [29,30] or bimetallic alloys, which improve the performance of classical catalysts [30-32].

The effective integration of a suitable and sensitive detection is one of the most important tasks in the development of miniaturized analytical devices, such as those named lab-on-a-chip. Electrochemical detection and grown CNTs, which follow a bottom-up fabrication scheme, have demonstrated to be a very convenient and promising alternative to

conventional solid electrodes. They can be directly integrated in miniaturized devices and their dimensions are easily controlled, showing the convenience of this approach for electrode manufacture. Surfaces with very different properties can be achieved only with slightly variations of CNTs synthesis procedure [33]. Therefore for a specific application a careful choice of the nanomaterial has to be made in order to obtain those with desired properties.

In this work we report and discuss about the influence of the orientation, density, underlayer deposition, or CVD reaction time on the grown CNTs properties (physical, electrochemical and analytical). The effect of these parameters was investigated by voltammetric and chronoamperometric measurements and dopamine (DA), an important catecholamine which is involved in Parkinson's and Alzheimer's diseases, was employed as electroactive redox molecule considering that it is easily converted to quinone by electrochemical oxidation. The carbon nanotubes electrodes were fabricated on glass substrates by means of chemical vapor deposition (CVD) and their performance has been compared to this presented on those conventional screen-printed carbon electrodes (SPCEs). Precision and surface stability over time have also been checked.

2. Materials and Methods

2.1. Growth of MWCNTs by Chemical Vapor Deposition (CVD)

Multiwall carbon nanotubes (MWCNTs) were grown by means of CVD in a commercial reactor (ET3000, FirstNano, CVD Equipment Corp., U.S.A.) onto Corning-glass substrates (Corning Inc., U.S.A.). With this purpose substrates were placed in a quartz tube at atmospheric pressure inside the furnace, in which the process gases (argon, hydrogen, and ethylene) were introduced in a controlled way.

For spaghetti-like MWCNTs synthesis, 40 mg of iron nitrate (Iron (III) nitrate monohydrate, 98%, Aldrich), 30 mg of alumina (Aeroxide Alu C, Evonik) and 3 mg of a molybdenum salt (Bis(acetylacetonato)-dioxomolybdenum (VI), Aldrich) were added in 30 ml of methanol, which is used to form a suspension and allow catalyst deposition. After sonication, the so-prepared liquid catalyst was spin-coated on the substrates at 2500 rpm for 30 s. Finally, the wafers were baked in an oven at 100 °C for 30 min, evaporating methanol and fixing the catalyst to the surface.

On the other hand, forest-like CNTs were grown from a Fe thin-film (5 nm) thermally evaporated in a Pfeiffer system (Classic 500) under high vacuum conditions (10-5 mbar). The

same procedure was followed for underlayered substrates (Fe/ITO and Fe/Al), in this cases a thin layer of ITO (200 nm) or Al (5 nm) was deposited onto Corning glass surfaces prior to catalyst deposition.

After catalyst deposition substrates were first annealed at 600 °C for 15 min under hydrogen atmosphere, generating Fe nanoparticles in both kinds of samples, and then hydrogen, argon and ethylene were flowed through the reactor chamber at a 1/1.6/0.3 rate. Finally, MWCNTs were grown at 750 °C for 30 min and the substrates were cooled to room temperature under an Ar flow of 0.3 slpm, obtaining both desired spaghetti and forest-like configurations on glass wafers.

2.2. Electrochemical measurements

Surfaces were electrochemically characterized by cyclic voltammetry and chronoamperometry.

Cyclic voltammetry was performed using a three-electrode configuration (working, reference and auxiliary), in which an Autolab PGSTAT 10 (ECO Chemie, The Netherlands) bipotentiostat was controlled by Autolab GPES 4.9 version for Windows 98. The grown MWCNTs (spaghetti and forest) surfaces were used as working electrodes (WE), Ag/AgCl as reference electrode (RE), and a Pt wire as auxiliary electrode (AE) (**Fig. in supplementary data**). The working area was delimited with an adhesive tape of 3 mm in diameter; notice that no leakage is produced between the tape and substrate, ensuring that there is no area fluctuation between electrodes. Cyclic voltammetry measurements were performed between 0 and 1.1 V at a scan rate of 100 mV s⁻¹. Screen-printed carbon electrodes (SPCE, Dropsens, Oviedo, Spain) were previously modified by 5 μL of 0.1 mg mL⁻¹ MWCNTs dispersion in DMF/H₂O [34].

Chronoamperometry were carried out with the same software and computer. Measurements of the anodic current at constant potential (+ 0.7 V) were recorded for 100 s.

3. Results and Discussion

3.1. CNTs Growth Procedure

The choice of an adequate substrate on which CNTs are going to be grown is one important parameter. It provides a solid foundation and must be able to inhibit the catalyst particles mobility [iError! Marcador no definido.]. Therefore, for the development of this work glass wafers were chosen as an ideal candidate due to their large area capability, robustness and low cost [35], particularly Corning-glass. This type of glass provides an upper limit of serviceability, as it is capable of withstanding higher temperatures (890 °C) than other glasses like soda-lime (473 °C) or borosilicate (521 °C). **Fig. 1** shows a schematic diagram of the procedures followed in MWCNTs growth (details regarding with the CVD process are described in the Methods section).

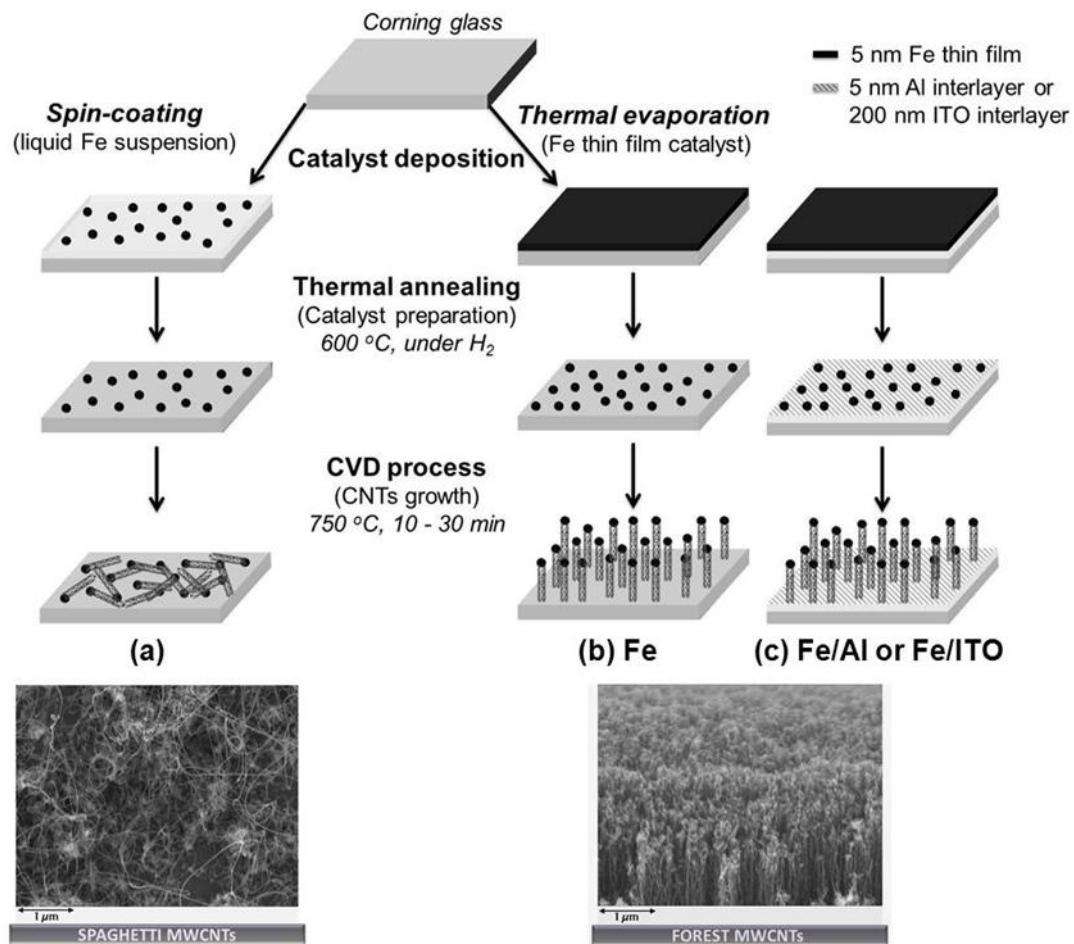


Figure 1. Scheme of the CVD process employed for CNTs growth. Spaghetti (a) and forest: without (b) or with Al (c) or ITO (d) underlayers. FE-SEM micrographs of the resulting working electrode surfaces.

In this work, MWCNTs with different orientation (spaghetti and forest) have been grown with the assistance of two kinds of iron catalyst (liquid solution or sputtered thin-film). It is widely accepted that Fe and their compounds show the highest catalytic activity when compared to other transition metals [36]. For the spaghetti configuration (**Fig. 1a**), the liquid catalyst was prepared in methanol by suspension of iron nitrate (Fe acting as catalyst after undergoing a thermal treatment), alumina (catalyst seeds support), and a molybdenum salt (growth promoter). The resulting suspension was then deposited on the substrate by means of spin-coating. Finally, methanol was evaporated and the catalyst was fixed to the surface by baking the samples in an oven at 100 °C for 30 minutes. For forest the configuration a Fe thin film (5 nm) catalyst was obtained by thermal evaporation (**Fig. 1b**). In both cases after the CVD process, MWCNTs morphology was examined by field emission scanning electron microscopy (FE-SEM). From the micrographs it can be concluded that well-aligned forest-like MWCNTs of approximately 100 μm in height and homogeneous diameters comprised between 10 and 15 nm had been obtained.

The first measures made on bare surfaces show significantly lower signals for spaghetti configuration than for forest one (**Fig. 2**). In view of these results, it was decided to increase the spaghetti-like MWCNTs density on the surface. Thus, catalyst suspension was deposited onto substrates by means of drop-casting, obtaining (after the CVD process) high-density spaghetti carbon nanotubes. On the other hand and concerning the forest configuration, Fe catalyzed MWCNTs were not stable with time and after several measures no signal was observed. To overcome this problem and improve forest-like carbon nanotubes adhesion to the substrate, a thin film underlayer of 5 nm Al or 200 nm indium-tin-oxide (ITO) [37-39], which isolate glass from the active catalyst, was deposited onto glass wafer prior to Fe thermal evaporation (**Fig. 1c**). The catalyst was then deposited, and wafers were introduced into a CVD system where MWCNTs were grown under the same experimental conditions. One of the reasons that could explain the improved adhesion is that Fe nanoparticles become embedded in the underlayer during the CNTs growth procedure, which leads to high number of nucleation centers and a strong interaction amidst Fe nanoparticles-underlayer-CNTs [40].

3.2. CNTs Electrochemical Characterization

To investigate whether grown MWCNTs could improve the electron transfer process, and evaluate the influence of the configuration (non-oriented or oriented) and thickness in the electrochemical signal, cyclic voltammetry (CV) was employed. This technique is an effective and valuable tool widely used to study surfaces electrochemical properties [41-43]. In addition,

DA was chosen as electrochemical specie and model system for the development of this work because it is an electrochemically active molecule, which has been widespread used in fundamental electrochemical studies [44]. On the other hand, dopamine is also known for its relationship with neurological disorders, such as Schizophrenia, Parkinson's disease, and drugs addiction [45].

3.2.1. Electrochemical Processes

First, the electrochemical behavior of bare MWCNTs surfaces was checked by cyclic voltammetry. It should be pointed out that working electrodes showed well-defined DA anodic and cathodic peaks, with potential values almost equal regardless of the electrode (E_{pa} 0.65 ± 0.07 V and E_{pc} 0.43 ± 0.07 V as an average for all surfaces, except for Fe catalyzed without underlayer whose particular behavior is detailed at the end of this section). At the same time they show good intra-day and inter-day reproducibility, with relative standard deviations (RSD) lower than 3, 6 and 7 % for intra-well (same electrode different DA drops), inter-well (same DA solution different electrodes) and inter-day (same electrode different days) respectively. Noteworthy is that the capacitive current observed at forest MWCNTs was significantly smaller than the spaghetti ones.

Working electrode surfaces can be grouped in function of the reversibility of the CV process. Thus, the peak potential separation ($\Delta E = E_{pa} - E_{pc}$) found for spaghetti and Fe/Al forest-like MWCNTs (0.17 ± 0.03 V) was greater than the value of 0.030 V (0.059 V / $2e^-$) expected for a reversible system, suggesting a quasi-reversible DA redox process. Even though, the Fe catalyzed forest MWCNTs without underlayer, showed a reversible process ($\Delta E = 0.02$ V), suggesting that the electron transfer reaction is more favorable than for the other surfaces. And, the higher irreversibility was for Fe/ITO surfaces ($\Delta E = 0.44$ V).

On the other hand, the anodic peak current (I_{pa}) was proportional to the square root of the scan rate in the range 10-200 mV s^{-1} (data not shown) thus confirming that the electrochemical process was diffusion-controlled.

Anodic peak intensities of 1 mM DA solution in 0.1 M H_2SO_4 are compared in **Fig. 2**. The electrochemical response of MWCNTs grown in both configurations was compared against conventional SPCEs modified with MWCNTs-COOH (MWCNTs-COOH SPCE), which have been widely employed in the literature to enhance electrochemical signals [5].

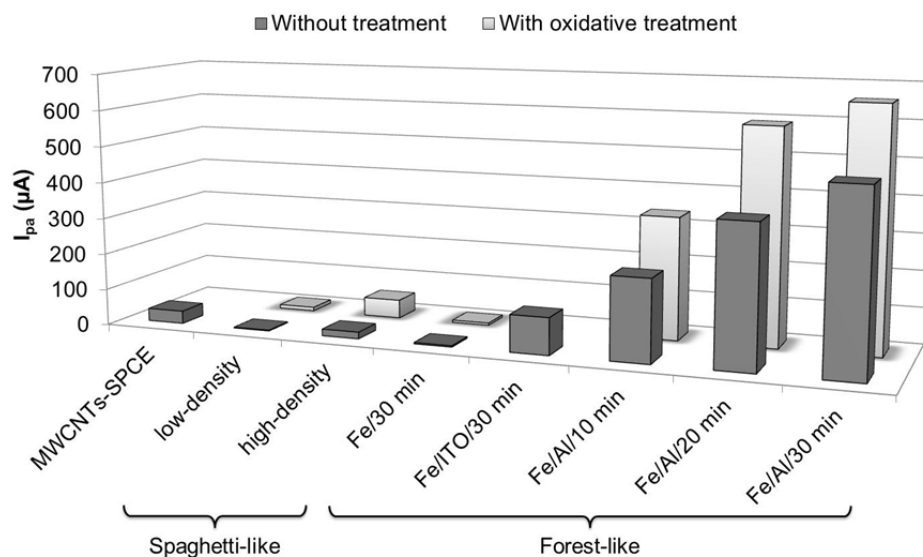


Figure 2. Anodic peak currents obtained from Cyclic Voltammetry measurements of 1 mM DA in 0.1 M H_2SO_4 recorded between 0 and 1.1 V for bare surfaces and treated with 1M HNO_3 . MWCNTs-COOH SPCE is included for comparison.

For spaghetti-like MWCNTs as working electrode, peaks were notoriously higher with increasing amounts of catalyst (1.97 ± 0.06 and $18.4 \pm 0.3 \mu A$ for low and high density respectively). While non-oriented configuration (both low and high density) provides lower peak intensities than MWCNTs-COOH SPCEs ($29 \pm 2 \mu A$) the opposite is true for oriented configuration, indicating an increase in their electroactive area. In this case and for the same CVD reaction times (30 min) the presence of an underlayer (ITO or Al) in the growth procedure results in much higher peak currents (101 ± 2 and $489 \pm 36 \mu A$ for Fe/ITO and Fe/Al respectively) than that obtained for Fe/30 forest MWCNTs catalyzed without underlayer ($3.3 \pm 0.4 \mu A$).

A particular mention deserves the electrochemical behavior of Fe/30 min forest MWCNTs as working electrodes. As shows **Fig. 3**, the cyclic voltammograms recorded on this surface exhibit a mixture of two electrochemical processes, adsorption and diffusion. When the measures were performed in three different days (with the dry electrode stored in a Petri dish between each measure) the adsorption process decreased with time, while the diffusion process increased. This could be explained for the higher MWCNTs hydrophilicity, caused by successive voltammetric measures, giving priority to the diffusion process. Anyway, this surface was not stable with time and gave a mixture of electrochemical processes thus it is not suitable for using as WE. This means that the choice of an adequate underlayer is extremely important, since it is going to influence surface stability and electrochemical properties. Another decisive parameter is the orientation (**Fig. 2**), achieving the higher DA signals on

underlayered forest MWCNTs. This effect has been explained in the bibliography as a consequence of the abnormally fast electron transfer at the end of the tube compared with side walls [46].

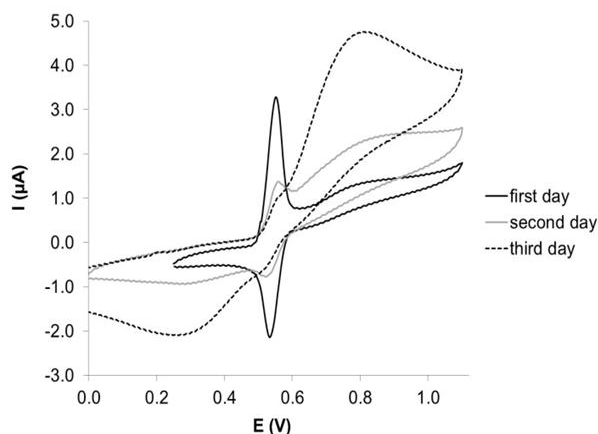


Figure 3. Cyclic Voltammograms of 1 mM DA in 0.1 M H_2SO_4 ($100\text{ mV}\cdot\text{s}^{-1}$) for Fe/30 min forest-like CNTs working electrode surface in three consecutive days.

3.2.2. Oxidative Pretreatment

Through the literature it has been reported that oxidative treatments with oxidizing agents like nitric acid are capable of changing both MWCNTs physical and chemical properties [47,48], which results in more hydrophilic surfaces and more efficient oxidation processes [49]. To determine if an oxidative treatment is capable of creating changes in both grown spaghetti and forest MWCNTs electrochemical properties, they were electrochemically treated with 1 M HNO_3 by 10 successive scans between -1.0 and 1.2 V potential window.

As it is illustrated in **Fig. 2**, the performance of spaghetti-like and Fe/Al forest-like surfaces improved with the oxidative treatment. In case of spaghetti-like, peak intensity increases from 1.97 ± 0.06 to 9.68 ± 0.03 μA for low density MWCNTs and from 18.4 ± 0.3 to 51 ± 6 μA for high density MWCNTs. This behavior could be explained by the fact that the carbon nanotube surface has initially high hydrophobicity, which avoids good contact between working electrode surface and DA drop. The oxidative treatment improves this contact, which favored DA oxidation and provides enhanced signals. Another remarkable fact is that when the oxidative treatment is performed on high-density spaghetti MWCNTs, resulting DA current is higher when compared with conventional modified screen printed carbon electrode (COOH functionalized MWCNTs-SPCE).

It should be emphasized that the highest DA oxidation signal was achieved on pre-oxidized Fe/Al/30 min forest-like MWCNTs, improving from 490 ± 36 for the bare electrode to $660 \pm 15 \mu\text{A}$ for the pretreated one. In spite of changes in peak currents, E_p remains almost constant ($0.66 \pm 0.07 \text{ V}$) for all surfaces. It should be said that this treatment was not possible to be performed on Fe/ITO/30 min forest MWCNTs owing to a detachment of the surface.

An increase in the background currents when the oxidative treatment is employed should be also commented. One of the reasons that might explain this behavior is that the capacitive current depends directly on the WE effective area. With the oxidative treatment defects in the CNTs structure are created and, consequently the effective area increases.

3.2.3. CNTs Density

As has been seeing Fe/Al/30 min forest-like MWCNTs provide the highest peak intensity thus a complementary experiment was conducted, in which the electrode response as a function of CNTs density was evaluated. **Fig. 4** shows the effect that the CVD reaction time (10, 20 and 30 min) has on the recorded cyclic voltammograms.

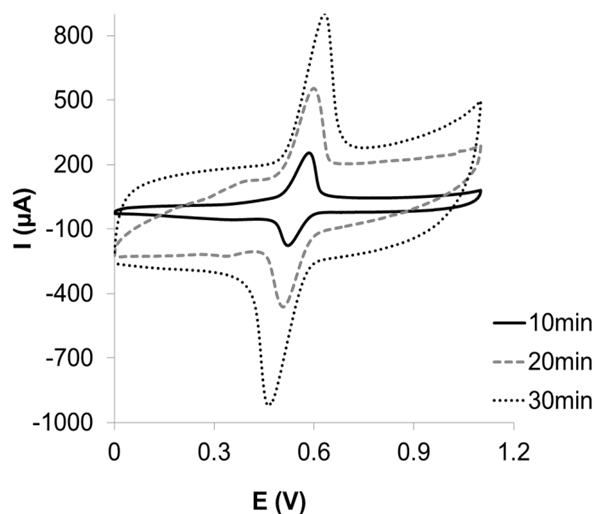


Figure 4. Cyclic Voltammograms of 1 mM DA in 0.1 M H_2SO_4 ($100 \text{ mV}\cdot\text{s}^{-1}$) for Fe/Al forest-like CNTs working electrode surfaces with different CVD reaction times.

In this case, a proportional increase of both DA anodic and cathodic peak currents with increasing reaction time (from 223 ± 6 to $490 \pm 36 \mu\text{A}$ and from 140 ± 16 to $571 \pm 7 \mu\text{A}$ for anodic and cathodic signals respectively) was observed, suggesting that peak current increases with MWCNTs density. However, this increase in MWCNTs density induces DA adsorption on the WE surface (**Fig. 5**), which could be avoided after an oxidative treatment like the one described in the previous section.

This figure exhibits as an example the procedure followed to avoid the DA adsorption on working electrodes. It has to be noticed that between measures, the surface was washed first with Milli-Q H₂O and then with two drops of the solution that is going to be measured later. This figure also displays the cyclic voltammograms corresponding to Fe/Al/20 min MWCNTs backgrounds (0.1M H₂SO₄) obtained before and after DA measures, finding out that even when the drop has been washed off DA process still being present in the background solution, which indicates an analyte adsorption on the WE surface. On the other hand, the same cyclic voltammetry measures are given for the spaghetti configuration with the aim of proving that DA is not adsorbed on this surface. Particular attention deserves the fact that after oxidative treatment the Fe/Al MWCNTs adsorption is significantly reduced at the same time that the DA signal is enhanced. The same behavior was observed for a Fe/Al/30 min MWCNTs.

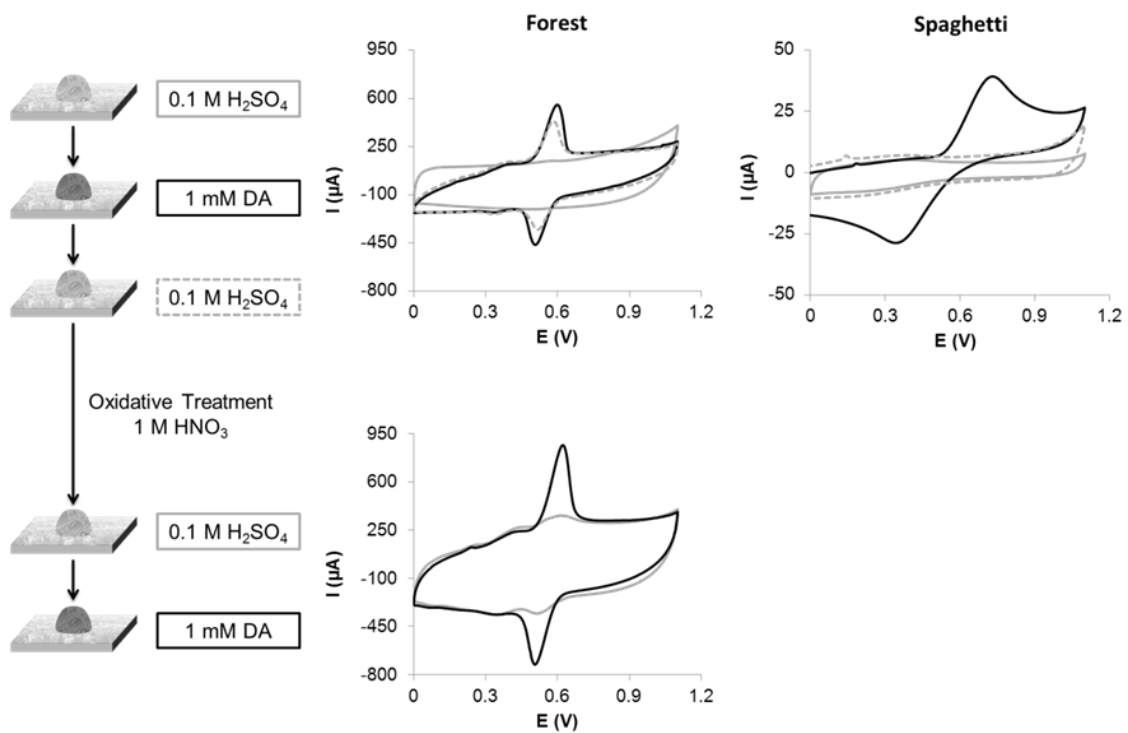


Figure 5. Scheme of the procedure followed for avoiding DA adsorption in case of forest-like CNTs. Cyclic voltammograms on both spaghetti and forest carbon nanotubes highlighting the need and effectiveness of the oxidative treatment for forest and the non-adsorption for spaghetti.

3.3. Surface Reproducibility and Stability

It should be noted that the reaction time is going to strongly influence the surface stability. While in Fe/Al/10 min only 60 scans could be made (not time-resistant surface) the Fe/Al/30 min proved to be more stable allowing measures for months. However, times over 30 min were not suitable because strong adsorption of DA was noticed on the surface. In

conclusion, a strong compromise between surface adsorption and stability in function of CVD reaction time has to be made.

Choosing high-density spaghetti-like, Fe/ITO/20 min and Fe/Al/30 min forest-like as the best surfaces of both MWCNTs types (non-oriented and oriented), the precision of analytical signals was studied by cyclic voltammetry. The intra-electrode RSD was determined by recording 5 consecutive scans at 100 mV s^{-1} . Values of 1, 2 and 14% were obtained for high-density spaghetti-like, Fe/ITO/30 min and Fe/Al/30 min forest-like CNTs respectively, indicating good reproducible behavior of synthesized surfaces. In the case of Fe/Al/30 min surface, a higher value of RSD was found owing to the already mentioned DA adsorption, which has been eliminated by the oxidative treatment with RSD values of 2%.

The surface performance has also been evaluated for MWCNTs grown in different days, obtaining RSD inter-day values of 8, 4 and 3% for high-density spaghetti-like, Fe/ITO/30 min and Fe/Al/30 min forest-like CNTs, respectively. Surface stability with time was studied too, with this aim the electrode was dry-stored in a Petri dish and periodic CV measures were performed. In light of this it was found that both spaghetti-like CNTs and underlayered forest-like CNTs (Fe/ITO and Fe/Al) were stable for at least 6 months (RSD of 9, 7 and 9% were obtained respectively). The result of these studies could be of great importance as it involves a good reproducibility of the electrochemical behavior over the time for the different synthesized MWCNTs surfaces.

3.4. Analytical Features

After a complete study of electrochemical parameters, the analytical performance of grown MWCNTs surfaces has been evaluated. Thus, cyclic voltammetry and chronoamperometry techniques were employed in order to study their characteristics.

3.4.1. Cyclic Voltammetry

Table 1 summarizes the most relevant parameters obtained by CV for different DA concentrations comprised between 0.5 and 3 mM. The sensitivity (slope of the calibration curve) and limit of detection (LOD, calculated as the concentration corresponding to three times the standard deviation of the estimate) were calculated based on peak intensities of the recorded cyclic voltammograms in both spaghetti and forest-like CNTs surfaces. A study of analytical features after 1 M HNO_3 surface oxidation pretreatment was also performed, and same studies were held on MWCNTs-COOH SPCEs with the aim of interpreting more deeply the results.

Among all studied surfaces, grown Fe/Al/30 min MWCNTs showed the highest sensitivity ($104 \pm 16 \mu\text{A mM}^{-1}$), approximately five times greater than the value obtained for MWCNTs-COOH SPCE ($21.2 \pm 0.1 \mu\text{A mM}^{-1}$), three times when it is compared with high-density spaghetti-like CNTs ($38 \pm 1 \mu\text{A mM}^{-1}$) and, slightly higher than that obtained for Fe/ITO/30 min forest CNTs ($80 \pm 7 \mu\text{A mM}^{-1}$). Even though, the lowest LOD corresponds to high-density spaghetti-like MWCNTs (0.03 mM), while the highest was for Fe/Al/30 min forest-like MWCNTs (0.88 mM). Similar limits of detection were observed in case of MWCNTs-COOH SPCE and Fe/ITO/30 min forest-like MWCNTs (0.31 and 0.48 mM respectively). Particular attention deserves the behavior of low-density spaghetti-like MWCNTs, where the density is a critical parameter that leads to the lowest sensitivity and highest LOD.

Table 1. Values of the analytical features obtained for DA (from 0.5 to 3 mM) calibration plots without and with oxidative pretreatment of the WE surface.

| | Oxidative Treatment | Sensitivity ($\mu\text{A.mM}^{-1}$) | Limit of Detection (mM) | Correlation Coefficient (r) |
|-----------------------|---------------------|---------------------------------------|-------------------------|-----------------------------|
| MWCNTs-SPCE | no | 21.2 ± 0.1 | 0.31 | 0.998 |
| <i>Low-density</i> | no | 0.16 ± 0.04 | 1.48 | 0.939 |
| Spaghetti-like | no | 38 ± 1 | 0.03 | 0.999 |
| | <i>High-density</i> | yes | 10.9 ± 0.4 | 0.998 |
| Forest-like | no | 80 ± 7 | 0.48 | 0.993 |
| | yes | <i>Surface Detached</i> | | |
| | no | 104 ± 16 | 0.88 | 0.977 |
| | <i>Fe/Al/30 min</i> | yes | 272 ± 8 | 0.999 |

When the oxidative pretreatment with 1 mM HNO_3 was carried out on the WE surface before measures, two kinds of situations could be observed depending on MWCNTs orientation. For high-density spaghetti-like CNTs there is a decrease in the analytical parameters, whereas the opposite is true for forest Fe/Al/30 min and, an improvement of them could be noticed. Remarkable is the fact that in Fe/Al/30 min surfaces, the sensitivity on pretreated surfaces is twice as much higher than non-pretreated surfaces (it changes from 104 ± 16 to $272 \pm 8 \mu\text{A mM}^{-1}$) while a significant decrease in LOD (from 0.88 to 0.16 mM) is observed, achieving a better regression coefficient (from 0.977 to 0.999). In case of Fe/Al/30 min carbon nanotubes, the improved analytical parameters demonstrated by the pre-oxidized compared with the bare surface may be attributed to defects created in the tube structure, which speed up the electron transfer kinetics [50], and to DA avoided adsorption.

With this study it can be concluded that slight changes in MWCNTs properties like orientation, density, kind of underlayer, and oxidative pretreatment lead to very different analytical properties with best sensitivity for Fe/Al/30 min pretreated MWCNTs and best LOD for high-density spaghetti-like MWCNTs. Therefore, depending on their use a careful choice of the surface material has to be made.

3.4.2. Chronoamperometry

The amperometric response of high-density spaghetti and pretreated Fe/Al/30 min MWCNTs surfaces to DA was investigated with chronoamperometry measures, in which a potential of + 0.7 V is applied over 100 s (in order to obtain a steady state). This technique was proposed as a closer approximation to the behavior of these WE surfaces when they are going to be employed in flow systems. **Fig. 6** shows DA oxidation recorded chronoamperograms on high-density spaghetti MWCNTs. These measures also confirm a linear response between I_a and DA at concentrations ranging from 0.025 to 2 mM. The analytical signal is the average of the intensity recorded on the last 20 seconds of the chronoamperogram and it is plotted against DA concentration in order to obtain the calibration curves (**Fig. 6 inset**).

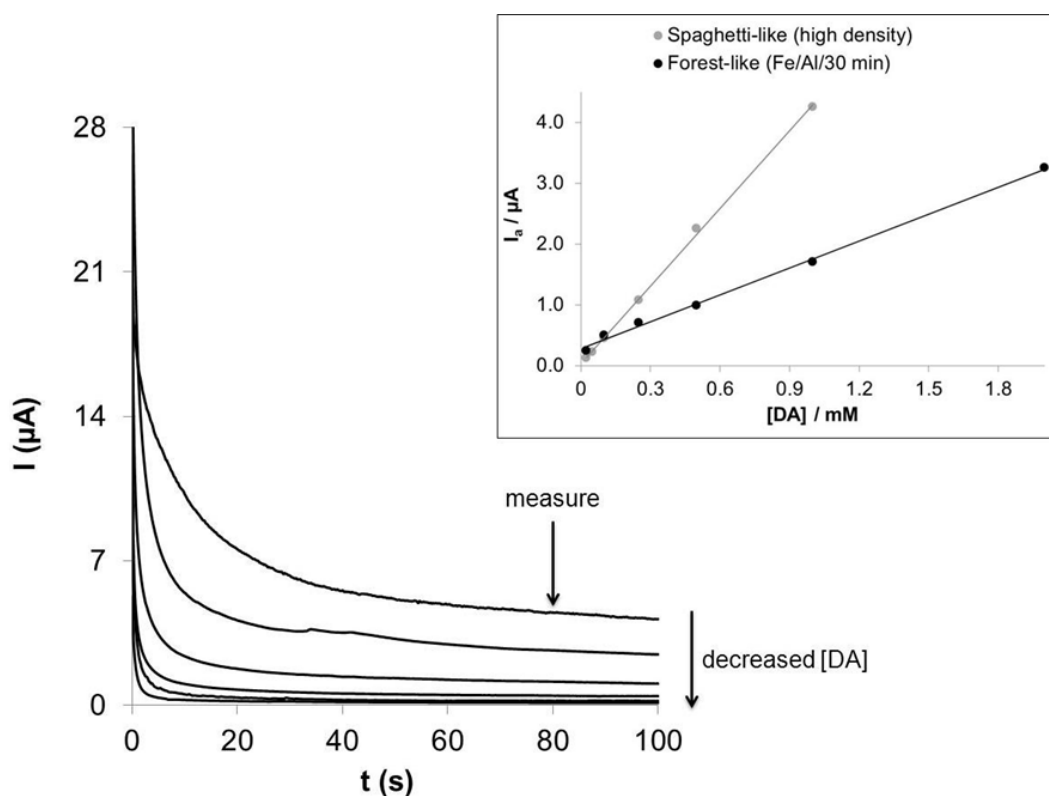


Fig. 6. Chronoamperogram of DA oxidation (from 0.025 to 2 mM) in 0.1 M H_2SO_4 for high-density spaghetti-like CNTs at +0.7 V (vs. Ag/AgCl) for 100s and the corresponding calibration plots (obtained averaging the measurements obtained in the last 20 s) for high-density spaghetti-like CNTs and pretreated Fe/Al forest-like CNTs.

In this case the sensitivity obtained for both surfaces ($4.26 \pm 0.06 \mu\text{A mM}^{-1}$ vs. $1.47 \pm 0.04 \mu\text{A mM}^{-1}$ for high-density spaghetti-like and pretreated Fe/Al/30 min forest-like CNTs respectively) are in the same order of magnitude, whereas those obtained for CV measures had been very different (**Table 1**), almost 7 times higher for the Fe/Al surface. However, achieved high-density spaghetti (0.04 mM) and pretreated Fe/Al/30 min (0.14 mM) LODs were very similar to those obtained by CV technique. In chronoamperometry, the flux of DA, hence the current as well, is proportional to the concentration gradient at the electrode surface [51]. Therefore, the fact that the diffusion process is easier in spaghetti-like CNTs, where adsorption does not exist (**Fig. 5**), explains the higher peak intensities obtained in this case.

In view of this, good performance of the electrode surfaces could be expected when they are used as WE electrodes, also in flow analysis with amperometric detection.

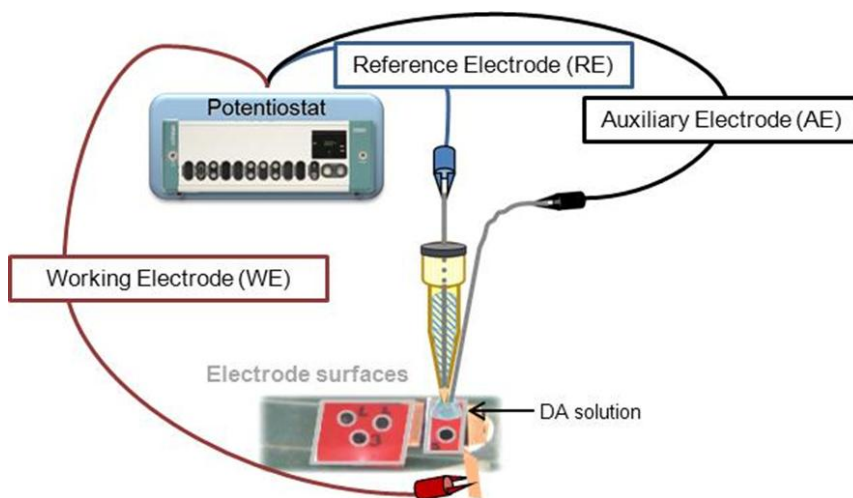
4. Conclusions

Glass is the ideal substrate for carrier wafers because of its chemical durability and thermal stability. Corning glass, particularly, provides outstanding mechanical and temperature strength ($750 \text{ }^\circ\text{C}$). In this work, successful spaghetti and vertical CNTs growth on Corning glass substrates through CVD technique has been performed. Both kinds of CNTs were evaluated as working electrodes, exhibiting excellent voltammetric and chronoamperometric performance and effectively respond to changes in DA concentrations, being adequate for carrying out analytical determinations. This work provides useful information on how parameters like CNTs orientation, density, underlayer deposition, reaction time or oxidative treatment may influence subsequent electrochemical and analytical properties. The results of CV indicated that higher amounts of catalyst in spaghetti-like and higher reaction times in forest-like CNTs synthesis can significantly enhance the analytical signal (peak currents). The grown CNTs can be used several times, providing low cost WEs and extremely time-resistant surfaces. On the other hand, the direct fabrication of the CNTs WE on glass substrates has several advantages compared with conventional electrode modification methods: (1) high controlled electrode fabrication, (2) improved LOD ($30 \mu\text{M}$ for bare high-density spaghetti-like CNTs) and (3) enhanced sensitivities ($272 \mu\text{A mM}^{-1} \text{ mm}^{-2}$ for oxidative treated forest-like CNTs with Al underlayer). Thus, the present forest-like carbon nanotubes growth procedure is highly recommended for electrochemical sensing thus it makes easy their integration in microfluidic devices avoiding tedious dispersion procedures.

Acknowledgements

This work has been supported by MICINN under project CTQ2011-25814 and by the Asturias Government with funds from PCTI 2006-2009, cofinanced with FEDER funds (Programa Operativo FEDER del Principado de Asturias 2007-2013) under project FC-11-PC10-30. Isabel Álvarez-Martos and Adrián Fernández-Gavela thank the MICINN and FICYT respectively for the award of PhD grants (AP2008-04451 and BP09-007).

Supplementary Data



Supplementary data. Schematic representation of the electrochemical cell for cyclic and chronoamperometric measurements.

REFERENCES

- [1] L.M. Bellan, D. Wu, R.S. Langer. Current trends in nanobiosensor technology. *Wiley Interdisciplinary Review of Nanomedicine and Nanobiotechnology* 3 (2011) 229-246
- [2] S. Marín, A. Merkoçi. Nanomaterials based electrochemical sensing applications for safety and security. *Electroanalysis* 24 (2012) 459-469.
- [3] R.L. McCreery. Advanced carbon electrode materials for molecular electrochemistry. *Chemical Reviews* 108 (2008) 2646-2687.
- [4] K. Scida, P.W. Stege, G. Haby, G.A. Messina, C.D. García. Recent applications of carbon-based nanomaterials in analytical chemistry: critical review. *Analytica Chimica Acta* 691 (2011) 6-17.
- [5] N. Xiao, B.J. Venton. Rapid, sensitive detection of neurotransmitters at microelectrodes modified with self-assembled SWCNT forests. *Analytical Chemistry* 84 (2012) 7816-7822.
- [6] P. Yáñez-Sedeño, J. Riu, J.M. Pingarrón, F.X. Rius. Electrochemical sensing based on carbon nanotubes. *Trac-Trends in Analytical Chemistry* 29 (2010) 939-953.
- [7] M.T. Fernández-Abedul, A. Costa-García. Carbon nanotubes (CNTs)-based electroanalysis. *Analytical and Bioanalytical Chemistry* 390 (2008) 293-298.
- [8] N.S. Lawrence, R.P. Deo, J. Wang. Detection of homocysteine at carbon nanotube paste electrodes. *Talanta* 63 (2004) 443-449.
- [9] R.R. Moore, C.E. Banks, R.G. Compton. Basal Plane Pyrolytic Graphite Modified Electrodes: Comparison of Carbon Nanotubes and Graphite Powder as Electrocatalysts. *Analytical Chemistry* 76 (2004) 2677-2682.
- [10] J.M. Goran, J.L. Lyon, K.J. Stevenson. Amperometric Detection of L-Lactate Using Nitrogen-Doped Carbon Nanotubes Modified with Lactate Oxidase . *Analytical Chemistry* 83 (2011) 8123-8129.
- [11] Y. Fu, L. Zhang, G. Chen. Preparation of a carbon nanotube-copper nanoparticle hybrid by chemical reduction for use in the electrochemical sensing of carbohydrates. *Carbon* 50 (2012) 2563-2570.
- [12] Y.-H. Li, J. Ding, Z. Luan, Z. Di, Y. Zhu, C. Xu, D. Wu, B. Wei. Competitive adsorption of Pb²⁺, Cu²⁺ and Cd²⁺ ions from aqueous solutions by multiwalled carbon nanotubes. *Carbon* 41 (2003) 2787-2792.
- [13] G. Lin, S.L. Riechers, M.C. Mellen, Y. Li. Sensitive electrochemical detection of enzymatically generated thiocholine at carbon nanotube modified glassy carbon electrode. *Electrochemistry Communications* 7 (2005) 1163-1169.
- [14] T. Premkumar, R. Mezzenga, K.E. Geckeler. Carbon nanotubes in the liquid phase: addressing the issue of dispersion. *Small* 8 (2012) 1299–1313.
- [15] T.J. Simmons, J. Bult, D.P. Hashim, R.J. Linhardt, P.M. Ajayan. Noncovalent functionalization as an alternative to oxidative acid treatment of single wall carbon nanotubes with applications for polymer composites. *ACS Nano* 3 (2009) 865-870.
- [16] J. Wang. Carbon-nanotube based electrochemical biosensors: a review. *Electroanalysis* 17 (2005) 7-14.

- [17] X. Yu, D. Chattopadhyay, I. Galeska, F. Papadimitrakopoulos, J.F. Rusling. Peroxidase activity of enzymes bound to the ends of single-wall carbon nanotube forest electrodes. *Electrochemical Communications* 5 (2003) 408-411.
- [18] X. Niu, H. Zhao, C. Chen, M. Lan. Platinum nanoparticle-decorated carbon nanotube clusters on screen-printed gold nanofilm electrode for enhanced electrocatalytic reduction of hydrogen peroxide. *Electrochimica acta* 65 (2013) 87-103.
- [19] S. Talapatra, S. Kar, S.K. Pal, R. Vajtai, L. Ci, P. Victor, M.M. Shaijumon, S. Kaur, O. Nalamasu, P.M. Ajayan. Direct growth of aligned carbon nanotubes on bulk metals. *Nature Nanotechnol* 1 (2006) 112-116.
- [20] C.M. Seah, S.P. Chai, A.R. Mohamed. Synthesis of aligned carbon nanotubes. *Carbon* 49 (2011) 4613-4635.
- [21] C.M. Orofeo, H. Ago, T. Ikuta, K. Takahasi, M. Tsuji. Growth of horizontally aligned single-walled carbon nanotubes on anisotropically etched silicon substrate. *Nanoscale* 2 (2010) 1708-1714.
- [22] A. Merkoçi, M. Pumera, X. Llopis, B. Pérez, M. del Valle, S. Alegret. New materials for electrochemical sensing VI: carbon nanotubes. *Trac-Trends in Analytical Chemistry* 24 (2005) 826-838.
- [23] G.D. Nessim, M. Seita, K.P. O'Brien, A.J. Hart, R.K. Bonaparte, R.R. Mitchell, C.V. Thompson. Low temperature synthesis of vertically aligned carbon nanotubes with electrical contact to metallic substrates enabled by thermal decomposition of the carbon feedstock. *Nano Letters* 9 (2009) 3398-3405.
- [24] G.D. Nessim, D. Acquaviva, M. Seita, K.P. O'Brien, C.V. Thompson. The critical role of the underlayer material and thickness in growing vertically aligned carbon nanotubes and nanofibers on metallic substrates by chemical vapor deposition. *Advanced Functional Materials* 20 (2010) 1306-1312.
- [25] X. Liu, K.H.R. Baronian, A.J. Downard. Direct growth of vertically aligned carbon nanotubes on a planar carbon substrate by thermal chemical vapour deposition. *Carbon* 47 (2009) 500-506.
- [26] S. Park, D.-W. Park, C.-S. Yang, K.-R. Kim, J.-H. Kwak, H.-M. So, C.W. Ahn, B.S. Kim, H. Chang, J.-O. Lee. Vertically aligned carbon nanotube electrodes directly grown on a glassy carbon electrode. *ACS Nano* 9 (2011) 7061-7068.
- [27] I. Taurino, S. Carrara, M. Giorcelli, A. Tagliaferro, G. De Micheli. Comparison of two different carbon nanotube-based surfaces with respect to potassium ferricyanide electrochemistry. *Surface Science* 606 (2012) 156-160.
- [28] C. Journet, M. Picher, V. Jourdain. Carbon nanotube synthesis: from large-scale production to atom-by-atom growth. *Nanotechnology* 23 (2012) 1-19.
- [29] W. Zhou, Z. Han, J. Wang, Y. Zhang, Z. Jin, X. Sun, Y. Zhang, C. Yan, Y. Li. Copper catalyzing growth of single-walled carbon nanotubes on substrates. *Nano Letters* 6 (2006) 2987-2990.
- [30] A.C. Dupuis. The catalyst in the CCVD of carbon nanotubes-a review. *Progress in Materials Science* 50 (2005) 929-961.

- [31] R.Y. Zhang, I. Amlani, J. Baker, J. Tresek, R.K. Tsui. Chemical vapor deposition of single-walled carbon nanotubes using ultrathin Ni/Al film as catalyst. *Nano Letters* 3 (2003) 731-735.
- [32] M.C. Altay, S. Eroglu. Synthesis of multi-walled C nanotubes by Fe-Ni (70 wt.%) catalyzed chemical vapor deposition from pre-heated CH₄. *Materials Letters* 67 (2012) 124-127.
- [33] J. Li, Y. Zhang, S. To, L. You, Y. Sun. Effect of nanowire number, diameter, and doping density on nano-FET biosensor sensitivity. *ACS Nano* 5 (2011) 6661-6668.
- [34] P. Fanjul-Bolado, P. Queipo, P.J. Lamas-Ardisana, A. Costa-García. Manufacture and evaluation of carbon nanotube modified screen-printed electrodes as electrochemical tools. *Talanta* 74 (2007) 427-433.
- [35] I.Y.Y. Bu, S.P. Oei. Hydrophobic vertically aligned carbon nanotubes on Corning glass for self cleaning applications. *Applied Surface Science* 256 (2010) 6699-6704.
- [36] S. Esconjauregui, C.M. Whelan, K. Maex. The reasons why metals catalyze the nucleation and growth of carbon nanotubes and other carbon nanomorphologies. *Carbon* 47 (2009) 659-669.
- [37] Y. Nakayama, L.J. Pan, G. Takeda. Low-temperature growth of vertically aligned carbon nanotubes using binary catalysts. *Japanese Journal of Applied Physics* 45 (2006) 369-371.
- [38] H.-C. Su, C.-H. Chen, Y.-C. chen, D.-J. Yao, H. Chen, Y.-C. Chang, T.-R. Yew. Improving the adhesion of carbon nanotubes to a substrate using microwave treatment. *Carbon* 48 (2010) 805-812.
- [39] H. Liu, Y. Zhang, D. Arato, R. Li, P. Mérel, X. Sun. Aligned multi-walled carbon nanotubes on different substrates by floating catalyst chemical vapor deposition: critical effects of buffer layer. *Surface & Coatings Technology* 202 (2008) 4114-4120.
- [40] Y. Zhang, N.W. Franklin, R.J. Chen, H. Dai. Metal coating on suspended carbon nanotubes and its implication to metal-tube interaction. *Chemical Physics Letters* 331 (2000) 35-41.
- [41] D. Antiohos, S.E. Moulton, A.I. Minett, G.G. Wallace, J. Chen. Electrochemical investigation of carbon nanoweb architecture in biological media. *Electrochemical Communications* 12 (2012) 1471-1474.
- [42] G. Yue, J. Wu, J.Y. Lin, Y. Xiao, S.Y. Tai, J. Lin, M. Huang, Z. Lan. A counter electrode of multi-wall carbon nanotubes decorated with tungsten sulfide used in dye-sensitized solar cells. *Carbon* 55 (2013) 1-9.
- [43] W. Li, C. Tan, M.A. Lowe, H.D. Abruña, D.C. Ralph. Electrochemistry of individual monolayer grapheme sheets. *ACS Nano* 5 (2011) 2264-2270.
- [44] Y. Xian, H. Wang, Y. Zhou, D. Pan, F. Liu, L. Jin. Preparation of L-Cys-Au colloid self-assembled nanoarray electrode based on the microporous aluminium anodic oxide film and its application to the measurement of dopamine. *Electrochemical Communications* 6 (2004) 1270-1275.
- [45] J. Park, P. Takmakov, R.M. Wightman. In vivo comparison of norepinephrine and dopamine release in rat brain by simultaneous measurements with fast-scan cyclic voltammetry. *Journal of Neurochemistry* 119 (2011) 932-944.
- [46] C.E. Banks, R.R. Moore, T.J. Davies, R.G. Compton. Investigation of modified basal plane pyrolytic graphite electrodes: definitive evidence for the electrocatalytic properties of the ends of carbon nanotubes. *Chemical Communications* 16 (2004) 1804-1805.

- [47] G.U. Sumanasekera, J.L. Allen, S.L. Fang, A.L. Loper, A.M. Rao, P.C. Eklund. Electrochemical oxidation of single wall carbon nanotube bundles in sulfuric acid. *Journal of Physical Chemistry B* 103 (1999) 4292-4297.
- [48] A. Doepke, C. Han, T. Back, W. Cho, D.D. Dionysiou, V. Shanov, H.B. Halsall, W.R. Heineman. Analysis of the electrochemical oxidation of multiwalled carbon nanotube tower electrodes in sodium hydroxide. *Electroanalysis* 24 (2012) 1501-1508.
- [49] P.J. Britto, K.S.V. Santhanam, P.M. Ajayan. Carbon nanotube electrode for oxidation of dopamine. *Bioelectrochemistry and Bioenergetics* 41 (1996) 121-125.
- [50] A. Chou, T. Böcking, N.K. Singh, J.J. Gooding. Demonstration of the importance of oxygenated species at the ends of carbon nanotubes for their valuable electrochemical properties. *Chemical Communications* 7 (2005) 842-844.
- [51] A.J. Bard, L.R. Faulkner. *Electrochemical Methods: Fundamentals and Applications*. second ed., J. Wiley & Sons, New York, 2001.

Biographies

Isabel Álvarez-Martos obtained her B.Sc. degree in 2009 with the work “Polymer modification of microchip electrophoresis: influence in catecholamines resolution”. One year later she has obtained her MSc. entitled “Microchip electrophoresis microchannel modification”. Her research is focused on the employment of electrochemical microfluidic devices (electrophoresis and paper), their modification (static and dynamic) with polymers and ionic liquids and the enhancement of their electrochemical properties, based on the employment of grown carbon nanotubes (disordered and forest).

Adrián Fernández Gavela received the degree in physics from the University of Oviedo, Spain. Since 2008, he is working in optical waveguide fabrication and characterization in the Physics Department of the University of Oviedo. In 2009, he received a grant from the FICYT (Principado de Asturias, Spain) to doctoral courses from this University. He is currently working as researcher for a coordinated project between the immunoelectroanalysis group and the integrated optic group of the University of Oviedo. His research interests are design, fabrication and characterization of optical waveguides, capillary electrophoresis microchips (MCE) and biosensors microdevices based on Mach–Zehnder interferometer.

José Rodríguez García received the Teaching degree from the University of Oviedo, Spain, and the BSc Extraordinary PhD degrees in physics from University of Santander, Spain. From 1982 to 1988 he worked in electromagnetic field analysis on dielectric waveguides in the Electronics Department of the University of Santander. Nowadays he is Professor in the Physics Department of University of Oviedo and he conducts research in the following areas: electromagnetic field theory, modeling, characterization, and evaluation of integrated optical waveguides and devices.

Nuria Campos-Alfaraz obtained her degree in Physics from the Autonomous University of Madrid in 2007. In that year she joined ITMA Materials Technology, working for the Nanotechnology department in nanomaterials characterization and microfabrication techniques. At the time, she enrolled the PhD program in Science and Technology of Materials

at the University of Oviedo, and did her project on soft lithography techniques. In 2009, she passed to the Energy Area of ITMA, whose activities are mainly focused on the development of vapor deposition processes for thin film photovoltaics. At the moment, she is working on the development of CVD processes for the synthesis of carbon nanostructures.

Ana Belén García-Delgado. PhD in Chemistry from University of Oviedo (Spain) in 2006. Her scientific career has been focused on organic chemistry, polymeric materials and nanotechnology. Since 2007 is working as researcher of the Energy Area at ITMA Materials Technology. During the last three years her activity has been involved in the development of new solar encapsulants and lamination strategies for cell encapsulation.

David Gómez-Plaza. PhD in Physics from University of Basque Country (2000). He has more than ten years of experience in the development of thin film and laser technology for manufacturing, energy and biotechnology applications. He has been researcher at Fundacion Tekniker (2001-2006), Head of the Nanotechnology Department at Fundación ITMA (2007-2009) and currently Director of Energy Area at ITMA Materials Technology (since 2009).

Agustín Costa-García obtained his B.Sc. degree in Chemistry, focus on Analytical Chemistry, in 1974 (University of Oviedo) and the Ph.D. in chemistry in 1977 (University of Oviedo). Since February 2000 he is Professor in Analytical Chemistry (University of Oviedo). He leads the Immunoanalytical Research Group of the University of Oviedo and has been supervisor of several research projects developed at the electrochemistry laboratories of the Department of Physical and Analytical Chemistry of the University of Oviedo. Nowadays his research is focused on the development of nanostructured electrodic surfaces and its use as transducers for electrochemical immunosensors and genosensors employing electrochemical labels.

M. Teresa Fernández-Abedul received her PhD in Chemistry in 1995 at the University of Oviedo, Spain. Since 2002 is working as Associate Professor in Analytical Chemistry at the University of Oviedo. Her current research interests are the development of immunosensors and genosensors employing nanostructured transducers as well as the development of miniaturized analytical devices (microchip electrophoresis and paper microfluidic devices) for the sensitive electrochemical detection of analytes of interest, even those non-electroactive through adequate electroactive labeling systems.

CHAPTER 3: NOVEL MATERIALS

3.1. Background

3.2. Research & Development:

- ▣ **Article 6:** Paper/Transparency-based Analytical Devices for the Sensitive Detection of Lead and Cadmium.
-

3.1. Background

Background

Microfluidic paper-based analytical devices (μ PADs) began as the idea of making conventional microfluidic devices out of paper instead of glass or polymers. The goal of this Chapter was to **develop low-cost devices for sensitive heavy metals detection**.

The inspiration for starting to work with paper came from its versatility. As material is cheap and has the ability to move fluids as a consequence of its capillary action, thus no pumps or power sources are going to be needed. Furthermore, paper also has a high surface-to-volume ratio, represent an excellent background for colorimetric detection, is flammable, which make it easily disposed, and its chemistry is well known from the test strips.

On the other hand, the interest in heavy metals comes from their toxic effects as they are non-degradable and thus persistent in the human body. They are natural elements presents in rocks, soils or water, but there are other extrasources like plastic industry, agricultural use (fertilizers) or sewage sludge which increase their levels in the environment. Cadmium and lead are in the most common environmental pollutants found in water samples. Marine organisms have a tendency to accumulate these metals, and humans therefore are exposed to these harmful compounds through any diet that includes seafood.

All these reasons explained the extremely importance of developing sensitive detection systems for this kind of compounds and the need of in situ monitoring.

This Chapter 3 contains data as a result of a research stay, which have not been published yet (**Article 6**).

3.2. Research & Development

Article 6

*Paper/Transparency-based Analytical Devices
for the Sensitive Detection of Lead and
Cadmium*

(unpublished results)



Unpublished Results



Paper/Transparency-based Analytical Devices for the Sensitive Detection of Lead and Cadmium

1. Introduction

Since their introduction there has been an ongoing interest in the development of paper-based analytical devices (μ PAD) [1,2], *i.e.* the use of paper as an inexpensive platform for diagnostic devices. Paper substrates are capable of drastically decrease the time of analysis due to their high surface-to- volume ratio, porous structure, and small volume, and in comparison with other microfluidic substrates it is less expensive (about 1000 times cheaper than glass) with fabrication process that take only few minutes.

There are a wide variety of paper materials available for the fabrication of these devices, being Whatman® cellulose range the most commonly used. The differences between these papers is given by porosity, particle retention and flow rate. The most popular is Whatman® No. 1 filter paper [3-9] with a medium flow rate/retention, and 0.18 mm thickness (allowing its printing in commercial machines). Its chemical composition consists of 98 % α -cellulose with no strengthening or whitening additives, which reduces the possibility of interferences. Other Whatman® filter papers are the No. 4 (with a larger pore size) [10-12] or No. P81 (cationic exchanger paper) [13] with the aim of increasing liquid penetration or facilitate the separation process respectively. There are also other commercially available paper substrates that have been employed as paper-based analytical devices. For example composite filter papers consisting on hydroentangled polyester (45 %)–cellulose (55 %) blend [14], cartridge paper [15], bioactive paper [16], glossy paper (flexible substrate made of cellulose fiber blended with an inorganic filler) [17], and even cloth [18] or thread [19].

The main application fields of these paper-based analytical devices include biochemical molecules [6,10,20,21] and environmental samples [3,9,12,14]. In particular, environmental monitoring is needed of accurate in-field detection for heavy metals and other pollutants. This

importance arises from their fluctuations over day and even over hours (*e.g.* between sample collection and laboratory analysis).

On the other hand, suitable detection methods are needed, which must be compatible with the simplicity, affordability and portability characteristics of these μ PADs. There are several reported techniques through the bibliography: colorimetric [20,22], electrochemical [6], chemiluminescence [23,24], electrochemiluminescence [25,26], fluorescence [22], photochemical [27], and even Raman spectroscopy [28]. Even though, only colorimetric and electrochemical have been widely used because of fulfill these requirements. The first is recommended for semi-quantitative analysis, since it relies on a chemical reaction or enzyme to induce a color change, which is proportional to analyte's concentration and commonly detected by a scanner or a digital/cell-phone camera. Nevertheless, colorimetric techniques are considered not suitable for an analyte accurate quantification since errors can occur as a consequence of background color variation, the lighting or the manufacture process. On the other hand, electrochemical techniques are fitted with the advantages of colorimetric methods but they also are capable of a selective and sensitive analyte determination.

Following this trend, the electrochemical detection usually is integrated in the paper-based analytical device (ePAD) by printing techniques, which possess some remarkable advantages like fastness or low-cost. There is not a single technique suitable for electrodes printing thus; its choice is going to be decided by lateral resolution, thickness, homogeneity, speed, material, or ink properties requirements [29]. In the particular case of screen printing the ink layer is dragged across the substrate and it impregnates the open pores of the paper. Ink properties are going to influence not only the printing resolution and thickness but also the electrochemical behavior.

The aim of this work was to develop a new sensitive carbon based electrochemical detection for determination of Pb and Cd by SWASV. Polyester transparency sheets were compared with filter paper, demonstrating to be a promising alternative substrate for zero-cost analysis. A thorough study of the variables involved in the performance of the transducer like oxidative treatment, bismuth concentration, buffer solution pH or Nafion[®] film thickness was carried out. The optimal conditions were applied to lead and cadmium detection, being able to detect concentrations of 0.1 ppb of both metals. To our knowledge there is no previous report about the application of transparency sheets for the quantification of heavy metals.

2. Experimental

2.1. Reagents and materials

All chemicals were analytical grade. Acetic acid and sodium acetate were purchased from Fischer Scientific (NJ). Graphite powder (particle size < 20 μm), carbon nanotubes, Nafion[®], and the standards of lead (II), cadmium (II) and bismuth (III) were acquired from Sigma-Aldrich (St. Louis, MO). Potassium ferrocyanide was obtained from Mallinckrodt (St. Louis, MO). Carbon ink E3178 was purchased from Ercon Incorporated (Wareham, MA).

Whatman No. 1 chromatographic paper and polyester transparency sheets (215 x 279 mm x 0.11 mm thick) were acquired from Whatman (Buckinghamshire, UK) and Highland 901 (Austin, TX) respectively.

Solutions were prepared by using purified water (18.2 M Ω) employing a Milli-Q Millipore (Bedford, MA, USA) water purification system. Heavy metal solutions were prepared daily by an appropriate dilution of standards in 0.1 M acetate buffer (pH 4.6).

2.2. Instrumentation

A XEROX Phaser 8860 printer was used to print the paper-based analytical devices following previously established protocols. An Isotemp hot plate from Fischer Scientific set at 150 $^{\circ}\text{C}$ was used to melt the wax on the paper. A Zygo SeScope optical profilometer was used to measure the electrode surface roughness and thickness. Buffer solution pH was determined with a Denver Instrument UltraBASIC UB-5 pH meter (Denver, CO).

2.3. Procedures

2.3.1. Masks and carbon paste/ink preparation

Masks for screen printing were fabricated using polyester transparency sheets. The sheets were used as received and cut using a laser engraving system (Epilog, Golden, CO). The CO₂ laser system had a peak power of 30 W and was controlled by Epilog software after uploading drawing files.

The pattern for transparency sheets was designed with CorelDRAW X5 software. The laser engraving system was used to cut the transparency and prepare the mask. In this work two designs of masks were employed: (i) the three electrode system patterned in the same

mask, and (ii) electrical contact pads, auxiliary (AE) and reference (RE) electrodes in one mask and working electrode (WE) in other.

For electrodes screen-printing, hydrophobic wax circles of 10 mm in diameter were drawn using CorelDRAW X5 software and printed with a XEROX Phaser 8860. The printed paper was placed on a hot plate at 150 °C for 2 min to melt the wax. Finally, the paper was allowed to cool to room temperature before screen-printing.

For the carbon paste preparation a mixture containing acetone:ciclohexanone (1:1) and cellulose acetate (7.5 %) was stirred for 1h. Then the resulting solution was hand mixed with graphite powder (5:2). The carbon paste was kept in a closed vial.

For modified carbon ink preparation, carbon nanotubes, graphite powder and carbon ink (5:5:200) were hand mixed. The carbon ink was kept in the same way as before.

2.3.2. Electrochemical paper/transparency-based microfluidic device fabrication

The same procedure was followed for the electrochemical integration on both paper and transparency substrates.

For the three electrodes made with the same carbon mixture (**method 1**) the mask was placed on the substrate (paper or transparency), which was previously immobilized on the table with the aid of an adhesive tape, and the carbon mixture was spread over the surface. Then the mask was carefully removed and the resulting screen-printed electrodes were baked at 60 °C for 30 min. For the other case (**method 2**) the followed procedure was the same unlike in this case the contact pads, CE and RE where screen-printed and baked first and then the WE. In both cases after the baking procedure the devices were allowed to cool and an adhesive tape was put in the back part.

The main difference between paper and transparency screen-printing procedure is that in the former the hydrophobic barriers constituting the electrochemical cell were printed previous to the carbon screen-printed procedure, and in the latter the electrochemical cell is delimited with the aid of an isolating tape at the end of the carbon screen-printing procedure.

2.3.3. *Cyclic voltammetry and square wave anodic stripping voltammetry (SWASV)*

Electrochemical measures were performed employing a three electrode system connected with a potentiostat model 660B (CH Instruments, Austin, TX). For characterizing the electrode performance an aliquot of 50 μL of the target analyte solution was deposited on the electrochemical cell.

Cyclic voltammetry measurements were performed by scanning the potential between -0.5 and 0.5 V .

For SWASV with *ex situ* bismuth (III) deposition the solution was deposited on the electrode and yielded to -1.2 V for 120s. After this the solution was removed and the electrode surface was cleaned with MQ water. Preconcentration step was then performed by applying a potential of -1.5 V for a time (240 s). Finally, the SWASV scan was carried out from -1.4 to -0.4 V under these conditions: square wave amplitude of 25 mV, frequency of 20 Hz, step potential of 5 mV, and equilibration time of 30 s.

3. Results and Discussion

It is well known that for their toxicity heavy metals like lead and cadmium have a considerable risk to human health and the environment, even exposures to minuscule quantities can be life threatening [30,31]. Thus, the search of a rapid and sensitive detection method for heavy metals monitoring is needed, and both paper and transparency represent a promising supporting material.

3.1. *Paper vs transparency*

The first part of this work was to compare the electrochemical performance of both paper and polyester transparency substrates in order to determine which one give the best electrochemical characteristics. Thus, the surfaces were screen-printed with the carbon paste (*section 2.3.2*), and characterized in terms of cyclic voltammetry with $\text{Fe}(\text{CN})_6^{4-}$ as redox molecule. As displays **Fig.1** both substrates provide good electrochemical signals, being slightly higher for transparency (40 ± 3 and 37 ± 1 μA for I_{pa} and I_{pc} respectively) than for paper (31 ± 3 and 25 ± 1 μA for I_{pa} and I_{pc} respectively).

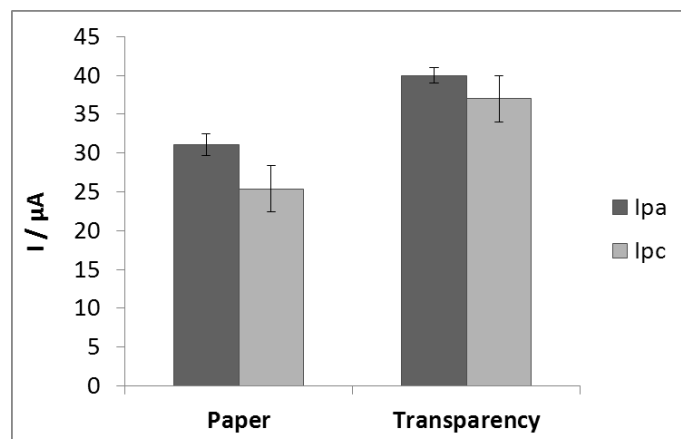


Figure 1. Anodic (I_{pa}) and cathodic (I_{pc}) peak intensity values obtained in paper and transparency substrates with carbon paste electrodes for a solution of 5 mM $Fe(CN_6)^{4-}$ in 0.1 M KCl ($n = 3$).

On the other hand, the peak potential separation ($\Delta E = E_{pa} - E_{pc}$) achieved for both surfaces was higher than the value 0.059 V (0.059 V / 1 e^-) expected for a reversible electrochemical system, suggesting a quasi-reversible $Fe(CN_6)^{4-}$ redox processes. Moreover, the results obtained in transparency substrates showed a slightly higher reversibility compared with paper, with values of 0.4 ± 0.02 and 0.26 ± 0.02 V respectively.

To establish if the working electrode effective area is influenced by the substrate material, a study of the anodic peak intensity vs scan rate was carried out, and knowing that for diffusion controlled processes the current can be defined by Randles-Sevcik equation (1), this area could be easily calculated.

$$i_p = 2.69 \cdot 10^{-5} n^{3/2} A D^{1/2} V^{1/2} C \quad (1)$$

Where n is the number of electrons involved in the redox reaction, A is the area of the working electrode (cm^2), D is the diffusion coefficient of the electroactive species ($cm^2 s^{-1}$), V is the scan rate ($V s^{-1}$), and C is the concentration of the electroactive specie at the electrode ($mol cm^{-3}$).

After this study, it was found a linear dependence between peak intensity and the square root of the scan rate in the range 10-150 mVs^{-1} regardless of the surface (**Figure 2**), evidencing that processes are diffusion-controlled, and surprisingly the WE effective area was almost the same in both substrates with values of 0.033 ± 0.003 and 0.038 ± 0.006 cm^2 ($n = 4$) for paper and transparency respectively.

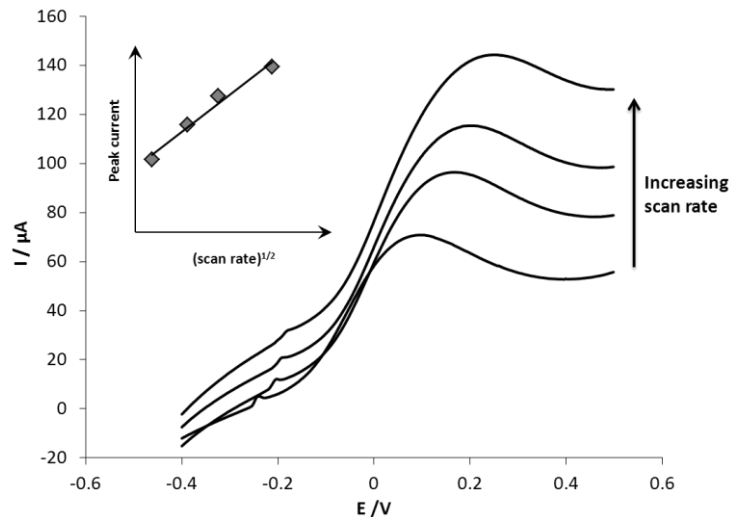


Figure 2. Influence of the scan rate in cyclic voltammetry measures performed on transparency, and linear dependence between the peak intensity with the square root of the scan rate (inset).

From these studies it could be concluded that the electrochemical characteristics of both substrates are very similar, and that transparency is going to be as suitable as paper for the performance of the electrochemical detection.

3.2. Optimization of the electrode for lead and cadmium detection

Heavy metals are considered one of the main sources of pollution in the environment. Among them, lead and cadmium are the most widespread studied because of represent a concern for the public-health. On the other hand, anodic stripping voltammetry technique has been widely used for these metals detection with remarkable sensitivity, allowing the detection of trace/ultratrace levels. The recent trend towards green chemistry (reduce the use and generation of hazardous substances) has made that conventional electrodes employed to carry out this technique (mercury) have been replaced by other more environmental-friendly like bismuth. All the following studies were performed on transparency sheets.

3.2.1. Bismuth modified electrodes: effect of the deposition method

In order to achieve a sensitive detection of lead and cadmium the way in which bismuth was incorporated on the electrode has been studied. For this, the three electrodes were screen-printed with the carbon paste detailed in *section 2.3.1*, and bismuth was incorporated by electrochemical deposition, adsorption, and on the carbon paste itself. To the development of these studies a 10 ppm lead and cadmium solution has been employed.

The bismuth electrochemical deposition was carried out in two different ways: *in situ* (Bi electrodeposition at the same that Pb and Cd) and *ex situ* (Bi electrodeposition prior to Pb and Cd). Thus, the bismuth concentration was 10 : 1 (Bi : Pb and Cd) [32], and for the *ex situ* approach the Bi electrodeposition conditions were -1.2 V for 120 s. Background currents result to be lower in the second case ($\approx 35 \mu\text{A}$) than for the first ($\approx 70 \mu\text{A}$). However, for lead the *in situ* approach provide higher anodic peak intensities ($3.57 \pm 0.02 \mu\text{A}$) than *ex situ* ($2.1 \pm 0.9 \mu\text{A}$), while for cadmium both strategies (*in situ* and *ex situ*) provide the same peak currents ($1.3 \pm 0.1 \mu\text{A}$ and 1.3 ± 0.5 and respectively). For both cases, the anodic peak potential remains almost constant regardless of the bismuth way of deposition, being $-0.86 \pm 0.1 \text{ V}$ for Pb and $-1.14 \pm 0.02 \text{ V}$ for Cd.

To improve these results a new approach based on the bismuth adsorption was checked. For this purpose, a drop of 5 μL (100 ppm Bi solution) was deposited covering only the WE surface and let it dry at room temperature overnight. The electrochemical cell was then washed thoroughly with MQ water prior lead and cadmium measures. If the recorded background currents of this method are compared with the above these are slightly reduced ($\approx 20 \mu\text{A}$), but only the cadmium peak is observed ($2.1 \pm 0.9 \mu\text{A}$). Therefore, this strategy was considered not suitable.

In the last method the bismuth-based working electrode was prepared by mixing the carbon paste with a bismuth (III) precursor (*i.e.* Bi_2O_3) before the screen-printing procedure (**method 2** in section 2.3.2). It is reported that at negative potentials, Bi_2O_3 is reduced to metallic bismuth becoming part of the electrode [33]. The precursor concentration (3 %) was chosen according to the literature [34]. The background currents of about 55 μA and the anodic peak intensities of 2.10 ± 0.09 and 2.0 ± 0.2 for lead and cadmium respectively were in accordance to the previous studies.

In spite of the strategy chosen for bismuth incorporation, it was difficult to see the lead and cadmium electrochemical processes bellow 10 ppm, making this carbon paste not suitable for heavy metals detection. Thus, a commercial carbon ink, modified with graphite powder and carbon nanotubes (MWCNTs) was tried as an alternative (section 2.3.1). In this case 10 ppm Pb (II) and Cd (II) with *in situ* Bi (III) deposition was employed, and the effect of the carbon ink on the SWASV response was evaluated with a pre-concentration time of 240 s. Well defined SWASV peaks were achieved on electrodes made with this carbon ink, being able to easily detect lead and cadmium concentrations of 25 ppb. Taking this carbon composition as the optimal for target analytes detection, several operational parameters that influence the

electroanalytical response (oxidative pretreatment, bismuth concentration, buffer solution pH, and Nafion® film thickness) were evaluated.

3.2.2. Oxidative pretreatment

It has been reported that carbon-based electrodes can improve their electrochemical behavior by an oxidative pre-treatment [35]. Moreover, the carbon nanotubes (unfunctionalized) present in the carbon ink are amenable to generate defects in their structure improving their electronic transference properties. Thus, electrodes were subjected to successive complete voltammetric scans (between -1.4 and 1.4 V) in an oxidizing medium with the aim of improving the sensitivity. To optimize the nature of the oxidizing agent, 0.1 M nitric and sulfuric acid were employed. As it was expected an improvement of the anodic peak current was observed, being slightly higher for sulfuric pretreatment than for nitric one **Fig. 3A**. The length of the oxidative treatment was also assessed in terms of number of scans (15-40 complete scans) with 0.1M H₂SO₄ as oxidizing agent. As displays **Fig. 3B** peak currents increase with the number of scans until reached 30 scans, where no further improvements were observed and the current starts to decrease. Therefore, 30 scans have been chosen as the best to achieve an improved electrochemical behavior, and this oxidative pretreatment was performed in all the subsequent optimizations.

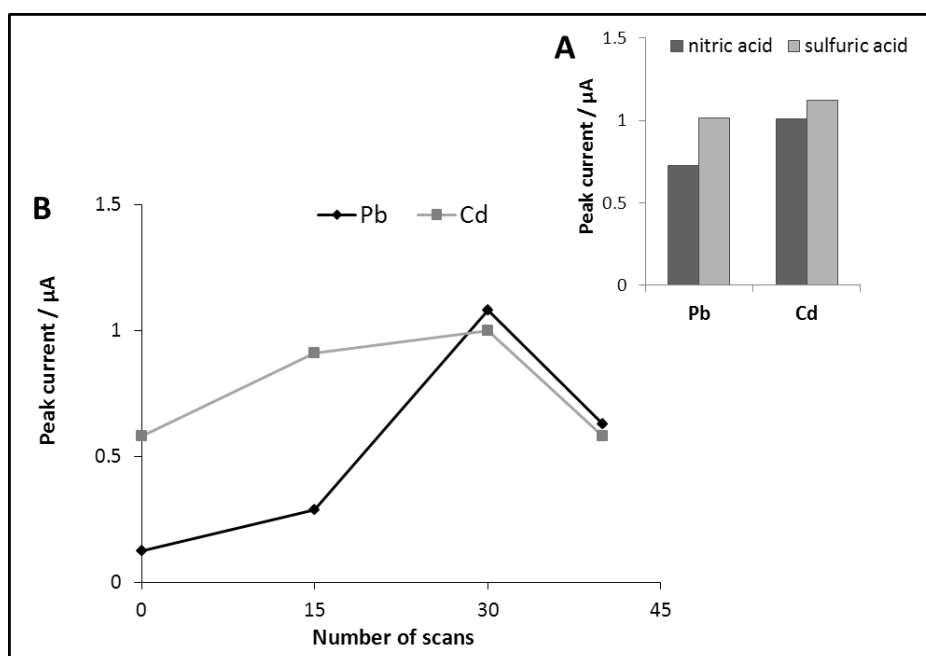


Figure 3. Peak current dependence with A) the oxidizing agent and B) the length of the treatment. Oxidative pretreatment conditions: potential window -1.4-1.4 V at scan rate of 0.1 mV s⁻¹. SWASV conditions: 150 ppb Pb (II) and Cd (II), 10 ppm Bi(III), 0.1 M acetate buffer (pH 4.3). Other conditions detailed in section 2.3.3.

3.2.3. Effect of bismuth (III) concentration on the SWASV response

The concentration of Bi (III) is an important parameter to be considered thus it decides not only the thickness of the Bi film on the electrode but also the lead and cadmium peak heights. To evaluate the stripping peak currents dependency with the thickness of the Bi film, concentrations of Bi (III) comprised between 3-200 ppm, each containing 150 ppb of Pb and Cd, with a deposition time of 240 s were chosen. The stripping peak currents displayed a clear dependence on the Bi film thickness (**Fig. 4**) as they increased rapidly at first, until reached a maximum (10 ppm) they start to decrease. The first behavior has been attributed in the literature as a consequence of the increasing number of nucleation sites and therefore a more efficient alloy formation. Even though, when Bi (III) concentration is too high the electrode surface is partially blocked by the thick layer of Bi, reducing the number of these sites [36]. It should be noted that film thickness does not affect the peak position of Pb (II) and Cd (II). Therefore, the proportion 1:67 for Pb²⁺ and Cd²⁺ vs Bi³⁺ was taken as the optimal.

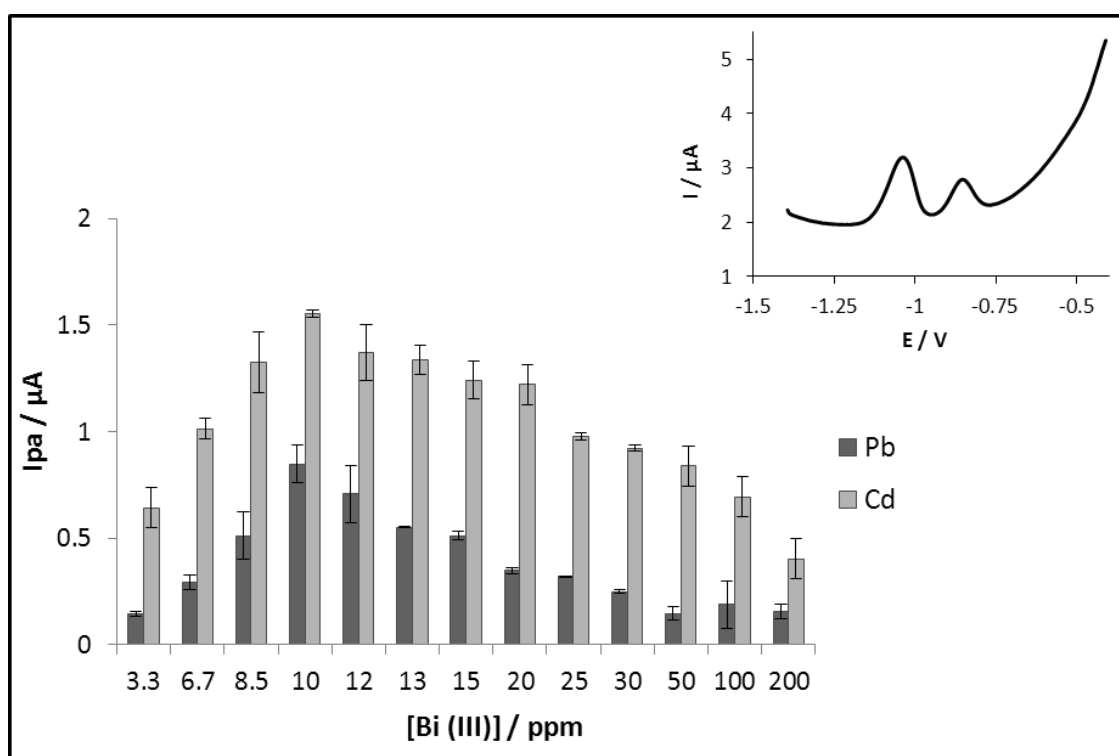
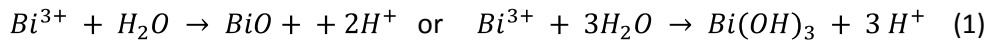


Figure 4. Influence of the Bi (III) concentration on the anodic stripping peak currents of 150 ppb Pb (II) and Cd (II) solution. In the inset the square wave anodic stripping voltammogram of lead and cadmium with 10 ppm Bi (III). Conditions: Pb (II) and Cd (II) preconcentration step -1.5 V for 240 s, 0.1M acetic buffer (pH 4.3), and pre-oxidized electrodes. SWASV detailed in section 2.3.3.

3.2.4. Buffer solution pH

The pH of the buffer solution is another variable to consider as it is going to influence the quality of the Bi film. On the one hand, neutral and alkaline-media are unsuitable because of Bi (III) hydrolysis, forming precipitates (1) [37]. Even though, it has been reported in the literature that the formation of these compounds can be avoided in highly alkaline media (NaOH), due to the formation of water soluble hydroxocomplexes [38].



On the other hand, strong acids should also be avoided as the potential window is reduced owing to the background hydrolysis, forming hydrogen which interferes in the Bi (III) deposition process [39]. Because of these restrictions, the so far dominant buffer solution for lead and cadmium determination is the acetate (pH 4-5) [37]. **Fig. 5** shows the SWASV measurements for three different pHs comprised in this range. Notice that the increase in pH is accompanied by a gradual rise in the lead signal and steeper one for cadmium, indicating a more effective complexation between Bi (III) and metal species. Thus, pH 4.6 was chosen for the development of the following optimizations.

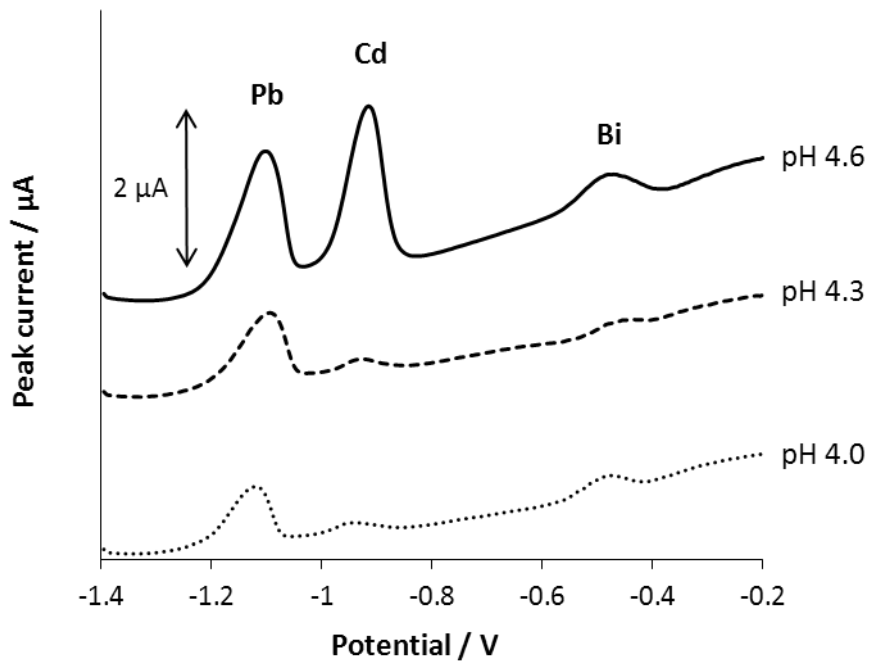


Figure 5. Square-wave anodic stripping voltammograms of 150 ppb Cd (II) and Pb (II) at different pHs. Other conditions as in Fig. 4.

3.3.5. Effect of the Nafion® thickness on the SWASV response

Nafion® is a well-known permselective membrane, capable of cation-exchange, allowing cationic species preconcentration excluding anionic interferences. This is the main cause of its widespread use as electrode modifier for trace metal analysis [40,41]. The working electrode was modified by drop coating (after the oxidative pretreatment) applying 5 μL of a Nafion® solution (0.3 v/v %). Then the solution was evaporated by heat treatment at 30 °C for 30 min.

As displays **Fig. 6**, peak current increases notoriously when compared bare and coated working electrodes (from 2.2 ± 0.5 to 4.0 ± 0.2 μA for lead and from 2.2 ± 0.4 to 4.2 ± 0.2 μA for cadmium). This behavior can be attributed to a more efficient plating of Pb^{2+} and Cd^{2+} as the Nafion® film helped to confine the cationic species close to the electrode surface. Notice also a slightly displacement of the peak potentials from -8.88 ± 0.05 to -0.91 ± 0.04 V for lead and -1.0 ± 0.1 to -1.12 ± 0.04 V for cadmium. This behavior has been explained in the bibliography as a consequence of metals deposited *via* cation-exchange mechanism need higher potentials for replating than the ones deposited directly on the electrode surface [42].

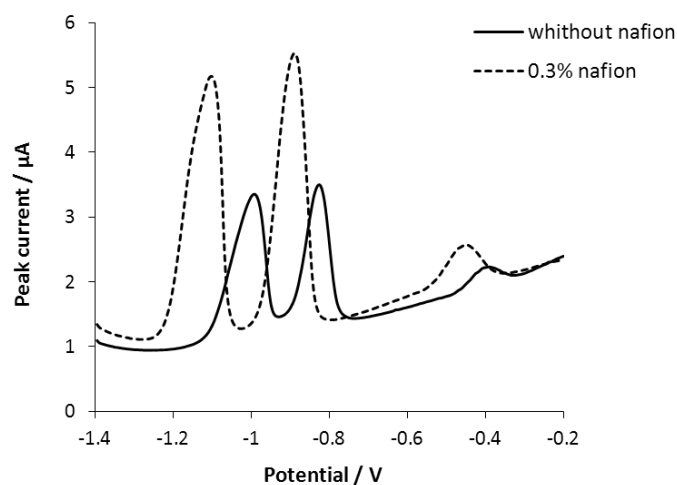


Figure 6. Square-wave anodic stripping voltammetry of 150 ppb Pb(II) and Cd(II) on bare electrode and Nafion® coated electrode. Conditions as in Fig. 4.

The effect of the film thickness on the SWASV response of Pb(II) and Cd(II) with *in situ* Bi(III) has been also studied. In this case the working electrode was modified in the same way as before, but with Nafion® solutions ranging from 0.025 to 1 v/v %. As can be deduce from **Fig. 7** initially the peak current increases with the Nafion® film thickness until reached a maximum (0.3 %) a large decline in peak current can be noticed. This phenomenon could be account for different reasons (i) polymer cracking and diffusion of the species away from the electrode before replating, thereby impeding the redox cycling mechanism [43] or (ii) steric effects, thick

films reduce the working electrode effective area leading to less metal deposited [40]. From results, 0.3 v/v% Nafion[®] was chosen as optimal for improving sensitivity.

Finally, the same study as in *section 3.2.2* (length of the oxidative treatment) was performed but this time coating the pretreated electrodes with 0.3 v/v% of Nafion[®]. For this instance the peak current behavior was slightly different, and for more than 15 scans no further improvements were observed (**Fig. 7 inset**). Then, a pretreatment of 15 scans between -1.4 and 1.4 V was chosen as the best compromise to achieve an improved electrochemical behavior in the shortest time.

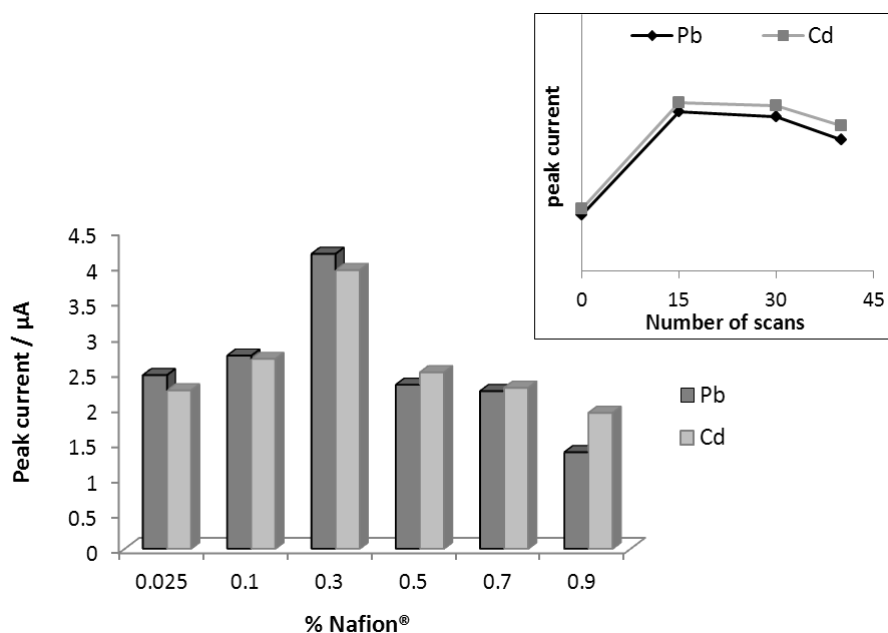


Figure 7. Effect of Nafion[®] film thickness on peak current and on pre-oxidized working electrode surfaces (inset). Conditions as in Fig. 4.

3.4. Calibration data

Calibration curves for the simultaneous determination of Pb (II) and Cd (II) were carried out in the range 0.1-50 ppb by SWASV under optimal conditions. The resulting calibration plots were linear over the range for both metals, and details regarding with slope and correlation coefficients are included in **Fig. 8**. The good intra-electrode reproducibility was demonstrated by performing three calibration curves on the same electrode, obtaining standard deviation (RSD) values of 3 and 4 % for Pb and Cd sensitivities. The limits of detection (calculated as $LOD = 3\sigma/S$, where σ is the standard deviation of the intercept and S is the slope) were 0.77 ppb for Pb and 1.4 ppb for Cd. On the other hand, the inter-electrode sensitivity was also checked, obtaining higher RSD values about 20 % for both metals.

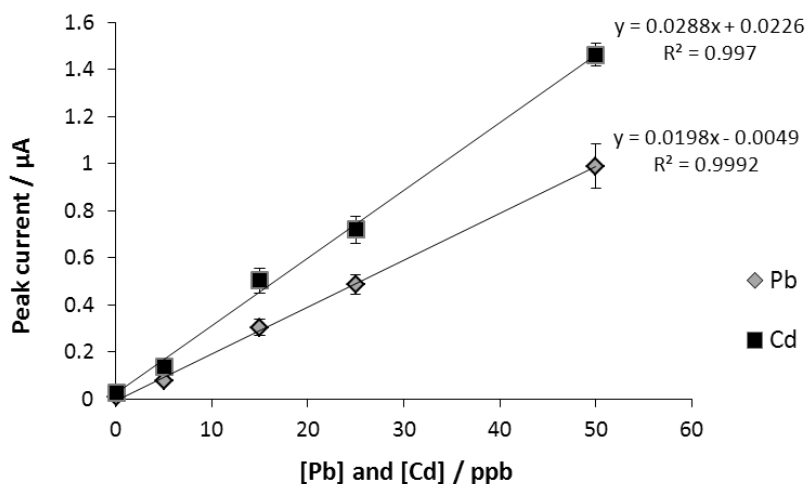


Figure 8. Calibration plots of Pb (II) and Cd (II) in 0.1 M acetate buffer (pH 4.6) under the optimized conditions.

Although RSD values for inter-electrode measures are high with the proposed method 0.1 ppb of Pb and Cd have been observed in stable and inexpensive electrodes. This meets the legal requirements that placed the minimum amount of lead for drinking water in 10 ppb and cadmium in 5 ppb (RD 140/2003).

4. Conclusions

In this work a novel method for heavy metals determination based on polyester transparency sheets with electrochemical detection is proposed. Different parameters (oxidative pretreatment, buffer solution pH, Bi^{3+} concentration, and Nafion® film thickness) have been optimized in order to achieve a sensitive detection system. Transparency has demonstrated that it is as suitable substrate as paper, which is able to provide alternative cheap tool of analysis for lead and cadmium quantification.

The results presented herein are in progress in order to improve the inter-electrode reproducibility and test real samples.

REFERENCES

- [1] D.D. Iliana, B. Raguse, J.J. Gooding, E. Chow. *Sensors* 12(2012) 11505-11526.
- [2] E.W. Nery, L.T. Kubota. *Anal. Bioanal. Chem.* 405 (2013) 7573-7595.
- [3] A.W. Martinez, S.T. Phillips, E. Carrilho, S.W. Thomas, H. Sindi, G.M. Whitesides. *Anal. Chem.* 80 (2008) 3699-3707.
- [4] A. Apilux, W. Dungchai, W. Siangproh, N. Praphairaksit, C.S. Henry, O. Chailapakul. *Anal. Chem.* 82 (2010) 1727-1732.
- [5] W. Dungchai, O. Chailapakul, C.S. Henry. *Anal. Chim. Acta* 674 (2010) 227-233.
- [6] M. Santhiago, L.T. Kubota. *Sens. Actuators B* 177 (2013) 224-230.
- [7] J. Noiphung, T. Songjaroen, W. Dungchai, C.S. Henry, O. Chailapakul, W. Laiwattanapaisa. *Anal. Chim. Acta* 788 (2013) 39-45.
- [8] T.-T. Tsai, S.-W. Shen, C.-M. Cheng, C.-F. Chen. *Sci. Technol. Adv. Mater.* 14 (2013) 1-7.
- [9] V. Mani, K. Kadimisetty, S. Malla, A.A. Joshi, J.F. Rusling. *Environ. Sci. Technol.* 47 (2013) 1937-1944.
- [10] X. Li, J. Tian, W. Shen. *Anal. Bioanal. Chem.* 396 (2010) 495-501.
- [11] X. Li, J. Tian, G. Garnier, W. Shen. *Colloid. Surface. B* 76 (2010) 564-570.
- [12] L. Feng, X. Li, H. Li, W. Yang, L. Chen, Y. Guan. *Anal. Chim. Acta* 780 (2013) 74-80.
- [13] L.Y. Shiroma, M. Santhiago, A.L. Gobbi, L.T. Kubota. *Anal. Chim. Acta* 725 (2012) 44-50.
- [14] Z. Nie, C.A. Nijhuis, J. Gong, X. Chen, A. Kumachev, A.W. Martinez, M. Narovlyansky, G.M. Whitesides. *Lab Chip* 10 (2010) 477-483.
- [15] M.P. Sousa, J.F. Mano. *ACS Appl. Mater. Interfaces* 5 (2013) 3731-3737.
- [16] M. Li, J. Tian, M. Al-Tamimi, W. Shen. *Angew. Chem. Int. Ed.* 51 (2012) 5497-5501.
- [17] A. Arena, N. Donato, G. Saitta, A. Bonavita, G. Rizzo, G. Neri. *Sens. Actuators B* 145 (2010) 488-494.
- [18] A. Nilghaz, D.H.B. Wicaksono, D. Gustiono, F.A.A. Majid, E. Supriyanto, M.R.A. Kadir. *Lab Chip* 12 (2012) 209-218.
- [19] M. Reches, K.A. Mirica, R. Dasgupta, M.D. Dickey, M.J. Butte, G.M. Whitesides. *ACS Appl. Mater. Inter.* 2 (2010) 1722-1728.
- [20] A.W. Martinez, S.T. Phillips, M.J. Butte, G.M. Whitesides. *Angew. Chem. Int. Ed.* 46 (2007) 1318-1320.
- [21] J. Lankelma, Z. Nie, E. Carrilho, G.M. Whitesides. *Anal. Chem.* 84 (2012) 4147-4152.
- [22] H. Liu, R.M. Crooks. *J. Am. Chem. Soc.* 133(2011) 17564-17566.
- [23] J.H. Yu, L. Ge, J.D. Huang, S.M. Wang, S.G. Ge. *Lab chip* 11 (2011) 1286-1291.
- [24] L. Ge, S. Wang, X. Song, S. Ge, J. Yu. *Lab Chip* 12 (2012) 3150-3158.
- [25] J.L. Delaney, C.F. Hogan, J. Tian, W. Shen. *Anal. Chem.* 83 (2011) 1300-1306.
- [26] J.L. Delaney, E.H. Doeven, A.J. Harsant, C.F. Hogan. *Anal. Chim. Acta* 790 (2013) 56-60.

- [27] L. Ge, P. Wang, S. Ge, N. Li, J. Yu, M. Yan, J. Huang. *Anal. Chem.* 85 (2013) 3961–3970.
- [28] W. Wei, I.M. White. *Anal. Chem.* 22 (2010) 9626–9630.
- [29] D. Tobjörk, R. Österbacka. *Adv. Mater.* 23 (2011) 1935–1961.
- [30] D.A. Gidlow. *Occup. Med.-Oxford* 54 (2004) 76–81.
- [31] V. Matovic, A. Buha, Z. Bulat, D. Đukic-Ćosic. *Arh. Hig. Rada Toksiko.* 62 (2011) 65-76.
- [32] L. Cao, J. Jia, Z. Wang. *Electrochim. Acta* 53 (2008) 2177-2182.
- [33] R.O. Kadara, N. Jenkinson, C.E. Banks. *Electroanalysis* 21 (2009) 2410-2414.
- [34] J. Calvo Quintana, F. Arduini, A. Amine, F. Punzo, G. Li Destri, C. Bianchini, D. Zane, A. Curulli, G. Palleschi, D. Moscone. *Anal. Chim. Acta* 707 (2011) 171-177.
- [35] J. Wang, M. Pedrero, H. Sakslund, O. Hammerich, J. Pingarron. *Analyst* 121 (1996) 345-350.
- [36] R.T. Kachoosangi, C.E. Banks, X. Ji, R.G. Compton. *Anal. Sci.* 23 (2007) 283-289.
- [37] A. Economou. *Trac-Trend. Anal. Chem.* 24 (2005) 334-340.
- [38] I. Svancara, L. Baldrianova', E. Tesarova', S.B. Hocevar, S.A.A. Elsuccary, A. Economou, S. Sotiropoulos, B. Ogorevc, K. Vytras. *Electroanalysis* 18 (2006) 177-185.
- [39] E.A. Hutton, B. Ogorevc, S.B. Hocevar, F. Weldon, M.R. Smyth, J. Wang. *Electrochem. Comm.* 3 (2001) 707-711.
- [40] G. Kefala, A. Economou, A. Voulgaropoulos. *Analyst* 129 (2004) 1082-1090.
- [41] J. Calvo Quintana, F. Arduini, A. Amine, K. van Velzen, G. Palleschi, D. Moscone. *Anal. Chim. Acta* 736 (2012) 92-99.
- [42] C. Kokkinos, A. Economou. *Talanta* 84 (2011) 696-701.
- [43] H. Li, J. Li, Z. Yang, Q. Xu, C. Hou, J. Peng, X. Hu. *J. Hazard. Mater.* 191 (2011) 26-31.

CONCLUSIONS

CONCLUSION

Las conclusiones obtenidas al término de esta investigación han ido comentándose a lo largo de la memoria de esta Tesis doctoral, pero de forma general, son las siguientes:

- ▣ Se ha demostrado el potencial de los microchips de electroforesis como herramienta de análisis competitiva.
- ▣ A lo largo de esta memoria se han propuesto varias estrategias para superar los problemas asociados al proceso de miniaturización, centradas principalmente en solventar los problemas relacionados con la selectividad y sensibilidad:
 - Por un lado, se ha demostrado la necesidad de un recubrimiento del microcanal para poder conseguir la separación de mezclas complejas, como por ejemplo las catecolaminas, analitos estructuralmente similares. Así, se ha puesto a punto un protocolo reproducible para la modificación estática de microcanales de vidrio. A su vez se han evaluado nuevos modificadores dinámicos, como son los líquidos iónicos y polímeros derivados del poli(glicidil metacrilato) de síntesis propia, resultando ser esta última la estrategia que ha proporcionado unos mejores resultados.
 - Por otro lado, la respuesta del sistema de detección ha sido considerablemente amplificada mediante el empleo de nanotubos de carbono crecidos directamente en el sustrato. Así, se ha visto que estos nanomateriales son capaces de ofrecer mejores prestaciones analíticas que los electrodos convencionales modificados con dispersiones de estos nanotubos. Además mediante su posterior integración en el sistema microfluídico supondrán una importante mejora de la sensibilidad.
- ▣ Finalmente la última contribución de esta Tesis estuvo relacionada con el campo de los dispositivos microfluídicos en papel. El incremento de la sensibilidad en los llamados “paper-based analytical devices” es una tarea extremadamente importante, ya que lo que se pretende conseguir son herramientas de análisis de bajo coste que permitan la detección de trazas. Así se ha integrado la detección electroquímica tanto en papel como en transparencias, demostrando el potencial de estas últimas para la detección sensible de metales pesados.